Modeling the biota population impact on polychlorinated biphenyls transport and simulating PCBs anaerobic biodegradation in the lake system

Submitted in partial fulfillment of the requirements for

the degree of

Doctor of Philosophy

in

Civil and Environmental Engineering

Xiangfei Sun

B.S., Environmental Science, University of Science and Technology of China

M.S., Environmental Engineering, Carnegie Mellon University

M.S., Engineering & Technology Innovation Management, Carnegie Mellon University

Carnegie Mellon University

Pittsburgh, PA

April, 2018

Acknowledgement

Firstly, I would like to express my sincere gratitude to my advisor Prof. Mitchell J. Small for the continuous support of my Ph.D. study and related research, for his patience, motivation, and immense knowledge. His guidance helped me in all the time of study and writing of this thesis. I could not have imagined having a better advisor and mentor for my Ph.D. study.

Besides my advisor, I would like to thank the rest of my thesis committee: Prof. Ng Carla, Prof. David Yaron, and Prof. Peter Adams, for their insightful comments and encouragement, but also for the hard questions which motivated me to widen my research from various perspectives.

My sincere thanks also go to the China Scholarship Council (CSC), who provided most of the funding for my Ph.D. studies. Without their valuable support, it would be impossible to conduct this research. The rest funding is provided by my family, and I really appreciate their support.

I thank my colleagues at Carnegie Mellon for the valuable discussions, suggestions, and for all the fun we have had in the last four years. Also, I appreciate Prof. Eddy Zeng, Dean of School of Environment, Jinan University, for providing me with my first exposure to research and all these years of continuous support in my academic career.

Last but not the least, I would like to thank my family: my parents and to my brothers and sister for supporting and encouraging me financially and spiritually throughout this period and my life in general.

Abstract

Persistent organic pollution (POPs) is one of the top environmental issues worldwide. Most of these chemicals are synthetic, introduced through industry production for particular purposes. Due to the persistence and stability, POPs can travel long distances, and some of them can accumulate in biota tissues with high lipid contents and cause long-term toxicity and affect organism's health when certain concentration levels are reached.

This thesis aims to improve the understanding of organism impacts during POPs transport and to model the mechanisms of biota degradation processes. We are focusing on a specific type of POPs, polychlorinated biphenyls (PCBs). The chemical complexity and composition uncertainty of PCBs make it an excellent research object. Moreover, since the PCBs have been banned for production and background concentration is dropping, we could acquire a completed figure of POPs pollution for model development. By analyzing the PCBs transport history, we could improve current model designs to predict other POPs transport behaviors in various environmental media, assist further development on POPs control policy, and prevent issues and damages on public health in future.

The first study intends to upgrade the current model performance for simulating complex PCBs fate and transport in a lake system, especially the organism effects during PCBs transport. Several improvements are made, such as integrating multiple biotic terms regarding the PCB

transport to rebuild the feedback routines from biotic compartments to the environmental media. Facilitated intermedia transport through biota compartments is shown in the analysis and its contributions to overall PCBs transport is carefully evaluated and discussed.

The second project aims to evaluate the performance of current empirical rules on PCB dechlorination study. The study aims to explore the mechanisms and principles behind PCB anaerobic biodegradation further since the empirical regulations are rough and unprecise for mathematical modeling. Moreover, the empirical rules mainly reflect the biotic features in PCB dechlorination process. Since the reaction involves both the biology and chemistry, it is rational to dig more information on impacts from the chemical side. The research not only reviews the microorganism's bio-selectivity behind the existing empirical rule, but also discusses the possible mechanism based on chemical kinetics, trying to develop a hypothesis to explain and quantify the anaerobic degradation behaviors, such as quantum chemistry theory, molecule orbit theory, and so on.

The final research focuses on simulating the PCB dechlorination through a redox potential based model. By introducing redox-potential as the thermal dynamic selection tool. This study provides one possible solution for predicting PCB dechlorination patterns and posting reaction products by tracking redox potential, as well as the bio-selectivity from microorganism features. The redox potentials of each dechlorination reaction can be calculated by evaluating the Gibbs free energy through quantum chemistry theories and several environmental factors. To realize a practical procedure, we created a model, using the Markov Chain method to monitor the continuous changes in the PCB concentration distribution. The new model proves its capability and accuracy by comparing the simulation results with several published reports on PCB dechlorination study.

Contents

Acknowledgement i

Abstract ii

List of Tables ix

List of Figures and Illustrations xi

Preface 1

Part 1: Modeling the impact of biota on polychlorinated biphenyls (PCBs) fate and transport in Lake Ontario using a population-based multi-compartment fugacity approach 4

1. Introduction 6

1.1. Background & Literature Review *6*

1.1.1. Persistent Organic Pollutants (POPs) 6

1.1.2. Polychlorinated Biphenyls (PCBs) 9

1.1.3. Multi-compartment Model 10

1.1.4. Fugacity Approach 11

1.1.5. Lake Ontario 12

1.2. Achievements and Problems *13*

1.2.1. Isotope Procedure 13

1.2.2. Potential Solution 14

2. Improved Model Design for Pollution Transport Study 16

2.1. General Model Design *16*

2.1.1. Formula for Population-Based Fugacity Model 16

2.1.2. Model Assumptions 26

2.2. Simultaneous Structure *26*

2.2.1. The Fugacity Capacity 26

2.2.2. PCBs Mass Variation 31
2.2.3. Fugacity Capacity Variation 40
2.2.4. The Compartment Volume Variation 44

2.3. Loading Pattern 48

2.4. Population Behavior during PCB Mass Exchange 51

3. Organic Impacts on PCBs transport 54

3.1. Mass Balance and Observations Comparison 54

3.2. Facilitated Biotic Intermedia Transport 63

3.3. Storage Effect 71

3.4. Overall model prediction evaluation 74

3.5. General sensitive analysis 76

3.6. Temperature variance on overall PCB transport 80

4. Conclusion 85

4.1. FBIT & Storage Effect 86

4.2. Future Study 86

Part 2 A cross-validation analysis of the empirical rules on polychlorinated biphenyls (PCBs) anaerobic dechlorination 88

5. Introduction 89

5.1. Polychlorinated Biphenyls (PCBs) Natural Degradation 89

5.2. PCBs Toxicity 91

5.3. Empirical Rules 91

5.4. Dehalogenation Process 93

6. Model Design and Data Collection 95

6.1. Observation Data Collection ... *95*

6.2. Rules and Assumptions ... *95*

6.3. Model Structure ... *98*

7. Results and Discussion ... 101

7.1. Limitation from PCB congener structure ... *101*

7.2. Observation on PCBs Dechlorination Preference ... *103*

7.3. Cross-Validation for Optimal Dechlorination Rule Selection ... *106*

7.3.1. Reactive Chlorophenyl Group Rules (RCGR) ... 106

7.3.2. General Nine Class Rules (GNCR) ... 108

8. Conclusion ... 111

Part 3: Using reduction potential and bio-selectivity to simulate PCB dechlorination process in anaerobic environment ... 112

9. Issues and Motivation ... 113

9.1. Synchronization Issues in PCB Dechlorination Model Design ... *113*

9.2. Redox Potential & Gibbs Free Energy ... *113*

9.3. Quantum Chemistry ... *114*

10. Model Design & Data Collection ... 116

10.1. Estimate Redox Potential of PCB Dechlorination Half-Reaction ... *116*

10.2. Model Assumptions and mechanisms ... *118*

10.3. Markov Chain PCB Dechlorination Model ... *120*

10.4. Model Performance Evaluation ... *123*

11. Results & Discussions ... 124

11.1. The Fundamental Effects of Redox Potential *124*

11.2. Redox Potential vs. Empirical Rules *128*

11.3. PCB Dechlorination Simulation *130*

12. Conclusion **140**

References **141**

Appendix A: Original Results and Datasets **157**

List of Tables

Table 1.1 POPs Chemical Summarize 7

Table 2.1. Lake Ontario Approximate Representative Domain 16

Table 2.2 PCBs Main Exchange Processes 21

Table 2.3 Parameter Estimation Formula 23

Table 2.4 General Parameter Information 25

Table 2.5. The Physical & Chemical Properties of Selected PCB Congeners 48

Table 2.6. The Physical & Chemical Properties of PCB Homolog Groups 49

Table 2.7. Species Biotic Information 53

Table 2.8. Food Web (pij) 53

Table 3.1. Observation vs. Simulation in Lake Ontario Pollution History 57

Table 5.1. Eight processes dechlorination rules 92

Table 6.1. Observed Data Collection 95

Table 6.2. PCB dechlorination classification based on empirical rules 97

Table 7.1. Most Frequent Trained Rules under Current Observation 110

Table 11.1 PCB-194 dechlorination simulation with final products allocation 127

Table A.1. The mass flows of selected PCB congeners under steady state (high biomass). 157

Table A.2. The mass flows of selected PCB congeners under steady state (low biomass) .. 158

Table A.3. PCB-18 Mass flow details under steady state with high biomass density 159

Table A.4. PCB-153 Mass flow details under steady state with high biomass density 160

Table A.5. PCB-194 Mass flow details under steady state with high biomass density........ 161

Table A.6. PCB-18 Mass flow details under steady state with low biomass density 162

Table A.7. PCB-153 Mass flow details under steady state with low biomass density 163

Table A.8. PCB-194 Mass flow details under steady state with low biomass density 164

Table A.9 Calculated standard redox potential for PCB dechlorination............................. 165

List of Figures and Illustrations

Figure 1.1. The Difference between Traditional Design and Improved Approach............................. 15

Figure 2.1. PCBs Exchange between Organism and Environment (New Design) 20

Figure 2.2. PCBs Exchange between Organism and Environment (Traditional Design)................... 20

Figure 2.3. PCBs Loading Pattern for Lake Ontario (Gobas et al. 1995).. 50

Figure 2.4. The Accumulated Inputs of All Three PCB Congeners.. 51

Figure 3.1. Model-Predicted Relative Distribution of Accumulated PCB-18 in 1960 & 1980 55

Figure 3.2. Model-Predicted Relative Distribution of Accumulated PCB-153 in 1960 & 1980 55

Figure 3.3. Model-Predicted Relative Distribution of Accumulated PCB-194 in 1960 & 1980 56

Figure 3.4. Total PCBs Concentration Comparison: Observation vs. Simulation in Aroclor 1248... 60

Figure 3.5. Total PCBs Concentration Comparison: Observation vs. Simulation in Aroclor 1254... 61

Figure 3.6. Total PCBs Concentration Comparison: Traditional Design, in Aroclor 1254 62

Figure 3.6. PCB-18 Facilitated Biotic Intermedia Transport under Two Bio-density 64

Figure 3.7. PCB-153 Facilitated Biotic Intermedia Transport under Two Bio-density 66

Figure 3.8. PCB-194 Facilitated Biotic Intermedia Transport under Two Bio-density 66

Figure 3.9. PCB-18 FBIT Effect under Different Bio-density (Steady State)...................................... 68

Figure 3.10. PCB-153 FBIT Effect under Different Bio-density (Steady State)................................. 68

Figure 3.11. PCB-194 FBIT Effect under Different Bio-density (Steady State) 69

Figure 3.12. PCB-18 Mass Content with Different Biota Density... 72

Figure 3.13. PCB-153 Mass Content with Different Biota Density... 72

Figure 3.14. PCB-194 Mass Content with Different Biota Density 73

Figure 3.15. Time Dependent Total PCB Concentration of Water and Salmonid 75

Figure 3.18. Annual Water Temperature Variations of Lake Ontario 81

Figure 3.19. Temperature Variations Impacts on total PCBs concentration in Lake Ontario 82

Figure 7.1. Theoretical PCB Dechlorination Pathways 101

Figure 7.2. Histogram of PCB Theoretical Dechlorination Pathways (blue) and Observed Pathways (yellow). 102

Figure 7.3 Observed PCB Dechlorination Pathways 105

Figure 7.4. RCGR Rule Preference Distribution over 100,000 Training Cycles 107

Figure 7.5. GNCR Rule Preference Distribution over 100,000 Training Cycles 108

Figure 7.6. The Relationship between RCGR Rules and GNCR Rules 109

Figure 10.1. PCB dechlorination model design 121

Figure 11.1. Comparison between parallel dropping vs. free dropping (black curve) 125

Figure 11.2. Parallel dropping vs. free dropping (black curve, PCB-172) 126

Figure 11.3. Gibbs Free Energy of 840 PCB dechlorination under Standard Condition 130

Figure 11.4a. Original PCBs Distribution & Observed Post-Dechlorinated Products (%mol, Bedard 1997) 132

Figure 11.4b. Simulated Dechlorinated Product Difference & Simulated PCBs Distribution (%mol, meta priming, Bedard 1997) 133

Figure 11.4c. Simulated Dechlorinated Product Difference & Simulated PCBs Distribution (%mol, no priming, Bedard 1997) 134

Figure 11.5a. Original PCBs Distribution & Observed Post-Dechlorinated Products (%mol,

Demirtepe 2015) 135

Figure 11.5b. Simulated Dechlorinated Product Difference & Simulated PCBs Distribution (%mol, no priming, Demirtepe 2015) 136

Figure 11.6a. Original PCBs Distribution & Observed Post-Dechlorinated Products (%mol, Van Dort 1997) 137

Figure 11.6b. Simulated Dechlorinated Product Difference & Simulated PCBs Distribution (%mol, meta priming, Van Dort 1997) 138

Figure 11.6c. Simulated Dechlorinated Product Difference & Simulated PCBs Distribution (%mol, no priming, Van Dort 1997).......... 139

Preface

Understanding the fate and transport of polychlorinated biphenyls (PCBs) in the environment is essential for pollution control and remediation technology development. Although the production of PCBs has been banned for almost thirty years, persistence and stability allow these chemical compounds to maintain their existence in the environment due to leakage from improper disposal and old electronic devices. A recent study also indicates that some of the PCB congeners can be synthsized as byproducts in related industrial processes.

In this thesis, three current issues affecting PCBs fate and transport are carefully discussed. Although the whole study is about modeling the PCB fate and transport in the environment, these three problems are quite distinguished from each other. As a result, the entire thesis is divided into three topics to reduce confusion. Each topic has its introduction, model, results, and discussion.

The first part of the thesis focuses on understanding organism population impacts on PCB distribution in the environment, based on a new modeling approach. In the classic modeling design, organisms have been treated as pure receptors instead of functional compartments during exposure studies, because of their small group sizes compared to other environmental compartments. However, since most of the PCB congeners have significant octane solubility and quickly accumulate in organisms, it becomes uncertain whether these high concentrations of

PCBs in biota could modify the overall PCB mass transport in the system, despite the relatively small biotic volumes. We design a new processing model using a populated organism design and try to evaluate the impacts of highly bioconcentrated PCB congeners on general PCB transport in the system.

The second part and the third part of the thesis focus on PCB biodegradation in the anaerobic environment, which is critical for developing useful remediation technology and eliminating PCB pollution. PCB anaerobic biodegradation belongs to the class of dehalogenation reactions where the microorganisms and bacteria utilize highly chlorinated PCB congeners as electronic receptors and generate lower chlorinated substitutes. Since PCB dechlorination could naturally occur in the environment, it might become one of the potential remediation techniques to eliminate PCB residues in the future.

In the second part, statistical analysis is introduced to evaluate the potentials of the empirical rules for PCB dechlorination simulation in an anaerobic environment. The cross-validation method is utilized by categorizing the 840 theoretical one-step reactions of PCB dechlorination into 90 classes and comparing them to over 200 observations in previous literature. The analysis proves that the empirical rules have a strong relationship with bio-selectivity of the microorganisms and bacteria. However, the study also indicates that a PCB dechlorination model cannot be produced solely by the empirical rules since these cannot provide a quantitative order of PCB dechlorination pathway selection within each pathway category.

In the third part, a new model program is developed to simulate PCB dechlorination using both the empirical rules and redox potential. Redox potential represents the potential of a direct measure of the thermodynamic feasibility of an oxidation-reduction half-reaction. According to the literature, it can quantitatively distinguish among similar chemical processes. However, it is difficult to directly measure redox potentials of multiple PCB congeners participating in the mechanically complex dechlorination reactions. As a result, quantum chemistry is introduced into the study and the redox potential is calculated indirectly through Gibbs free energy of each dechlorination reactions. The model is tested and compared with observations in the published literature. The differences between the observations and simulations indicate that the proposed mechanisms could provide improved prediction of PCB dechlorination in the environment.

Part 1: Modeling the impact of biota on polychlorinated biphenyls (PCBs) fate and transport in Lake Ontario using a population-based multi-compartment fugacity approach

Organisms have long been treated as receptors in exposure studies of polychlorinated biphenyls (PCBs) and other persistent organic pollutants (POPs). The influences of pollution exposure on organisms are well recognized. However, the impact of biota on PCB transport in an environmental system has not been considered in sufficient detail. In this study, a population-based multi-compartment fugacity model is developed by reconfiguring the organisms as populated compartments and reconstructing all the exchange processes between the organism compartments and environmental compartments, especially the previously ignored feedback routes from biota to the environment. We evaluate the model performance by simulating the PCB concentration distribution in Lake Ontario using published loading records. The lake system is divided into three environment compartments (air, water, and sediment) and several organism groups according to the dominant local biotic species. The comparison indicates that the simulated results are well-matched by a list of published field measurements from different years. We identify a new process, called Facilitated Biotic Intermedia Transport (FBIT), to describe the enhanced pollution transport that occurs between environmental media and organisms. As the hydrophobicity of PCB congener increases, the organism population exerts greater influence on PCB mass flows. In a high biomass scenario, the model simulation indicates significant FBIT effects and biotic storage effects with hydrophobic PCB congeners, which also lead to significant shifts in systemic contaminant exchange rates between organisms and the environment.

1. Introduction

1.1. Background & Literature Review

1.1.1. Persistent Organic Pollutants (POPs)

Persistent organic pollutants (POPs) are a group of organic compounds (carbon-based) that, to a varying degree, resist photolytic, biological and chemical degradation. POPs are characterized by low water solubility and high-octane solubility, leading to their bioaccumulation in organism fatty tissues, eutrophication water, and humus enriched soil & sediment. POPs are also semi-volatile, enabling them to move long distances in the atmosphere before deposition occurs (Ritter et al., 1995).

Although some types of POPs, such as dioxins and dibenzofurans, can naturally arise from volcanic activity and vegetation fires, most of the existing POPs come from artificial synthesis of modern chemical industry (El-Shahawi et al., 2010). The commercial manufacture of anthropogenically synthesized organic chemicals began in the 1920s. Since then, the synthetic industry has produced thousands of organic compounds, as well as many other byproducts during the process. Some products are used as pesticides, which are incredibly useful in pest control, while others are excellent intermediate material for other industries. After World War II, the production and usage of these chemical componds expand rapidly, driven by a desire to increase the food production, protect public health, and facilitate industrial development (Krueger and

Selin, 2002). All these organic chemicals indeed improved our life quality and solved many urgent problems associated with agriculture and industry during that period. However, some products, such as DDT, Aldrin, PCBs, and so on, are extremely toxic and resistant to most natural degradation processes. Moreover, the high hydrophobic features lead these organic compounds to dissolve and accumulate in organism tissues and organs through ingestion, gill uptake, and direct exposure, causing significant bioaccumulation behaviors, and generating lots of toxicity and reproduction issues to more species than their designed sphere of influence. (Gobas et al. 1986; Oliver 1987; Campfens et al. 1997; Arnot et al. 2004; De Laender et al. 2010).

Table 1.1 POPs Chemical Summarize

Annex	Chemical Name	Generation
Annex A (Elimination) [Parties must take measures to ***eliminate*** the production, and use of the chemicals listed under Annex A. Specific exemptions for the use of production are listed in the Annex and apply only to Parties that register for them]	Aldrin*	*Pesticide*
	Chlordane*	*Pesticide*
	Chlordecone	*Pesticide*
	Dieldrin*	*Pesticide*
	Endrin*	*Pesticide*
	Heptachlor*	*Pesticide*
	Hexabromobiphenyl	*Industrial chemical*
	Hexabromocyclododecane (HBCD)	*Industrial chemical*
	Hexabromodiphenyl ether & Heptabromodiphenyl ether	*Industrial chemical*
	Hexachlorobenzene (HCB)*	*Pesticide & Industrial chemical*
	Hexachlorobutadiene	*Industrial chemical*
	Alpha hexachlorocyclohexane	*Pesticide*
	Beta hexachlorocyclohexane	*Pesticide*

	Lindane	*Pesticide*
	Mirex*	*Pesticide*
	Pentachlorobenzene	*Pesticide*
	Polychlorinated biphenyls (PCB)*	*Industrial chemical*
	Polychlorinated naphthalenes	*Industrial chemical*
	Pentachlorophenol and its salts and esters	*Pesticide*
	Technical endosulfan and its related isomers	*Pesticide*
	Tetrabromodiphenyl ether and pentabromodiphenyl ether	*Industrial chemical*
	Toxaphene*	*Pesticide*
Annex B (Restriction) [Parties must take measures to ***restrict*** the production and use of the chemicals listed under Annex B in light of any applicable acceptable purposes and specific exemptions listed in the Annex.]	DDT*	*Pesticide*
	Perfluorooctane sulfonic acid, its salts and Perfluorooctane sulfonyl fluoride	*Industrial chemical*
Annex C (Unintentional Production) [Parties must take measures to ***reduce*** the unintentional release of the chemicals listed under Annex C with the goal of continuing minimization and, where feasible, ultimate elimination.]	Hexachlorobenzene (HCB)	*Unintentional Production*
	Pentachlorobenzene	*Unintentional Production*
	Polychlorinated biphenyls (PCB)	*Unintentional Production*
	Polychlorinated dibenzo-*p*-dioxins (PCDD)*	*Unintentional Production*
	Polychlorinated dibenzofurans (PCDF)*	*Unintentional Production*
	Polychlorinated naphthalenes	*Unintentional Production*
Chemicals proposed for listing under the Convention	Decabromodiphenyl ether	*Unknown*
	Dicofol	*Unknown*
	Short-chain chlorinated paraffin	*Unknown*
	Pentadecafluorooctanoic acid	*Unknown*

Note: * represents the initial 12 POPs

Persistent organic pollutants (POPs) are officially recognized by the Stockholm Convention under the United Nations Environment Programme. Following the extensive negotiation, it was adopted on May 22, 2001 (Harrad, 2009). Since then, features, sources, transport, and impacts of POPs are carefully measured and evaluated across the world. In late 2008, over 180 participants were contributing to this subject, and new types of POPs are kept identified. Up to 2017, 26 groups of chemicals have been classified as persistent organic pollutants, comparing to the initial 12 group chemicals. Moreover, another four categories of organic chemicals are currently proposed for listing under the POPs index. Table 1.1 listed all the chemical compounds presently identified as POPs or under reviewing. As described in Table 1.1, the sources of POPs include industrial production, pesticides usage, and unintentional production.

1.1.2. Polychlorinated Biphenyls (PCBs)

Polychlorinated Biphenyls (PCBs) are a group of anthropogenically synthesized organic compounds, including 209 isomers which belong to ten homolog groups based on the chlorine contents. Due to their persistence, long-distance transport, bioaccumulation, and toxicity, PCBs have been identified as a group of persistent organic pollutants (POPs) (Porta and Zumeta 2002).

The commercial products of PCBs in the United States have a uniformed trade name, Aroclor, which is distinguished by their chlorine contents. Over 600,000 tons of Aroclor products are solely produced by the Monsanto Company between 1930 and 1977 (approximately 40%-60% of the global PCBs production). Although the PCBs production in the U.S. is completely stopped in 1977, other countries still produced them for another 16 years (Breivik et al. 2002). Because of its vast inventory, 40% of total manufactured PCB was thought to remain in use in 2006 (Rossberg et al. 2000).

The commercial products of PCBs are isomers mixtures with different degrees of chlorination (Kaley et al. 2007). Depending on the manufacturing techniques, each product contains different combination and content of PCB isomers. Each product only includes part of the isomers listed in the literature, and the proportion of each isomer also varies significantly. In fact, some of the isomers were never existed in any commercial products. For example, more than 97% products sold and used in the U.S. are Aroclor 1016: 1242: 1248: 1254: 1260 (de Voogt and Brinkman, 1989; Rossberg et al. 2000). Each Aroclor only contains 30%-56% of the entire 209 isomers, and 32 isomers never appear in all these mixtures.

1.1.3. Multi-compartment Model

Mathematical modeling provides an essential basis for estimating the fate and transport of PCBs through an environmental system (Bates et al. 2017; Kelce et al. 1998). Chemical potential and fugacity are two frequently used methods (Mackay et al. 2001; Campfens et al. 1997). The chemical potential approach utilizes the phase equilibrium thermodynamics, yielding rates of mass diffusion directly proportional to measured concentrations (Neely et al. 1974; Kamaya et al.

1981; Barber, Suérez, and Lassiter 1988). In 2004, Arnot and Gobas developed a bioaccumulation food web model based on the chemical potential formulation (Arnot et al. 2004), which has been widely used as a standard approach in PCB transport and bioaccumulation studies (McLeod et al. 2015; Selck et al. 2012; De Laender et al. 2010).

1.1.4. Fugacity Approach

However, redox potential is logarithmically related to concentration (non-linear) and can vary significantly due to environmental sensitivity. Therefore it is necessary to establish some standard state at which it has a reference value and separate the environmental sensitivity from contaminant diffusion. (Bates et al. 2017; Mackay et al. 2006; MacLeod et al. 2002; Mackay 1979). As a result, the fugacity approach was introduced in the 1980s as a more convenient convention to describe thermodynamic equilibrium. Recent model development also integrates information on multiple and interacting processes on PCBs partitioning and transport in the environment (Hollander et al. 2007).

In 2006, Wania created the fugacity-based CoZMo-POP2 model. The model includes 19 environmental compartments and works under dynamic conditions. The model also takes into account seasonal variables and allows for the definition of time-variant emission scenarios (Wania et al. 2006). Furthermore, the fugacity approach has been applied in bioaccumulation and exposure studies for PCBs. A review of bioaccumulation studies using the fugacity approach is provided by Gobas and Morrison (Gobas and Morrison 2000). In 2016, Mackay used the fugacity model to study the processes influencing chemical biomagnification and trophic magnification factors in aquatic ecosystems (Mackay et al. 2016). To allow for further insight, Monte Carlo analysis was introduced to characterize uncertainty under various environmental conditions (De Laender et al. 2010).

1.1.5. Lake Ontario

Lake Ontario belongs to the Great Lakes of North American continent. It is one of the largest freshwater lakes on earth. Its primary inlet is the Niagara River from Lake Erie. As the last lake in the Great Lakes chain, Lake Ontario serves as the outlet to the Atlantic Ocean via the Saint Lawrence River (Fine and Carneiro 1999). Lake Ontario is well-known for its biodiversity among the Great Lake system. However, surrounded by some of the earliest developed cities, Lake Ontario has experienced a long history of substantial industrial activities, resulting in massive pollution scenarios (Ashworth 1987). These toxic chemicals not only affected the normal bioactivities of living stock in the lake area but also disturbed the existing trophic structures and nutrition levels. For instance, the high nutrition level in spring and summer is thought to be the cause of frequent algal blooms to occur in the 1960s and 1970s (Christie 1974), which killed a large number of fishes and damaged the ecosystem of Lake Ontario. Furthermore, the species population and distribution also shifted significantly during recent years. Although part of this alternation is caused by the invasion of alien species, the massive pollution is also a critical factor to inhibit the expansion and growth of native species.

As one of the earliest areas for POPs pollution research, a substantial amount of field data has been compiled since the 1970s in Lake Ontario district (Rukavina 1976; Oliver and Niimi 1988; Soonthornnonda et al. 2011). These measurements provide a valuable basis to explore biological impacts on PCB transport process.

1.2. Achievements and Problems

1.2.1. Isotope Procedure

Despite these previous improvements, organisms have long been treated as pollution exposure assessment targets, and their biological impacts on pollutant fate and transport are considered only in recent years, regarding specifically the contaminant transport through species migration (Walters and Christensen 2018; McGill et al. 2017; Krümmel et al. 2003). When establishing the contaminant mass balance within the organisms, the direct exchange processes of PCB mass through biotic compartments are well categorized and formulated. However, the biotic compartments respond more rapidly than the environmental sectors. Depending on the nutrition level, mortality rate, food web, and temperature, the population of a species may shift substantially over relatively short periods. Previous models use growth dilution to represent the volumetric changes of biotic compartments rather than direct contaminant exchanges (Gewurtz et al. 2006; Arnot and Gobas 2004; Campfens and Mackay 1997). Since growth dilution expresses reductions in concentration due to an organism's volume expansion, it neither describes the effects of organism population behavior on overall PCB transport in the system nor clarifies the destination of contaminant discharged from the organism.

Highly chlorinated PCB congeners are highly hydrophobic, and the high lipid content of organisms provides an excellent location for storage (Kaur et al. 2012; Kelly et al. 2004; Gobas et al. 1988; Barber et al. 1988). Recent studies have confirmed that the PCB bioaccumulation and storage effects on organism population scales may have a significant impact on PCB transport in an ecosystem (Walters and Christensen 2018; McGill et al. 2017; Krümmel et al. 2003).

1.2.2. Potential Solution

To quantify organism impacts on PCB transport, we extend the existing fugacity approach by integrating completed organism interactions with environmental media and using a population-based structure. The new design allows us to evaluate the influence of organism population dynamics on PCB mass flow. As a result, PCB transport among biotic groups not only relies on direct individual exchange processes, such as respiration, food ingestion, metabolism, and so on, but also depends on population features, such as birth, growth, predation, and natural mortality rates (Bates et al. 2017).

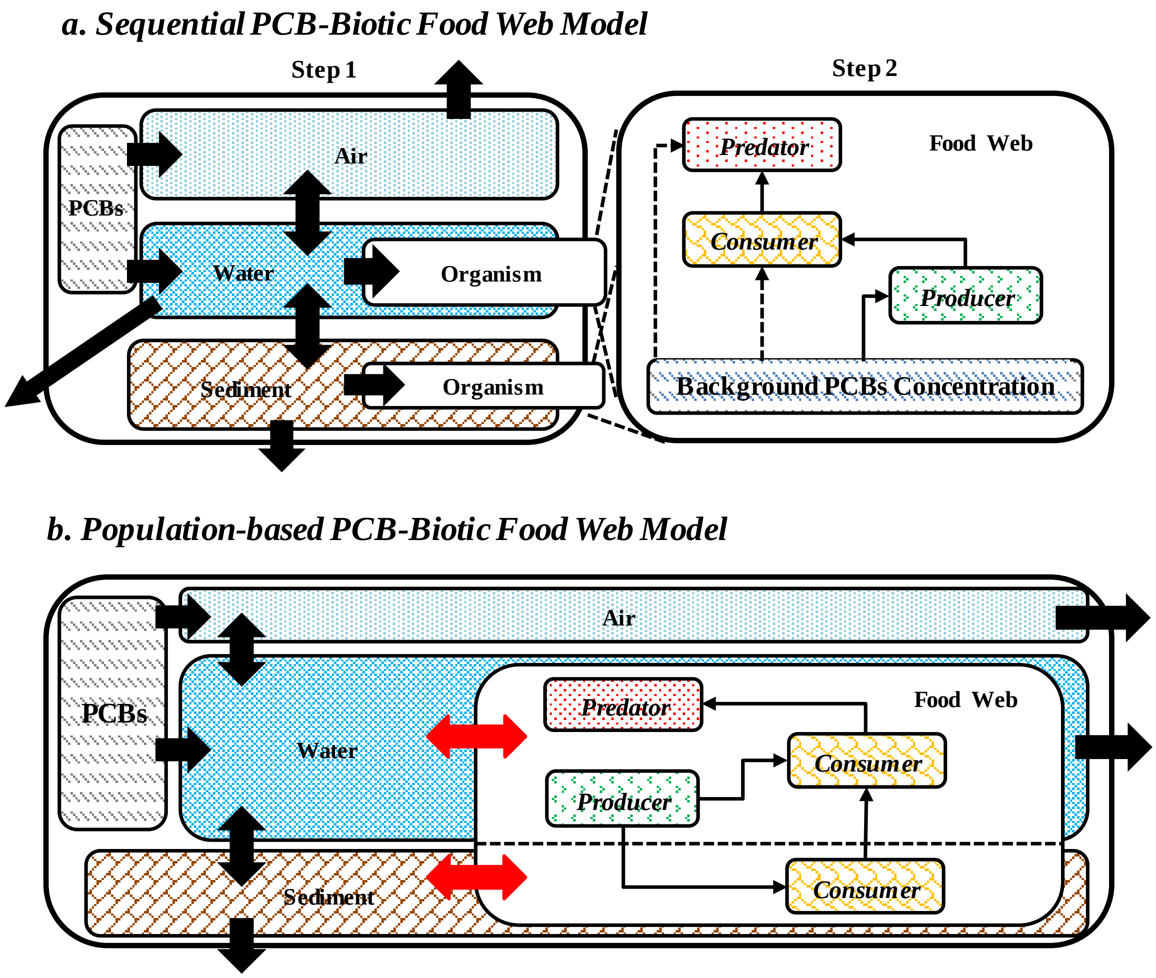

Figure 1.1. The Difference between Traditional Design and Improved Approach

2. Improved Model Design for Pollution Transport Study

2.1. General Model Design

2.1.1. Formula for Population-Based Fugacity Model

The extended approach is a multi-compartment fugacity model; it is proposed to estimate the mass distribution of PCB congeners simultaneously in environmental compartments and organisms. For lake systems, only three environmental compartments are taken into consideration: air, water, and sediment. The study area is simulated by an idealized but representative space (Table 2.1.).

Table 2.1. Lake Ontario Approximate Representative Domain

<table>
<tr><td rowspan="4">Air</td><td>Area (m^2)</td><td>1.90E+10</td><td>Aerosol</td><td>Volume fraction (typical)</td><td>2.00E-11</td></tr>
<tr><td>Height (m)</td><td>6000</td><td rowspan="2">Suspended Sediment</td><td>Density (kg/m^3)</td><td>1500</td></tr>
<tr><td>Density (kg/m^3)</td><td>1.175</td><td>Volume fraction (typical)</td><td>0.001</td></tr>
<tr><td>Resident Time ($years$)</td><td>1</td><td rowspan="6">Sediment</td><td>Area (m^2)</td><td>1.17E+10</td></tr>
<tr><td rowspan="5">Water</td><td>Area (m^2)</td><td>1.90E+10</td><td>Thickness (m)</td><td>0.1</td></tr>
<tr><td>Depth (m)</td><td>86</td><td rowspan="2">Organic Particle Density (kg/m^3)</td><td rowspan="2">1250</td></tr>
<tr><td>Density (kg/m^3)</td><td>1000</td></tr>
<tr><td>Fraction of Organic Carbon in Water</td><td>0</td><td>Inorganic Particle Density (kg/m^3)</td><td>2650</td></tr>
<tr><td>Retention Time ($years$)</td><td>6</td><td>Water Volume Fraction</td><td>0.9</td></tr>
</table>

For mathematical simplicity, internal homogeneity is applied to all compartments. For instance, the air compartment is represented as an equilibrium space with constant density, and aerosols and gaseous air are at equilibrium with aerosols evenly distributed throughout the sub-compartment (MacLeod et al. 2002). We include the air compartment in our model because of its role in atmospheric transport and deposition of PCBs (LimnoTech 2011; Harner and Bidleman 1996). Furthermore, a recent study shows a potential inhalation problem of lower-chlorinated congeners in the atmosphere (Grimm et al. 2015). The water compartment includes both the water phase and uniformly suspended particles. However, assuming vertical homogeneity in the sediment compartment is unrealistic, since the PCB content with sediment depth depends on the PCB contamination level during the deposition period. As a computational tradeoff, the current sediment compartment only includes the very top layer of bio-active sediment (~0.1m) which contains about 10% dry residual mixed with the remaining 90% of the saturated water (in volume fraction). We only use one box to represent each environmental media, because of previous studies that indicate little variation of PCBs concentration regardless of the number of boxes within the water or air media (Kaur et al. 2012). A very recent study by Cai and Reavie (2018) found that water quality data in Lake Ontario is suggestive of two horizontal zones, with the eastern portion exhibiting higher nutrients in summer. Future applications should thus consider whether such spatial differences in water column biomass and associated sedimentation rates could lead to significantly different predictions for PCB fate and transport in a two- vs. a one-zone lake model.

In this study, we do not divide each environmental media into further detailed sub-division compartment. A previous study of PCB transport in Lake Ontario indicates that the sub-divisions of each environmental media shows little differences from a mathematical point of view. In 2012, Kaur et al. published an article evaluating the historical PCBs level in Lake Ontario, and it is the most detailed and up-to-date model of PCB transport in Lake Ontario. In their designs, water and sediment are further divided into multiple boxes and layers based on locations and compositions. However, their simulation indicates little variation of PCBs concentration regardless the number of boxes (Kaur et al. 2012). One possible explanation is that the water flows of Lake Ontario are highly mobilized. The active water flows cause the PCB input can mixed within the media and distribution evenly within relatively shorter period.

According to the fugacity approach, the accumulated PCB mass in compartment i is expressed as:

$$M_i = V_i Z_i f_i \dots\dots\dots\dots\dots\dots\dots\dots\dots\dots\dots\dots\dots\dots\dots\dots\dots (1)$$

Where M_i represents the mass of PCBs accumulated in compartment i; $V_i(m^3)$ is the volume of compartment i; $Z_i(mol/Pa \cdot m^3)$ is the fugacity capacity of compartment i; $f_i(Pa)$ is the PCB fugacity which represents the level of PCB mass in compartment i. Thus, the dynamic change of PCBs in compartment i is estimated as:

$$\frac{dM_i}{dt} = \frac{d(Z_i V_i f_i)}{dt} \dots\dots\dots\dots\dots\dots\dots\dots\dots\dots\dots\dots\dots\dots (2)$$

The formula is transformed through partial difference to become,

$$Z_i V_i \frac{df_i}{dt} = \frac{dM_i}{dt} - V_i f_i \frac{dZ_i}{dt} - Z_i f_i \frac{dV_i}{dt} \dots\dots\dots\dots\dots\dots (3)$$

As shown in formula 3, the change of PCBs fugacity in compartment i can be divided into three categories: the PCBs mass variation (dM_i/dt), the change in fugacity capacity (dZ_i/dt), and the change in compartment volume (dV_i/dt). All compartments related to PCBs transport involve at least one of these three general processes. To determine the fugacity variation in the certain compartment, we need to separately define the process and parameters in each media according to their physical, chemical, and biological features. Furthermore, we need to define the exchanging terms among different compartments. Moreover, we need to apply a method to estimate the existing biomass/population volume in each biotic compartment for population scale.

Figure 2.1 shows a general flowchart to describe the PCB exchange between organisms and the environment in the proposed model. The green arrows represent PCB inputs to species from other compartments, while the red arrows show all elimination routes for PCBs from the organism. The dotted line of food ingestion from the environment is specific for the benthic species which acquire their food from detritus and organic matter in sediment. The colored shadow areas represent the organism volume/size gain (green)/loss (red). The colored dotted frame represents the actual PCBs gain (green)/loss (red) during the volume change. For comparison, the traditional model design is shown in figure 2.2.

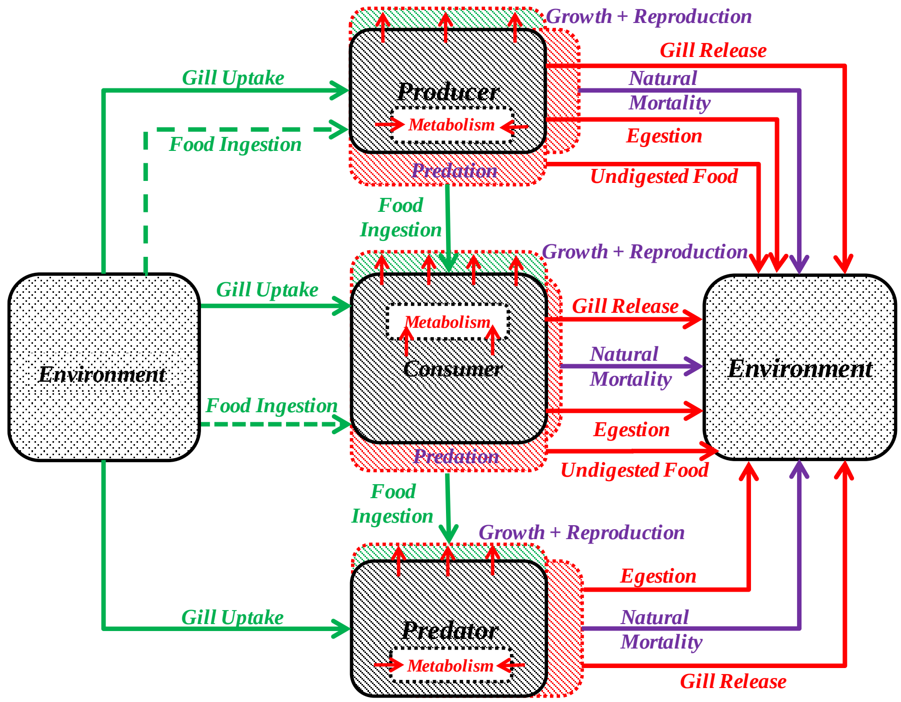

Figure 2.1. PCBs Exchange between Organism and Environment (New Design)

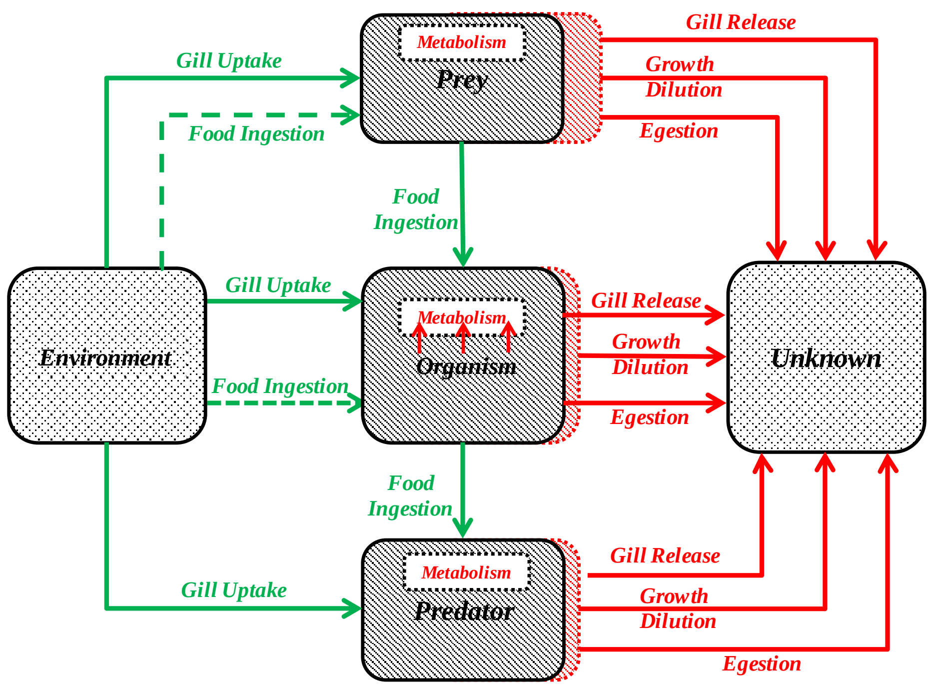

Figure 2.2. PCBs Exchange between Organism and Environment (Traditional Design)

The uptake routes of PCBs from the environment into organisms include gill uptake and food ingestion (for low-level benthic species, scavenging the decomposed individuals might occur), while the elimination routes include gill loss, natural mortality, egestion (undigested food & associated PCBs), and predation. Metabolism can also degrade a small fraction of PCB congeners, with rates that vary substantially among species and congeners. The primary exchanges among the biotic compartments are through the complex food web. However, no food ingestion is considered in primary producers since they acquire energy and food through photosynthesis. A summary of model configuration is listed in table 2.2, 2.3, and 2.4.

Table 2.2 PCBs Main Exchange Processes

Process	Compartment Name	Term	Formula
PCBs Mass Transfer Terms	Air (A)	Advection $(D_{AA}(f_{in1} - f_A))$	$G_A Z_A (f_{in1} - f_A)$
		Reaction $(R_A f_A)$	$-V_A Z_A f_A / t_A$
		Emission (E_A)	E_A
	Air(-)-Water(+) Exchange	Diffusion $(D_V(f_A - f_W))$	$\frac{(f_A - f_W)}{(k_{VA} A_{AW} Z_1)^{-1} + (k_{VW} A_{AW} Z_2)^{-1}}$
		Wet Dissolution $(D_{RWW} f_A)$	$A_{AW} U_Q Z_2 f_A$
		Dry Deposition $(D_{QDW} f_A)$	$A_{AW} U_Q v_Q Z_7 f_A$
		Wet Particle Deposition $(D_{RWW} f_A)$	$A_{AW} U_R Q v_Q Z_7 f_A$
	Water (W)	Advection $(D_{AW}(f_{in2} - f_W))$	$G_W Z_W (f_{in2} - f_W)$
		Reaction $(R_W f_W)$	$-V_W Z_W f_W / t_W$
		Emission (E_W)	E_W
	Water(-)-Biota(+) Exchange	Pelagic Gill Uptake $(D_{GGW} f_W)$	$k_1 V_P \rho_B Z_W f_W$
		Pelagic Gill Release	$-\mu_1 k_1 V_P \rho_B Z_W f_{BP}$

	$(D_{GGW}f_{BP})$	
	Pelagic Egestion $(\boldsymbol{\mu_1 D_{E,BP} f_j})$	$-\frac{\boldsymbol{\mu_1 E_D \rho_i V_{Pi} G_{Di}}}{\boldsymbol{W_{Bi}}}\sum_{\boldsymbol{i\neq j}}^{\boldsymbol{n}}\frac{\boldsymbol{p_{ij} Z_{Bj} f_j}}{\boldsymbol{(TL_i - TL_j)}} * \boldsymbol{TMF}$
	Pelagic Undigested Food $(\boldsymbol{\mu_1 D_{P,BP}})$	$-\frac{\boldsymbol{\mu_1(1-E_D)}}{\boldsymbol{E_D}}\sum_{\boldsymbol{i=pelagic\&i\neq j}}^{\boldsymbol{n}}\boldsymbol{p_{ij} D_{FIj} f_j}$
Sediment(-)-Water (+) Exchange	Diffusion $(D_Y(f_S - f_W))$	$k_{SW}A_{SW}Z_2(f_{SE} - f_W)$
	Deposition $(D_{DS}f_W)$	$-U_{DP}A_{SW}Z_5 f_{SE}$
	Resuspension $(D_{RS}f_S)$	$U_{RS}A_{SW}Z_4 f_W$
Sediment (SE)	Reaction $(R_S f_S)$	$-V_{SE}Z_{SE}f_{SE}/t_{SE}$
	Advection $(D_{AS}(f_{in3} - f_S))$	$G_{SE}Z_{SE}f_{SE}$
	Emission (E_S)	E_{SE}
Sediment(-)-Biota(+) Exchange	**Pelagic Egestion** $(\boldsymbol{(1-\mu_1) D_{E,BP} f_j})$	$-\boldsymbol{(1-\mu_1)}\left(\frac{\boldsymbol{E_D \rho_i V_{Pi} G_{Di}}}{\boldsymbol{W_{Bi}}}\sum_{\boldsymbol{i\neq j}}^{\boldsymbol{n}}\frac{\boldsymbol{p_{ij} Z_{Bj} f_j}}{\boldsymbol{(TL_i - TL_j)}} * \boldsymbol{TMF}\right)$
	Pelagic Undigested Food $(\boldsymbol{(1-\mu_1) D_{P,BP}})$	$-\frac{\boldsymbol{(1-\mu_1)(1-E_D)}}{\boldsymbol{E_D}}\sum_{\boldsymbol{i=pelagic\&i\neq j}}^{\boldsymbol{n}}\boldsymbol{p_{ij} D_{FIj} f_j}$
	Benthic Gill Uptake $(D_{GGS}f_S)$	$k_1 V_P \rho_B Z_{SE} f_{SE}$
	Benthic Gill Release $(D_{GGS}f_{BP})$	$-\mu_1 k_1 V_P \rho_B Z_{SE} f_{BB}$
	Benthic Egestion $(\boldsymbol{D_{E,BB} f_j})$	$-\frac{\boldsymbol{E_D \rho_i V_{Pi} G_{Di}}}{\boldsymbol{W_{Bi}}}\sum_{\boldsymbol{i\neq j}}^{\boldsymbol{n}}\frac{\boldsymbol{p_{ij} Z_{Bj} f_j}}{\boldsymbol{(TL_i - TL_j)}} * \boldsymbol{TMF}$
	Benthic Undigested Food $(\boldsymbol{\mu_1 D_{P,BP} f_j})$	$-\frac{\boldsymbol{(1-E_D)}}{\boldsymbol{E_D}}\sum_{\boldsymbol{i=benthic\&i\neq j}}^{\boldsymbol{n}}\boldsymbol{p_{ij} D_{FIj} f_j}$
Biota (Benthic Species, BB, i for target, j for food)	Food Ingestion $(\sum_{i=benthic\&i\neq j}^{n} p_{ij} D_{FIj} f_j)$	$\left(\sum_{i=benthic\&i\neq j}^{n} p_{ij} k_{iD} V_{iP} Z_j f_j\right)$
	Metabolism $(R_{BB}f_{BB})$	$V_{P,BB}Z_{BB}k_{M,BB}f_{BB}$
Biota (B)	**Natural Mortality Rate** $(\boldsymbol{Z_B V_P\, dV_{Mi}/dt})$	$\boldsymbol{Z_B V_P}\frac{\boldsymbol{4.899 t_{max}^{-0.916} V_P}}{\boldsymbol{365000}}$
	Predation (Excluded Natural Mortality)	$\sum_{\boldsymbol{i\neq k}}^{\boldsymbol{n}}\frac{\boldsymbol{\rho_k V_{Pk} p_{ik} G_{Dk} Z_i f_i}}{\boldsymbol{W_{Bk}}}$
Biota (Pelagic Species,	Food Ingestion $(\sum_{i=pelagic\&i\neq j}^{n} p_{ij} D_{FIj} f_j)$	$\left(\sum_{i=pelagic\&i\neq j}^{n} p_{ij} k_{iD} V_{iP} Z_j f_j\right)$

	BP, i for target, j for food)	Metabolism $(R_{BP}f_{BP})$	$V_{P,BP}Z_{BP}k_{M,BP}f_{BP}$
Fugacity Capacity Change	Air	**Fugacity Change** $\boldsymbol{V_Af_A(dZ_A/dt)}$	$\boldsymbol{-V_Af_A\left[\frac{(\tau_1 0.1K_{OA}+1)}{RT_A^2}+\frac{\tau_1 0.1ln(10)10^{\frac{a}{T_A}+b}}{RT_A^3}\right]\frac{dT_A}{dt}}$
	Water	**Fugacity Change** $\boldsymbol{V_Wf_W(dZ_W/dt)}$	$\boldsymbol{-V_Wf_W\left(1+0.41*\frac{\tau_2\rho_5\delta_5K_{OW}}{1000}\right)\frac{\Delta U_{AW}}{HRT_W^2}\frac{dT_W}{dt}}$
	Sediment	**Fugacity Change** $\boldsymbol{V_{SE}f_{SE}(dZ_{SE}/dt)}$	$\boldsymbol{V_{SE}f_{SE}\left(1-\tau_3+\frac{0.41\tau_3\rho_4\delta_4K_{OW}}{1000}\right)\frac{\Delta U_{AW}}{HRT_S^2}\frac{dT_S}{dt}}$
	Biota (Pelagic Species, BP)	**Fugacity Change** $\boldsymbol{V_Pf_{BP}(dZ_{BP}/dt)}$	$\boldsymbol{V_{BP}f_{BP}\left(Z_WK_{OW}\frac{dL}{dt}-LK_{OW}\frac{\Delta U_{AW}}{HRT_W^2}\frac{dT_W}{dt}\right)}$
	Biota (Benthic Species, BB)	**Fugacity Change** $\boldsymbol{V_Pf_{BB}(dZ_{BB}/dt)}$	$\boldsymbol{V_{BB}f_{BB}\left(Z_WK_{OW}\frac{dL}{dt}-LK_{OW}\frac{\Delta U_{AW}}{HRT_S^2}\frac{dT_S}{dt}\right)}$
Volume Change	Biota (B)	**Biomass Volume Variation**	$\boldsymbol{G_i=P_i+MO_i}$
	Air, Water, Sediment	Assuming Constant Volume	$G_{in}-G_{out}$

Table 2.3 Parameter Estimation Formula

Term	Figure	Description	Unit	Formula	Reference
Fugacity Capacity	Z_1	Gas Phase in Air	$\mathrm{mol/Pa\cdot m^3}$	$1/RT_A$	(Mackay, 2001)
	Z_2	Water Phase in Water	$\mathrm{mol/Pa\cdot m^3}$	$1/H$	
	Z_4	Dry Sediment in Sediment	$\mathrm{mol/Pa\cdot m^3}$	$0.41Z_2\rho_4\delta K_{OW}/1000$	
	Z_5	Suspended Sediment	$\mathrm{mol/Pa\cdot m^3}$	$0.41Z_2\rho_5\delta K_{OW}/1000$	
	Z_7	Aerosols in Air	$\mathrm{mol/Pa\cdot m^3}$	$0.1Z_1K_{OA}$	
	Z_A	Air Compartment	$\mathrm{mol/Pa\cdot m^3}$	$Z_1+\tau_1Z_7$	
	Z_W	Water Compartment	$\mathrm{mol/Pa\cdot m^3}$	$Z_2+\tau_2Z_5$	
	Z_{SE}	Sediment Compartment	$\mathrm{mol/Pa\cdot m^3}$	$(1-\tau_3)Z_2+\tau_3Z_4$	
	$Z_{B,i}$	Biota Compartment	$\mathrm{mol/Pa\cdot m^3}$	LZ_2K_{OW}	
Advection Flow Rate	G_A	Air Flow	$\mathrm{m^3/day}$	$V_A/t_{A,refill}$	(Mackay, 2001)
	G_W	Water Flow	$\mathrm{m^3/day}$	$V_W/t_{W,refill}$	

	G_{SE}	Sediment Burial	$\mathrm{m^3/day}$	$A_{SE}U_{BSE}$	
Henry's Law Constant	H	Henry's Law Constant	$\mathrm{Pa \cdot m^3/mol}$	$H^{ref} exp\left[-\frac{\Delta U_{AW}}{R}\left(\frac{1}{T_W}-\frac{1}{T^{ref}}\right)\right.$	(Schwarzenbach, 2003)
Octanol/Air Partition Coefficient	K_{OA}	Octanol/Air Partition Coefficient	(Unitless)	$10^{\frac{a}{T_A}+b}$	(Harner and Bidleman 1996)
Food Ingestion	k_D	Diet Uptake Rate	kg/kg/day	$E_D G_D / W_B$	(Arnot & Gobas, 2004)
	E_D	Chemical Dietary Efficiency	(Unitless)	$1/(2 + 3 \times 10^{-7} K_{OW})$	
	G_D	Food ingestion rate	kg/day	$0.022 W_B^{0.85} e^{0.06(T-273)}$	(Gobas, et al., 1988)
Gill Uptake	k_1	Phytoplankton, Algae	L/kg/day	$(6.0 \times 10^{-5} + 5.5/K_{OW})^{-1}$	(Arnot & Gobas, 2004)
		Fish & General Species		$E_W G_V / W_B$	
	E_W	Gill Chemical Transfer Efficiency	(Unitless)	$1/(1.85 + 155/K_{OW})$	
	G_V	Gill Ventilation Rate	L/day	$1400 W_B^{0.65} / C_{OX}$	
	C_{OX}	Oxygen Concentration	mg/L	$[-0.24 * (1.85 + 155 / K_{OW}) S]$	
Gill Loss	k_2	Gill loss rate	L/kg/day	k_1 / BCF	(Gewurtz, et al., 2006)
	BCF	Bioconcentration factor	(Unitless)	$L K_{OW}$	
Bottom Sediment Density	ρ_D	Sediment Dry Bulk Density	$\mathrm{kg/m^3}$	$(1 - \tau_3) * \rho_P$	(Klute 1986)
	δ	Organic Carbon Mass Fraction in Sediment	(Unitless)	$0.001 e^{\frac{1.776 - \rho_D/1000}{0.363}}$	(Avnimelech, et al., 2001)
	ρ_4	Bottom Sediment Density	$\mathrm{kg/m^3}$	$(1 - \delta) * \rho_P + \delta \rho_{OC}$	
Organism Trophic Level	TL	Organism Trophic Level Estimation	(Unitless)	$TL_i = 1 + \sum TL_j \cdot p_{ij}$	(Pauly & Palomares, 2005)
Organism Group Size Estimation	G_i	Biomass Growth Rate	kg/day	$0.00586(1.113)^{T-20}(1000 W_{Bi})^{-0.2}$	(Gewurtz, et al., 2006)
	P_i	Biomass Predation Rate	kg/day	$\sum_{i \neq k}^{n} \frac{\rho_k V_{Pk} p_{ik} G_{Dk}}{W_{Bk}}$	(Arnot & Gobas, 2004)
	M_i	Biomass Natural Mortality	kg/day	$\frac{4.899 t_{max,i}^{-0.916} V_{P,i}}{365000}$	(Then, et al., 2005)

Table 2.4 General Parameter Information

Term	Figure	Unit	Mean Value	Range	Reference
Air Temp.	T_A	K	285.5	273-303	(NDBC)
Surface Water Temp.	T_W	K	285.5	273-298	(NDBC)
Bottom Water (Sediment) Temp.	T_{SE}	K	279	277-281	(GLSEA)
Ideal Gas Constant	R	$J \cdot mol/K$	8.314	N/A	(NIST)
Air Density	ρ_A	kg/m^3	1.175	N/A	
Water Density	ρ_W	kg/m^3	1000	N/A	(Mackay, 2001)
Suspended Sediment Density	ρ_5	kg/m^3	1500	N/A	
Inorganic Sediment Particle Density	ρ_P	kg/m^3	2650	N/A	(Blake & Hartge, 1986a)
Organic Particle Density	ρ_{OC}	kg/m^3	1250	N/A	(Boyd, 1995)
Average Organism Density	ρ_B	kg/m^3	1000	N/A	(Estimated)
Aerosol Volume Fraction	τ_1	(Unitless)	2.0E-11	±50%	(Mackay, 2001)
Sediment Volume Fraction	τ_2	(Unitless)	0.001	N/A	
Water Content	τ_3	(Unitless)	0.9	0.85-0.95	(Estimated)
Air Retention Time	$t_{A,refill}$	years	1	±50%	(Estimated)
Water Retention Time	$t_{W,refill}$	years	6	±50%	(EPA)
Dissolved Oxygen Saturation	S	(Unitless)	0.85	N/A	(Arnot & Gobas, 2004)
Air Side MTC over Water	k_{VA}	m/day	72	±50%	
Water Side MTC to Air	k_{VW}	m/day	0.72	±50%	
Rain Rate	U_R	m/day	2.33E-03	±50%	
Scavenging ratio	S_Q	(Unitless)	200000	N/A	
Dry Deposition Velocity (Air)	U_Q	m/day	259.2	N/A	(Mackay, 2001)
Water Side MTC over Sediment	k_{SW}	m/day	0.24	±50%	
Sediment Deposition Rate	U_{DP}	m/day	1.10E-06	±50%	
Sediment Resuspension Rate	U_{RS}	m/day	2.64E-07	±50%	
Sediment Burial Rate	U_{BSE}	m/day	2.19E-06	±50%	
Photosynthesis efficiency	φ_P	(Unitless)	0.002	N/A	(Estimated)
Vegetation coverage	φ_V	(Unitless)	0.0075	±50%	
Biota Average Weight	W_B	kg	Table 4	±50%	(Campfens & Mackay, 1997)
Biota Population	V_P	m^3	Table 5	±50%	(Table S.2)
Organism Longest Lifespan	t_{max}	year	Table 4	±50%	(Estimated)

Air Height	H_A	m	6000	N/A	(Mackay, 2001)
Water Depth	H_W	m	86	N/A	(EPA)
Sediment Thickness	H_{SE}	m	0.2	N/A	(Estimated)
Air Surface Area	A_A	m^2	1.90E+10	N/A	(EPA)
Water Surface Area	A_W	m^2	1.90E+10	N/A	(EPA)
Sediment Surface Area	A_{SE}	m^2	1.17E+10	N/A	(EPA)
Organic Matter Deposition Rate	μ_1	(Unitless)	0.5	$\pm 50\%$	(Estimated)
Trophic Magnification Factor	TMF	(Unitless)	Table S.5	N/A	

2.1.2. Model Assumptions

a. All compartments are homogeneity and PCBs are evenly distributed inside each compartment. No spreading delay is considered;

b. The biota population size is varied by growth rate, mortality rate, and predation rate;

c. The fugacity capacity varies based on the compartmental temperature. The organism fugacity capacity is also affected by the lipid content. However, we lack proper lipid content variation data. As a compromise, current model assumes constant lipid content for each species.

2.2. Simultaneous Structure

2.2.1. The Fugacity Capacity

2.2.1.1. Air

The main components related to PCBs transport in the air are air parcel and aerosol. The fugacity capacity in each component could be expressed as (Mackay, 2001):

$$Z_1 = \frac{1}{RT_A}\ (Air) \ldots\ldots\ldots\ldots\ldots\ldots\ldots\ldots (4)$$

$$Z_7 = 0.1 Z_1 K_{OA}\ (Aerosol) \ldots\ldots\ldots\ldots\ldots\ldots\ldots\ldots (5)$$

Where R is the ideal gas constant ($8.314 J/mol \cdot K$); K_{OA} is the octanol-air partition coefficient; T_A is the air temperature (*K*). Thus, the fugacity capacity in air compartment should be:

$$Z_A = Z_1 + \tau_1 Z_7 \ldots\ldots\ldots\ldots\ldots\ldots\ldots\ldots (6)$$

Where τ_1 is the volume fraction of aerosol.

2.2.1.2. Water

The water compartment contains water column and suspended sediment. In some model designs, water compartment also includes aquatic species. However, since organisms are isolated and calculated separately, we isolate most of the organisms from the water compartment. The fugacity capacity could be expressed as:

$$Z_2 = \frac{1}{H}\ (Water) \ldots\ldots\ldots\ldots\ldots\ldots\ldots\ldots (7)$$

$$Z_5 = \frac{Z_2 \rho_5 \delta_5 K_{OC}}{1000} (Suspended\ Sediment) \ldots\ldots\ldots\ldots\ldots\ldots\ldots\ldots (8)$$

Where H is the Henry's Law constant ($Pa \cdot m^3/mol$); ρ_5 is the suspended sediment density (kg/m^3); δ_5 is the mass fraction of the organic carbon; K_{OC} is the organic carbon partition coefficient (L/kg), which is calculated (Karickhoff, 1981):

$$K_{OC} = 0.41K_{OW} \dots\dots\dots\dots\dots\dots\dots\dots (8)$$

Thus, the capacity of water compartment should be:

$$Z_W = Z_2 + \tau_2 Z_5 \dots\dots\dots\dots\dots\dots\dots\dots (9)$$

Where τ_2 is the volume fraction of suspended sediment.

According to assumption (a), we have:

$$f_{water} = f_{suspended\ sediment} \dots\dots\dots\dots\dots\dots\dots\dots (10)$$

In 2011, LimnoTech published a study report regarding the PCB loading patterns in Lake Ontario (LimnoTech, 2011). According to the study, the PCB input of Lake Ontario in 2005 came from air transmission (20%) and water flows (80%). Moreover, a detailed analysis on aquatic PCBs input indicates a 70%/30% allocation between dissolved PCBs (water column) and particle PCBs (suspended sediment). Thus,

$$\frac{m_{water}^{PCBs}}{m_{susp.\ sedi.}^{PCBs}} = \frac{0.56}{0.24} = \frac{V_{water} Z_{water} f_{water}}{V_{susp.\ sedi.} Z_{susp.\ sedi.} f_{susp.\ sedi.}} \dots\dots\dots\dots\dots\dots\dots\dots (10)$$

$$\frac{V_{water} Z_2 f_{water}}{\tau_2 V_{water} Z_5 f_{susp.\ sedi.}} = \frac{1000 V_{water} Z_2}{\tau_2 V_{water} Z_2 \rho_5 \delta_5 K_{OC}} = \frac{0.56}{0.24}$$

$$\frac{1000}{\tau_2 \rho_5 \delta_5 K_{OC}} = \frac{0.56}{0.24}$$

Thus

$$\tau_2 = \frac{3000}{7\rho_5\delta_5 K_{OC}} \dots\dots\dots\dots\dots\dots\dots\dots (11)$$

2.2.1.3. Sediment

The vertical homogeneity conversion of the sediment compartment is difficult since the PCBs content with sediment depth depends on the PCB contamination level during the deposition period. The current sediment compartment only includes the very top layer of bio-active sediment (~0.1m). The sediment is considered as flooded sediment, where little air existed in the compartment. As a result, the sediment compartment is a mixture of water and sediment solid with organic particle attached to the organic matters. The dry sediment bulk has a fugacity capacity as:

$$Z_4 = \frac{Z_2\rho_4\delta_4 K_{OC}}{1000} (dry\ sediment) \dots\dots\dots\dots\dots\dots\dots\dots (12)$$

Thus the fugacity capacity of the sediment compartment is:

$$Z_S = (1-\tau_3)Z_2 + \tau_3 Z_4 \dots\dots\dots\dots\dots\dots\dots\dots (13)$$

Where τ_3 is the volume fraction of solid sediment.

For rough estimation, the fraction of organic carbon in flooded sediment could be calculated through water content and dry bulk density (Avnimelech et al. 2001):

$$Dry\ Bulk\ Density(g/cm^3) = 1.776 - 0.363 lnOC \dots\dots\dots\dots\dots\dots\dots\dots (14)$$

Where OC is the organic carbon concentration ($mg/dw\ g$). The inorganic sediment particle density is conventionally taken 2.65 g/cm^3; the density of organic matters can be corrected assuming a density of 1.25 g/cm^3. Thus, the sediment solid density can be expressed as:

$$Soild\ Density(g/cm^3) = 1.25 * (\%\ OM) + 2.65 * (1 - \%\ OM)$$

$$OM = 1.7OC \dots\dots\dots\dots\dots\dots\dots\dots (15)$$

Thus, the water content is:

$$\tau_3 = \left(1 - \frac{Dry\ Bulk\ Density}{Soild\ Density}\right) \times 100\% \dots\dots\dots\dots\dots\dots\dots\dots (16)$$

Finally, the fraction of OC is:

$$\frac{1.776 - 0.363 ln(1000 * OM/1.7)}{2.65 - 1.4\%\ OM} = 1 - \tau_3 \dots\dots\dots\dots\dots\dots\dots\dots (17)$$

This equation means we can use water content to estimate the fraction of organic carbon in the sediment.

2.2.1.4. Organism

According to Mackay, the fugacity capacity of biota is defined as (Mackay 2001):

$$Z_B = LZ_L = LZ_O = LZ_W K_{OW} \dots\dots\dots\dots\dots\dots\dots\dots (18)$$

Where L is the lipid fraction in the organism.

2.2.2. PCBs Mass Variation

The PCB mass variation, or dM_i/dt, is defined as the absolute PCB masses enter or exit the system through the general transport processes. The basic form for the changes of fugacity in compartment i can be expressed as,

$$\frac{dM_i}{dt} = E_i + \sum_{j=1}^{n}(D_{ji}f_j) - D_{T_i}f_i \dots\dots\dots\dots\dots\dots\dots\dots\dots\dots (19)$$

In this formula, i represents the different media; j represents other media that interact with media i; $M_i(mol)$ represents the current PCB mass in medium i ; $V_i(m^3)$ represents the volume of medium i; $Z_i(mol/Pa \cdot m^3)$ represents the fugacity capacity of medium i; t represents the PCB transport and allocation time; $E_\mathrm{i}(\mathrm{mol/day})$ represents the direct pollution exchange rate to medium i; $f_j(Pa)$ represents the PCB fugacity in medium j; $f_i(Pa)$ represents the fugacity of medium i; $D_{ji}(mol/Pa \cdot day)$ represents the PCB transport processes from medium j to medium i $(i \neq j)$; $D_{T_i}(mol/Pa \cdot day)$ represents the total PCB elimination/exit from medium i. To obtain the detailed expression for each compartment, further detailes about the compartment features should be provided accordingly.

2.2.2.1. Air

Pollutant transport processes related to air compartment include three routes: the inter-media exchange, the self-elimination, the systematic exchange (Mackay et al. 1983). During the inter-media transport, the entrée is mainly through water volatilization (air-water diffusion, D_V), while the exit pathways include absorption (water-air diffusion, D_V), wet dissolution (D_{RWW}), dry deposition (D_{QDW}), wet particle deposition (D_{QWW}). Since no biota is considered in the air, no direct exchange exists between the air compartment and any organisms. The self-elimination, or reaction (R_A) within the compartment eliminate contaminate through photodegradation and is related to the compartmental-based lifetime. Finally, the systematic exchange is mainly through the advection (D_{AI}/D_{AO}). As a result, the fugacity variation in the air compartment could be written as:

$$\frac{dM_A}{dt} = (f_{in1}D_{AI} - f_A D_{AO}) + D_V(f_W - f_A) - (D_{RWW} + D_{QDW} + D_{QWW} + R_A)f_A \dots\dots\dots (20)$$

Where

$$\text{Diffusion: } D_V = \left(\frac{1}{k_{VA}A_{AW}Z_1} + \frac{1}{k_{VW}A_{AW}Z_2}\right)^{-1} \dots\dots\dots\dots\dots\dots (21)$$

$$\text{Wet Dissolution: } D_{RWW} = A_{AW}U_Q Z_2 \dots\dots\dots\dots\dots\dots\dots\dots.\dots\dots (22)$$

$$\text{Dry Deposition: } D_{QDW} = A_{AW}U_Q v_Q Z_7 \dots\dots\dots\dots\dots\dots\dots..\dots\dots (23)$$

$$\text{Wet Particle Deposition: } D_{QWW} = A_{AW}U_R Q v_Q Z_7 \dots\dots\dots\dots.. (24)$$

$$\text{Reaction: } R_A = \frac{V_A Z_A}{t_A} \dots\dots\dots\dots\dots\dots\dots\dots\dots\dots\dots\dots.\dots\dots\dots\dots\dots (25)$$

$$\text{Advection Input: } D_{AI} = G_{in} Z_A \dots\dots\dots\dots\dots\dots\dots\dots\dots\dots\dots\dots..(26)$$

$$\text{Advections Output: } D_{AO} = G_{out} Z_A \dots\dots\dots\dots\dots\dots\dots\dots\dots\dots.\dots(27)$$

The parameters used in formula (21) through (27) are listed in table 2.4. Thus,

$$Z_A V_A \frac{df_A}{dt} = (f_{in1} G_{in} - f_A G_{out}) Z_A + \left(\frac{1}{k_{VA} A_{AW} Z_1} + \frac{1}{k_{VW} A_{AW} Z_2}\right)^{-1} (f_W - f_A) -$$

$$(A_{AW} U_Q Z_2 + A_{AW} U_Q v_Q Z_7 + A_{AW} U_R Q v_Q Z_7 + \frac{V_A Z_A}{t_A}) f_A \dots\dots\dots\dots\dots\dots\dots\dots\dots(28)$$

2.2.2.2. Biota

Biotic compartments are discussed previously for better understanding their interactions with the environment phases. In this study, the definition of the inter-exchange process among different biota groups occurs only within the food web, while the processes with the environmental groups are identified as a systematic exchange. In the inter-exchange process, PCBs are absorbed by organisms through food ingestion (D_{FI}), and are released through predation (D_{Pred}).

When studying the PCB transport between environment and organism in water compartment, organisms are divided into pelagic and benthic species, because habitat location will lead to different calculation method PCB exchange rate. Gill uptake is one of the primary routes to transfer PCBs into organisms (D_{GGW}/D_{GGS}). The pathways to transport PCBs to the environment includes gill release (D_{GLW}/D_{GLS}), natural mortality (D_{MD}), and egestion (D_E). Egestion is combined by the undigested food ($1 - E_D$) and PCB exchange between gut and the fences (D_{EX}).

Undigested food is usually estimated as a proportion of the total food ingestion, while the gut/fences exchange rate is estimated through trophic magnification factor (TMF) and trophic levels. The PCB self-elimination in biota group is mainly through metabolism (R_B).

Considering the existence of the decomposing process, we assume that the PCB inside dead organisms caused by natural mortality will be initially decomposed and released to the environment before regaining through the food web. For the pelagic species, PCBs from decomposed organisms return to both water and sediment; for benthic groups, all released PCBs go to the sediment compartment. Thus, the changes of fugacity in biota could be expressed as:

Pelagic species

$$\frac{dM_P}{dt} = D_{GG}f_W + \sum\nolimits_{i=pelagic\&i\neq j}^{n} p_{ij}D_{FIj}f_j - D_{GLW}f_i - (R_{Bi} + D_{MDi} + D_{Predi})f_i - \sum D_{EXi}f_j \ldots (29)$$

Benthic species

$$\frac{dM_B}{dt} = D_{GG}f_S + \sum\nolimits_{i=benthic\&i\neq j}^{n} p_{ij}D_{FIj}f_j - D_{GLS}f_i - (R_{Bi} + D_{MDi} + D_{Predi})f_i - \sum D_{EXi}f_j \ldots\ldots (30)$$

Where

$$Gill\ Uptake: D_{GG} = k_1 V_P \rho_B Z_W \ \ldots\ldots\ldots\ldots\ldots\ldots\ldots\ldots\ldots\ldots.\ldots (31)$$

$$Food\ Ingestion: D_{FIi} = E_D \frac{\rho_i V_{Pi} G_{Di} Z_{Bj}}{W_{Bi}} \ldots\ldots\ldots\ldots\ldots\ldots\ldots.\ldots (32)$$

$$Gill\ Release: D_{GL} = D_{GG} \ldots\ldots\ldots\ldots\ldots\ldots\ldots\ldots\ldots\ldots\ldots\ldots\ldots\ldots. \ldots (33)$$

$$Metabiolism: R_{Bi} = V_P Z_i k_M \ldots\ldots\ldots\ldots\ldots\ldots\ldots\ldots\ldots\ldots\ldots\ldots. \ldots (34)$$

The parameters used in formula (31) through (34) are listed in Table 2.4.

2.2.2.2.1. PCB Exchange Between Gut and Fences

The PCB exchange rate between the gut and the fences can be calculated through TMF and trophic levels. TMF, or trophic magnification factor, could be used to evaluate the proportion of PCB escape from the system through fences. The species trophic level can be calculated by the following formula (Pauly and Palomares 2005):

$$TL_i = 1 + \sum TL_j \cdot p_{ij} \ldots\ldots\ldots\ldots\ldots\ldots\ldots\ldots\ldots\ldots\ldots\ldots\ldots\ldots\ldots\ldots\ldots\ldots\ldots\ldots\ldots\ldots (35)$$

Where TL_j represents the fractional trophic level of prey j, and p_{ij} represents the fraction of j in the diet of i. The PCB released through the fence is then decided by the true TMF differences between food and diet:

$$D_{EX} = \frac{E_D \rho_i V_{Pi} G_{Di}}{W_{Bi}} \sum_{i \neq j}^{n} \frac{p_{ij} Z_{Bj} f_j}{\left(TL_i - TL_j\right)} * TMF \ldots\ldots\ldots\ldots\ldots\ldots\ldots\ldots\ldots\ldots\ldots\ldots (36)$$

2.2.2.2.2. Predation

$$D_{Predi} = \sum_{i \neq k}^{n} \frac{\rho_k V_{Pk} p_{ik} G_{Dk}}{W_{Bk}} = \sum_{i \neq k}^{n} \frac{0.022 e^{0.06T} \rho_k V_{Pk} p_{ik}}{W_{Bk}^{0.15}} * Z_{Bi} \ldots\ldots (37)$$

2.2.2.2.3. Natural Mortality (Mortality without Predation)

The natural mortality rate is estimated by Then et al. in 2015, who used over 200 fish species to evaluate the current existing empirical models for natural mortality rate estimation (Then et al. 2015). We selected one of the best models as our fundamental to estimate the natural mortality loss.

$$D_{MDi} = \frac{4.899 t_{max}^{-0.916} V_{Pi}}{365000} * Z_{Bi} \dots\dots\dots\dots\dots\dots\dots\dots\dots\dots\dots\dots\dots \text{(38)}$$

Where, t_{max} is the maximum surviving time for species i (years);

2.2.2.2.4. Growth Dilution

According to the new diversity in formula 1, the growth dilution does not belong to the first category since there is no actual entrée or exit of any PCB during the process. It is merely a volume change. As a result, it should be moved to the third part.

In sum, the extended expressions for formula (29) and (30) are:

Pelagic species

$$\frac{dM_{BP}}{dt} = k_{1i} V_{Pi} \rho_B Z_W f_W + \frac{E_D \rho_i V_{Pi} G_{Di}}{W_{Bi}} \sum_{i \neq j}^{n} \frac{TL_i - TL_j - 1}{TL_i - TL_j} * TMF * p_{ij} Z_{Bj} f_j - f_i \left(k_{1i} V_{Pi} \rho_B Z_W + V_{Pi} Z_i k_{Mi} + \frac{4.899 t_{max}^{-0.916} V_{Pi}}{365000} * Z_{Bi} + \sum_{i \neq k}^{n} \frac{0.022 e^{0.06T} \rho_k V_{Pk} p_{ik}}{W_{Bk}^{0.15}} * Z_{Bi} \right) \dots\dots\dots\dots\dots\dots\dots\dots \text{(39)}$$

Benthic species

$$\frac{dM_{BB}}{dt} = k_{1i}V_{Pi}\rho_B Z_W f_S + \frac{E_D \rho_i V_{Pi} G_{Di}}{W_{Bi}} \sum_{i \neq j}^{n} \frac{TL_i - TL_j - 1}{TL_i - TL_j} * TMF * p_{ij} Z_{Bj} f_j - f_i \left(k_{1i} V_{Pi} \rho_B Z_W + V_{Pi} Z_i k_{Mi} + \frac{4.899 t_{max}^{-0.916} V_{Pi}}{365000} * Z_{Bi} + \sum_{i \neq k}^{n} \frac{0.022 e^{0.06T} \rho_k V_{Pk} p_{ik}}{W_{Bk}^{0.15}} * Z_{Bi} \right) \ldots \ldots \ldots \ldots \ldots \ldots \ldots \ldots \ldots (40)$$

2.2.2.3. Water

The pollution transport through water is more complex than the air section because of the existence of organisms. To achieve the fidelity as the reality as possible, we recreated the PCB exchange processes between the environment and organisms. Similarly, the pollutant exchange in the water section is divided into three parts. The entrée processes in intermedia exchange include

Air-Water: absorption (water-air diffusion, D_V), wet dissolution (D_{RWW}), dry deposition (D_{QDW}), wet particle deposition (D_{QWW});

Water-Sediment: diffusion (D_Y), resuspension (D_{RS});

Water-Biota: gill release (D_{GLW}), death loss (mortality, D_{ML}), egestion (Q_E);

The exit processes in intermedia exchange:

Air-Water: volatilization (air-water diffusion, D_V);

Water-Sediment: diffusion (D_Y), deposition (D_{DS});

Water-Biota: gill uptake (D_{GGW});

The self-elimination, or reaction (R_W) within the compartment generally eliminate contaminate under a first-order decay rate, which is relative to its compartment-based lifetime. Finally, the systematic exchange is mainly through the advections in/out (D_{WI}/D_{WO}) of the system. As a result, the fugacity variation in the water compartment could be written as:

$$\frac{dM_W}{dt} = (f_{in2}D_{WI} - f_W D_{WO}) + D_V(f_A - f_W) + \left(D_{RWW} + D_{QDW} + D_{QWW}\right)f_A + \sum_{i=pelagic}^{n} [D_{GLi}f_i - D_{GGi}f_W] - R_W f_W + D_Y(f_S - f_W) + D_{RS}f_S - D_{DS}f_W \dots\dots(41)$$

$$Advection\ in/out:\ D_{WI} = D_{WO} = G_W Z_W \dots\dots(42)$$

$$Water - sediment\ Diffusion: D_Y = \frac{K_{SW}}{Y_4} A_{SW} Z_2 \dots\dots(43)$$

$$Water - Sediment\ Deposition: D_{DS} = U_{DP} A_{SW} Z_5 \dots\dots(44)$$

$$Water - Sediment\ Resuspension: D_{RS} = U_{RS} A_{SW} Z_4 \dots\dots(45)$$

$$Reaction:\ R_W = \frac{V_W Z_W}{t_W} \dots\dots(46)$$

In sum the extended expression for water compartment could be written as:

$$\frac{dM_W}{dt} = G_W Z_W (f_{in2} - f_W) + \left(\frac{1}{k_{VA} A_{AW} Z_1} + \frac{1}{k_{VW} A_{AW} Z_2}\right)^{-1} (f_A - f_W)$$
$$+ \left(A_{AW} U_Q Z_2 + A_{AW} U_Q v_Q Z_7 + A_{AW} U_R Q v_Q Z_7\right) f_A + \frac{B_{MS}}{Y_4} A_{SW} Z_2 (f_S - f_W)$$
$$+ U_{RS} A_{SW} Z_4 f_S - U_{DP} A_{SW} Z_5 f_W - \frac{V_W Z_W f_W}{t_W}$$
$$+ \sum_{i=pelagic}^{n} [(f_i - f_W) k_{1i} V_{Pi} \rho_B Z_W] \dots\dots\dots\dots\dots (47)$$

2.2.2.4. Sediment

Similarly, the sediment compartment includes biotic activities. Thus it also contains similar processes. The entrée processes in intermedia exchange include

Water-Sediment: diffusion (D_Y), resuspension (D_{RS});

Sediment-Biota: gill release (D_{GL}), egestion (Q_E);

Water-Biota: part of the egestion (Q_E);

The exit processes in intermedia exchange:

Water-Sediment: diffusion (D_Y), deposition (D_{DS});

Sediment-Biota: gill uptake (D_{GG});

The self-elimination, or reaction (R_W) within the compartment eliminates PCB through biodegradation (aerobic remediation only), which is relative to its compartment-based lifetime. The sediment compartment does not have a direct PCB input route, but sediment compartment can push PCBs out of the system by deposition. As a result, the fugacity variation in the sediment compartment could be written as:

$$\frac{dM_S}{dt} = \sum_{i=1}^{n} \frac{E_D \rho_i V_{Pi} G_{Di}}{W_{Bi}} \sum_{i \neq j}^{n} \frac{TMF * p_{ij} Z_{Bj} f_j}{TL_i - TL_j} + \sum_{i=1}^{n} (1 - E_D) * \frac{\rho_i V_{Pi} G_{Di}}{W_{Bi}} \sum_{i \neq j}^{n} p_{ij} Z_{Bj} f_j + \sum_{i=1}^{n} D_{MDi} f_i + \sum_{i=benthic}^{n} [D_{GLi} f_i - D_{GGi} f_S] + D_{DS} f_W - R_S f_S - D_Y (f_S - f_W) - D_{RS} f_S \dots \dots \dots (48)$$

$$Deposition: D_{SO} = G_S Z_S \dots \dots \dots (49)$$

$$Reaction: \ R_S = V_S Z_S / t_S \dots \dots \dots (50)$$

In sum the extended expression for sediment compartment could be written as:

$$\frac{dM_S}{dt} = \sum_{i=j}^{n} \frac{E_D \rho_i V_{Pi} G_{Di}}{W_{Bi}} \sum_{i \neq j}^{n} \frac{TMF * p_{ij} Z_{Bj} f_j}{TL_i - TL_j} + \sum_{i=j}^{n} (1 - E_D) * \frac{\rho_i V_{Pi} G_{Di}}{W_{Bi}} \sum_{i \neq j}^{n} p_{ij} Z_{Bj} f_j + \sum_{i=benthic}^{n} [(f_i - f_S) k_{1i} V_{Pi} \rho_B Z_W] + U_{DP} A_{SW} Z_5 f_W - \frac{V_S Z_S f_S}{t_S} - \frac{B_{MS}}{Y_4} A_{SW} Z_2 (f_S - f_W) - U_{RS} A_{SW} Z_4 f_S + \sum_{i=1}^{n} \frac{4.899 t_{max}^{-0.916} V_{Pi}}{365000} * Z_{Bi} f_i \ \dots \dots \dots (51)$$

2.2.3. Fugacity Capacity Variation

2.2.3.1. Air

The fugacity capacity of air compartment could be expressed as:

$$Z_A = \frac{1}{RT_A} (\tau_1 0.1 K_{OA} + 1) \dots \dots \dots (52)$$

According to Li et al., the Octanol/Air partition coefficient is temperature sensitive with an estimation of:

$$logK_{OA}(T) = \frac{a}{T_A} + b \ldots\ldots\ldots\ldots\ldots\ldots..\ldots\ldots\ldots\ldots.\ldots.(53)$$

Thus, the fugacity capacity variation in air compartment is expressed as:

$$\frac{dZ_A}{dt} = \frac{d(\frac{\tau_1 0.1K_{OA} + 1}{RT_A})}{dt} = -\frac{(\tau_1 0.1K_{OA} + 1)}{RT_A^2}\frac{dT_A}{dt} + \frac{\tau_1 0.1}{RT_A}\frac{d(K_{OA})}{dt} \ldots\ldots.(54)$$

For

$$\frac{d(K_{OA})}{dt} = \frac{d(10^{\frac{a}{T_A}+b})}{dt} = -\frac{\ln(10)10^{\frac{a}{T_A}+b}}{T_A^2}\frac{dT_A}{dt}$$

Thus,

$$\frac{dZ_A}{dt} = \frac{d(\frac{\tau_1 0.1K_{OA} + 1}{RT_A})}{dt} = -\left[\frac{(\tau_1 0.1K_{OA} + 1)}{RT_A^2} + \frac{\tau_1 0.1\ln(10)10^{\frac{a}{T_A}+b}}{RT_A^3}\right]\frac{dT_A}{dt} \ldots\ldots.(55)$$

2.2.3.2. Water

The fugacity capacity in water could be expressed as:

$$Z_W = \frac{1}{H}\left(1 + 0.41 * \frac{\tau_2\rho_5\delta_5 K_{OW}}{1000}\right) \ldots\ldots\ldots\ldots\ldots\ldots\ldots\ldots\ldots(56)$$

H is Henry's law constant. According to research by Schwarzenbach in 2003, the Henry's Law constant could be affected by the temperature with the following formula, also as known as van't

Hoff correction. (Bates et al. 2017):

$$H(T_W) = H^{ref} exp\left[-\frac{\Delta U_{AW}}{R}\left(\frac{1}{T_W} - \frac{1}{T^{ref}}\right)\right] \dots\dots\dots\dots\dots (57)$$

Where H^{ref} is the referenced Henry's Law constant at T^{ref}; U_{AW} is the is the difference in internal energies of PCB in phase change from air to water (kJ/mol). Similarly, the K_{OW} also adept in van't Hoff correction:

$$K_{OW}(T) = K_{OW}^{ref} exp\left[-\frac{\Delta U_{OW}}{R}\left(\frac{1}{T} - \frac{1}{T^{ref}}\right)\right] \dots\dots\dots\dots\dots (58)$$

Where ΔU_{OW} is the internal energies requirement for PCB going from octanol to water (kJ/mol). However, the K_{OW} is much less sensitive to the temperature variation. In this study we can assume a constant K_{OW} to simplify the calculation. Thus the fugacity rate of change in water is:

$$\frac{dZ_W}{dt} = \frac{d\left(\frac{1 + 0.41 * \frac{\tau_2 \rho_5 \delta_5 K_{OW}}{1000}}{H}\right)}{dt} = \frac{1}{H^2}\frac{dH}{dt} \dots\dots\dots\dots\dots (59)$$

And

$$\frac{dH}{dt} = \frac{d\left\{H^{ref} exp\left[-\frac{\Delta U_{AW}}{R}\left(\frac{1}{T_W} - \frac{1}{T^{ref}}\right)\right]\right\}}{dt} = \frac{H * \Delta U_{AW}}{RT_W^2}\frac{dT_W}{dt} \dots\dots\dots (60)$$

Finally,

$$\frac{dZ_W}{dt} = -\left(1 + 0.41 * \frac{\tau_2 \rho_5 \delta_5 K_{OW}}{1000}\right)\frac{\Delta U_{AW}}{HRT_W^2}\frac{dT_W}{dt} \dots\dots\dots\dots\dots\dots\dots\dots\dots (61)$$

2.2.3.3. Sediment

The fugacity capacity in sediment could be expressed as:

$$Z_S = (1-\tau_3)Z_2 + \tau_3 Z_4 = (1-\tau_3)Z_2 + \tau_3 \frac{Z_2\rho_4\delta_4 K_{OC}}{1000} \dots\dots\dots\dots\dots (62)$$

Thus,

$$Z_S = \frac{1-\tau_3}{H} + \frac{0.41\tau_3\rho_4\delta_4 K_{OW}}{1000H} \dots\dots\dots\dots\dots\dots\dots\dots\dots\dots\dots\dots\dots\dots\dots\dots (63)$$

Where ρ_4 is the sediment density (kg/L). Thus, the fugacity capacity change in sediment is:

$$\frac{dZ_S}{dt} = \frac{d(\frac{1-\tau_3}{H} + \frac{0.41\tau_3\rho_4\delta_4 K_{OW}}{1000H})}{dt} = \left(1-\tau_3 + \frac{0.41\tau_3\rho_4\delta_4 K_{OW}}{1000}\right)\frac{1}{H^2}\frac{dH}{dt} \dots\dots (64)$$

Finally,

$$\frac{dZ_S}{dt} = \left(1-\tau_3 + \frac{0.41\tau_3\rho_4\delta_4 K_{OW}}{1000}\right)\frac{\Delta U_{AW}}{HRT_W^2}\frac{dT_W}{dt} \dots\dots\dots\dots\dots\dots\dots\dots\dots (65)$$

2.2.3.4. Biota

According to Mackay, the fugacity capacity of biota is defined as:

$$Z_B = LZ_L = LZ_O = LZ_4 K_{OW} \dots\dots\dots\dots\dots\dots\dots\dots\dots\dots\dots\dots\dots\dots (66)$$

Where L is the lipid fraction in biota, then

$$\frac{dZ_B}{dt} = \frac{d(LZ_4 K_{OW})}{dt} = Z_W K_{OW}\frac{dL}{dt} + LK_{OW}\frac{dZ_W}{dt} \dots\dots\dots\dots\dots\dots (67)$$

Then

$$\frac{dZ_B}{dt} = Z_W K_{OW} \frac{dL}{dt} - LK_{OW} \frac{\Delta U_{AW}}{HRT_W^2} \frac{dT_W}{dt} \dots \dots \dots \dots \dots \dots \dots \dots \dots \dots (68)$$

2.2.4. The Compartment Volume Variation

2.2.4.1. Environmental Compartment

In this study, we assume that no volume change occurs in the environmental compartment.

2.2.4.2. Organism Volume through Natural Mortality, Growth Rate, and Predation

The organism population size is an essential factor for the improved model. Pre-existing methods for biomass size estimation involve field investigation and measurement. To estimate the biomass volumes, we develop an energy-mass method using energy flow as the critical parameter, which could be used to calculate the primary producer biomass/volume and the following species on the connected food web can be calculated accordingly.

To estimation the biomass of primary producer, two assumptions must be made before the application. First, the primary producers have long been existed and stabilized. Second, the identified energy source can be measured and quantified. However, it is also important to acknowledge that energy is not the only dominant factor to control the primary producer biomass. Other environmental factors, such as nutritional levels, water supply, energy absorption efficiency is also critical for primary producers. For solar energy-based ecosystems, most of these parameters cannot be measured directly, but they can be quantified via other parameters, such as photosynthetic efficiency and vegetation coverage (Ssebiyonga et al. 2013). Based on the pre-assumptions, the following formula is used to estimate the primary producer population which depends on solar energy:

$$m_{phytoplankton,algae} = \frac{E_{Solar} \times \varphi_i^{PE} \times \sigma_i^C \times \varphi_i^T \times \vartheta_i^C \times A_i}{\varphi_i^C} \times \tau_i \dots\dots\dots\dots (69)$$

Where $E_{Solar}(\mathrm{J/s \cdot m^2})$ represents the total solar energy input to the unit surface; $\varphi_i^{PE}(\%)$ represents the photosynthetic efficiency of plant i; $\sigma_i^C(\%)$ represents vegetation coverage rate of each type of plant in the study area; $\varphi_i^T(\%)$ is the energy transport factor, the efficient proportion of energy stored in the system; $\vartheta_i^C(\mathrm{g/J})$ represents the carbon production factor which is the energy transferred to carbon in the system; $\varphi_i^C(\%)$ represents the carbon fraction, that is, the weight percentage of carbon in the target organism i; $\tau_i(\text{days})$ represents the average lifetime of the species; $A_i(\mathrm{m^2})$ is the area of species covered surface.

In formula (69), the total solar radiation is acquired from the Solargis (SolarGIS, 2014). Notice the Photosynthetic Efficiency and Carbon Production Factor are measured together. For the aquatic system, the combined parameter of Photosynthetic Efficiency and Carbon Production Factor is based on the Green Solar Collector; converting sunlight into algal biomass (Wageningen University project, 2005—2008). The estimation of the biomass growth efficiency not only depends on the photosynthesis efficiency but also takes into account daily consumption for organism consumption and self-maintenance. The vegetation coverage rate can also be found in books (Munawar and Munawar 1986) and the USGS GAP Land Cover Data Set. The calculation results are expressed as volume or mass since the density of most aquatic organisms is close to the water density. According to the observation records in Lake Ontario (Reavie et al. 2014), the biomass density of phytoplankton is around 0.01~1g/m^3. The formula (69) calculation results, depending on the coverage rate and seasonal features, are around 0.03 to 1.5 g/m^3.

The next step is to calculate other species biomass/volume through the trophic level and food webs. Since consumers and predators gain their energy through food ingestion, it is convenient to use food mass flows to find out the biomasses. In the current design, we assume constant population sizes among all the biotic compartments in the ecosystem. The population size could increase through growth/reproduction and lose its size through natural mortality and predation. We do not consider disasters or incidents which could dramatically alter the population.

Factors that control population size are considered for their impacts on PCB mass flows. Biota reproduction and growth processes do not trigger the actual loss of PCBs from the compartment but only reduce the PCB concentration in the biotic compartments as population size increases. In contrast, predation and natural mortality can cause both reductions in PCBs mass and loss in population size, while not affecting the concentration. Thus, both predation and natural death remove PCBs from the biotic compartments. In both processes, PCBs would either be released to the environment or be transferred to other biotic compartments. Under the constant population assumption, the growth rate is identical to the sum of the natural mortality rate and predation rate. Thus the variation in fugacity is merely caused by the change in PCBs mass transfer. The relationship between growth rate, mortality rate, and predation rate under steady-state population assumption for a given species i are described by the following equations:

$$GT_i = P_i + M_i \ldots \ldots \ldots \ldots \ldots \ldots \ldots \ldots \ldots \ldots \ldots \ldots \ldots \ldots \ldots \ldots \quad (70)$$

For species i, GT_i represents the growth rate (day^{-1}), P_i represents the predation rate (day^{-1}), and M_i is the natural mortality rate (day^{-1}).

The expressions for growth rate, predation rate, and natural mortality rate are:

$$Growth\ Rate: G = k_{Gi}V_{Pi} = 0.00586(1.113)^{T-20}(1000W_{Bi})^{-0.2}V_{Pi} \ldots \ldots \ldots \ldots (71)$$

$$Predation\ Rate: P = \sum_{i \neq k}^{n} \frac{0.022e^{0.06T}\rho_k V_{Pk} p_{ik}}{W_{Bk}^{0.15}} \ldots \ldots \ldots \ldots \ldots \ldots \ldots \ldots \ldots \ldots \ldots \ldots (72)$$

$$Natrual\ Mortality\ Rate: M = \frac{4.899t_{max}^{-0.916}V_{Pi}}{365000} \ldots \ldots \ldots \ldots \ldots \ldots \ldots \ldots \ldots \ldots \ldots \ldots \ldots (73)$$

The detailed information for each term is listed in Table 2.4. As a result,

$$\frac{dV_i}{dt} = 0.00586(1.113)^{T-20}(1000W_{Bi})^{-0.2}V_{Pi} - \frac{4.899t_{max}^{-0.916}V_{Pi}}{365000} - \sum_{i \neq k}^{n} \frac{0.022e^{0.06T}\rho_k V_{Pk} p_{ik}}{W_{Bk}^{0.15}} \ldots \ldots \ldots \ldots \ldots \ldots \ldots \ldots (74)$$

Under constant population scale,

$$\frac{dV_i}{dt} = 0 \ldots \ldots \ldots \ldots \ldots \ldots \ldots \ldots \ldots \ldots \ldots \ldots \ldots \ldots .. \ldots (75)$$

$$0.00586(1.113)^{T-20}(1000W_{Bi})^{-0.2}V_{Pi} = \frac{4.899t_{max}^{-0.916}V_{Pi}}{365000} + \sum_{i \neq k}^{n} \frac{0.022e^{0.06T}\rho_k V_{Pk} p_{ik}}{W_{Bk}^{0.15}} \ldots \ldots (76)$$

If the food web details and the scale of primary producers are known, the population equilibrium can be used to compute the population of any species if they are connected by the food web.

2.3. Loading Pattern

We use ten homolog groups to simulate the total PCB fluxes in Lake Ontario and compare the results to the observational records. Moreover, we select PCB-18, PCB-153, and PCB-194, which are prevalent PCB congeners in Lake Ontario (Soonthornnonda et al. 2011; Campfens and Mackay 1997; Oliver and Niiml 1988) for organism impact analysis. PCB-18 ($Log\ K_{OW} = 5.6$), PCB-153 ($Log\ K_{OW} = 7.5$), and PCB-194 ($Log\ K_{OW} = 7.65$) have K_{OW} values that extend across the range of values reported for PCB congeners (McLeod et al. 2015; Arnot and Gobas 2004), while the similarity of K_{OW} for PCB-153 and PCB-194 allow examination of the effects of a small to moderate change in hydrophobicity.

Table 2.5. The Physical & Chemical Properties of Selected PCB Congeners

Name	M (mol/g)	H(25°C) $(Pa \cdot m^3/mol)$	K_{OW}	Reaction Lifetime (day)			a	b	U_{OA}	TMF
				Air	Water	Sediment				
PCB-18	257.5	25.3	5.60	30	900	5265	4060	-6	35	3
PCB-153	360.9	20.0	7.50	90	7400	9918	3785	-7	66	4.2

PCB-194	429.8	4.37	7.65	90	7400	9918	4906	-5.33	169	6

Table 2.6. The Physical & Chemical Properties of PCB Homolog Groups

Homolog Groups	Mono	Di	Tri	Tetra	Penta	Hexa	Hepta	Octa	Nona	Deca
M (g/mol)	205	223	257	292	326	361	395	430	464	498.7
H(ref) (Pa*m^3/mol)	60	60	77	76	68	86	100	100	100	100
a	3520	3785	4060	4251	3785	3785	4845	4906	4906	4906
b	-5.0	-5.4	-6.0	-6.0	-5.4	-7	-6.1	-5.33	-5.3	-5.3
T(ref) (K)	298	298	298	298	298	298	298	298	298	298
Uoa	42.7	44.0	35.0	31.0	30.0	66	144.0	169	167.0	170.0
LKow	4.66	5.19	5.5	5.9	6.3	6.8	7.1	7.5	7.9	8.27
Air (day)	10	15	60.0	90	180	360	720	720	720	720
Water (day)	1800	1800	1800	1800	3600	7400	14430	14430	14430	14430
Sediment (day)	5265	5265	5265	5265	5265	9918	19841	19841	19841	19841
TMF	3.4	3.8	4.2	4.6	5.3	5.39	5.8	6.2	6.6	7
Identify No.	1	2	3	4	5	6	7	8	9	10
Combine 1242	0.3	14.7	42.1	33.9	8.1	0.8	0.1	0	0	0
Combine 1248	0.02	0.36	22.0	57.3	18.6	1.96	0.57	0	0	0
Combine 1254	0	0.5	0.7	18.3	55.6	22	2.5	0.4	0	0
Combine 1260	0	0.1	0.3	0.9	9.9	43.5	45.3	18.5	1.7	0

We use annual PCB loadings based on Gobas et al. 1995 and LimnoTech 2011 to parameterize PCB emissions in our model. 20% of the total PCB loading is emitted into the air compartment; while the rest enters the water column. The water inputs are combined with dissolved and particulate phases, and the proportion of dissolved/particulate phase was estimated as 70%/30%. Furthermore, we use standard homolog group properties and their technical mixture shares to calculate the total PCB concentration. This simplification shortens the calculation time while preserving differences among all PCB congeners. Field measurements indicate that Aroclor 1248

& 1254 mixtures dominate the PCBs present in Lake Ontario sediment cores, consistent with the historical production records (Hu et al. 2011; Breivik et al. 2002). The proportions of PCB-18, PCB-153, and PCB-194 in the total PCB loading in Lake Ontario have been estimated to be 3.8%, 9.85%, and 1.93%, respectively (Figure 2.4, Breivik et al. 2002a).

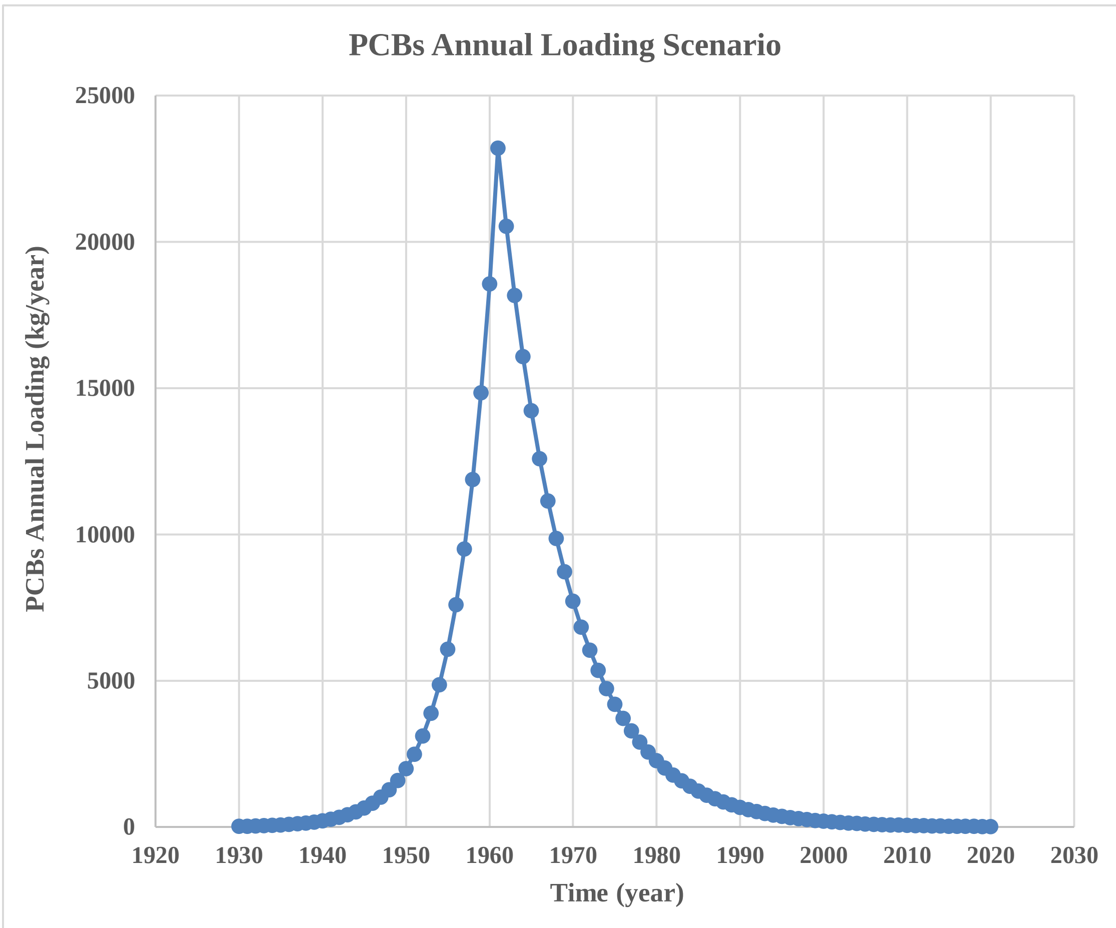

Figure 2.3. PCBs Loading Pattern for Lake Ontario (Gobas et al. 1995)

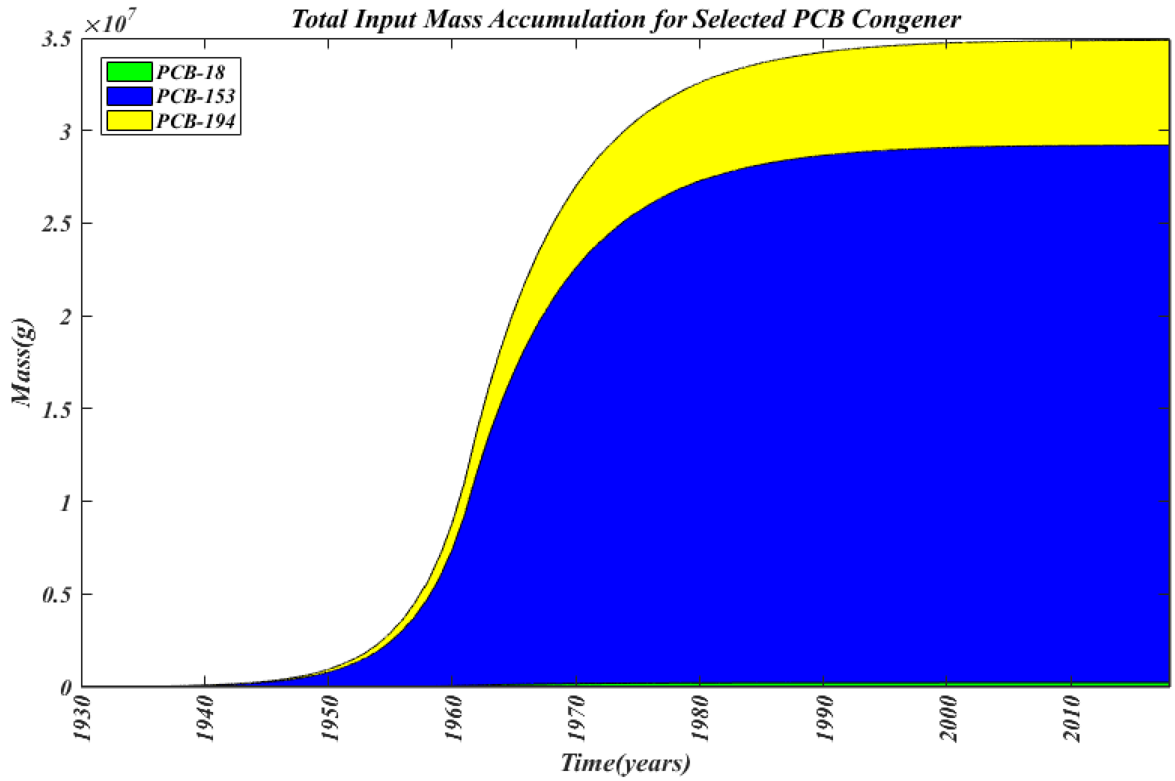

Figure 2.4. The Accumulated Inputs of All Three PCB Congeners

The general environmental parameters of Lake Ontario are applied. Using the Runge-Kutta numerical integration to solve for the ordinary differential equations, we estimate the total PCB mass flows and concentrations, comparing to the total PCB concentration in Lake Ontario (for the period 1930-2015) based on published studies. The predicted PCB mass flows among different compartments are then used to evaluate the organism impacts on overall PCB transport and fate in Lake Ontario.

2.4. Population Behavior during PCB Mass Exchange

In contrast to reliance on the simplified growth dilution formulation, we use the natural mortality rate, predation rate, birth rate, and growth rate to model the size of the biotic population. The population volume growth rate represents the sum of the organism's reproduction rate and growth rate. The new growth term is merely an extension of the previous growth formula (Gewurtz, 2006). Predation loss and natural mortality are two new processes we use to describe the population loss of the biotic compartments. Mortality is defined as the sum of the organism natural death rate and predation rate. Predation occurs when the species is consumed by its predators, while the natural mortality rate derives from the average lifespan, including all other causes of death (Then et al. 2005). Both processes cause PCBs removal from the applicable organism compartment.

The advantage of using the alternatives to replace the growth dilution is that natural mortality, predation, reproduction, and growth is more accurate to distinguish between volume expansion and contaminant loss. For example, although predation causes PCBs to leave the current biotic compartment with the dead organism, it is never entirely absorbed by its predator. According to Arnot and Gobas, only a portion of PCBs is taken up by the predator, as determined by the function of the dietary chemical transfer efficiency (E_D) (Arnot and Gobas 2004). The desorbed PCBs will be separated from the total mortality rate and count as part of the PCB transfer from organism to the environment.

The species information and food web structure come from previous studies on PCB bioaccumulation in Lake Ontario (Campfens and Mackay 1997). To evaluate organism population impacts, we select two specified biomass densities regarding the phytoplankton concentration: $1.4\,\mu g/L$ (low) and $1.4\,mg/L$ (high), based on a study on seasonal phytoplankton population variation in Lake Ontario (Estepp and Reavie 2015)

Table 2.7. Species Biotic Information

	mass(g)	lipid fraction	metabolism (day^{-1})	Maximum survival time (years)	Gill Uptake Type	Location
Plankton	0.0004	0.015	50000	0.1	0	*Pelagic*
Mysid	0.1	0.04	5000	0.8	1	*Pelagic*
Pontoporeia	0.02	0.03	5000	2	1	*Benthic*
Oligochaete	2	0.01	5000	3	1	*Benthic*
Sculpin	8	0.08	500	4	1	*Pelagic*
Alewife	32	0.07	500	5	1	*Pelagic*
Smelt	16	0.04	500	5	1	*Pelagic*
Salmonid	2400	0.16	500	12	1	*Pelagic*

Table 2.8. Food Web ($\mathbf{p_{ij}}$)

Predator	Prey							
	Plankton	Mysid	Pontoporeia	Oligochaete	Sculpin	Alewife	Smelt	Salmonid
Plankton	0	0	0	0	0	0	0	0
Mysid	0.8	0	0.2	0	0	0	0	0
Pontoporeia	0	0	0	0	0	0	0	0
Oligochaete	0	0	0	0	0	0	0	0
Sculpin	0	0.18	0.82	0	0	0	0	0
Alewife	0	0.6	0.4	0	0	0	0	0
Smelt	0	0.54	0.21	0	0	0.25	0	0
Salmonid	0	0	0	0	0.1	0.5	0.4	0

3. Organic Impacts on PCBs transport

3.1. Mass Balance and Observations Comparison

We simulate the PCB concentration distribution from 1930 to 2015 for selected PCB congeners, as well as the total PCBs concentration. Figure 3.1-3.3 show the simulated cumulative mass flows in 1960 and 1980 for PCB-18, PCB-153 & PCB-194. The accumulation accounts for all the mass through the system. The dashed box indicates the model boundary and the arrow represent the PCB mass flow direction and allocation/deposition proportion; the hollow circle indicates natural degradation in the environmental compartments and organism compartments. The percentage showed behind each compartment name represents the PCB mass remaining in that compartment among all accumulated PCB inputs. The left side color bar shows the shares of PCB congener among each compartment in the system at 1960 and 1980. According to the historical record, these two times represent the start and end of primary PCB inputs into Lake Ontario. We confirm that the sum of the PCB inputs matches the amount of all advection outflows and reactions in the system; thus closing the mass balance.

The shares of PCB mass flows indicate two primary destinations for these pollutants: reactions (degradation in the environment and biodegradation in organisms) and sediment deposition & burial. Comparing 1980 to 1960, the percentage of PCB-153 predicted to accumulate in buried sediment increases from 73% to 91%, with the difference associated primarily with decreases in the PCBs in the biota (12%) and water compartments (5%).

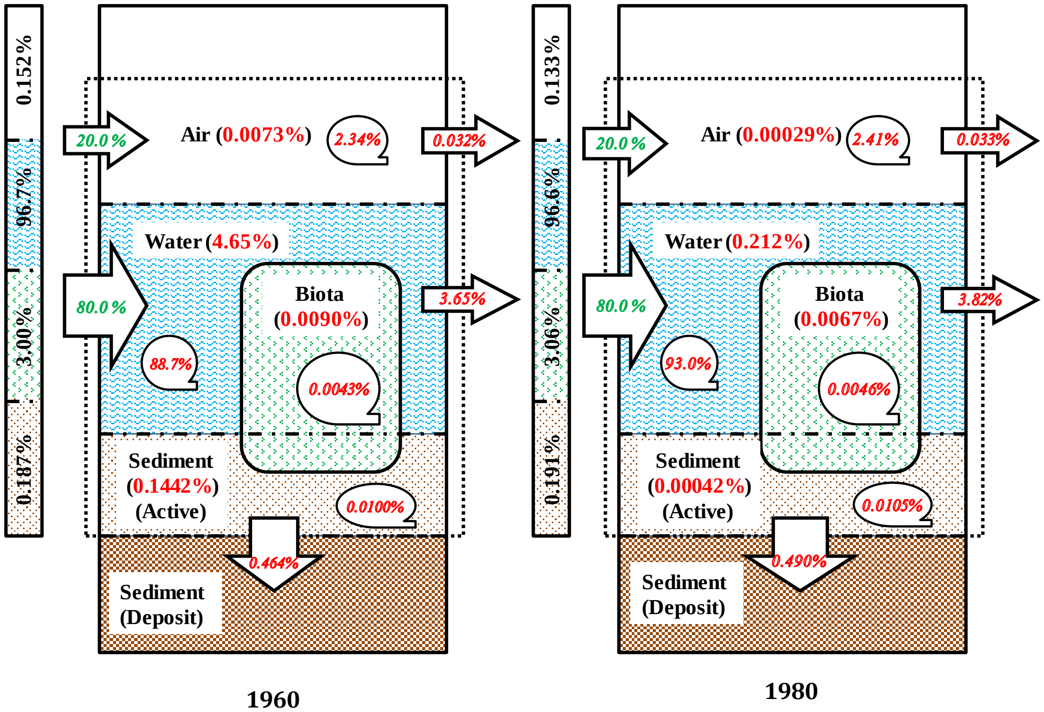

Figure 3.1. Model-Predicted Relative Distribution of Accumulated PCB-18 in 1960 & 1980

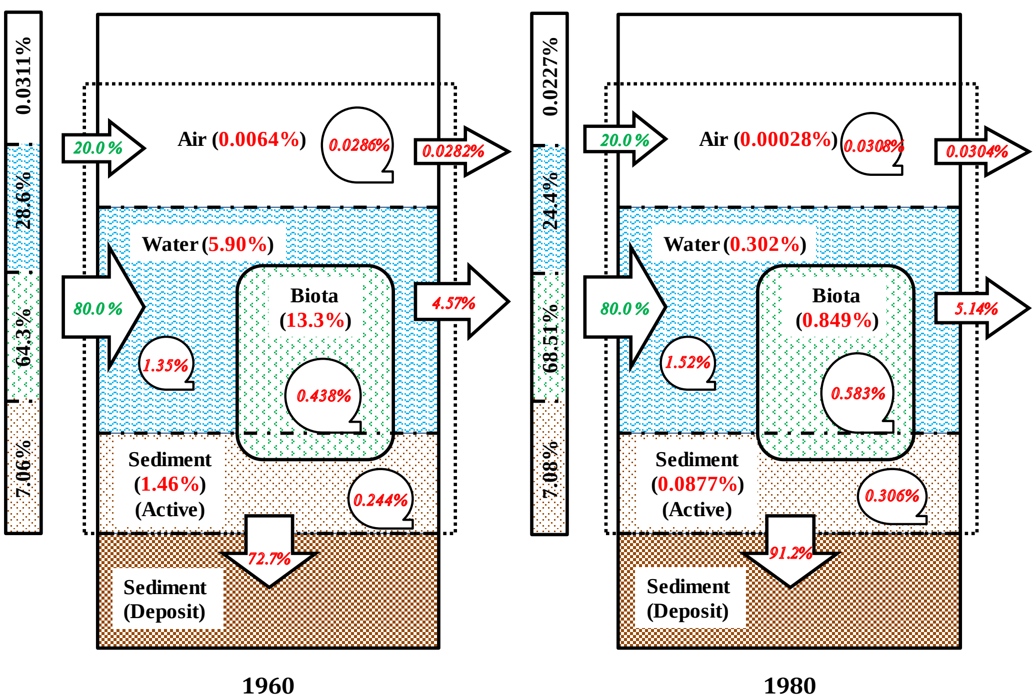

Figure 3.2. Model-Predicted Relative Distribution of Accumulated PCB-153 in 1960 & 1980

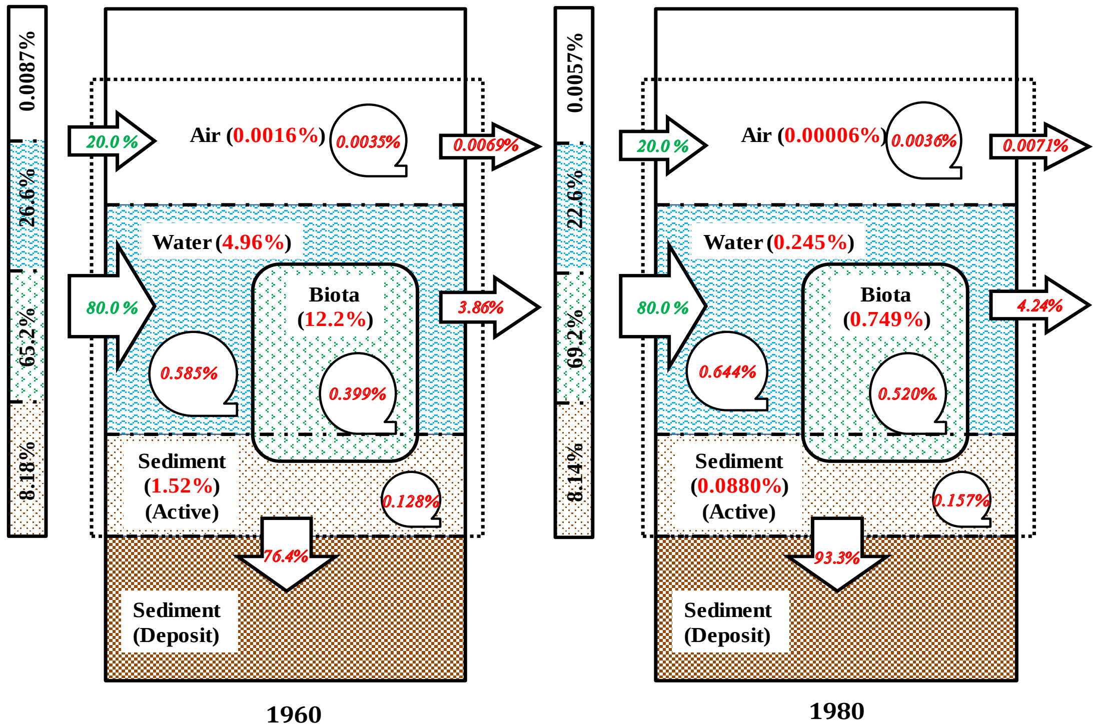

Figure 3.3. Model-Predicted Relative Distribution of Accumulated PCB-194 in 1960 & 1980

The fate of each PCB congener in figure 3.1–3.3 depends on lipophilicity. The $logK_{OW}$ value of most PCB congeners (PCB-17 to PCB-209) falls between 5.0 and 8.3 (25℃, Mackay et al., 2006). For lighter PCB congeners, such as PCB-18, a low K_{OW} indicates little lipid attraction, so that most of the PCB-18 remains in water and air. Due to its lower stability (compared to higher PCB congeners), aerobic microbial degradation and photodegradation would quickly eliminate PCB-18 in the natural environment. According to Neely, the typical surface water half-life for PCB-18 in the Great Lake system is around 43 days (Neely 1983). In contrast, heavy congeners, such as PCB-153 & PCB-194, are more persistent and have higher octanol/water partition coefficients, leading them to partition to organisms or organic matter on suspended sediment particles. Most of these particles then deposit onto the bottom sediment and are subsequently buried beneath the active layer.

To further test the model, we compare the simulation results to field observations collected from published literature from 1960 to 2015. The simulation uses the historical PCB loading data in Lake Ontario. Average temperatures are applied for all the environmental compartments, and the biota temperatures are the same as their habitat compartments. By running the model under two loading scenarios for Aroclor 1248 (figure 3.4) and Aroclor 1254 (figure 3.5), the simulation results are well-matched with the observed measurements, within one order of magnitude for all compartments at various time points. The simulation also confirms that the pollution source of Lake Ontario is some combination of Aroclor 1248 and Aroclor 1254. Although our current model formation cannot simulate PCB gradients within each compartment due to the homogeneity assumption, the comparison still supports the overall validity and accuracy of the model predictions. The original comparison data are listed in table 3.1.

Table 3.1. Observation vs. Simulation in Lake Ontario Pollution History

<table>
<tr><th>Location</th><th>Time</th><th>Unit</th><th>Observed Records</th><th>Simulation 1254</th><th>Simulation 1248</th><th>Type</th><th>Reference</th></tr>
<tr><td>Sediment</td><td>1968</td><td>ng/g wt</td><td>57</td><td>170</td><td>67</td><td>Total PCB</td><td>Frank et, al. 1979</td></tr>
<tr><td>Water</td><td>1969</td><td>ng/L</td><td>20</td><td>15</td><td>17.4</td><td>Total PCB</td><td rowspan="2">Mackay 1989</td></tr>
<tr><td>Air</td><td>1969</td><td>pg/m^3</td><td>7000</td><td>850</td><td>1030</td><td>Total PCB</td></tr>
<tr><td>Smelt</td><td>1978</td><td>ng/g wt</td><td>1000</td><td>3320.0</td><td>1054.0</td><td>Total PCB</td><td rowspan="3">Whittle et al. 1983</td></tr>
<tr><td>Smelt</td><td>1978</td><td>ng/g wt</td><td>858</td><td>3320.0</td><td>1054.0</td><td>Total PCB</td></tr>
<tr><td>Pontoporeia</td><td>1978</td><td>ng/g wt</td><td>1849</td><td>649</td><td>237</td><td>Total PCB</td></tr>
</table>

Pontoporeia	1978	ng/g wt	1378	649	237	Total PCB	
Phytoplankton	1978	ng/g wt	110	122	68	Total PCB	
Phytoplankton	1978	ng/g wt	280	122	68	Total PCB	
Mysid	1978	ng/g wt	580	510	237	Total PCB	
Mysid	1978	ng/g wt	150	510	237	Total PCB	
Sediment	1981	ng/g dt	510	760	300	Total PCB	Oliver et al. 1989
		ng/g dt	690	760	300	Total PCB	
		ng/g dt	630	760	300	Total PCB	
		ng/g dt	200	760	300	Total PCB	
Sediment	1981	ng/g dt	570	760	300	Total PCB	Oliver et al. 1988
Water	1984	ng/L	1.1	2.61	2.98	Total PCB	
Phytoplankton	1982	ng/g wt	50	75	42	Total PCB	
Mysid	1983	ng/g wt	330	275	146	Total PCB	
Pontoporeia	1985	ng/g wt	790	275	164	Total PCB	
Sculpin	1986	ng/g wt	1300	892	537	Total PCB	
Alewife	1982	ng/g wt	1600	1490	571	Total PCB	
Smelt	1982	ng/g wt	1400	2042	649	Total PCB	
Salmonid	1982	ng/g wt	4300	13160	4356	Total PCB	
Salmonid	1977	ng/g wt	6840	23910	7909	Total PCB	Borgmann et al. 1991
Salmonid	1978	ng/g wt	8040	21254	7031	Total PCB	
Salmonid	1979	ng/g wt	3670	18872	6245	Total PCB	
Salmonid	1980	ng/g wt	3940	16744	5541	Total PCB	
Salmonid	1981	ng/g wt	2850	14848	4914	Total PCB	
Salmonid	1982	ng/g wt	5310	13160	4356	Total PCB	
Salmonid	1983	ng/g wt	5430	11659	3860	Total PCB	
Salmonid	1984	ng/g wt	4840	10327	3419	Total PCB	
Salmonid	1985	ng/g wt	2540	9146	3028	Total PCB	
Salmonid	1986	ng/g wt	3130	8098	2681	Total PCB	
Salmonid	1987	ng/g wt	3430	7169	2339	Total PCB	
Salmonid	1988	ng/g wt	2540	6349	2101	Total PCB	
Sediment	1983	ng/g dt	1300	596	236	Total PCB	Oliver et al. 1989
Sediment	1983	ng/g dt	1900	596	236	Total PCB	
Sediment	1984	ng/g dt	500	528	209	Total PCB	
Sediment	1984	ng/g dt	570	528	209	Total PCB	
Sediment	1984	ng/g dt	350	528	209	Total PCB	
Sediment	1985	ng/g dt	470	467	180	Total PCB	
Sediment	1985	ng/g dt	680	467	180	Total PCB	

Sediment	1985	ng/g dt	410	467	180	Total PCB	
Sediment	1986	ng/g dt	80	413	164	Total PCB	
Sediment	1986	ng/g dt	290	413	164	Total PCB	
Air	1990	pg/m^3	128	71	85	Total PCB	Hillery et al. 1997

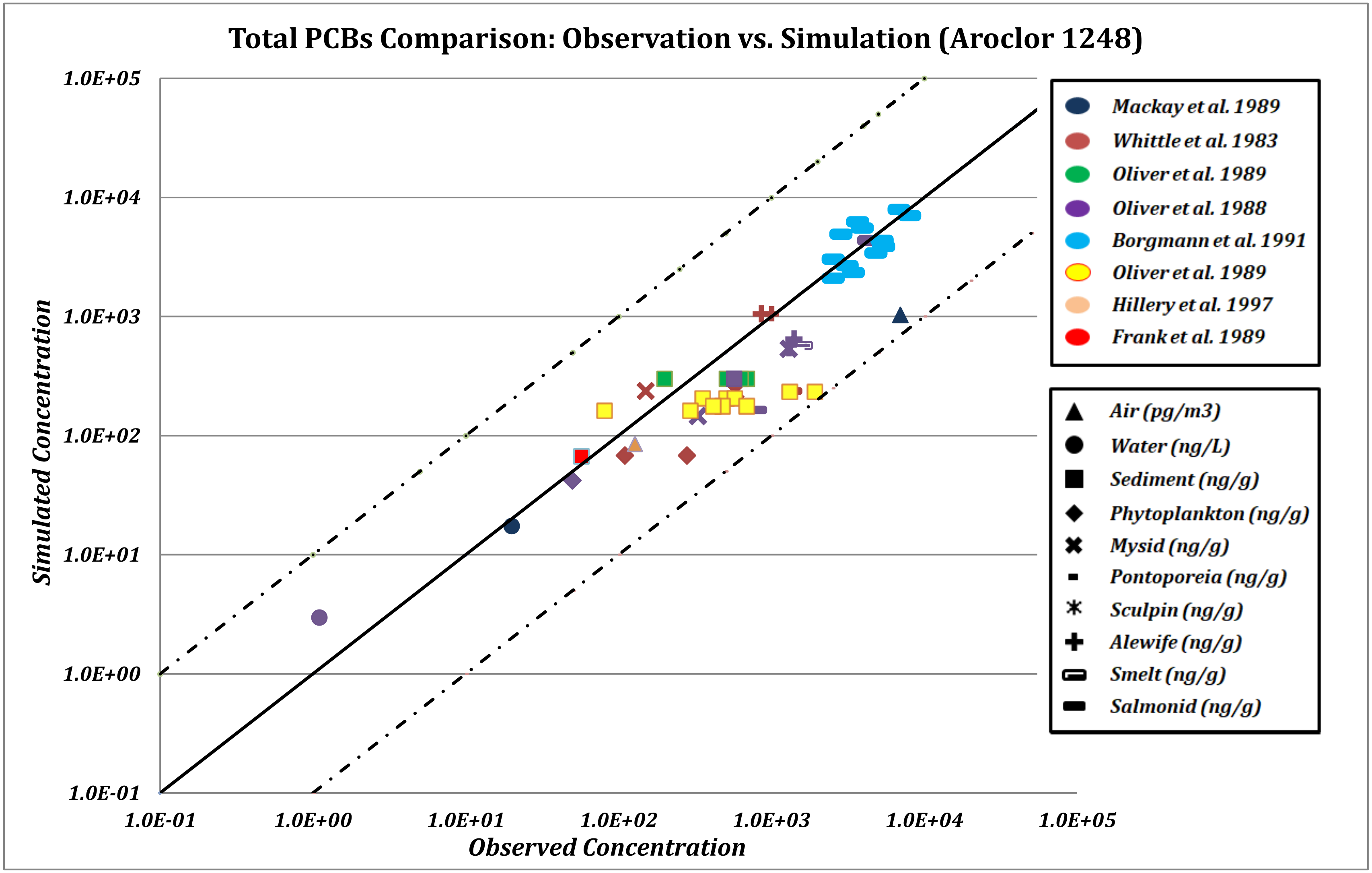

Figure 3.4. Total PCBs Concentration Comparison: Observation vs. Simulation in Aroclor 1248

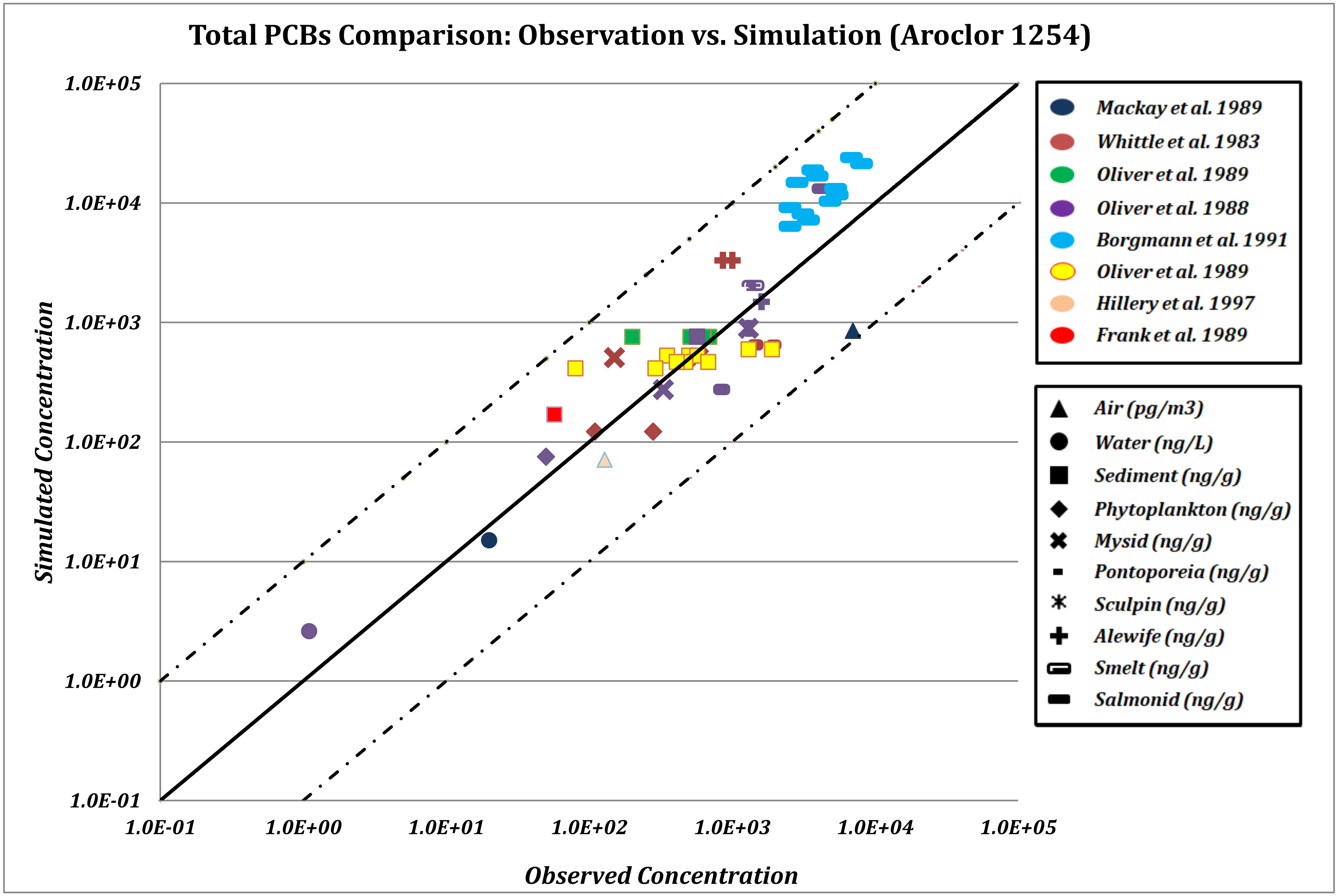

Figure 3.5. Total PCBs Concentration Comparison: Observation vs. Simulation in Aroclor 1254

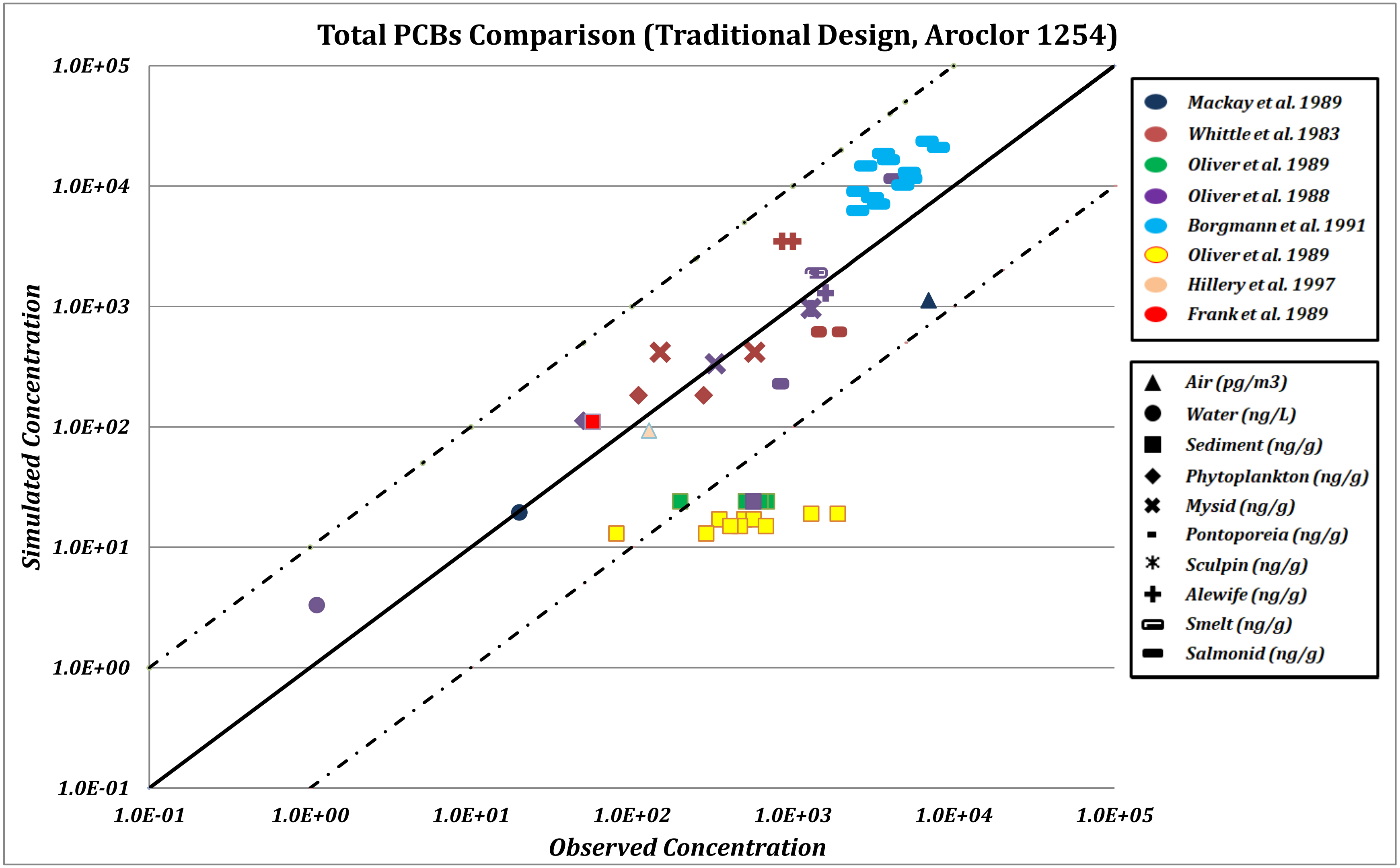

Figure 3.6. Total PCBs Concentration Comparison: Traditional Design, in Aroclor 1254

To evaluate the new model design, we also simulate the model under the traditional design and compare the results between simulation and observation using Aroclor 1254 (Figure 3.6). In this figure, it is clear that a number of the observed PCB concentrations are significantly higher than the simulation. The lack of FBIT effect by the populated organisms reduces the general exchange flux which transports PCB mass from water to sediment. Thus, while the sediment concentration data for Aroclor 1254 (yellow, green and purple squares) are well matched by the FBIT model in Figure 3.5, the same PCB concentrations are underpredicted in Figure 3.6 when the FBIT effect is omitted.

3.2. Facilitated Biotic Intermedia Transport

Facilitated biotic intermedia transport (FBIT) results from the additional transport routes provided by biotic compartments that affect the overall transport patterns in the system. The net flowchart is a useful tool to uncover the FBIT effect of the organisms. In figure 3.6-3.8, the magnitude of each flow flux is represented by the width of the arrows. Note that the net flows shown in the graph only include the net mass flow of each compartment, not all of the exchange processes occurring during the PCB transport (i.e., between organisms). The detailed mass transfer matrix is provided in Table 3.2-3.4 in the supplementary document. Due to the size of the original flow matrix, the eight biotic compartments (Plankton, Mysid, Pontoporeia, Oligochaete, Sculpin, Alewife, Smelt, and Salmonid) are compressed into one general group: biota. The values in the matrix result from an input amount of 1000 kg/year consistently for all three selected PCB congeners, with an input of 20% into the air, 56% into the water and 24% in suspended particles. A plankton density of 1.4 mg/m3 is used as low biota density, while a plankton density of 1.4 g/m3 is chosen for high biota density. Both scenarios are tested under average temperature scenario (bottom: 6°C, surface: 15°C).

The net flow chart indicates no significant biotic impact on hydrophilic PCB congeners, such as PCB-18. 97% of the PCB-18 flux remains in the water, most of which is eliminated by degradation. In both biotic density scenarios, less than 0.5% of the PCB-18 dissolves in biotic compartments, and the existence of high biomass has little impact on overall PCB-18 transport. Degradation in the water column dominates PCB-18 fate in Lake Ontario.

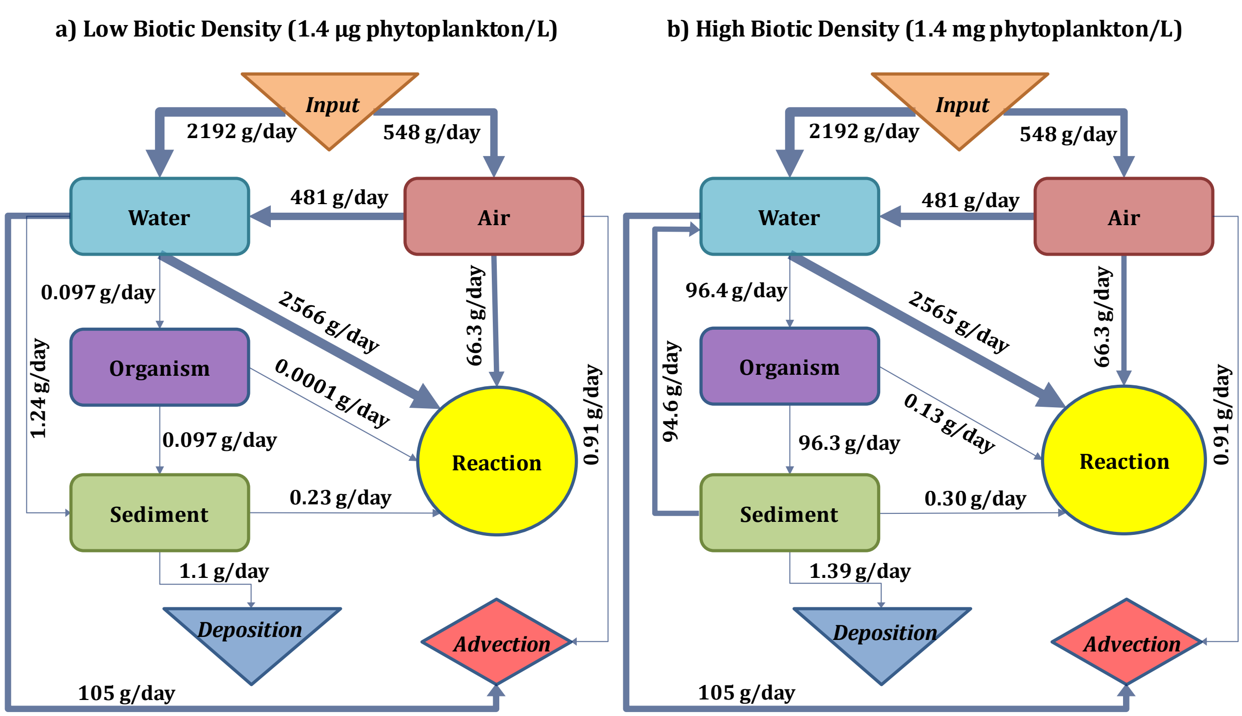

Figure 3.6. PCB-18 Facilitated Biotic Intermedia Transport under Two Bio-density

However, the results show quite the opposite for PCB-153 (figure 4) and PCB-194 (supplemental A5b) in the net flowchart. As shown in figures, the PCB congeners enter the system through water and air; almost all the contaminants are absorbed by the water column (diffusion, dry deposition, and wet deposition). Only 2-5% of the total PCB fluxes are removed by environmental and biological degradation; most of the PCB mass enters the sediment compartment through diffusion, particle deposition, and organism exchange (FBIT). Diffusion and deposition provide direct PCB exchange routes between water and sediment, and they dominant the PCB exchange flux in the low biomass scenario (figure 3.7 left). For PCB-153, organisms only capture less than 0.2% of the total PCB flux due to the small population size, serving as an alternative route to transfer PCB-153 from water to sediment. At this point, both the FBIT flux and the direct exchange flux have the same net transport direction from water to sediment. In the high biota density situation (figure 3.7 right with 1.4 mg phytoplankton/L), the FBIT effect becomes much stronger (i.e., 8210 g/day, PCB-153) and is more than triple the net PCB exchange rate (i.e., 2190 g/day, PCB-153) between water and sediment. The direction of the direct net exchange flux is reversed, dominated by resuspension and diffusion that balances PCB partitioning between water and sediment.

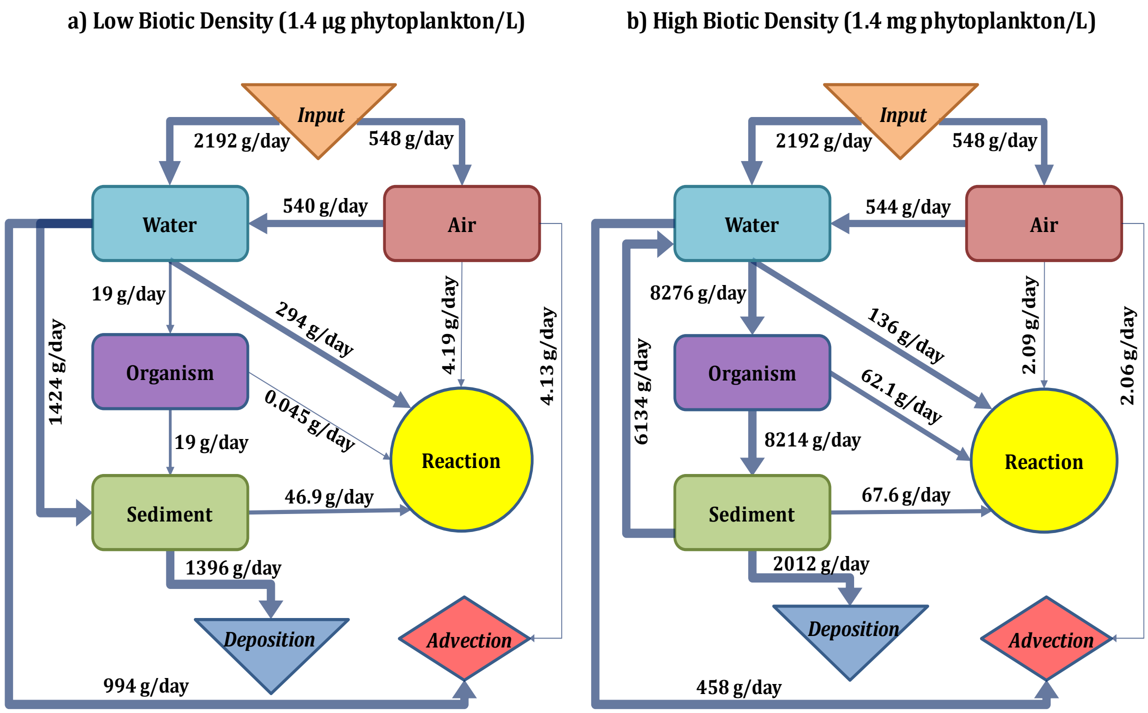

Figure 3.7. PCB-153 Facilitated Biotic Intermedia Transport under Two Bio-density

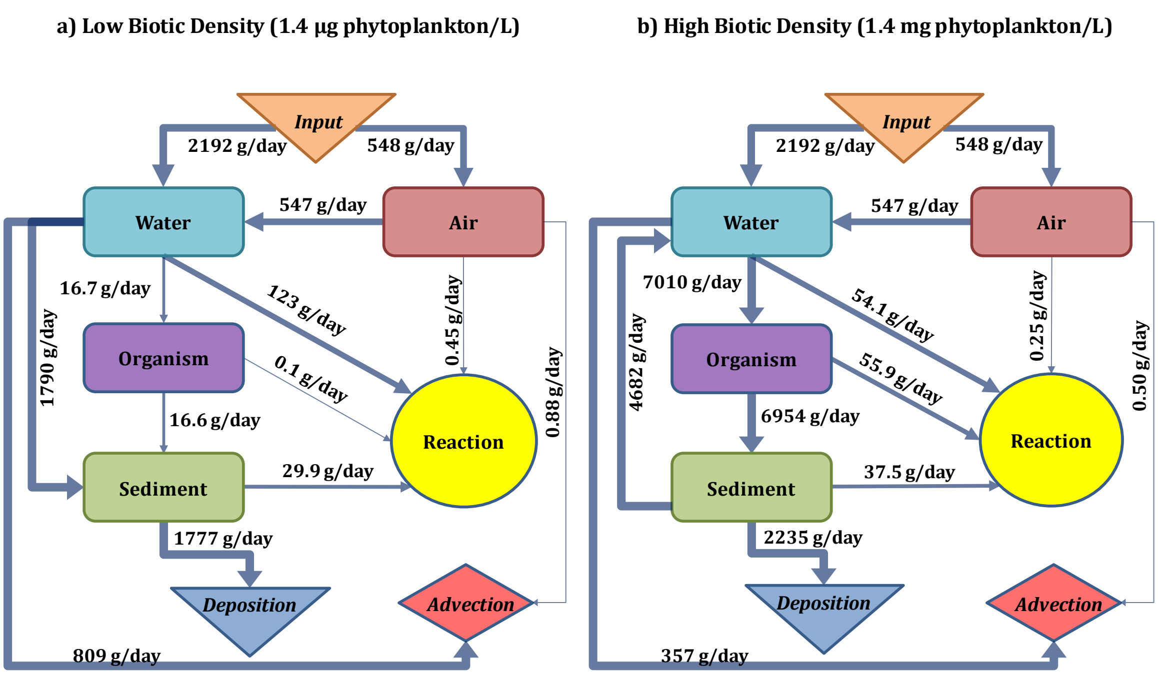

Figure 3.8. PCB-194 Facilitated Biotic Intermedia Transport under Two Bio-density

To further study the organism population impact on the FBIT effect, we analyze the PCB transport pattern between water and sediment under growing organism population. Four transport fluxes and their flow direction are tracked in the model under the same input rate, temperature, and species combination: the direct water-sediment net transport flux, the FBIT flux, the air & water removal flux (advection & degradation), and the active net exchange rate from water to sediment (figure 3.9-3.11). The contents of each flux are listed below:

$$Flux_{W\&S} = DF_{WS} + DP_S - DF_{SW} - RS_W \tag{77}$$

$$Flux_{FBIT} = \sum_{i=1}^{8} (G + FI - B)_i \tag{78}$$

$$Flux_{water/air} = DD_W + DD_A + AD_W + AD_A \tag{79}$$

$$Flux_{SW\ direct} = Flux_{W\&S} + Flux_{FBIT} \tag{80}$$

The general PCB flux from water to sediment (formula 77) is calculated by the diffusion of water and sediment (DF_{SW} & DF_{WS}), the deposition from water to sediment (DP_S), and the resuspension from sediment to water (RS_W); the FBIT flux (formula 78) is comprised of the gill uptake rate (G) and the food ingestion rate (FI), minus the biodegradation rate (B); The pollution removal by water and air (formula 79) is estimated by the water/air natural degradation & advection rate. Finally, PCB transport without bioactivity is expressed by formula 80.

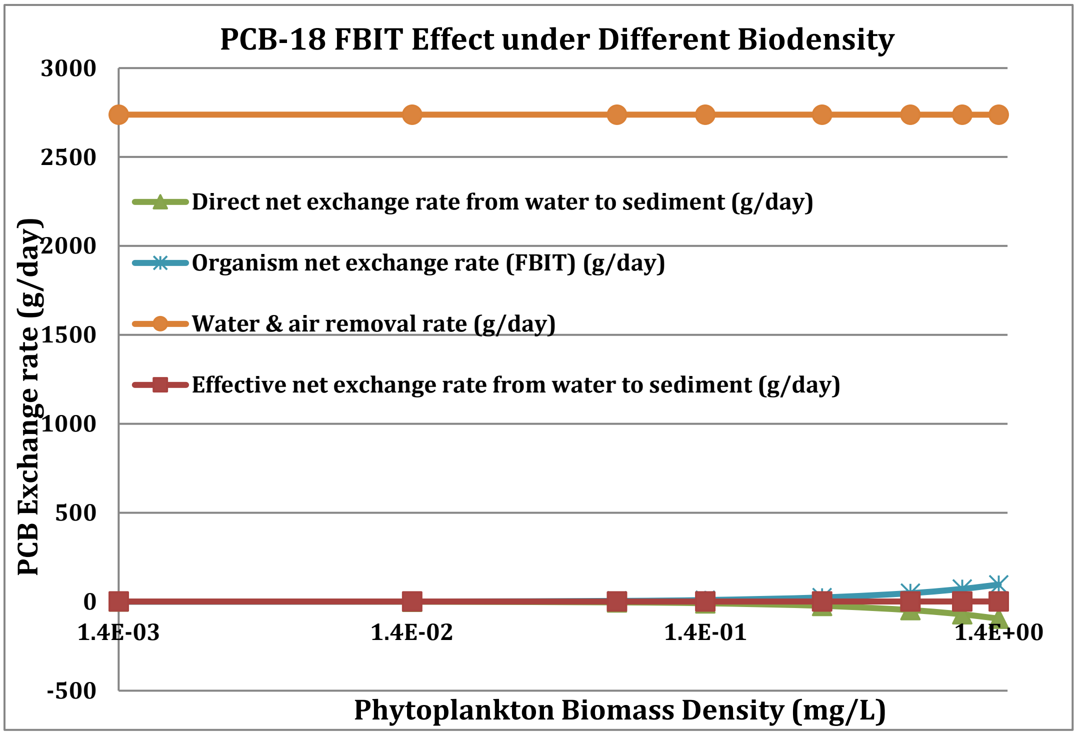

Figure 3.9. PCB-18 FBIT Effect under Different Bio-density (Steady State)

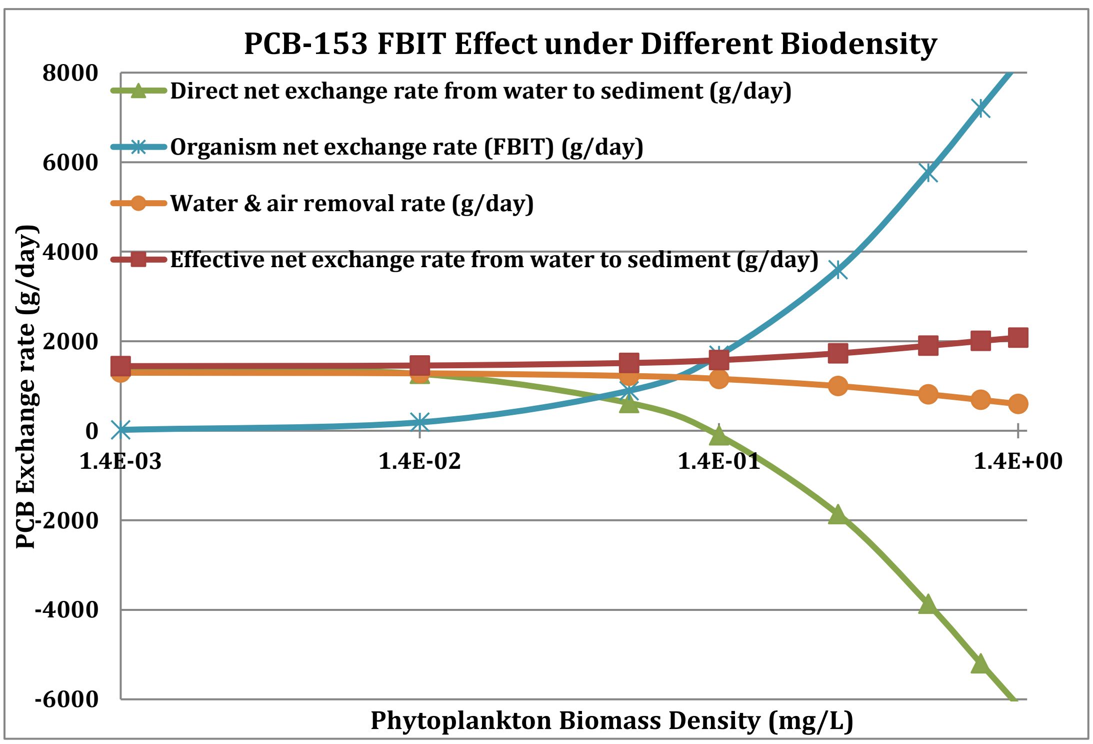

Figure 3.10. PCB-153 FBIT Effect under Different Bio-density (Steady State)

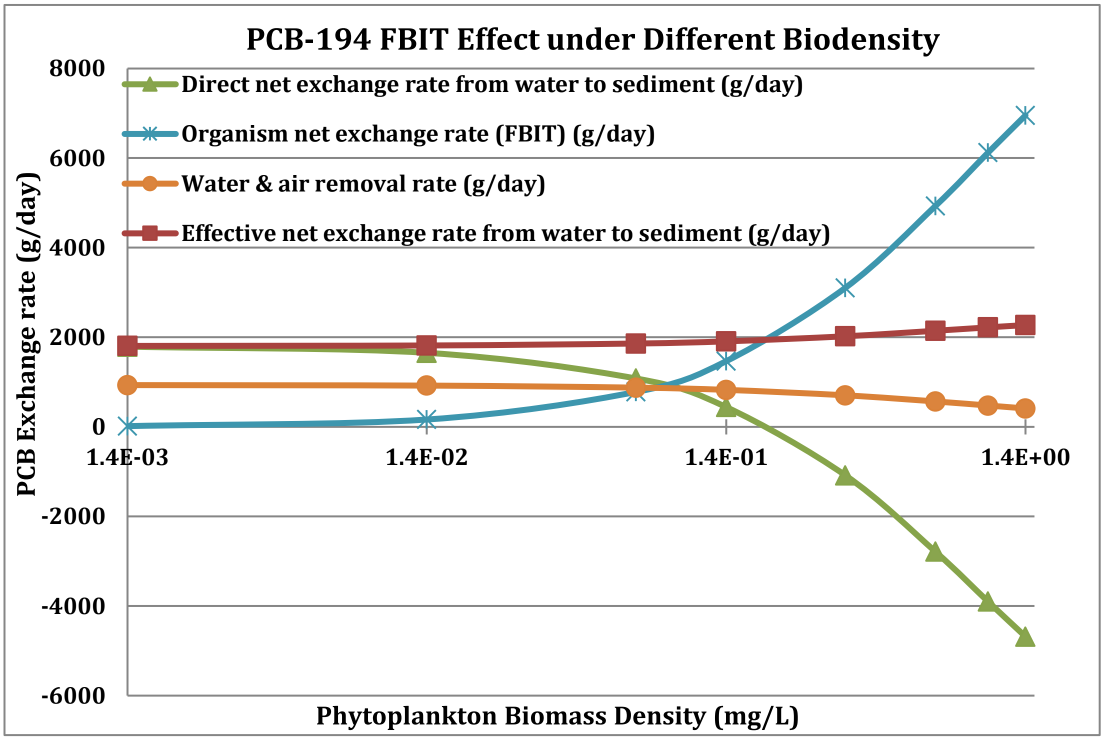

Figure 3.11. PCB-194 FBIT Effect under Different Bio-density (Steady State)

Figure 3.9, 3.10, and 3.11 show the intermedia exchange rate of selected PCB congeners under different organism density. Four simulated intermedia exchange rates are shown for PCB-18, PCB-153 & PCB-194 as the biomasses increase. The x-axis represents the biomass density (measured in phytoplankton density, mg/L); the y-axis represents the exchange rate (g/day). Positive rates indicate the net flow direction in the legend; a negative value means the opposite direction.

In the case of PCB-18 (figure 3.9), the air & water removal flux is the main PCB transport route and is close to the overall PCB net exchange rate through the system (2738 g/day vs. 2740 g/day). Since the air & water compartments are the same in all biomass scenarios, the air & water removal flux remains constant. In the meantime, we observe a growing FBIT effect, and the direct water-sediment net exchange flux reverses its transport direction at approximately 0.14 mg phytoplankton/L. Its impact can be neglected compared to the dominant air & water advection/degradation flux for this hydrophilic PCB congener.

For hydrophobic PCBs, such as PCB-153 & PCB-194, the FBIT flux plays a critical role in contaminant transport when the organism population is significant. As shown in figure 3.10 & 3.11, the direct water-sediment exchange flux and air & water removal flux constitute the overall PCB net exchange flux in the low biomass case. As the organism population increases, the FBIT flux starts to grow. When the phytoplankton density approaches 0.14 mg/L, the FBIT flux completely assumes the role of the direct water-sediment exchange flux and is the dominant route for PCB net transport from water to sediment. After this point, the direction of the direct net exchange flux reverses, with PCB mass transport from sediment back to the water column. As more PCB mass is captured by organisms and the sediment, the air & water removal flux also declines, resulting in approximately a 10%-20% increment in the effective net exchange rate from water to sediment.

However, the FBIT effect cannot contribute to overall PCB removal, unless biological migration is considered during the model simulation. The absolute amount of PCBs escaping from the model boundary depends on the sum of the environmental and natural degradation, as well as the sum of the outflows/deposition from the environmental compartments, with the extra amount of PCB in the sediment returning to the water column. Because the water-sediment deposition rate depends on the hydraulic and morphological conditions, the acceleration of the transport rate mainly comes from increments of organism biodegradation activities that follow the biotic population growth.

3.3. Storage Effect

The storage effect is defined as the PCB absorption by biotic compartments, causing PCB levels to drop in the surrounding environment. To evaluate the storage effects, we compare the selected PCB congener masses among different environmental compartments under steady state.

Figure 3.12-3.14 represents the mass distributions of PCB-18, PCB-153, and PCB-194 at a steady state corresponding to different biota densities in Lake Ontario. The different colors represent different model compartments. The x-axis represents different biota density in the system. At steady state, other organisms' population could be estimated based on the plankton density (g/m^3). Y-axis represents the contaminant mass content (g) using a log scale. The sediment compartment considers the top layer (~0.1m) of active sediment, and the PCB content in the sediment only represents the top layer rather than the entire sediment sector. For PCB-18 (figure 3.12), over 94% of the contaminant remains in the water column due to its low lipophilic feature ($logK_{OW} = 5.6$). The presence of organisms yields little storage effect (2.5%-3.4%) on the overall chemical distribution of PCB-18 and has little impact on its overall allocation and transport in the environment.

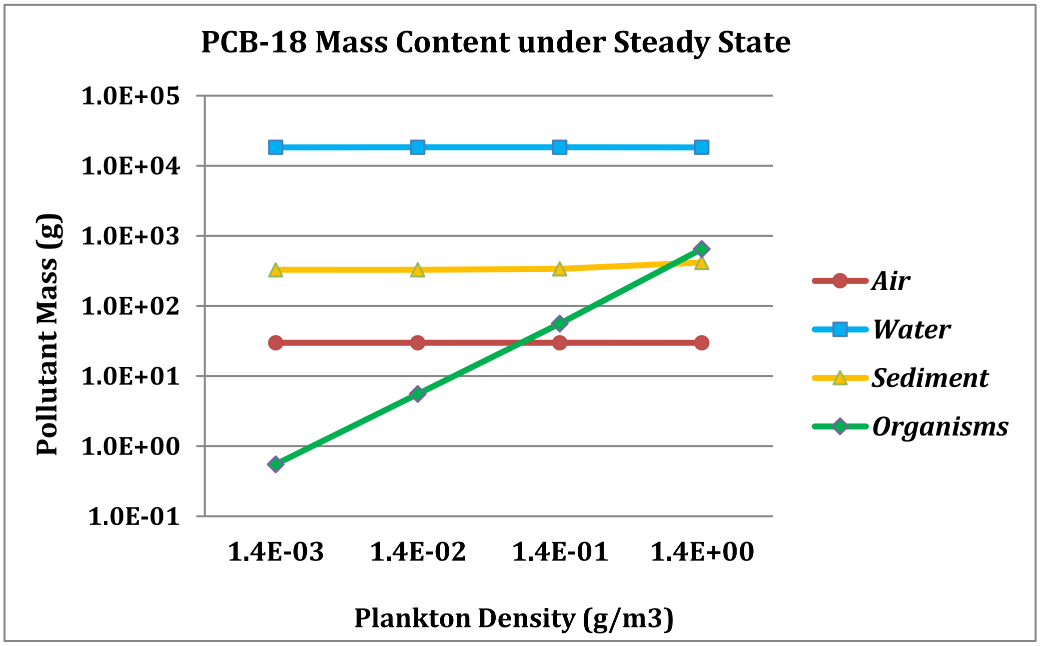

Figure 3.12. PCB-18 Mass Content with Different Biota Density

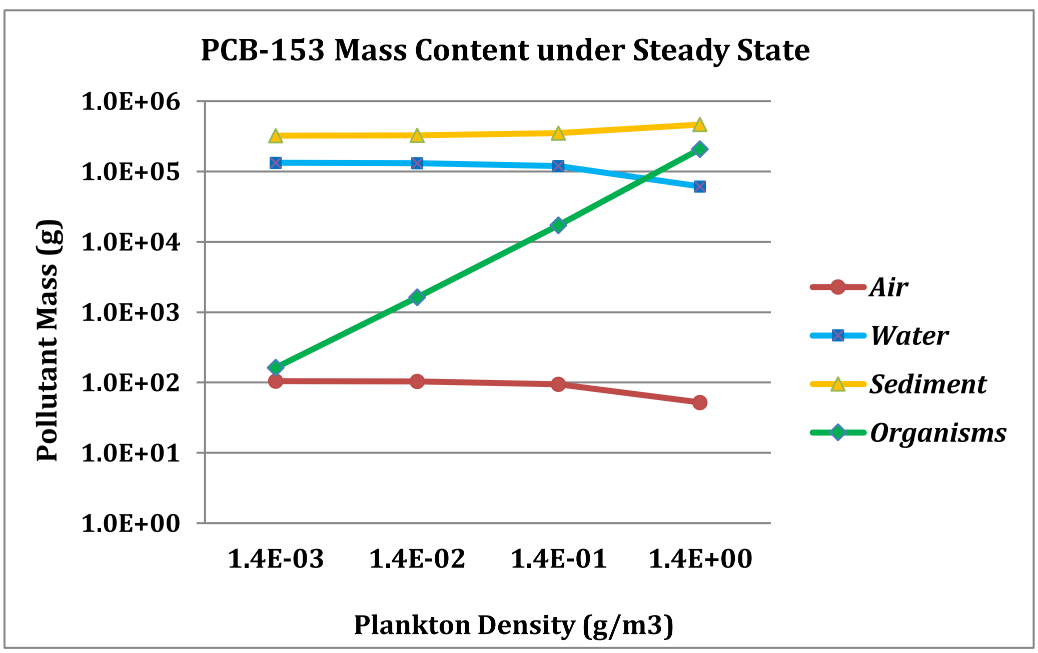

Figure 3.13. PCB-153 Mass Content with Different Biota Density

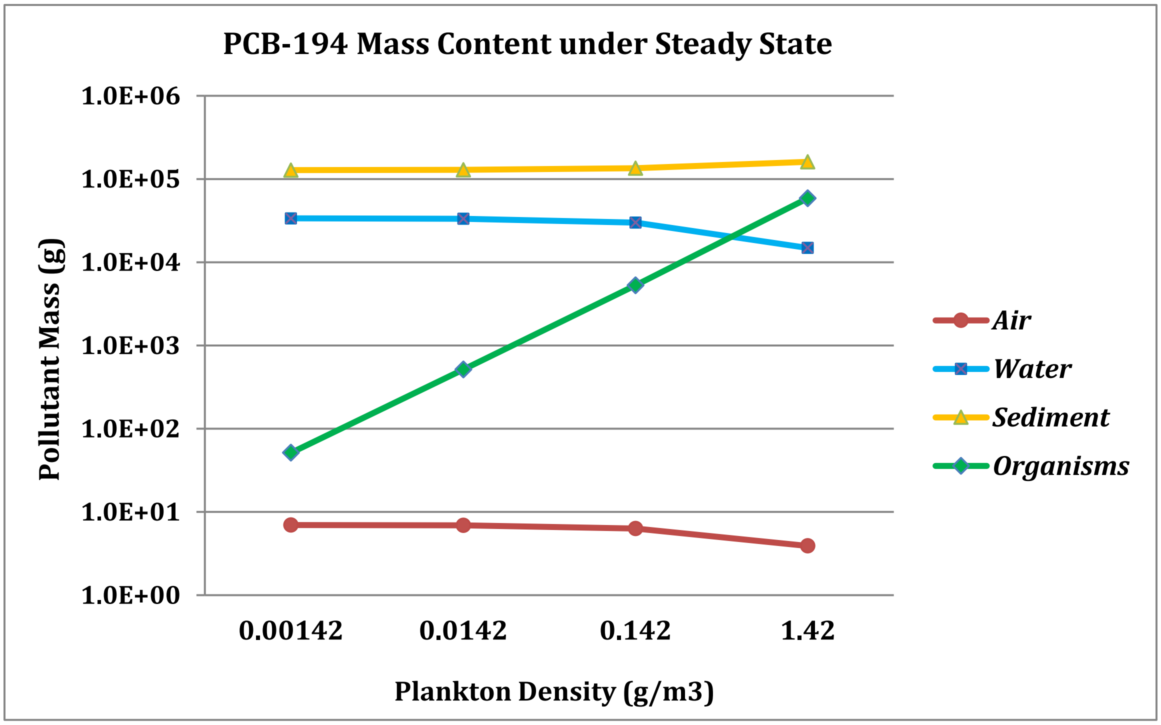

Figure 3.14. PCB-194 Mass Content with Different Biota Density

However, PCB congeners with high lipophilicity show obvious storage effects and the PCB levels in environmental compartments drop significantly as the organism density increases. In the case of PCB-153 ($logK_{OW} = 7.5$), a significant amount accumulates in organisms, as well as sediment (due to the high organic content of sediment and deposition of dead organisms), reducing nearly 50% of the PCB-153 mass in water and air (figure 3.13, 1.4 μg phytoplankton/L vs. 1.4 mg phytoplankton/L). This 1000-fold increment in the organism population enhances the storage effect of both the organism and the sediment compartment. In the PCB-194 scenario (figure 3.14), the organisms and sediment capture 93.7% of the total PCB-194 ($logK_{OW} = 7.65$) under high population density (1.4 mg phytoplankton/L). Among all biotic compartments in the system, the lower trophic levels (Plankton, Mysid, Pontoporeia, and Oligochaete) carry most of the PCB contents, although the PCBs concentration in these species is much smaller than the higher trophic level species. Because the upper trophic level species only acquire 10%-15% of the energy stored in the sub-trophic level due to the food web structure, the low trophic levels could maintain much larger populations compared to the high trophic levels. The significant population assists in creating efficient pathways for PCB storage and transport.

3.4. Overall model prediction evaluation

To evaluate the overall model performance, we summarize the model results and compare to the predictions of the LOTOX2 model, one of the most advanced models specially designed to estimate total PCB concentrations in Lake Ontario (Kaur et al. 2012). The new model simulates the total PCB concentration under different PCB mixture scenarios from 1930 to 2018 according to historical records (Figure 3.15). Although the parameter settings and loading scenarios vary significantly between the two programs, both models achieve similar results.

However, some differences are also noticeable between the two approaches. In the water column, the total PCB concentration in the new model is three to four times higher than predicted by the LOTOX2 model depending on the PCB type and combination. The higher total PCB concentration in water is thought to be partially related to the PCB feedback routines from organisms to the environment.

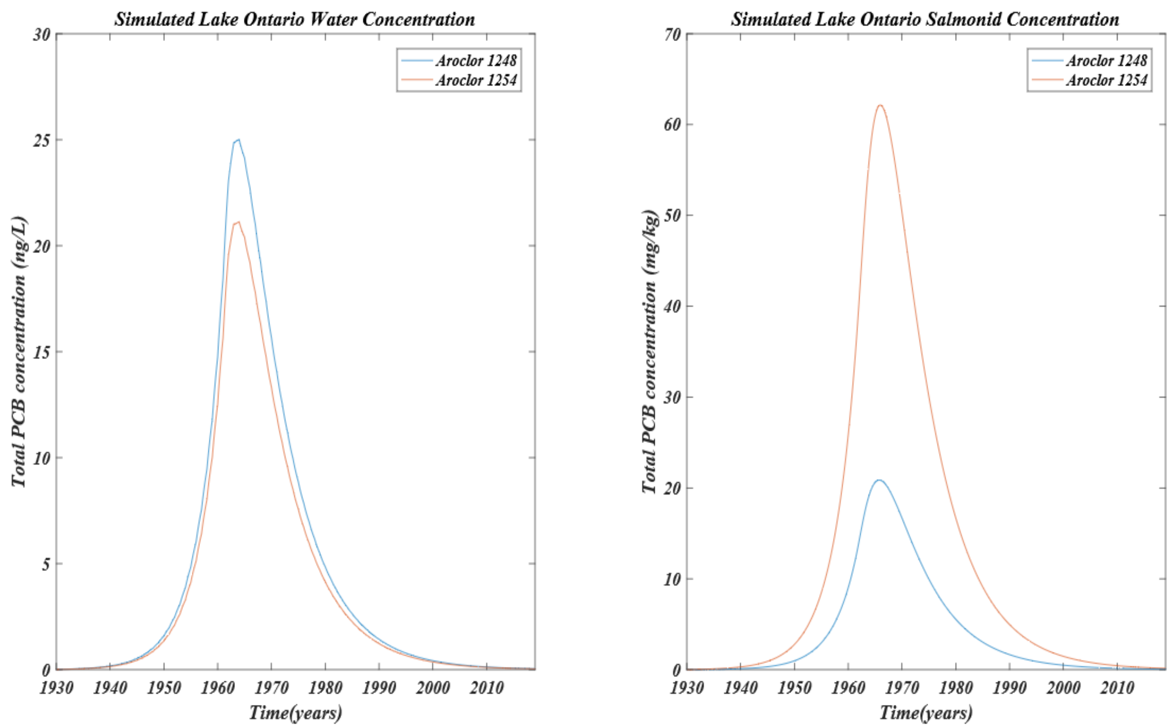

Figure 3.15. Time Dependent Total PCB Concentration of Water and Salmonid

On the other hand, the predictions of the total PCB concentration in lake trout is interesting. When the PCB mixture is assumed as Aroclor 1248, the total PCB concentration is approximately 80% of the LOTOX2 prediction. But if we select Aroclor 1254 to represent the PCB mixture in the model, the total PCB concentration is three times that of the LOTOX2 estimation. Our results are consistent with the inference that the actual PCB loading (chlorine content) in Lake Ontario is a combination of Aroclor 1248 and Aroclor 1254, based on core studies of PCB components in Lake Ontario sediments, this joint Arochlor contribution is also consistent with the trends of Aroclor production history (Hu et al. 2011).

3.5. General sensitive analysis

According to Table 2.3, we have identified a list of parameters which, in our opinion, can affect the PCB distribution and change its behavior during environmental transport. The variation range is determined in several ways. The ranges of some regular environmental parameters, such as temperature, water content, and dissolved oxygen saturation, could be settled from historical study and records. On the other side, parameters which are difficult to monitor or hard to find in previous studies, we use an assumed variation for the analysis. The typical variation range is $\pm 50\%$ of the typical values. Then the program runs under strict controlled condition with only one variable change each cycle. The results are compared to the standard values to determine the impact of the selected parameter. For constant input, all final results are converted into percentage:

$$variation = \frac{C_S - C_i}{C_S} * 100\%$$

Where C_S represents the PCB concentration under baseline values; C_i represents the simulated concentration with the ith parameter changed to a certain level. A group of tornado charts are provided in Figure 3.16. To begin with, the bar with blue color on the left represents a negative impact on the PCB-18 concentration. The negative impact means that if a selected parameter increases by a certain amount, the PCB-18 concentration will decrease under steady state. On the contrary, the bar with red color on the left side indicates that the selected parameter has a positive impact on the PCB congener's level. As observed in the chart, the impact of parameter variation varies significantly among compartments. In the air compartment, the diffusion rate has the most significant impact on PCB-18 concentration and it is a positive effect. It is followed by organism group volume, organism lipid fraction, water content and air retention time. Notice that the organism group volume and the organism lipid fractions are the two factors which belong to the biota compartment and no air-bore organism exists in the current model setting. This result indicates the indirect effects of biota activities during PCB-18 transport. On the other hand, the most sensitive factors in water and sediment are similar, although the impact significances are quite different in these two compartments. In general, sediment compartment is more sensitive to temperature variation than water. Water content, water retention time and water-sediment diffusion rate are the top three factors affecting the PCB-18 concentration distribution. In the water compartment, organism lipid fraction and organism group scale are the two main factors to affect PCB-18 concentration. In these charts, the y axis lists all selected parameters with variations that are considered to have impacts on the PCB-18 concentration distribution. The x axis represents the PCB-18 concentration alternation after applying a certain kind of parameter variation. The bar with blue color on the left represents a negative impact on PCB-18 concentration. The negative impact means that if a selected parameter increases by a certain amount, the PCB-18 concentration will decrease under steady state. In contrast, the bar with red color on the left side indicates that the selected parameter has a positive impact on the PCB congener's level.

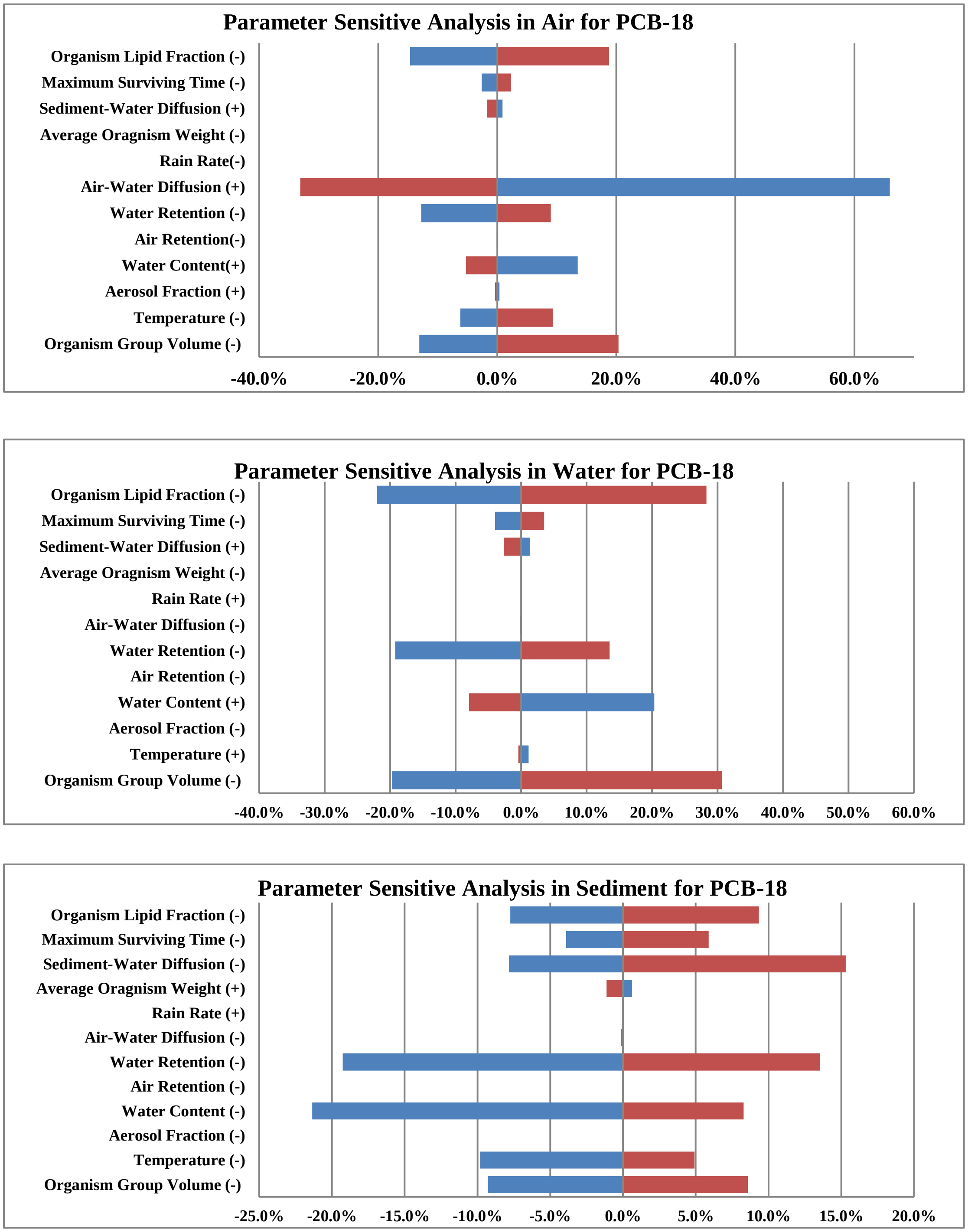

Figure 3.16 Sensitive Analysis for Selected Factors.

However, these patterns are not common rules for PCBs. Due to different physical and chemical properties, the effects of parameter variation shift among different PCB congeners. As shown in Figure 3.17, although for all three PCB congeners, the impact factors are similar, the impact levels are quite different. The effects from organism lipid fraction and scale become more and more significant as the congener number increases. It seems to show that higher PCB congeners are easier to be affected by the organism. One possible explanation is that higher PCB congeners tend to have high K_{OW} and are easier to be absorbed by the lipid content in sediment and organism. In the meantime, the impact levels of other factors seem quite similar among congeners.

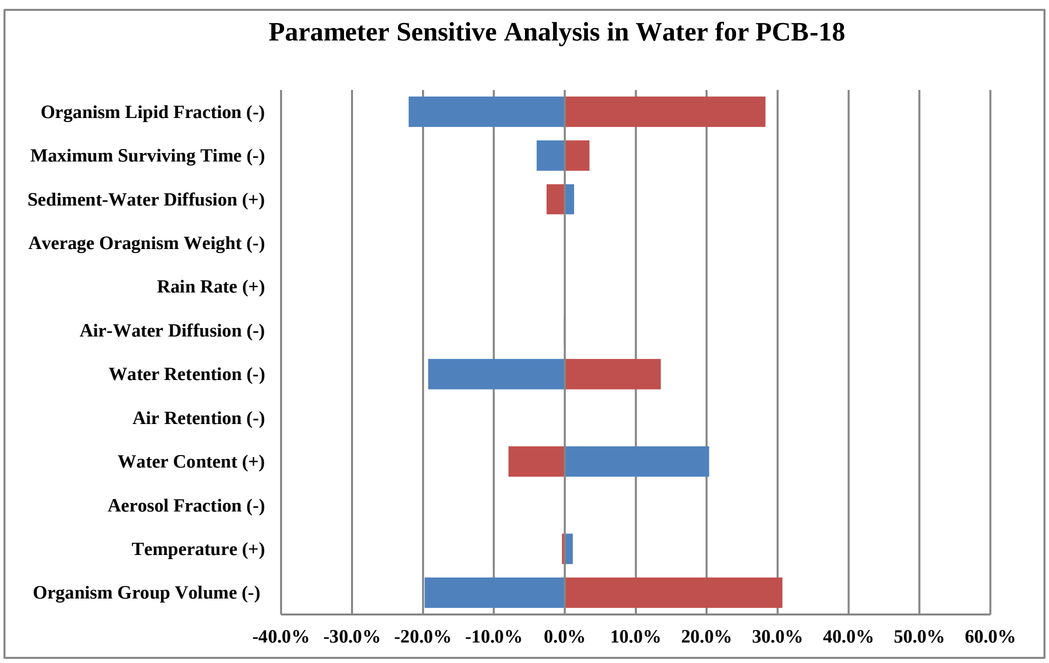

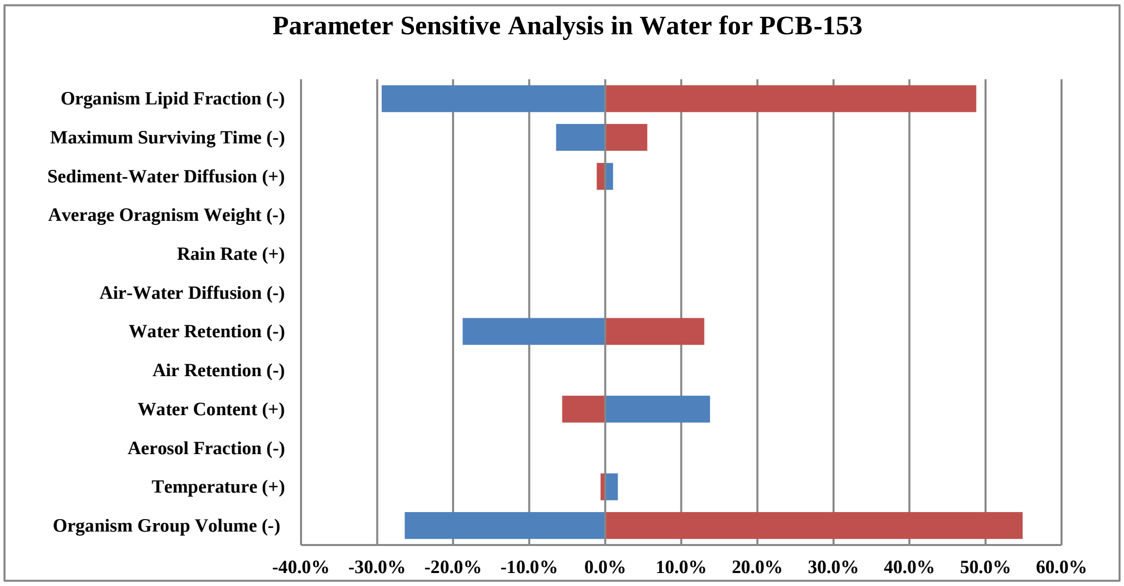

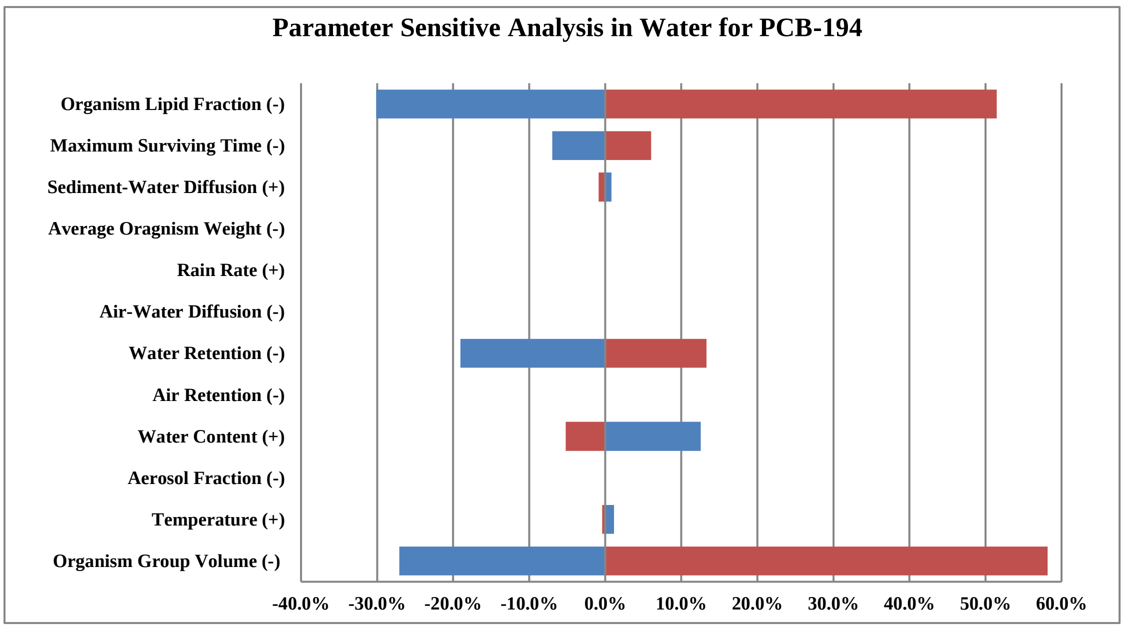

Figure 3.17 Sensitive Analysis for Selected Factors on different PCB congeners in water.

3.6. Temperature variance on overall PCB transport

In section 3.5, we know that the seasonal temperature variance of environmental media seems to have less impact on PCB transport due to the limited variance range of temperature in Lake Ontario, especially in water and air compartments. However, we understand that the fugacity capacity variation is the change of compartmental temperature from section 2.2.3. To study the temperature variation impacts on overall PCB transport and concentration variation, we simulated the model with historical PCB loading (Gobas et al, 1995) and historical temperature records from the Lake Ontario monitoring program (Figure 3.16, NOAA - Great Lakes Environmental Research Laboratory). The results are plotted in Figure 3.17. Notice that we still maintain the constant population assumption in current simulations due to the complex relationship between temperature and population variance among different biotic species.

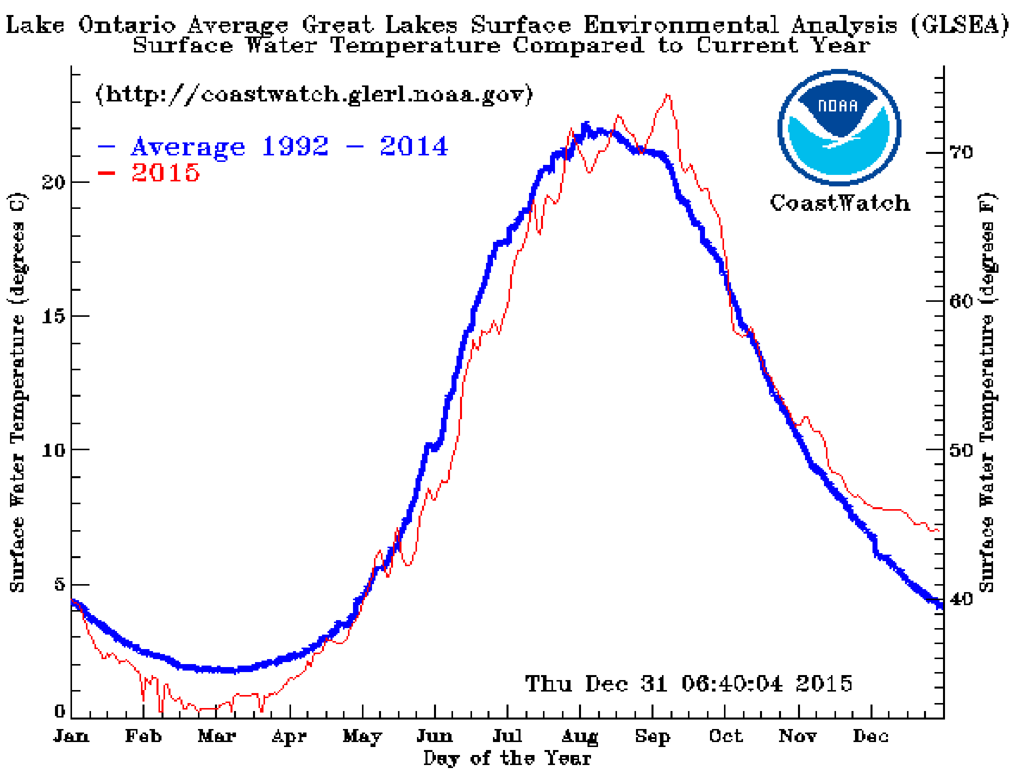

Figure 3.18. Annual Water Temperature Variations of Lake Ontario

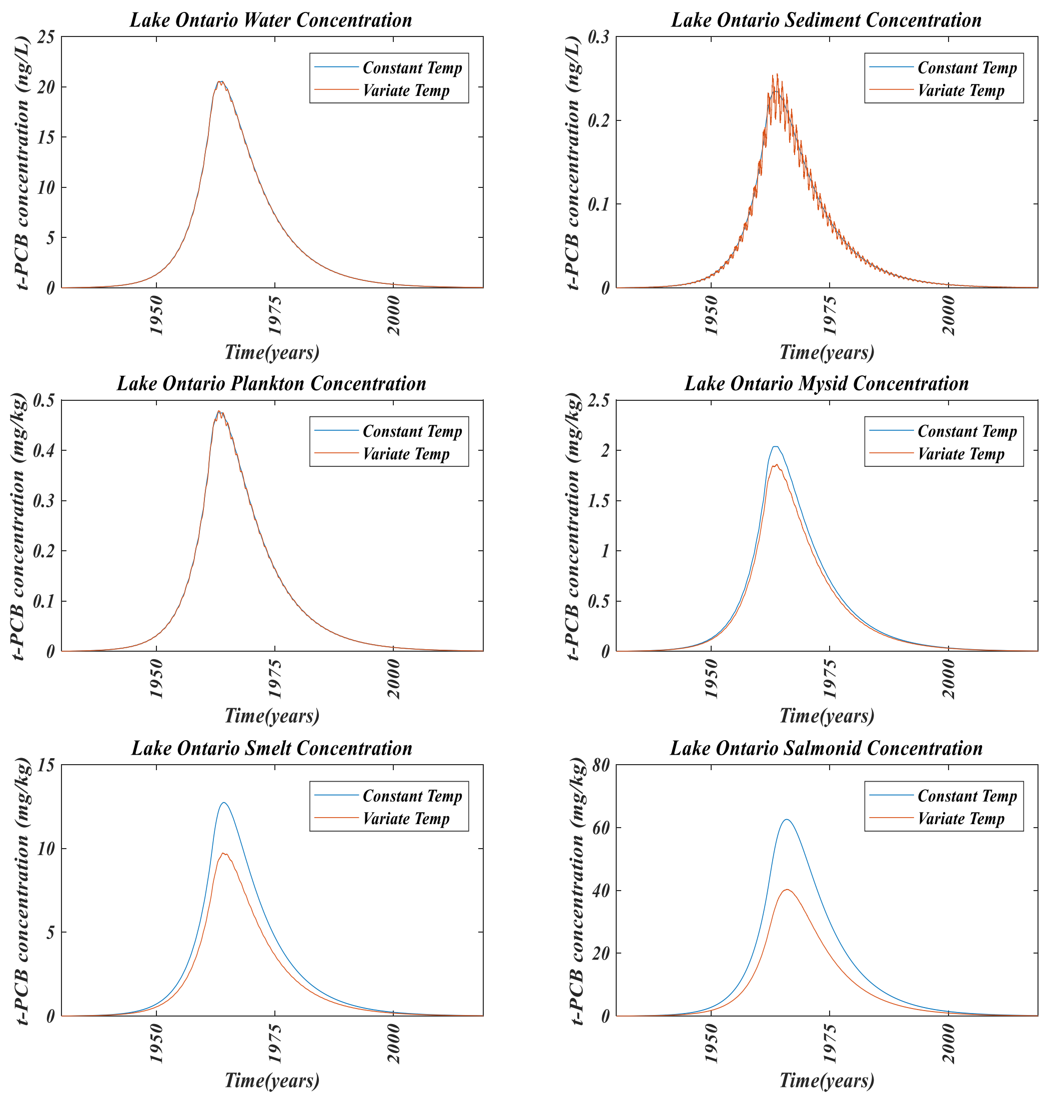

Figure 3.19. Temperature Variations Impacts on total PCBs concentration in Lake Ontario

The temperature variations in water and sediment only trigger a limited degree of oscillation on the underlying curve, but it does not affect the general trend of the PCB concentration changes along the timeline. The approximate average concentration of total PCBs remains similar as the results directly calculated through the average temperature. It is evident that the concentration variation caused by temperature changes is more significant in sediment compare to water. The sediment compartment has no direct PCB input, it only receives PCB contaminants indirectly through water-sediment diffusion and deposition or FBIT transport through organisms. As a result, its concentration is not only affected by its own fugacity capacity changes, but also the PCB input variation from other compartments. In figure 3.19, the PCB concentration oscillation in water is barely observed, but the PCB concentration swings in sediment are very distinct. From formula (55), (61), & (65), we understand that the temperature variation represents the fugacity capacity changes, thus these results indicate that the sediment compartment is more sensitive to the fugacity capacity variation compared to the water compartment.

However, the dynamic temperature reduces the concentration levels in high trophic level species compare to a constant temperature setup. In figure 3.19, the Smelt and Salmonid represent the typical high trophic level species, and we can observe an approximately 20%-40% drop in simulated total PCB concentration under dynamic temperature scenario. This phenomenon can be explained by the food ingestion and the growth of the organisms. From Table A3-A8, the primary route for PCBs to enter the high trophic level organism proved to be the food ingestion, especially for high trophic level species. During spring and summer, the temperature begins to rise and remains high, as well as the growth of primary producers and other low trophic level species. At this moment, although the systematic food ingestion rates are increasing, the growth rates of the low trophic level species are also high. The fast expansion of the individual size reduces the systematic PCB levels in the body, which lowers the PCB mass transfer efficiency through the food web. In contrast, as the temperature begins to drop and maintains low in fall and winter, the PCB concentration in the preys begin to rise due to the slow growth rates, but the diet rates of the predators also drop significantly. As a result, the PCB transport throughout the entire food web is reduced due to dynamic temperature variations, which weaken the long-term accumulation rate of the PCB mass in high trophic level species.

Moreover, these results also indicate that the high trophic level species have little impacts on overall PCB allocations in the environment. Although the accumulated PCB concentration in high trophic levels can be extremely high compared to other compartments, the small population sizes have weakened its effect to a large extent on the overall distribution of PCB mass. From the figure 3.19, it is clear that the concentration in high trophic levels species, such as Smelt and Salmonid, is entirely different under two temperature scenarios. But the PCB concentrations in water and sediment seem to have little changes on an average basis. As a result, when talking about the organism impacts on PCB mass allocation in the environment, we should focus on low trophic level species instead of high trophic level organisms

4. Conclusion

Our new model has been used to evaluate organism impacts on PCB transport through an ecosystem, to provide for a more robust modeling approach. Results indicate that the organism should be treated on a population basis to characterize PCB transport better, especially when the PCB congeners show strong hydrophobicity. Also, the model should not only predict the pollution mass transfer to and from the organism but also maintain equal mass flows to ensure that no pollutant is created or lost without attribution.

The use of an organism population approach allows for more robust explanations of PCB allocation and exchange through the lake system. We introduce a set of new terms to describe the population behavior of the organism and specify equilibrium on organism population. The facilitated biotic intermedia transport effect (FBIT) and the storage effect of organisms are described, and their impacts on the overall PCB fate and transport in the environment are identified. For high hydrophobic and lipophilic PCBs, the organism compartment plays a vital role during PCB transport and takes a significant share of PCB mass once their population size reaches certain levels. Our simulations indicate that organisms not only perform as the receptors during PCB exposure but also act as a primary carrier, providing several primary exchange pathways for PCBs allocation between water and sediment.

4.1. FBIT & Storage Effect

In this study, the facilitated biotic intermedia transport effect and the storage effect of the organism are described, and their impacts on the overall PCBs transport in the environment are identified. For high hydrophobic and lipophilic PCBs, the organism compartments take a significant share of the pollutant mass once their population scales reach certain levels, especially for low trophic levels due to their considerable biomass quantities. Our simulations show substantial evidence that the organism not only performs as the receptors but also acts as a primary carrier and provide the primary transport paths for PCBs exchange between water and sediment, especially for high hydrophobicity PCBs when the organism population is significant.

4.2. Future Study

Opportunities are present to extend the current model further. For example, the FBIT effects could be further expanded if organism migration is taken into consideration. The organism migration process will provide additional PCB removal pathways, reinforce the FBIT effects, and increase the overall net flow rates during PCB transport. Moreover, the fate of post mortality organisms needs more attention, since the details on predation and decomposition alter the PCB flow rate and direction among different environmental and biotic compartments, which eventually change the PCB transport and concentrations. Furthermore, we need additional solutions to evaluate the variation of PCB distributions within each compartment. The current model assumes a homogeneity design. However, a highly variant distribution of PCB concentration is inevitable for large dimension compartments. For instance, the requirement of homogeneity leads the current model to include only the top layer of the sediment. If we want to expand the application of the model into the whole sediment, it may be necessary to add a vertical gradient within the sediment layers.

Part 2 A cross-validation analysis of the empirical rules on polychlorinated biphenyls (PCBs) anaerobic dechlorination

Dechlorination is the dominant process to degrade Polychlorinated Biphenyls (PCBs) in an anaerobic environment. However, PCBs dechlorination mechanisms and their degradation products vary due to different microorganisms and environmental conditions. Our first project focuses on improving the understanding of the empirical rules by using updated observation records and the Monte Carlo cross-validation method, extracting the bio-selectivity features from the pre-existed empirical rules. General patterns of currently reported pathways are also summarized, and comparison of different rules with the PCB observation is given at the end.

5. Introduction

5.1. Polychlorinated Biphenyls (PCBs) Natural Degradation

As a group of the persistent organic compounds, the ultimate fate of Polychlorinated Biphenyls (PCBs), as well as other persistent organic pollutants (POPs), has become a focus of research in recent years. Biodegradation is the conventional process for PCB natural degradation in the environment. It is divided into two main categories: aerobic biodegradation and anaerobic biodegradation, depending on the bacteria presence and oxygen availability (Abramowicz 1995).

The natural elimination of PCBs in the aerobic environment is possible, but this kind of biodegradation is limited to lower homolog groups with fewer chlorine atoms attatched on the benzene rings. (Ahmed and Focht 1973; Zehnder 1988; Abramowicz 1990; Commandeur et al. 1996; Abraham 2002; Pieper 2005; Borja et al. 2005;). The mechanism of PCBs aerobic biodegradation has been identified and key enzymes, biphenyl 2,3-dioxygenases, have been intensively characterized and separated from the environmental background (Gibson and Parales 2000). In this reaction, the microorganisms with biphenyl catabolic genes break the biphenyls rings (the 2, 3-dioxygenase pathway), yielding benzoate and 2- hydroxypenta-2,4-dienoate as reaction products. The final products include water, carbon dioxide, and hydrogen chloride Abramowicz 1995).

On the other side, the PCB anaerobic biodegradation, or dechlorination, has been widely detected and examined in anaerobic sediment layers of several contaminated water sites (Brown et al.

1984; Alder et al. 1993; Bedard and May 1996; Bedard et al. 1997; Fagervold et al. 2007). PCB dechlorination is performed by halorespiring microorganisms and primarily occurs in highly chlorined substances. Unlike the aerobic degradation, the PCB dechlroination reaction removes chlorine atoms from the benze rings and produces a less chlorinated substitutes. This capability is believed to originate from pre-existed dehalogenation reactions, which evolved to degrade aliphatic and aromatic halogenated compounds (Häggblom & Bossert 2003; May et al. 2008). Evidence shows that the population growth of dehalogenation microorganisms has been identified to be positively correlated with PCBs homologous chlorinated levels (Hiraishi 2008). It is believed that the PCB dechlorination can be used as an effective remediation technology for the degradation of heavily contaminated site, such as sediment and deep layer soil in the future.

Understanding the mechanisms and stages of PCB dechlorination is important for practice. However, the separation and identification of PCB dechlorination related microorganisms and enzymes has proved to be extremely difficult and complex, and the engineering applications of controllable PCB dechlorination are still far off. Since the discovery of PCB anaerobic degradation, or dechlorination process, it has taken three decades from the first report of microbial polychlorinated biphenyl (PCB) dechlorination to identify even one of the enzymes responsible (Bedard 2014). Furthermore, the separated enzymes and microorganisms behave differently under various environmental conditions (Wu et al. 1997). As a result, predicting PCB dechlorination using laboratory experiments has become a major challenge in scientific studies

5.2. PCBs Toxicity

The toxicity of PCBs changes significantly among congeners (Robertson and Hansen, 2001). The PCBs toxicity on human health is believed to have short-term and long-term impacts. The most studied and confirmed toxicity comes from a very small number of PCB congeners which have dioxin-like chemical structures. In general, the dioxin-like PCB substitutes are non-ortho or mono-ortho chlorinated congeners. Since the lack of chlorine atoms on ortho positions allows the biphenyl structure to freely rotate along the carbon-carbon bond between the two benzene rings, these congeners might gain more bio-reactivity. In the short-term, the dioxin like PCB congeners usually cause restrictions of Heme synthesis, which triggers the Porphyrin disease, with multiple symptoms, including severe skin rash. The symptoms were first reported by the workers in PCB manufacture facilities, and widely discovered in PCB related accidents (Aoki 2001).

However, the mechanisms of long-term toxicity are still unclear, and the lack of quantitative evidence between PCB exposure levels and cancer incidences make it difficult to have a clear description of PCBs long-term toxicity. It is broadly believed that the accumulated PCB products in human tissues also intrude DNA molecules and induce mutations, thus have teratogenic and carcinogenic effects, causing cancer and leukemia.

5.3. Empirical Rules

Empirical rules are developed since the early stages of PCB dechlorination study as a way of exploring the mechanisms without knowing the specific microorganisms and enzymes. Based on the position of the targeted chlorine atom, the dechlorination pathways usually classified into three general groups: *para*, *meta*, and *ortho.* A dechlorination pathway is determined when a specific congener loses one chlorine atom and transforms into another PCB congener. Without proper rules, the difficulty and workload on distinguishing the correct dechlorination pathways would increase dramatically (VanBriesen 2011). Although the characteristics of PCB dechlorination microorganisms are still rarely known, eight PCB dechlorination categories are summarized based on homolog categories, organism groups, targeted chlorines, and their spatial relationships with other chlorine atoms on the congener structures (Bedard & Quensen 1995; Bedard et al. 1997; Wu et al. 1997). These rules provide excellent guidance for biodegradation degradation study.

Table 5.1. Eight processes dechlorination rules

Dechlorination activity	Targeted Chlorine	Homolog substrate range	Reactive chlorophenyl groups
P	single/doubly flanked para	4~6	34, 234, 245, 2345, 23456
H	single/doubly flanked para, doubly flanked meta	4~7	34, 245, 2345, 345, 234, 2346
H'	single/doubly flanked para & para flanked meta	3~5	23, 34, 234, 245, 2345
N	ortho/para/doubly flanked meta	5~9	234, 236, 245, 2345, 2346, 23456
M	ortho/para/doubly flanked meta & unflanked meta	2~4	3, 23, 25, 34, 234, 236
Q	ortho/doubly flanked meta & flanked/unflanked para	2~4	4, 23, 24, 34, 234, 245, 246
LP	flanked/unflanked para & ortho/doubly flanked meta	3~6	24, 245, 246, 34, 4, 23, 235, 234
T	doubly flanked meta	7~8	2345

The empirical rules (Table 5.1) are created based on in-situ samples & laboratory tests (Hughes 2010). The table was firstly modified by Bedard in 2001, and the red character indicates new supplementary by Hughes et al. in 2010. The characterization includes PCB homolog groups, targeted chlorines, and the spatial relationships with other chlorine atoms on the biphenyl structure (Tiedje et al. 1993; Bedard et al. 1997; Wu et al. 1997). It is believed that the PCB dechlorination preferences come from the bio-selectivity under various microorganisms and enzymes.

However, it is difficult to use the sole empirical rules as guidance to describe the complexity of PCB dechlorination behavior and congener distribution mathematically under specific congener combination and environmental conditions, since the empirical regulations represent the bio-selectivity features of microorganisms and cannot provide quantitative information to distinguish the thermodynamic differences among similar dechlorination.

5.4. Dehalogenation Process

During the dechlorination reaction, PCB molecules replace chlorine atoms with hydrogen atoms, forming lower chlorine content PCB isomers (Borja et al. 2005; Jönsson et al. 2003; Wiegel and Wu 2000). Under anaerobic environment, lack of electron receptors (oxygen, nitrate (NO_3^-)) becomes the main concern for microorganism respiration. To deal with the issue, microorganisms utilize high redox potential aliphatic and aromatic halogenated compounds as the electron receptors (e.g. PCBs, chloroethylene) and hydrogen or other small molecular organic compounds as the electron donators to perform a dehalogenation respiration (Mohn & Tiedje 1992). As a typical reduction-oxidation reaction, each halogenated molecular receives two electrons, and substitutes one chlorine ion (Cl^-) with one hydrogen ion (H^+). The dehalogenation process usually releases significant amount of energy and assists microorganism to realize normal metabolism and reproduction functions. The general formula of PCB dechlorination process is expressed as (Dolfing and Harrison 1992) ：

$$\mathrm{PCB}(C_{12}H_{10-n}Cl_n) + M \rightarrow \mathrm{PCB}(C_{12}H_{10-n}Cl_{n-1}) + M^+ + Cl^-$$

$$\mathrm{PCB}(C_{12}H_{10-n}Cl_{n-1}) + M + H^+ \rightarrow \mathrm{PCB}(C_{12}H_{11-n}Cl_{n-1}) + M^+$$

M represents the electron donors in the reaction. Moreover, the occurrence and termination of PCBs dechlorination reaction also depend on environmental conditions. Temperature, pH, electron donator availability, and electron receptor competition may affect the PCB dechlorination pathway selection (Abraham 2002; Wiegel & Wu 2000; Wu et al. 1997; Nies & Vogel 1991).

6. Model Design and Data Collection

6.1. Observation Data Collection

The observation data is collected from multiple studies in the last two decades. All data sources are listed in table 6.1. The table is modified based on explicitly reported observations from multiple studies on in situ and lab tests. Notice that repeated observations are frequent, but there is no difference using repeated data to train model. A total of 405 explicitly reported dechlorination pathways are collected in the dataset.

Table 6.1. Observed Data Collection

Explicitly Reported Observation	**Source**	**Number of Observation**	Observation Site
Process P	Wu et al. 1997	26	Woods Pond
Process H	Bedard and Quensen, 1995	21	Hudson River
Process H'	Bedard and Quensen, 1995	20	New Bedford; Hudson River
Process N	Bedard and Quensen, 1995	29	Silver River; Hudson River
Process M	Bedard and Quensen, 1995	16	Silver River; Hudson River
Process Q	Bedard and Quensen, 1995	20	Hudson River
Process LP	Bedard et al. 1997	31	Housatonic River
Process T	Wu et al. 1997	7	Woods Pond
Process ARO	Imamoglu et al. 2002	50	Ashtabula River; Hudson River
Process WHO	Van den Berg et al. 2006	18	None
Process LH	Bzdusek et al. 2006	40	Lake Hartwell
Process SBG	Bzdusek et al. 2006	20	Sheboygan River
Process 1260	Fagervold et al. 2007	31	The Chesapeake Bay
Process BH	Demirtepe et al. 2015	93	Baltimore Harbor

6.2. Rules and Assumptions

The improvement of current PCB dechlorination rules involves a deep understanding of the limitation and boundaries of possible dechlorination pathways. Several factors may limit the actual selection of dechlorination pathways: compound structure, PCB mixture combination, dechlorination preference, microorganism features, and environmental conditions. In this study, our purpose is to improve the general rules of PCB dechlorination, so that we only discuss the compound structure, PCB mixture combination, and dechlorination preference, since the microorganism features and environmental conditions may vary significantly from place to place.

First, the PCB congener structure provides the fundamental limitation for dechlorination pathway selection, and it would produce the initial boundary on the availability of dechlorination pathways. The chemical structure of PCB congeners would limit the dechlorination pathways in some cases. For example, double flanked *para* and double flanked *meta* are the most common dechlorination processes in Heptachlorobiphenyl (PCB-170~PCB193) groups. However, PCB-187 only dechlorides through single flanked *para* and single flanked *meta* (*ortho* or *para* flanked), because it does not contain any double flanked chlorine structures.

The second principle comes from the empirical rules. PCB dechlorination processes are divided into three groups: *para, meta*, and *ortho*, based on the position of the lost chlorine atom. For any given PCB congeners, there are four *meta* positions, four *ortho* positions, and two *para* positions for chlorine attachment. Each category is further split based on the side chlorine atom appearance, also known as flanked.

Table 6.2. PCB dechlorination classification based on empirical rules

No.	Dechlorination location	Flanked situation	Arrangement form		Typical group
1	para	unflanked para	X010X	-	4, 24, 246
2		single flanked para	X110X	X011X	34, 234, 245, 2346
3		doubly flanked para	X111X	-	345, 2345, 23456
4	meta	unflanked meta	010XX	XX010	3, 25, 235
5		para flanked meta	011XX	XX110	34, 345, 245, 2345
6		ortho flanked meta	110XX	XX011	23, 235, 236, 2356
7		doubly flanked meta	111XX	XX111	234, 2345, 2346, 23456,
8	ortho	unflanked ortho	10XXX	XXX01	2, 24, 25, 26, 245, 246,2456
9		single flanked ortho	11XXX	XXX11	23, 234, 235, 236, 2345, 2346, 23456

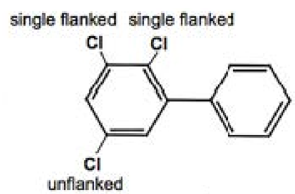

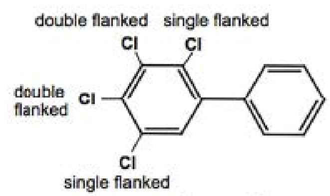

For *para* dechlorination process, it could be unflanked *para*, single flanked *para*, and double flanked *para*. Because the *para* position is axisymmetric, the flanked chlorine atom could only locate at the *meta* position. For *meta* dechlorination process, there are two single flanked *meta* structures: *para* flanked, and *ortho* flanked. No double flanked *ortho* exists under PCB structure. As a result, the current system includes 90 possible dechlorination categories. Table 6.2 is a summary of PCB dechlorination classification. “0” means the position is attached to a hydrogen atom; “1” means the position is attached to a chlorine atom; “X” represents the location could be either chlorine or a hydrogen atom. The red mark on the numbers represents the dechlorination location where the chlorine atom is replaced by a hydrogen atom. In a typical group, the number with underlines indicates the dechlorination position. However, in some *meta* dechlorination process, only one chlorine is removed each tie for the possible process.

The third rule is originated by studying the PCBs production procedure. As previously mentioned, all the commercial PCB products are mixtures of different PCB congeners, and each product contains a specific range of homolog groups. However, the appearances of PCB congeners are not continuous even in those homolog groups. As a result, a small share of congeners has never been observed in any existed product. Although the production process and dechlorination process are entirely different in directions, mechanisms, media, and environmental conditions, it can still provide useful information to generate dechlorination restrictions. The assumption is that if a particular congener has never been observed in commercial products, nor it can be observed in any degradation processes, we can remove the pathways related to these congeners. This rule becomes much more useful when the dechlorination pathways of a specific PCB mixture are evaluated because the single commercial mixture only contains 30%~60% of the total PCB congeners.

6.3. Model Structure

All classification is processed within a Matlab (ver. 2016b) program. The entire classification process begins with a structural database of PCB congeners. The targeted parent congener is broken into the left ring and right ring, and their chlorine structures are identified. The program would randomly remove one chlorine atom from the current structure. The position of the lost chlorine atom is determined by the flanked situation. Then the dechlorined structure is rejoined by the system to identify the child congener. Because of the PCB naming principles, the child congener may need to reshape its structure to meet with the correct order for program recognition. As a result, an additional process is used to reform the new structure for identification. After this procedure, the process is recorded by the program with a parent, child congener, and its dechlorination categories. At this stage, no rule is applied to the processes, and the program identifies all possible dechlorination pathways according to congener structures. After that, the remaining pathways are checked by the production restrictions to eliminate non-existed congeners and remove all related processes.

Next, the program processes a Monte Carlo cross-validation test to figure out the optimal classification method and compare to the current sorting method. In the beginning, the program randomly splits the observation dataset into two groups: the training group (80%) and the test group (20%). The program first runs a classification process of all the observation data with the sorting method in the table. The features of these observations are signed with a classification number and the parent congener's homolog group. Then the program uses the training group to find the dechlorination patterns and rules are generated during the process. However, the observation records may contain some errors which may lead to an unexpected extension in potential pathways. As a result, an extra restriction is provided that the number of observation in training group for each possible pathway must acquire a certain level of significance before identifying as a specific rule. Since the number of potential pathways in each dechlorination category is different, it is necessary to make sure that this restriction works evenly through the entire dechlorination category. We assume that if the number of observation could achieve 20% of the total number of potential pathways in current category, it is significant enough to be identified as a valid dechlorination category. The goal of the selecting process is to achieve a minimum number of potential dechlorination pathways to reduce the complexity of the rules and simplify the analysis, and maximize the prediction accuracy at the same time. According to the variance of different training groups, the rules may have some differences each time. When the training process is complete, the program removes all invalid dechlorination pathways which do not meet the rule requirements and also the repeated pathways in summary. Finally, the program runs the testing group to evaluate the accuracy of the predicted patterns. The entire process repeats for over 100,000 times to eliminate any statistical bias and over-fitting issue.

7. Results and Discussion

7.1. Limitation from PCB congener structure

The total number of the theoretical dechlorination pathways is 840 for all possible PCB dechlorination reactions. In figure 7.1, three colors are used to represent the ortho, para, & meta pathways of PCB dechlorination. Then the different shapes of the lines are used to describe the flanked-categories of the PCB congeners. The color of the frame represents the dechlorination characters of each congener: red frame means the conger has no parent; the blue frame means the congener has no child under current degradation rules; the green color indicates that the congener has neither parent nor child. Thus no dechlorination process occurs in this congener.

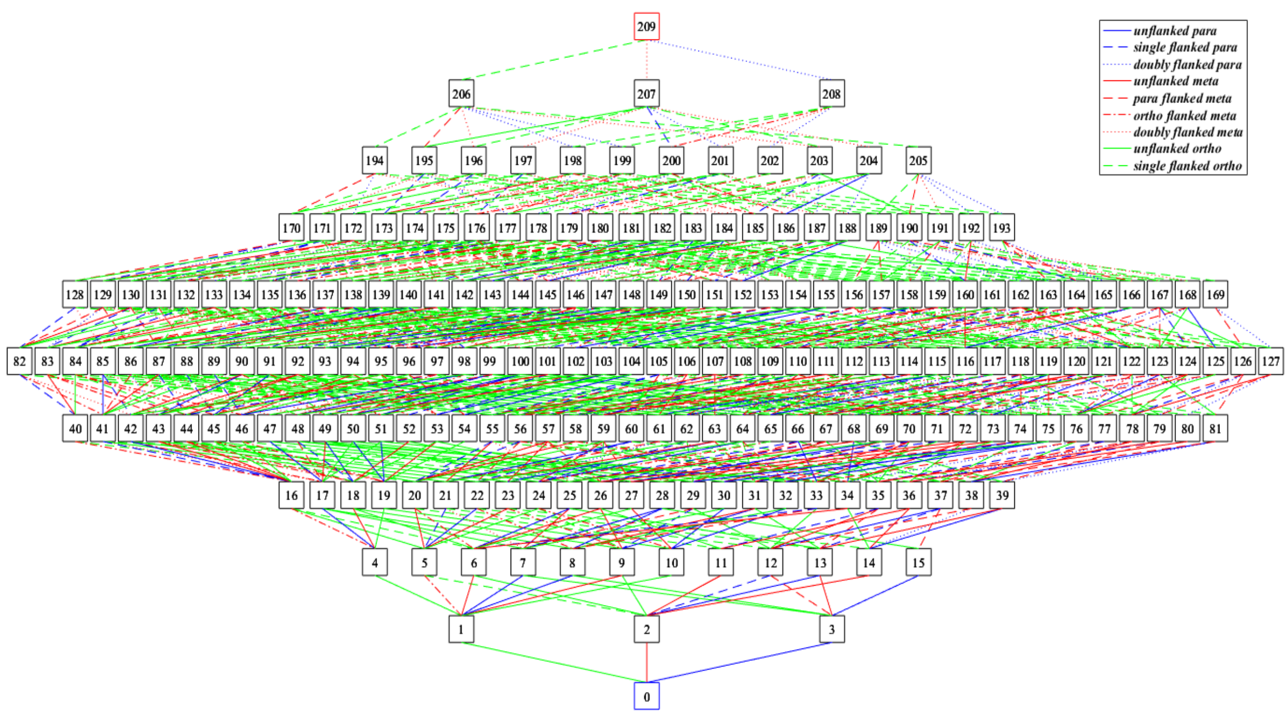

Figure 7.1. Theoretical PCB Dechlorination Pathways

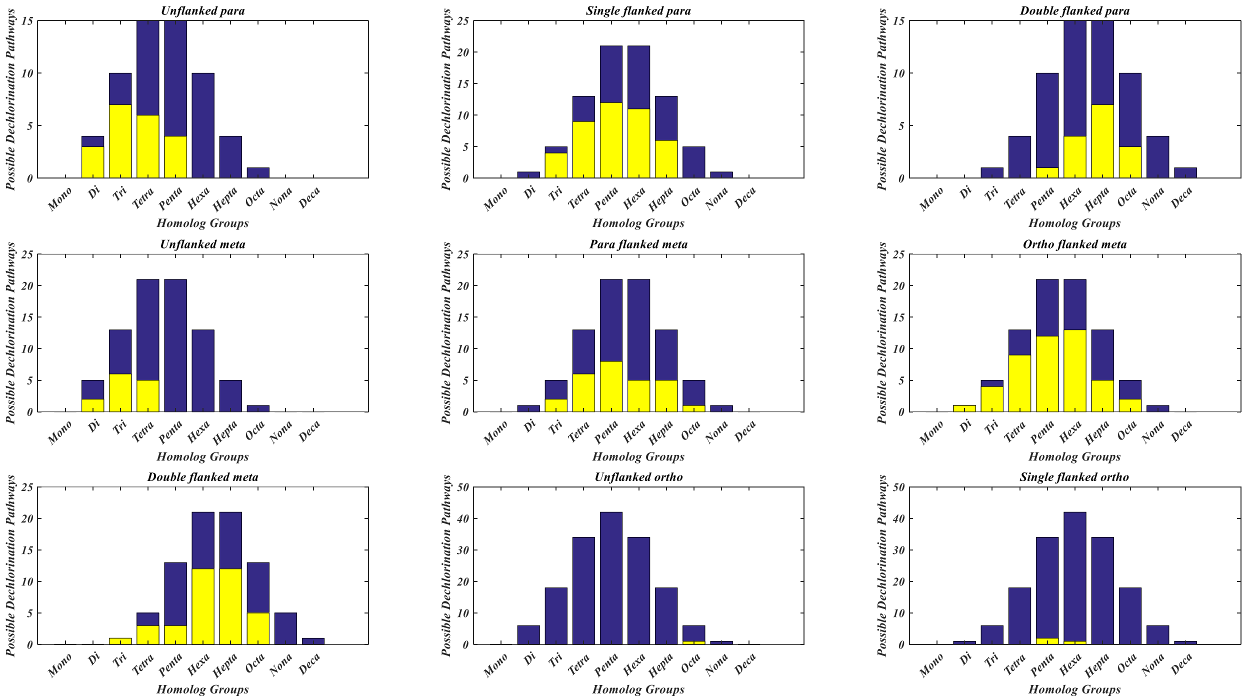

Figure 7.2. Histogram of PCB Theoretical Dechlorination Pathways (blue) and Observed Pathways (yellow).

The PCB theoretical dechlorination pathways do not limit or apply a bias to the dechlorination preference. The histograms of all possible PCB dechlorination pathways are performed in figure 7.2. All pathways are split based on the homolog group (parent) and dechlorination categories. The general dechlorination processes are split into different flank categories with different homolog groups. The repeated observations have been removed to reflect the actual number of existed pathways. The shapes in the entire dechlorination categories are typically distributed if no other factor is considered to affect the selection of specific dechlorination routines. The peak frequency appears in Tetrachlorobiphenyl (unflanked), Pentachlorobiphenyl (unflanked and single flanked), Hexachlorobiphenyl (single flanked and double flanked), and Heptachlorobiphenyl (double flanked) groups, where the homolog groups contain the most PCB congeners. The availability of flanked chlorine structures in each homolog group has small effects to bias the number of dechlorination pathways.

The theoretical dechlorination pathways could be used to determine the redundancy of the observation and make sure the observation pathways do not obey the structure restrictions. 404 valid observations are listed in the original data record. After eliminating the repeated records, 201 valid pathways are recognized from the dataset.

7.2. Observation on PCBs Dechlorination Preference

The preference of dechlorination pathways is challenging to predict since its mechanism with microorganisms is still not fully understood by the scientific community (Bedard 2001). However, previous research has managed to figure out the relationship between preferences and trends of dechlorination pathways under specific homolog groups using statistical analysis.

In general, our analysis confirmed that the *para* and *meta* removal still counted as the primary dechlorination pathways for PCB congeners (Bedard 1995). Figure 7.3 provides the frequency of observed dechlorination pathways in each category. The observed dechlorination pathways are separated into nine general categories based on the position of the removal chlorine atom and the flanked chlorine locations. The frequency counted all the recorded pathways. Some of them are repeated records in multiple studies. *Ortho* removal is very rare and appears randomly in PCB congeners. Unlike the previous study, our analysis indicates higher frequencies of single flanked *para* and *meta* removal than the double flanked removal in the general observation records. One explanation of this preference is that single flanked structures are more common than double flanked structures among PCB congener structures. Another feature of PCB dechlorination pathways is that the observations of *ortho* flanked *meta* pathway are significantly higher than *para* flanked *meta* pathways. According to Bedard, this is probably caused by the competitive relationship between *para* flanked *meta* and single flanked *para* (which is also known as *meta* flanked *para*).

According to the histogram, homolog groups prefer different *para* dechlorination pathways following a robust empirical pattern: the higher chlorine content of a homolog group contains, the more likely it would dechloride from higher flanked positions. For example, double flanked *para* is preferred by high homolog groups (Pentachlorobiphenyl to Octachlorobiphenyl); medium homolog congeners (Trichlorobiphenyl to Heptachlorobiphenyl) tend to dechloride through single flanked *para*; lower homolog groups remove their chlorine atoms through unflank *para*. For each general pathway, the frequency of observation among different homology groups form shapes close to normal distributions. From figure 7.2, we already know that all three dechlorination categories are normally distributed through the homolog groups, and the peak frequency of all three categories appears in Tetrachlorobiphenyl, Pentachlorobiphenyl, and

Hexachlorobiphenyl groups. Thus, the shifts of peak frequency in unflanked *para* and double flanked *para* indicate the relationship between the homolog groups and the preferred dechlorination pathways.

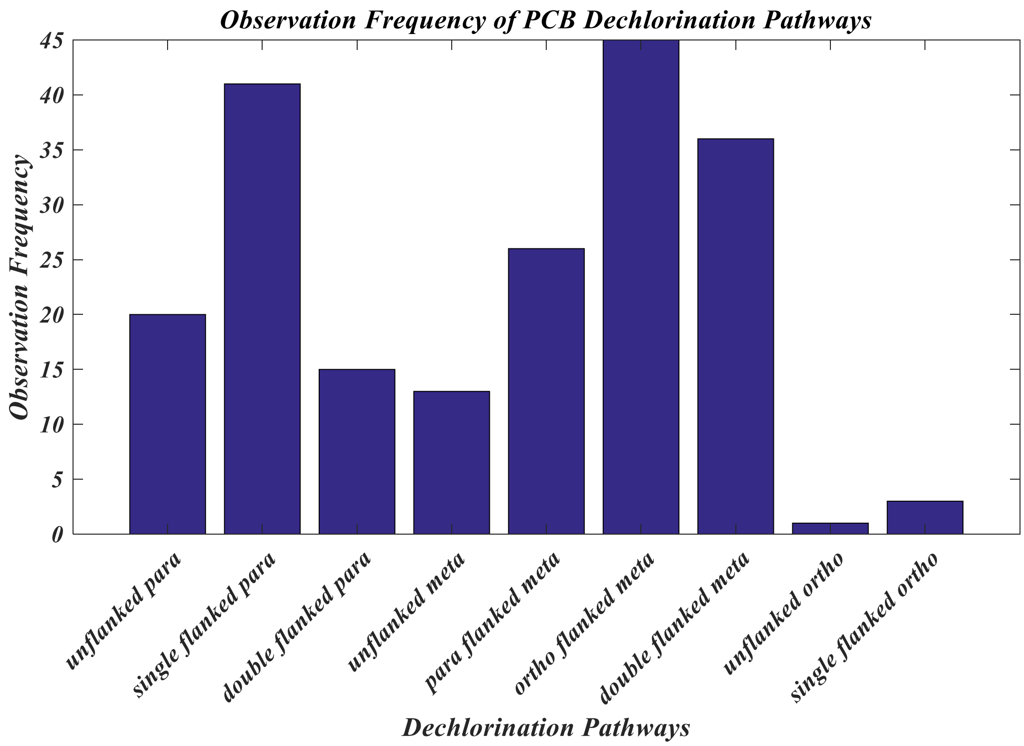

Figure 7.3 Observed PCB Dechlorination Pathways

For *meta* dechlorination pathways, there are two forms of single flanked meta dechlorination. The *ortho* flanked *meta* dechlorination pathways is the most common dechlorination method among PCB congeners. Although the *ortho* flanked *meta* dechlorination processes appear in every homolog groups, it mostly occurs in Tetrachlorobiphenyl, Pentachlorobiphenyl, and Hexachlorobiphenyl congeners. Similarly, the relationship between homolog groups and *meta* dechlorination preference is the same as *para* dechlorination. The double flanked *meta* is often observed in high chlorine homolog groups; *para* flanked *meta* and *ortho* flanked *meta* occur commonly in medium chlorine homolog groups; unflanked *meta* dechlorination appears more frequently in low chlorine homolog groups.

7.3. Cross-Validation for Optimal Dechlorination Rule Selection

Mote Carlo cross-validation method is used to figure out the optimal dechlorination rules. We use two rule systems to define the dechlorination category. The first classification method splits the PCB dechlorination pathways based on the reactive chlorophenyl groups, which can be used as a background rule or blank. The second categorization approach is based on the previous study on PCB structures. Nine general classes are divided based on the position of the removal chlorine (para, meta, ortho) and its flanked structure (unflanked, single flanked, double flanked). 100,000 training cycles give a list of different dechlorination rule combinations for each classification method, and each rule combination is tested for prediction performance. If the second classification method is statistically better than the reference test during training test, we can confirm that the current empirical rules are robust and could be used as bio-selectivity principles for PCB dechlorination modeling.

7.3.1. Reactive Chlorophenyl Group Rules (RCGR)

The reactive chlorophenyl group rules (RCGR) separates the rubrics based on each PCB dechlorination group. The RCGR dechlorination preferences distribution based on training process are listed in figure 7.4. The more a rule is selected during one training process, the brighter of the bar would be in the graph. The frequency chart of RCGR does not provide significant trends since the top 5 selections are entirely different compared to each other, and they are not significant enough to outstanding from other combinations. As a result, the RCGR method is not suitable to determine the optimum dechlorination rules all by its own.

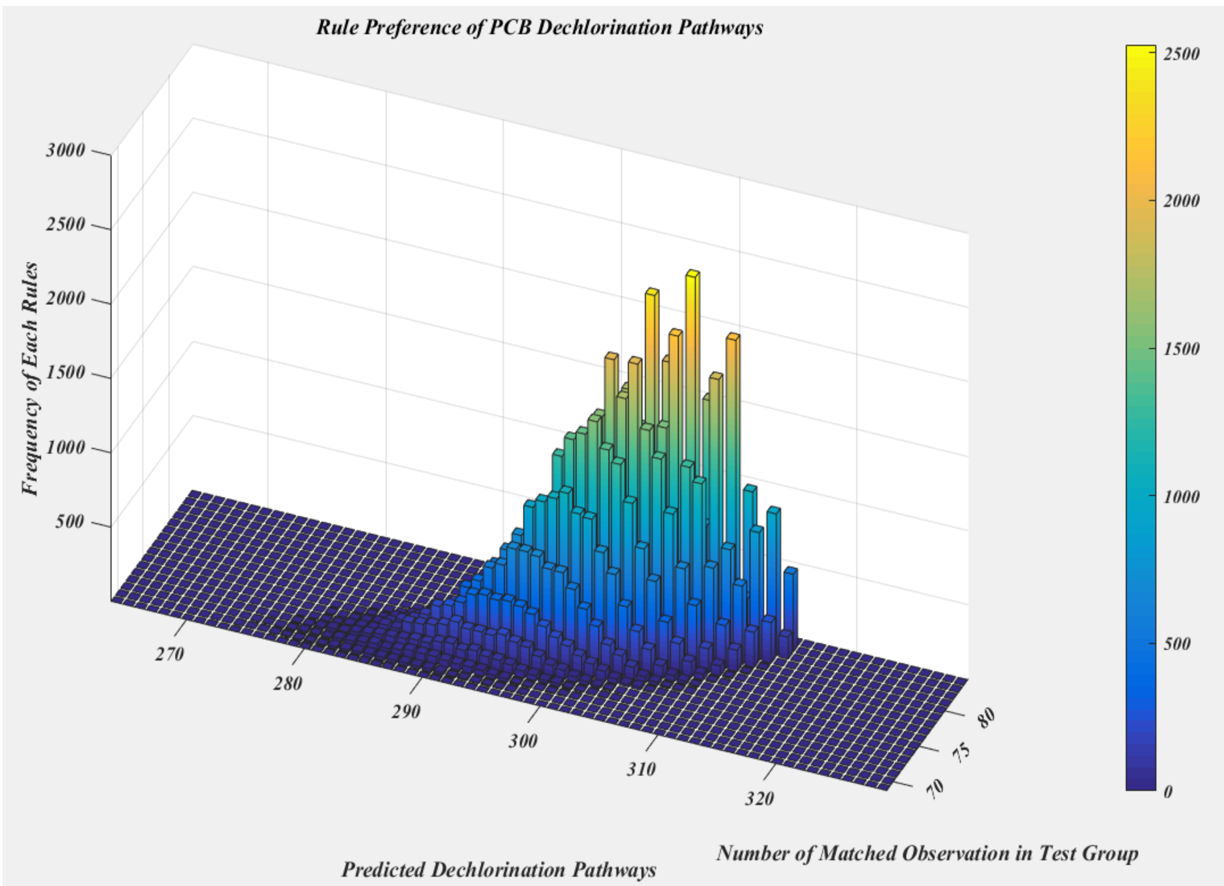

Figure 7.4. RCGR Rule Preference Distribution over 100,000 Training Cycles

7.3.2. General Nine Class Rules (GNCR)

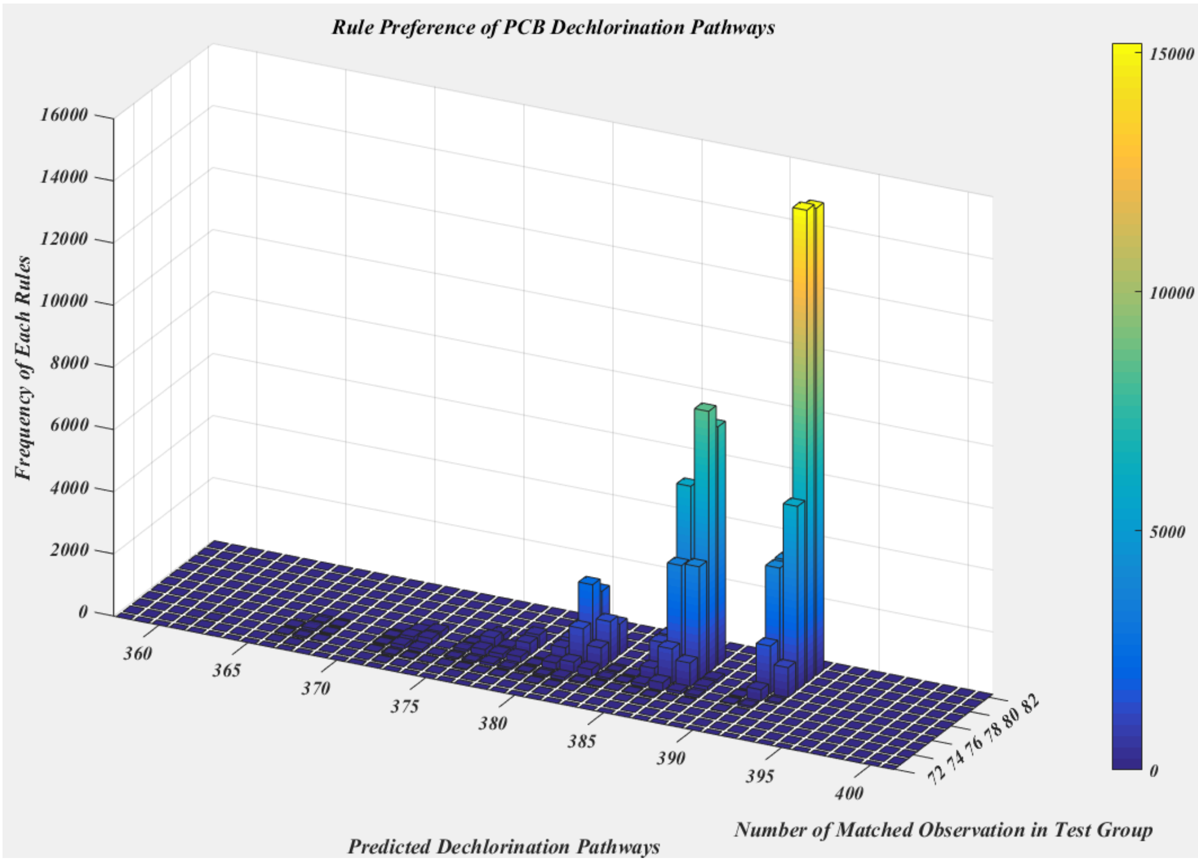

Figure 7.5. GNCR Rule Preference Distribution over 100,000 Training Cycles

On the other hand, the general nine class rules could provide many clear trends on categorizing the PCB dechlorination preference. The GNCR dechlorination preference distribution based on training process are listed in figure 7.5. The X-axis represents the total predicted dechlorination pathways under selected rules; Y-axis represents the testing group (n=81) hits under current prediction rules. The vertical axis (Z) means the frequency of a specific rule is selected by the system from the entire 100,000 tests. The higher frequency a rule is selected during one training process, the brighter of the bar would be in the graph.

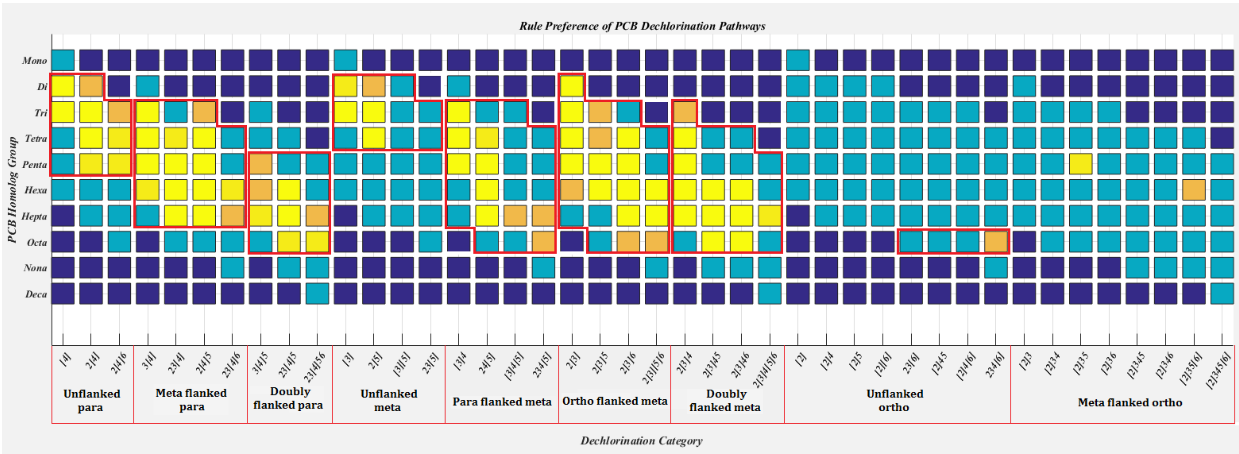

Figure 7.6. The Relationship between RCGR Rules and GNCR Rules

Significant preferences are observed for rule combinations. The top 5 rules (sum up to 51% of the total processes) based on the training process are quite similar with little differences in rule selection. All of them shares approximately 35 out of the entire 90 dechlorination rules. In these rule selections, the prediction accuracy is from 97.5% to 100% with some 387~392 potential dechlorination pathways, depending on the testing group selections. If no additional restriction exists, the rules listed in table 7.1 would be the best training results based on current observations. Current eight processes rules under the same circumstances provide prediction accuracy between 88.1% and 92.3%, depending on the reactive chlorophenyl groups included in the study. The GNCR rule provides more accurate predictions than the general eight processes rules.

However, the improvement in prediction performance of the new rules also leads to a more extensive dechlorination pathway index compare to the old method. Under the eight processes rules, the total number of predicted dechlorination pathways is 330. The prediction index in

GNCR rules increases significantly by 17.2%. Blind increase in pathway index reduces the efficiency of the rules and generates extra difficulties in PCB dechlorination study. As a result, further analysis is provided by introducing other principles as an assist to reduce the current prediction index.

Table 7.1. Most Frequent Trained Rules under Current Observation

No.	Dechlorination location	Flanked situation	Arrangement form		Homolog Group
1	para	unflanked para	$X0\underline{1}0X$	-	2, 3, 4, 5
2		single flanked para	$X1\underline{1}0X$	$X0\underline{1}1X$	3, 4, 5, 6, 7
3		doubly flanked para	$X1\underline{1}1X$	-	5, 6, 7, 8
4	meta	unflanked meta	$0\underline{1}0XX$	$XX0\underline{1}0$	2, 3, 4
5		para flanked meta	$0\underline{1}1XX$	$XX1\underline{1}0$	3, 4, 5, 6, 7
6		ortho flanked meta	$1\underline{1}0XX$	$XX0\underline{1}1$	2, 3, 4, 5, 6, 7, 8
7		doubly flanked meta	$1\underline{1}1XX$	$XX1\underline{1}1$	3, 4, 5, 6, 7, 8
8	ortho	unflanked ortho	$\underline{1}0XXX$	$XXX0\underline{1}$	8
9		single flanked ortho	$\underline{1}1XXX$	$XXX1\underline{1}$	-

8. Conclusion

The statistical analysis indicates that the empirical rules contain significant bio-selectivity features. Even without any thermodynamic principles, the current simulation can provide a clear framework to distinguish PCB dechlorination preference among different categories. However, it is also important to admit that the current selection methods do not include a mechanism to reflect the impacts of environmental conditions and dechlorination mechanisms, as well as the quantitative determination on the order of reaction occurring, when applying on specific PCB dechlorination scenario. Recent studies have shown that PCB dechlorination preference is closely related to temperature, microorganism type, pH, and other environmental conditions. Thus, further updates and new principles on PCB dechlorination predictions should be added for a predictive modeling process.

Part 3: Using reduction potential and bio-selectivity to simulate PCB dechlorination process in anaerobic environment

This study tries to find a possible approach to reappear PCBs dechlorination processes. As a biochemical process, PCB dechlorination not only follows the bio-selectivity principle but also obey the thermodynamic rules in chemistry. Our study shows that a combination of redox potential and bio-selectivity is one of the possible approaches to explain PCBs dechlorination preferences. By estimating the Gibbs free energies through quantum chemistry theories, we evaluate the redox potentials of all PCB dechlorination processes based on the Gibbs free energy and environmental factors, which provide quantitative evidence for pathway selection. A simulation model is created, and the Markov Chain method is applied to provide continuous tracking of the redox potential changes. With proper setup, the dechlorination model can reproduce most of the PCB dechlorination observations from several published reports.

9. Issues and Motivation

9.1. Synchronization Issues in PCB Dechlorination Model Design

To better understand PCB dechlorination in practice, researchers and scientists must deal with the synchronization issues of multiple PCB congeners. Although the empirical rules regulate the bio-selectivity for specific microorganism features, it is rather difficult to mathematically simulate PCB dechlorination behavior and congener distribution under specific isomer combination and environmental conditions, since the empirical regulations cannot distinguish reaction priorities among similar dechlorination pathways through quantitative comparison. The current lab experiments have encountered considerable difficulties in separating and categorizing the microorganisms related to PCB dechlorination process due to a list of technical limitations. As a result, we decide to circumvent the experimental approaches and look for theoretical explanations.

9.2. Redox Potential & Gibbs Free Energy

Redox potential is one of the conventional methods to describe the thermodynamic feasibility of a redox reaction. In 1993, research published by Dolfing pointed out that the redox potential can bu used as a parameter to predict the degradation pathway of chlorinated benzenes, which belongs to the general category of microbial reductive dehalogenaion, in ananerobic environments (Dofing and Harrizon 1993; Mohn and Tiedje, 1992). Although the redox potential cannot be used to estimate the chemical reaction rate directly, it can be used as a quantitative indicator to measure the thermodynamic feasibility of PCB dechlorination preference. The redox potential is usually assessed through laboratory tests. However, it is difficult to directly measure redox potentials of multiple PCB congeners participating in the mechanical complexity of dechlorination reactions (Ho et al. 2015).

As an alternative, we estimate the Gibbs free energy through the thermodynamicc procedure. Thermodynamicc principles have been applied to metabiolism related study since 1930, in an attempt to characterize the role of adenosine triphosphate (ATP) in organisms (Lipmann 1941). From then, the thermodynamic theory has been widely adopted in studying biological reactions and their reacting agents (Alberty 1968; Alberty 1969; Goldberg 1975; Tewari and Goldberg 1991; Alberty and Goldberg 1992; Alberty 2002; Goldberg et al. 2002; Held and Sadowski 2016). The key thermodynamic quantity is the Gibbs free energy of reaction, which can be used to estimate the redox potential of a reduction-oxidation reaction, such as PCB dechlorination.

9.3. Quantum Chemistry

The Gibbs free energy of a given chemical can be calculated through quantum chemistry theory. Quantum chemistry is a brand of computational chemistry which uses computational models to solve the Schrödinger equation for molecular structure analysis, electronic density, orbit distribution, energy content, and so on. In recent years, the development of computational methods and computer technology have become so advanced that it can provide accurate calculations of thermodynamic quantities for compounds with sophisticated molecule structures

(Szabo & Ostlund 2012). However, the accuracy of the theoretical prediction depends on the estimation of the molecular potential energy surface. For complicated molecule structures, the computation cost of accurate description of their molecular potential energy surface is too high. Thus some degree of simplification is necessary, and errors are inevitable during the process (Ho et al. 2015).

10.Model Design & Data Collection

10.1. Estimate Redox Potential of PCB Dechlorination Half-Reaction

According to quantum chemistry, the Gibbs free energy of a given chemical is calculated by finding a proper expression to describe the molecule potential energy (Miertuš̃ and Tomasi 1982). The Density Functional Theory (DFT) is one of the most widely applied methods (Kohn and Sham 1965; Parr et al 1979; Car and Parrinello 1985; Scott and Radom 1996; Orio et al. 2009). DFT uses electron density to calculate the molecular structure and orbit distribution. With proper basis sets, DFT method could provide relatively accurate estimations of molecular potential energy without expensive computation cost (Barone and Cossi 1998). However, the DFT method is not an appropriate solution to directly simulate reaction process, since the fundamental principles of DFT cannot describe the intermolecular interactions (Assadi & Hanaor 2013). Thus, we use the DFT to evaluate the energy levels of PCB congeners and calculate the Gibbs free energy for each dechlorination reaction indirectly.

The sequence of redox reactions in microorganisms follow the electron affinity of the electron acceptors present and can be understood by looking at the redox potentials of the appropriate half-reaction (Zehnder 1988). The half-reaction of the PCB dechlorination could be written in the following form:

$$\text{PCB}(C_{12}H_{10-n}Cl_n)(aq) + H_2O(l) + H^+(aq) + 2e^-(g)$$
$$\rightarrow \text{PCB}(C_{12}H_{11-n}Cl_{n-1})(aq) + [Cl(H_2O)]^-(aq) \dots\dots (81)$$

Since the PCB dechlorination reaction is believed to occur with anaerobic microorganisms, and the reaction is thought to process in the aquatic environment. Thus, the solvent effects should be taken into consideration (Mennucci et al. 1997; Barone and Cossi 1998). Gaussian 09 software provides the option to quantify the impacts of redox potential shifts with different solvent appearance. We select the SMD model and choose water solvent as reaction background to simulate the PCB dechlorination in the environment (Marenich et al. 2009a; Marenich et al. 2009b). However, the SMD solvent model is designed as a discrete-continuum model, and it is likely to neglect the first-solvent shell interaction of species with regions of concentrated charges (Kelly et al. 2006). As a result, it has been parameterized to reproduce the experimental aqueous solvation free energy of the $[Cl(H_2O)]^-$ instead of bare Cl^-.

The standard redox potential estimation could be expressed as:

$$E^0 = -\frac{\Delta G^\Theta}{nF} \dots\dots\dots\dots\dots\dots\dots (82)$$

Where E^0 is the absolute standard electrode potential (1.0 atm, 25°C, $a_{Ox}/a_{Red} = 1$); F is the Faraday constant (96485 C/mol); ΔG^Θ represents the absolute standard Gibbs free energy change of PCB dechlorination half-reaction (81); *n* is the number of electron transfer through the half reaction. The actual redox potential is then calculated through formula (83):

$$E = E^0 + \frac{RT}{F} ln\left(\frac{a_{Ox}}{a_{Red}}\right) - E_{SHE} \dots\dots\dots\dots\dots\dots\dots (83)$$

Where R represents the ideal gas constant; T is the environmental temperature (K); a_{Ox} and

a_{Red} is concentration related coefficients of oxidants and reductants of the half reaction; E_{SHE} represents the standard hydrogen electrode potential, which has been assigned a potential zero in experimental measurements. Since E^0 is the absolute standard redox potential, it needs to calibrate with E_{SHE} before comparing to the experimental measurements (relative value). As shown in formula (83), the redox potential would vary due to the concentration changes of both the reactants and products. Since each PCB congener may have multiple potential dechlorination pathways, redox potential can help us to determine which pathway shows the highest thermodynamic feasibility.

10.2. Model Assumptions and mechanisms

To configure the new model mechanism, we need to understand the limitations and boundaries of PCBs dechlorination: compound structure, PCB mixture combination, dechlorination preference, microorganism selectivity, and environmental conditions. As a result, we defined several regulations based on the study on PCB dechlorination features.

First, the PCB congener structure provides the fundamental limitation for pathway availability. A total of 840 possible dechlorination pathways exist among all PCB congeners (figure 1) if only the chemical structure is considered (Karcher 2007; Hughes et al. 2010). For example, double flanked para and double flanked meta are the most common dechlorination processes in Heptachlorobiphenyl (PCB-170~PCB193) groups. However, PCB-187 only dechlorides through single flanked para and single flanked meta (ortho or para flanked), since no double flanked structure exists in PCB-187.

The second limitation comes from the bio-selectivity (Table 3). Although the empirical rules cannot provide mathematical relationship among different dechlorination pathways, it does represent the general biological preferences of PCB dechlorination pathway selections among the various microorganisms. In most in-situ investigations and lab tests, meta and para dechlorination are frequently observed (Bedard et al. 1996; Bedard 2001; Hughes et al. 2010). In contrast, only a limited number of studies have reported the occurrence of ortho dechlorination, and most of which are site-specific with specific environmental conditions (Wu et al. 1997). Moreover, the bio-selectivity also appears on preference of specific chlorine content ranges. Most of the PCB dechlorination reactions occur between homolog group 3-9 (Imamoglu et al. 2002; Fagervold et al. 2007; Demirtepe et al. 2015). In the new model, bio-selectivity is realized by blocking certain types of dechlorination pathways or homolog groups, adding restrictions for pathway access. There is a total of ninety independent switches to create various of bio-selectivity scenarios.

The third regulation comes from the redox potential. The dechlorination pathway is selected when it fulfills two requirements: the reactant availability and the highest redox potential appearance under current environmental conditions. Since the redox potentials of each PCB congener change as the concentration varies, we introduce the Markov Chain method to realize a sequential simulation. Since dramatic redox potential shift would disrupt the current redox potential status, the program only allows a small amount of selected PCB mass transfer and reevaluate the redox potential shifts through the entire system each time, making sure the chosen dechlorination pathway always satisfies the requirements. The whole process terminates when a specific redox potential level is reached in the system. Notice that the simulation is time irrelevant since the redox potential cannot be used to estimate chemical reaction rate.

10.3. Markov Chain PCB Dechlorination Model

The new model approach is a natural extension to the work of Dolfing, and it involves a full implementation of multiple-step pathways. Although Dolfing uses a small molecule, chlorine benzene, with a simple reaction network, the use of redox potential to estimate anaerobic dechlorination seemed to work well. In our study, we create a series of "states" from the beginning of the dechlorination process to the end of their products, where each state contains a set of all PCB concentrations. Since the congener concentration distribution in subsequent states is established using only information from the previous state, it forms a Markov-Chain.

The simulation begins with the existing dechlorination pathway category. A total of 840 possible dechlorination pathways exist among all PCB congeners (figure 1) if only the chemical structure is considered (Karcher 2007; Hughes et al. 2010). The program then chooses the proper bio-selectivity for the simulation (Table 3). The bio-selectivity is either determined by the empirical rules among various microorganisms or selected by known studies of the targeted environment.

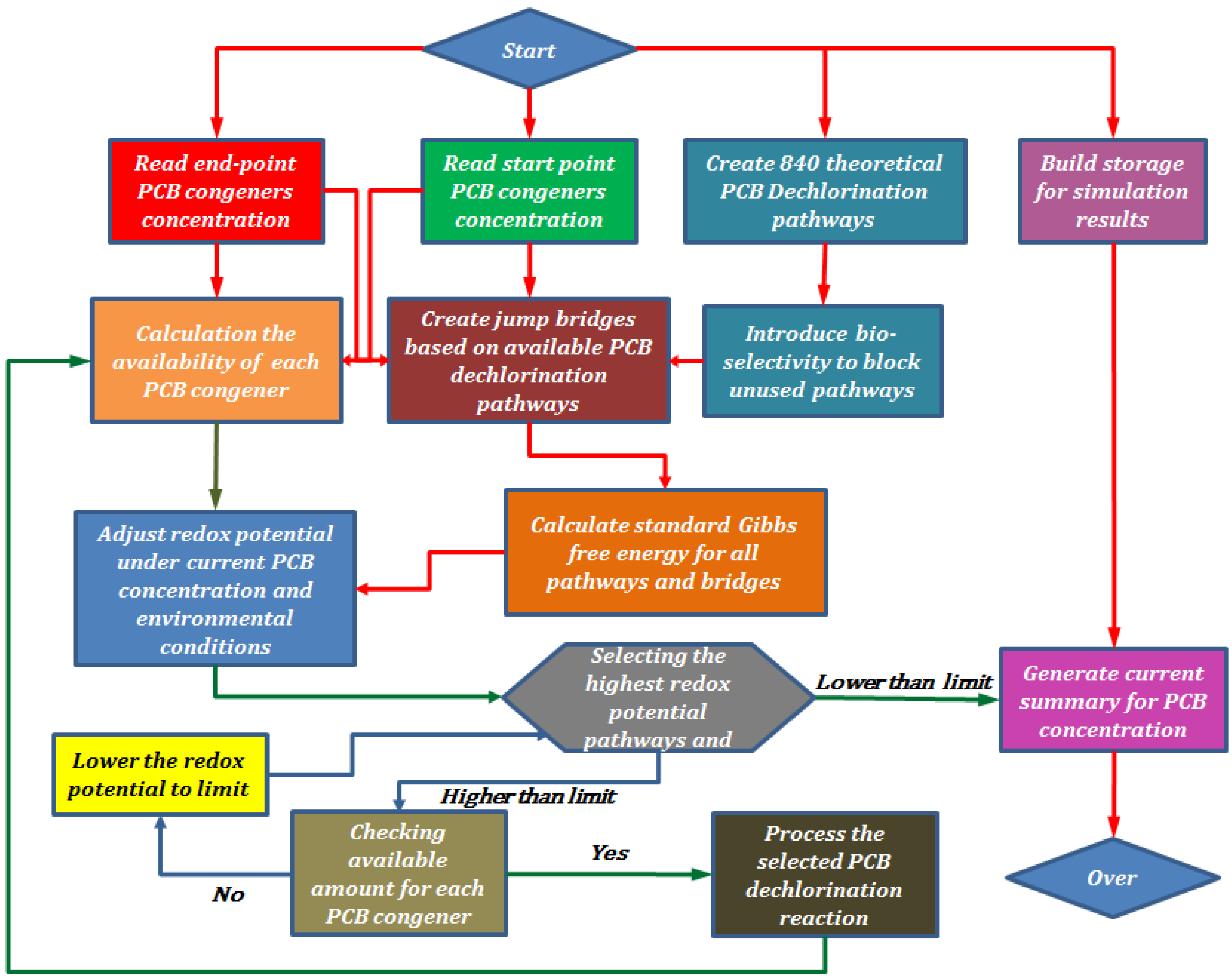

Figure 10.1. PCB dechlorination model design

After blocking the unused pathways, the program establishes multi-step bridges based on the existing one-step dechlorination pathways. This operation is processed based on the following assumption: some PCB congeners might react quickly as intermediate products and disappear in the final products. Since lacking information of those intermedia states in most observations, we introduce bridges to connect reactants to possible products through available one-step pathways and to avoid unintentional blocks. The redox potential of multiple-steps (bridges) is expressed in formula (84):

$$E = -\frac{\sum_{i=1}^{m} \Delta G^{\Theta}{}_{i}}{nmF} + \frac{RT}{nmF} ln \frac{([[Cl(H_2O)]^-]^m [PCB_{h-m}])}{([H^+]^m \, [PCB_h])} \dots \dots \dots \dots \dots \dots \dots \dots (84)$$

Where m is the step numbers; F is the Faraday constant (96485 C/mol); ΔG^{Θ} represents the absolute standard Gibbs free energy change of PCB dechlorination half-reaction from the reactant to product; *n* is the number of electron transfer through the half-reaction; h represents the homolog group number of the PCB reactant.

In each cycle, the model calculates the redox potential of the established dechlorination pathways to evaluate the primary driving force and determine the PCB mass transfer at the current step. The dechlorination pathway/bridge is selected when it fulfills two requirements: the reactant is available for mass transfer and is the highest redox potential appearing under current environmental conditions. Since the concentration distribution of PCB congeners change as the dechlorination process continues and the current redox potential distribution only depends on the previous steps, a Markov Chain is formed to realize a sequential simulation. To prevent disruption caused by dramatic mass shifts during simulation, a small amount of selected PCB reactant is allowed to transfer through the chosen pathway in each step, making sure the chosen dechlorination pathway always satisfies the requirements. The whole process terminates when a specific redox potential level is achieved in the system, or no PCB reactant is available through the system. Notice that the simulation is time irrelevant since the redox potential cannot be used to estimate chemical reaction rate.

10.4. Model Performance Evaluation

To evaluate the model performance, we select three PCB dechlorination observations from published literature. The first dataset comes from Demirtepe which is a typical PCB dechlorination test under lab conditions (Demirtepe et al. 2015). The second dataset is produced by Bedard. In this simulation, the PCB dechlorination is primed by 23456-CB and the flanked meta and unflanked para pathways are significant reinforced (Bedard et al. 1997). The last data source was generated by Van Dort in 1997. According to the literature, the dechlorination test is also primed by 23456-CB. The final product indicates a reinforcement on flanked meta pathways (Van Dort et al. 1997).

All three tests utilize Aroclor mixtures as the dechlorination source. The sole Aroclor 1260 is used in Van Dort and Demirtepe tests, and a combination of Aroclor 1248, 1256, & 1260 is used in Bedard experiment. All three studies provide detailed PCB congener distribution of both reactants and products. Moreover, the standard Gibbs free energy calculation is performed by Gaussian 09 software with Ampac 10.1 GUI software. In this article, we selected DFT method with 6-31+G(d) basis sets for the calculation. The solvent effect is realized through SMD model with the water solvent. The redox potential calculation and PCB dechlorination simulation are programmed and performed in MATLAB (ver. 2016b) software. The original code is available online.

11.Results & Discussions

11.1. The Fundamental Effects of Redox Potential

The redox potential not only assists in determining the pathway selection of each PCB congener but also act as a mathematical indicator and guidance on dechlorination orders among different PCB congeners. According to the step tracking of dechlorination pathway selection records, the program selects dominant high chlorinated PCB congeners with double flanked structures as the beginner, which usually carry the highest redox potential in the system. For these congeners, they typically have several available dechlorination options (after bio-selectivity filter), and the program selects the highest redox potential pathway to process the dechlorination mass transfer. The reactant concentration drops as well as their redox potentials. During this process, the product congeners gain their mass and rise the redox potential. Once the redox potential of these product congeners exceeds the current redox potential or the previous reactants consume all their load, the next congener would be selected to continue the reaction.

The bio-selectivity provides another critical factor in dechlorination pathway selection. For example, Bedard et al. experiment on Aroclor mixtures perform a priming process to reinforce the specific dechlorination pathways (Van Dort et al. 1997). Due to the availability of 2345-CB, the population of microorganisms which join the dechlorination process of PCB- are significantly increased and become the dominant groups in the system. As a result, the dechlorination rules are reshaped, and most of the PCB mixtures perform the flanked meta and unflanked para dechlorination based on monitoring results of the 2345-CB products. To test the importance of bio-selectivity, we use other combinations of PCB dechlorination categories to perform the same Aroclor mixtures, and none of them would reproduce a product set similarly to the observation. As a result, the bio-selectivity is necessary for PCB dechlorination modeling, and it cannot be neglected even if the redox potential is applied in the system.

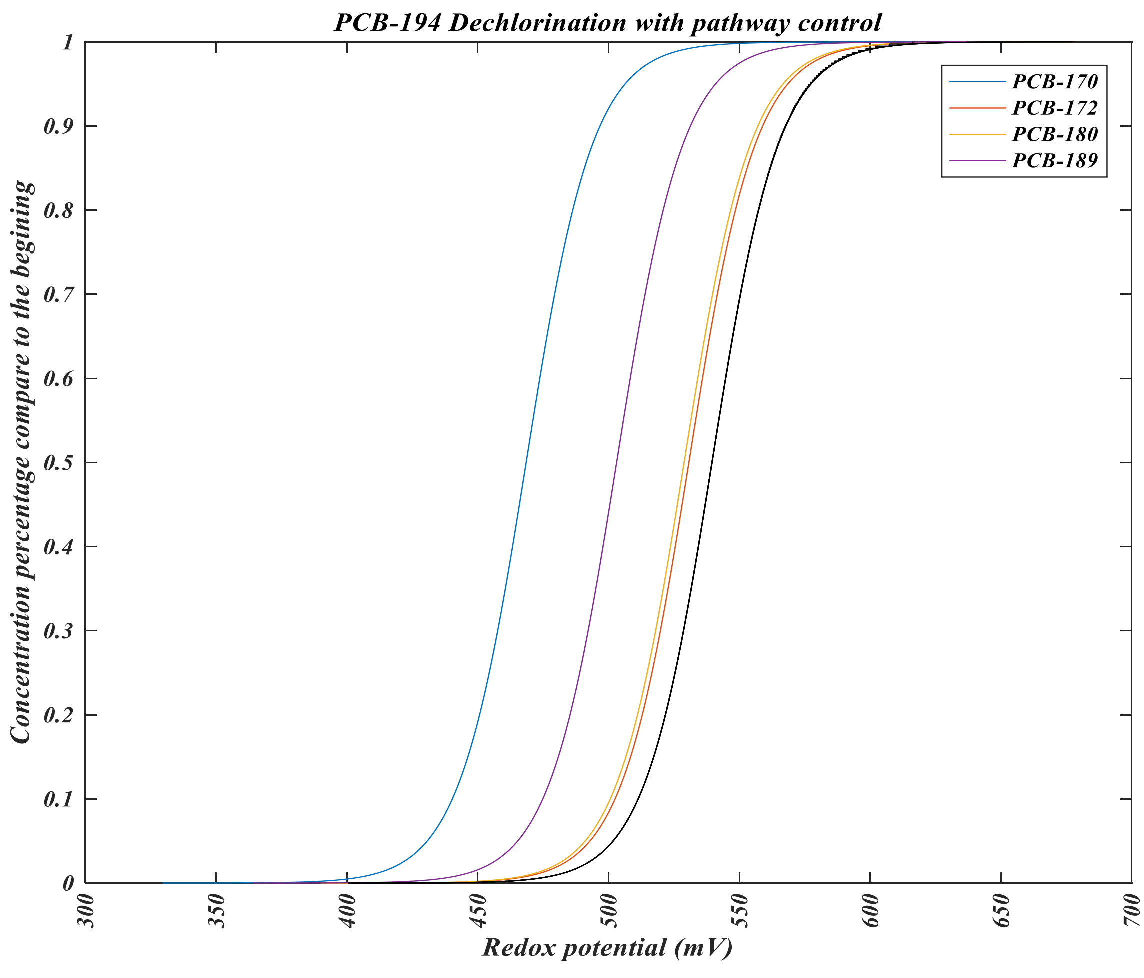

Figure 11.1. Comparison between parallel dropping vs. free dropping (black curve)

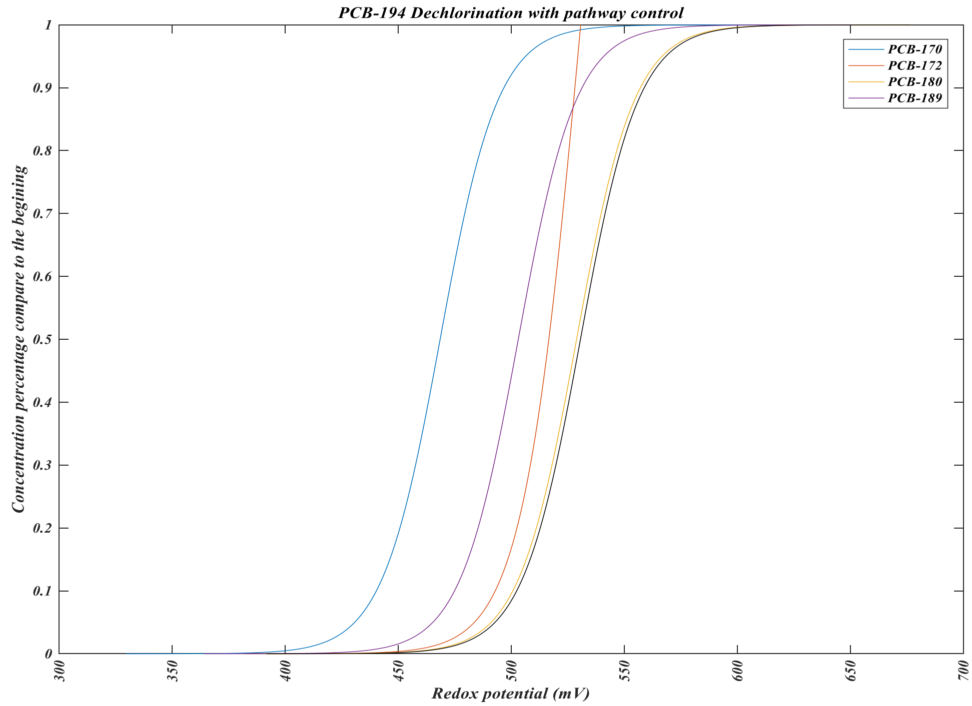

Figure 11.2. Parallel dropping vs. free dropping (black curve, PCB-172)

For any given PCB congener, the redox potential gaps among multiple dechlorination pathways provide the fundamental principle for final dechlorination product allocation. According to formula (83), the concentration ratio between products and reactants is the primary way to alter the gaps in each dechlorination pathways. To further discuss this issue, we begin with the situation where PCB dechlorination with only one path is allowed. If PCB congener is dechlorinated through only one pathway each time (using bio-selection, such as microorganism species, temperature, pH, and so on) and the PCB congener is assumed 100% with no product pre-existed in the system, each dechlorination curve will be parallel to each other along the redox potential drop. Figure 11.1 (colored curves) is an example using PCB-194 dechlorination drops, the standard redox potential for all dechlorination pathways are listed in table 10.1. PCB-194 has four potential dechlorination pathways with different redox potentials. The model is settled for simultaneous free dropping test. All four pathways are available during the simulation without restriction.

Table 11.1 PCB-194 dechlorination simulation with final products allocation

Reactant	Product	Standard Redox Potential (mV)	Accumulated Product Allocation (%)
PCB-194	PCB-170	469	0.40%
PCB-194	PCB-172	531	50.2%
PCB-194	PCB-180	529	43.6%
PCB-194	PCB-189	503	5.85%

In a practical case, all potential products share the same source. If the dechlorination pathway is only determined by the redox potential and the anaerobic organisms can dechlorinate all possible products at the same rate, then the dechlorination vs. redox potential could be plotted in figure 11.1 (black curve). If no restriction on pathway selection, the PCB congener can dechlorinate faster than any single pathway. Moreover, the dropping process will be further speed up if two or more dechlorination pathways exist in high redox potential category. Because the existence of the alternative routes could reduce the “dechlorination drag” formed by the increment of product concentration, which reduces the redox potential of current dechlorination reactions.

In free dropping simulation, we also measure the proportion of PCB dechlorinated products and compare them to the standard redox potential differences. Table 11.1 is an example of dechlorination simulation based on redox potential drop, and the allocation of each product corresponds to the redox potential differences under standard condition. The conclusion is obvious: the highest redox potential pathway gain, the most likely that pathway would generate a more dechlorinated product. In the meantime, the outcome of other routes depends on the redox potential differences with the highest redox potential pathway. As an efficient alternative dechlorination pathway, the redox potential gaps between the alternative pathway and primary pathway should be as small as possible.

Furthermore, since PCB pollution is released to the environment as commercial mixtures, the initial input of PCBs may already have some potential products existed in the system. Based on the redox potential formula, the concentration of reactants and products will affect the actual redox potential in the system, and it would reduce the redox potential of dechlorination specifically for that pathway. To show the case, we reconfigured the scenario with 1.0 nmol of PCB-172 pre-existed in the system, and the redox potential drops for all four possible dechlorination pathways are recalculated. The results are shown in figure 11.2. Notice that the PCB-172 redox potential dropping curve under pre-existed products is an actual part of the original curve. As a result, some of the dechlorination pathways may never occur at all in mixture dechlorination simulations due to low redox potential dropping curve, unless the bio selectivity can prevent most of the higher redox potential pathways.

11.2. Redox Potential vs. Empirical Rules

We evaluate the similarity between empirical regulations and redox potential on PCB dechlorination pathway preference. The empirical rules are created based on observations, and it includes both the bio-selectivity and thermodynamic feasibility. In contrast, the redox potential only reflects the thermodynamic feasibility of each dechlorination pathways, and the bio-selectivity is identified separately as another factor in model simulation. In figure 10.6, we calculate the redox potentials of all 840 dechlorination pathways and classifies the results based on empirical rules. The standard condition is defined as $\mathrm{T} = 25℃, \mathrm{pH} = 7.0, \text{and } [\mathrm{a}_{OX}/\mathrm{a}_{RED}] = 1$. The redox potential is calculated based on the PCB dechlorination half reaction (81) and formula (82). The results are then categorized based on the empirical rule classification. Moreover, we also divide all dechlorination pathways based on homolog groups. If no human factor or lab adjustment (e.g., priming procedure) involves during the process, the trends of the thermodynamic feasibility of the dechlorination pathways are matched with the empirical rules except for both ortho dechlorination groups. According to the empirical rules, ortho dechlorination is the least observed reactions under natural conditions, although the thermodynamic feasibility of both categories is not among the lowest. If the calculation is correct, the rare occurrence of ortho dechlorination may be explained by the bio-selectivity in natural conditions.

The highest similarity between observation and simulation when the redox potential reaches 330 mV ~ 350 mV in the system. According to the redox potential status, the PCB dechlorination terminates at tri- & tetra- homolog groups and most mono-, di-, tri- homolog group congeners cannot process, which matches the conclusion in empirical rules. Most of the dechlorination reactions occur with homolog group 3~9 (PCB-209 is not a typical product in commercial Aroclor mixtures) (Hughes et al. 2010; Kuipers et al. 1999). Notice that the summary of redox potential does not exclude lower redox potential pathways in each homolog groups, which could explain the lower boundaries of redox potential in each category.

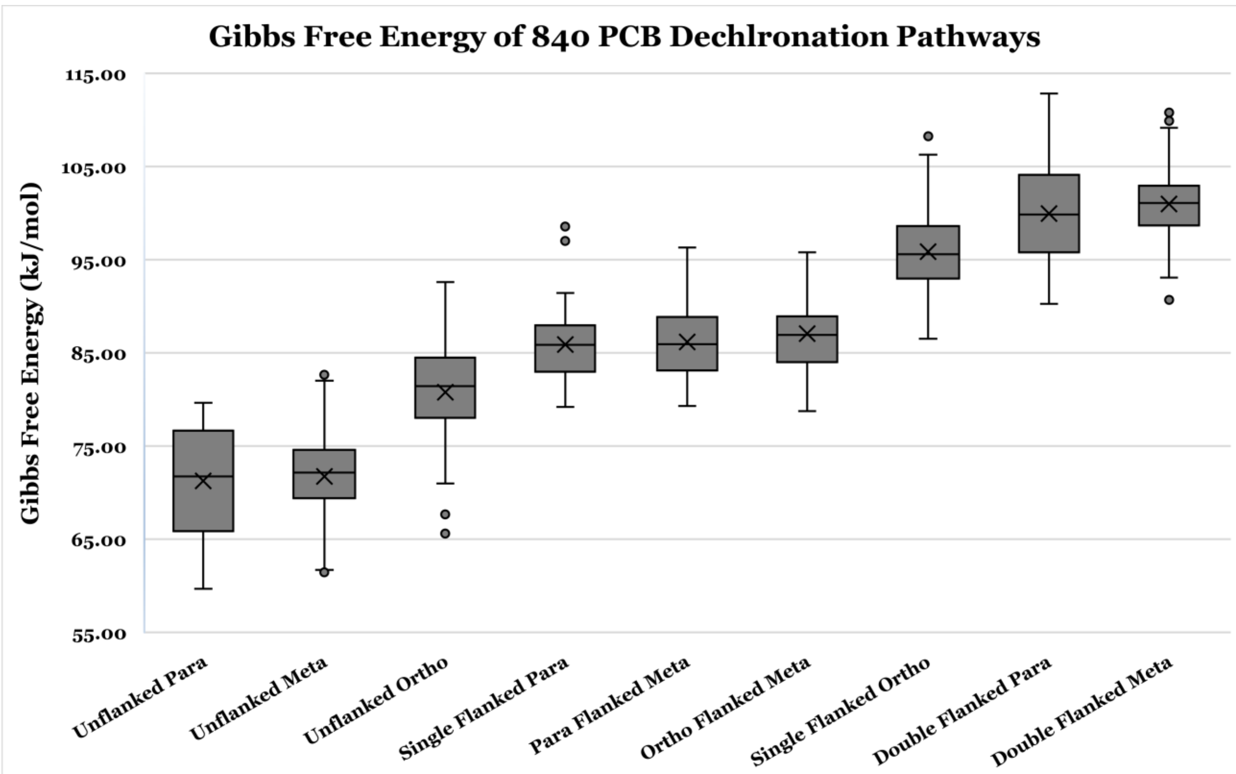

Figure 11.3. Gibbs Free Energy of 840 PCB dechlorination under Standard Condition

11.3. PCB Dechlorination Simulation

The simulation tests prove the capability of redox potential on tracking and predicting the PCB dechlorination under specific bio-selectivity situations. The summarize of all three simulations are listed in figure 11.4 to figure 11.6. Among all three figures, figure (a) represents the original

PCBs distribution & observed post-dechlorinated PCB mixtures; figure (b) and figure (c) show different bio-selectivity scenarios. Each figure set includes two figures: the difference comparison between simulation and observation, and the congener distribution when the prediction and observation are the closest. If the correct bio-selectivity (e.g., priming on microorganism species) is chosen, the model should produce a dechlorination mixture very much like the observation. All dechlorination simulation show a termination point between 330 mV and 350 mV, where the observations and simulations of post-dechlorinated PCB mixture have the highest similarity (8.5%~15%).

Two reasons can explain those prediction errors. First, PCB redox potential is calculated rather than directly measured, and the DFT method and 6-31+G(d) basis set sacrifices some level of accuracy to achieve computability. Since the influences of computational compromise are most likely uneven among different PCB congeners, the calculated redox potentials may change the status of each dechlorination pathways, and cause errors on the dechlorination pathway determination (Ho et al. 2015). Furthermore, due to the limitation of gas chromatography techniques, the analytical result of PCB mixture includes some small unseparated PCB congener groups (up to four PCB congeners). Under current technology, we can only distinguish the components of these mixtures based on the overall component record of similar products, which generate significant errors during dechlorination simulation. Because the combination of PCB mixtures is critical for the modeling program to establish initial status of PCB congeners.

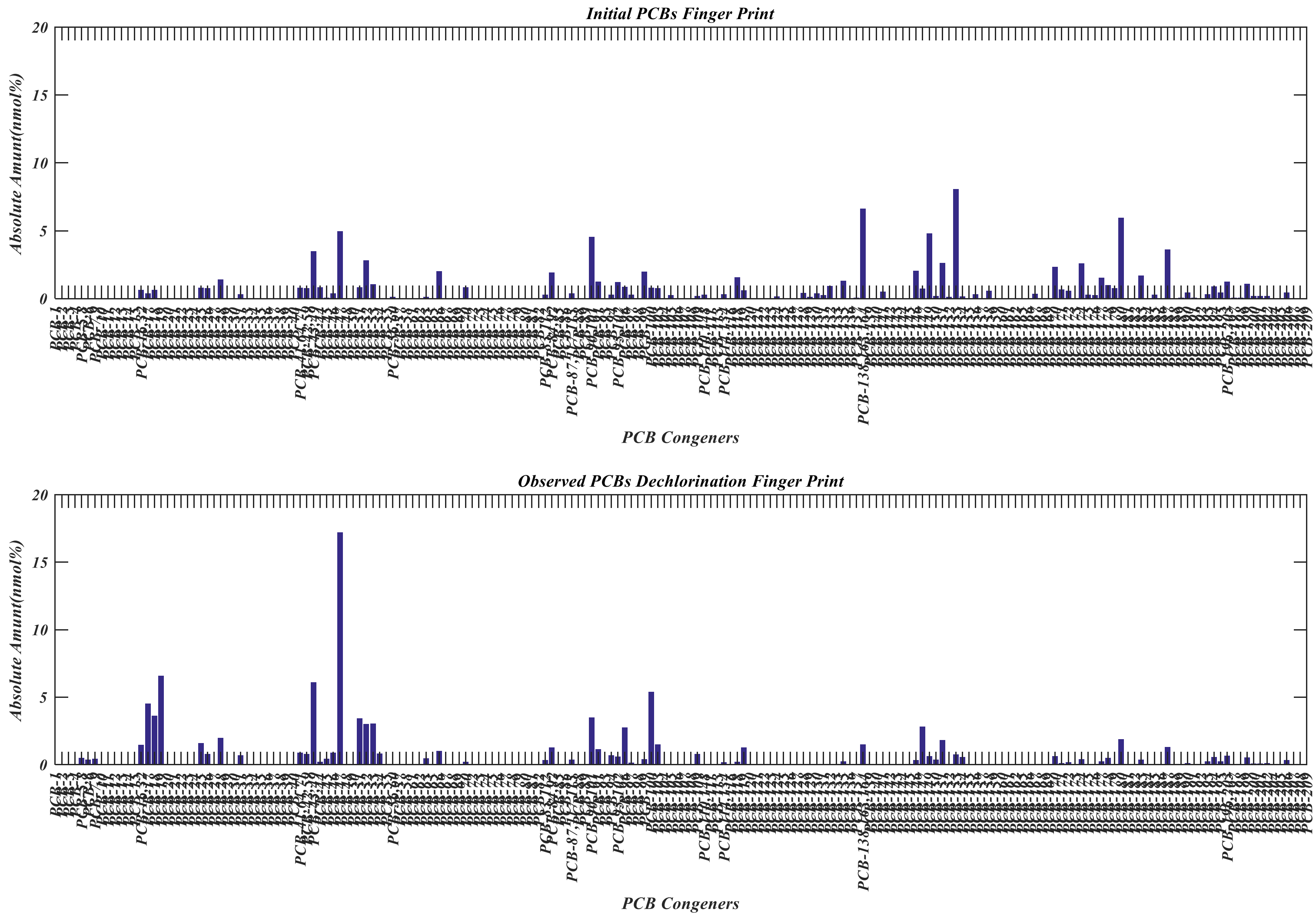

Figure 11.4a. Original PCBs Distribution & Observed Post-Dechlorinated Products (%mol, Bedard 1997)

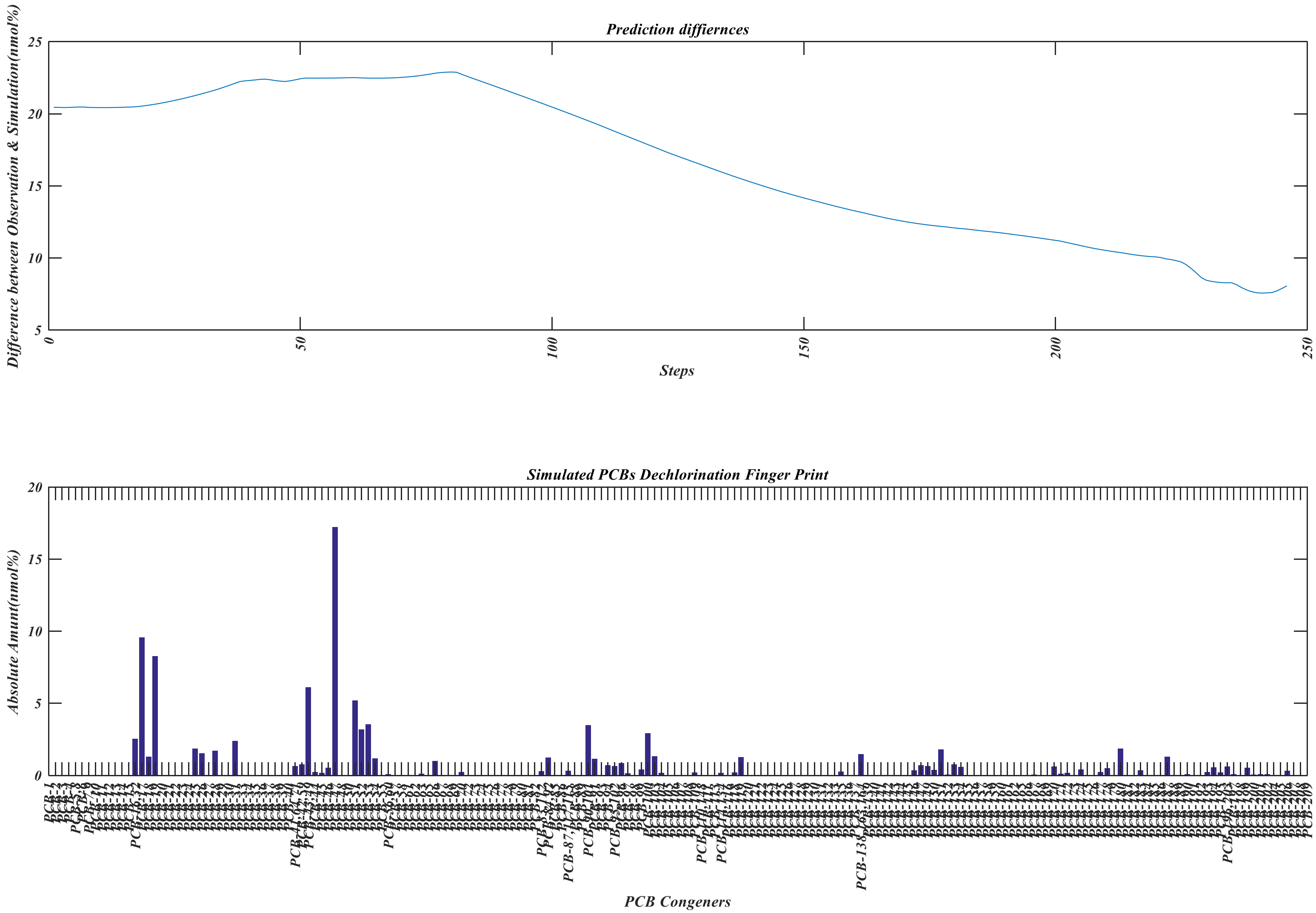

Figure 11.4b. Simulated Dechlorinated Product Difference & Simulated PCBs Distribution (%mol, meta priming, Bedard 1997)

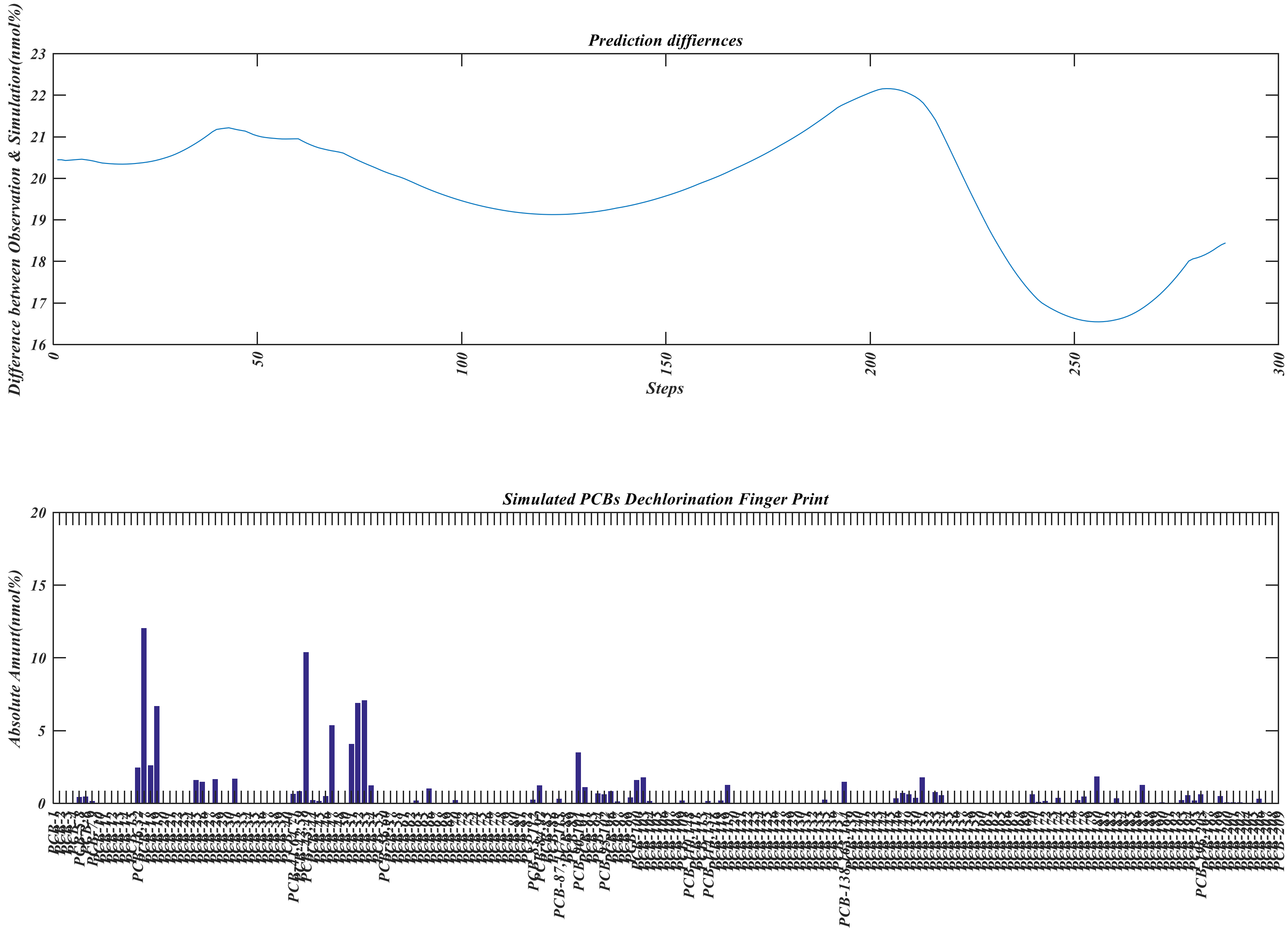

Figure 11.4c. Simulated Dechlorinated Product Difference & Simulated PCBs Distribution (%mol, no priming, Bedard 1997)

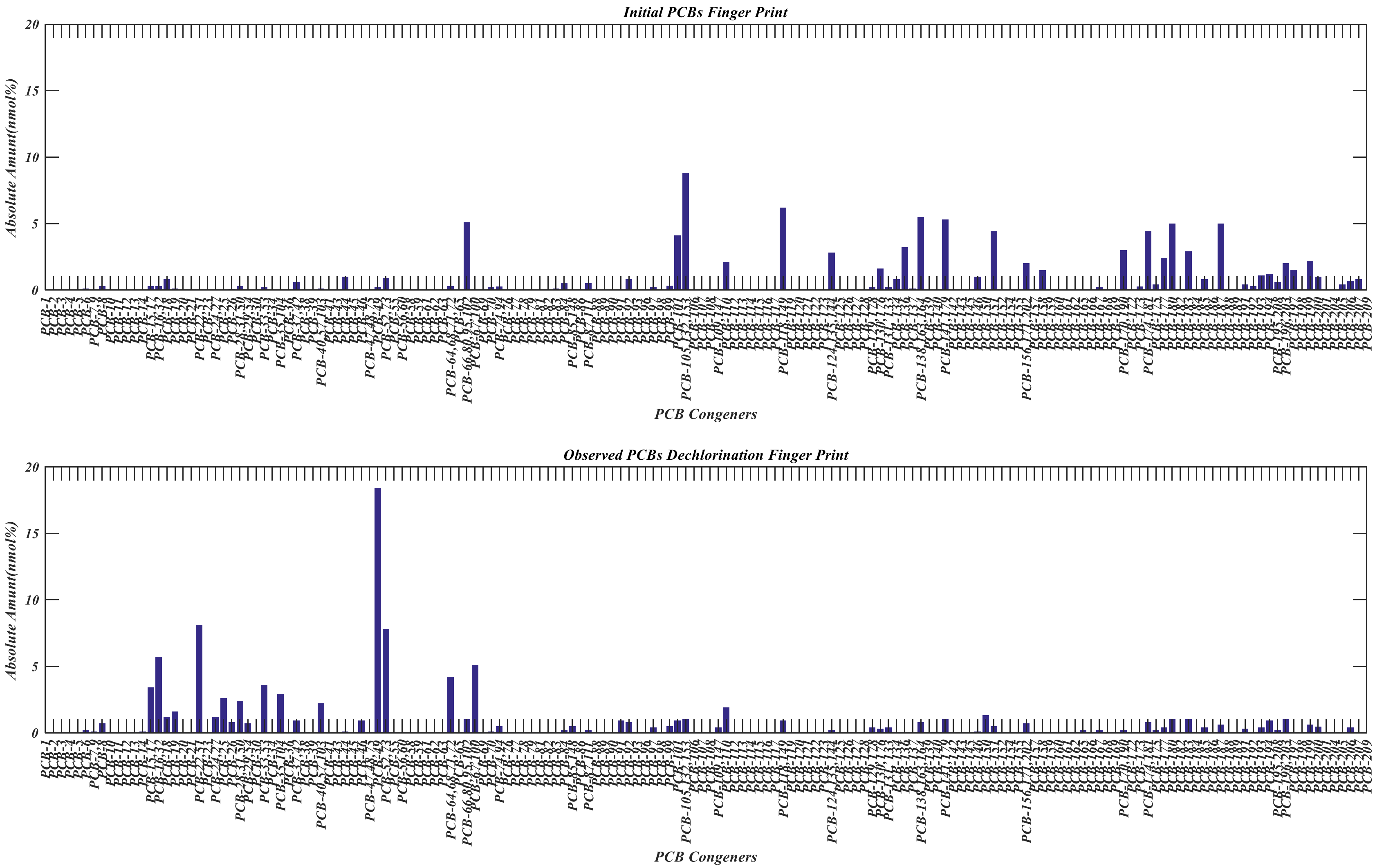

Figure 11.5a. Original PCBs Distribution & Observed Post-Dechlorinated Products (%mol, Demirtepe 2015)

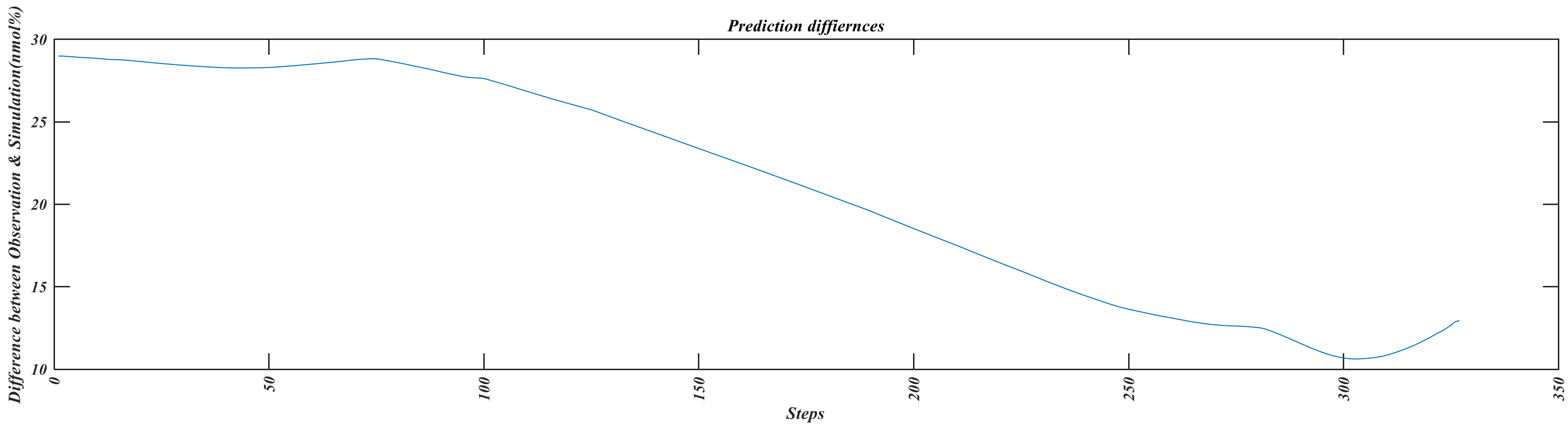

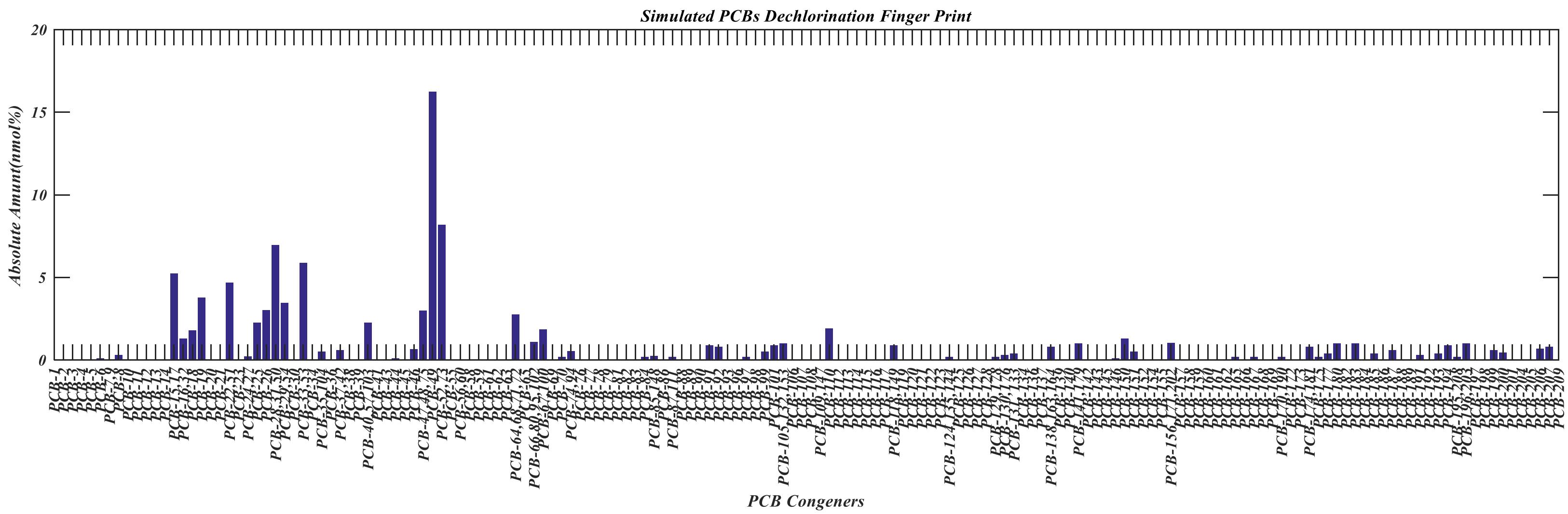

Figure 11.5b. Simulated Dechlorinated Product Difference & Simulated PCBs Distribution (%mol, no priming, Demirtepe 2015)

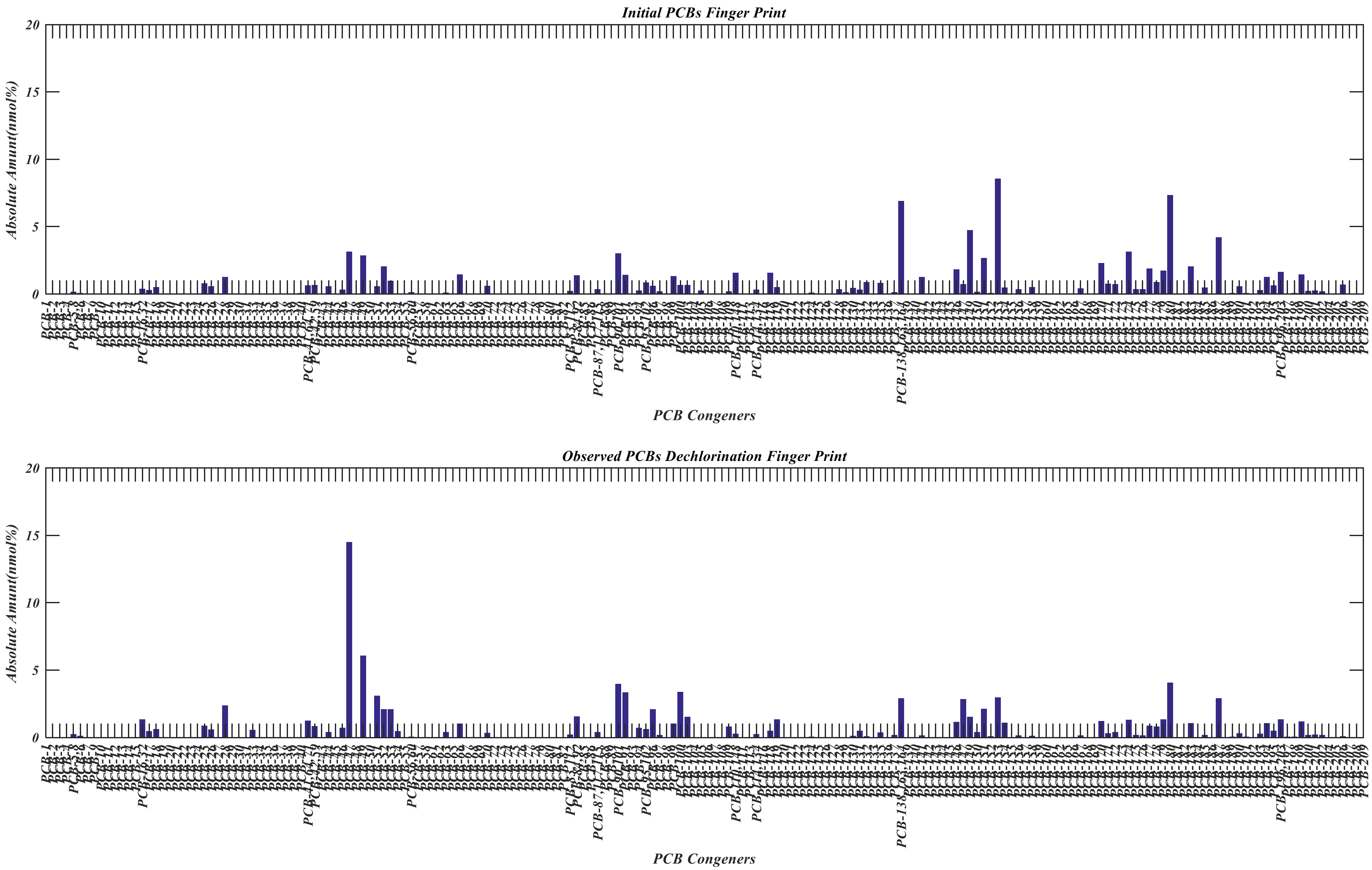

Figure 11.6a. Original PCBs Distribution & Observed Post-Dechlorinated Products (%mol, Van Dort 1997)

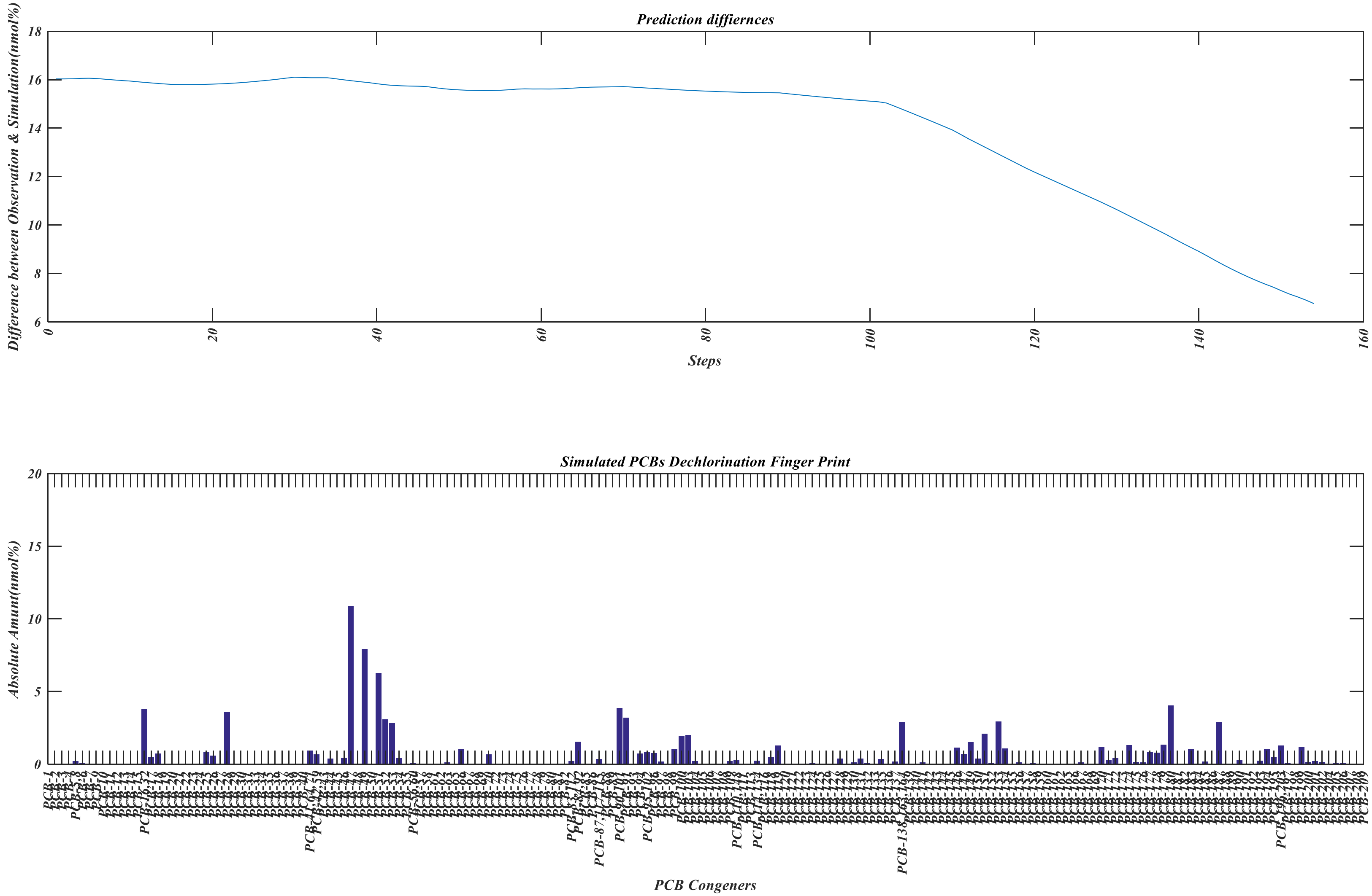

Figure 11.6b. Simulated Dechlorinated Product Difference & Simulated PCBs Distribution (%mol, meta priming, Van Dort 1997)

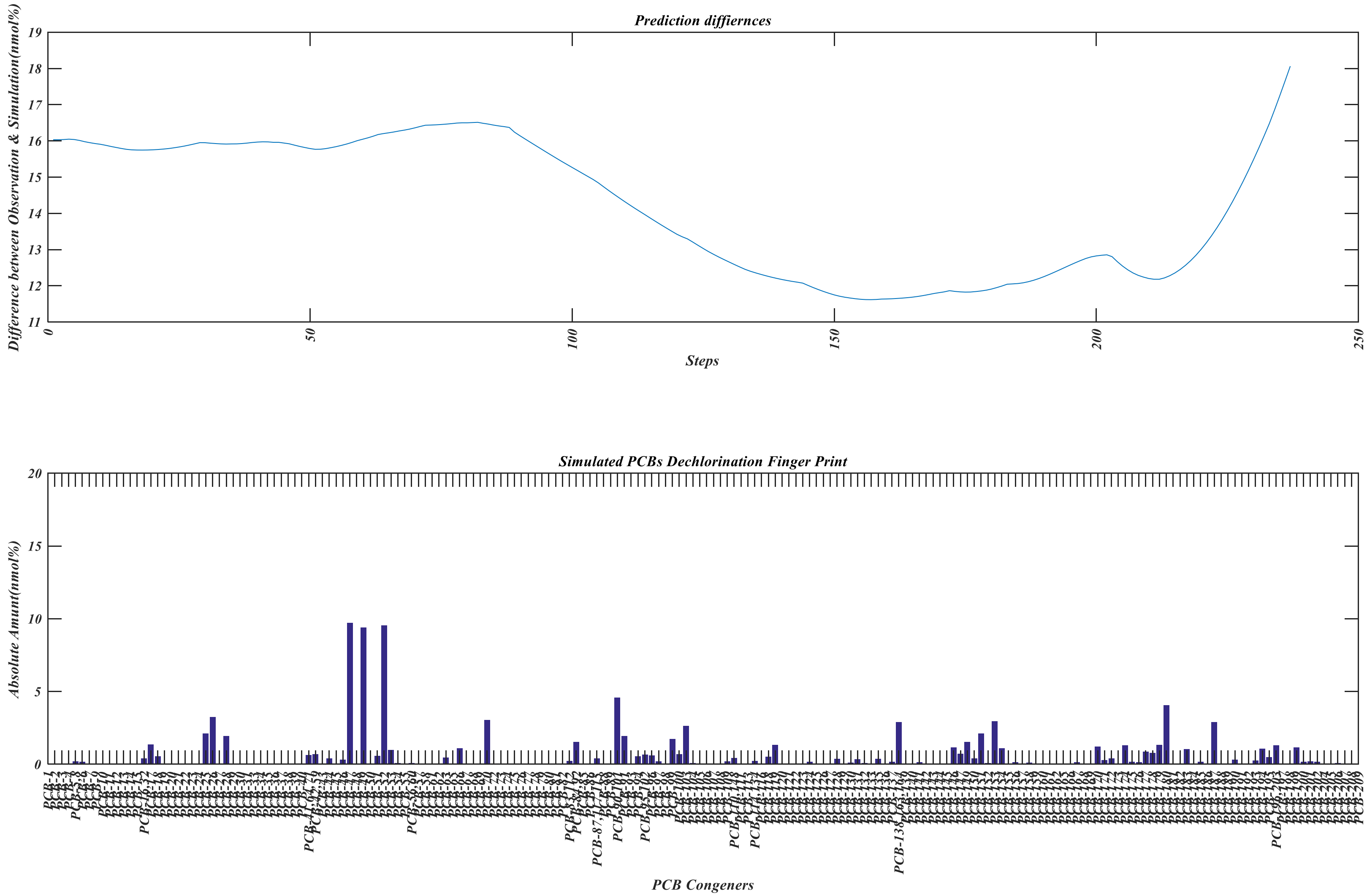

Figure 11.6c. Simulated Dechlorinated Product Difference & Simulated PCBs Distribution (%mol, no priming, Van Dort 1997)

12.Conclusion

The combination of redox potential and bio-selectivity is a better alternative to quantify the PCB dechlorination process compare to empirical rules. The redox potential provides a quantitative indicator to determine the PCB dechlorination pathway. Our simulation on three published literature has proven the potentials of redox potential as a useful tool to simulation the PCB dechlorination process and predict the outcomes if the bio-selectivity of the system is well known. On the other side, we can also use the comparison between different prediction results under the same initial PCB inputs to conjecture the bio-selectivity of the environment.

Understanding the mechanism and preference of PCB dechlorination pathway selection and the partition will help us explore the patterns and regulations of the PCBs dechlorination behaviors on a mathematical level, improve the understanding on PCB degradation and transformation, and optimize the prediction on PCB toxicity during in-situ remediation in the environment (Sowers and May 2013; Van den Berg et al. 2006).

References

Abraham, W.-R. (2002). Microbial degradation of polychlorinated biphenyls (PCBs) in the environment. In S. Ved Pal & S. Raymond D. (Eds.), *Progress in Industrial Microbiology* (Vol. 36, pp. 29–67). Elsevier. https://doi.org/10.1016/S0079-6352(02)80006-6

Ahmed, M., & Focht, D. D. (1973). Degradation of polychlorinated biphenyls by two species of Achromobacter. *Canadian Journal of Microbiology*, *19*(1), 47–52. https://doi.org/10.1139/m73-007

Alberty, R. A. (2002). Thermodynamics of Systems of Biochemical Reactions. *Journal of Theoretical Biology*, *215*(4), 491–501. https://doi.org/10.1006/jtbi.2001.2516

Alberty, Robert A. (1968). Effect of pH and Metal Ion Concentration on the Equilibrium Hydrolysis of Adenosine Triphosphate to Adenosine Diphosphate. *Journal of Biological Chemistry*, *243*(7), 1337–1343.

Alberty, Robert A. (1969). Standard Gibbs Free Energy, Enthalpy, and Entropy Changes as a Function of pH and pMg for Several Reactions Involving Adenosine Phosphates. *Journal of Biological Chemistry*, *244*(12), 3290–3302.

Alberty, Robert A., & Goldberg, R. N. (1992). Standard thermodynamic formation properties for the adenosine 5'-triphosphate series. *Biochemistry*, *31*(43), 10610–10615. https://doi.org/10.1021/bi00158a025

Alder, A. C., Haggblom, M. M., Oppenheimer, S. R., & Young, L. Y. (1993). Reductive dechlorination of polychlorinated biphenyls in anaerobic sediments. *Environmental Science & Technology*, *27*(3), 530–538. https://doi.org/10.1021/es00040a012

Aoki, Y. (2001). Polychlorinated biphenyls, polychlorinated dibenzo-p-dioxins, and polychlorinated dibenzofurans as endocrine disrupters--what we have learned from Yusho disease. *Environmental Research*, *86*(1), 2–11. https://doi.org/10.1006/enrs.2001.4244

Arnot, J. A., & Gobas, F. A. P. C. (2004). A food web bioaccumulation model for organic chemicals in aquatic ecosystems. *Environmental Toxicology and Chemistry*, *23*(10), 2343–2355. https://doi.org/10.1897/03-438

Assadi, M. H. N., & Hanaor, D. A. H. (2013). Theoretical study on copper's energetics and magnetism in TiO2 polymorphs. *Journal of Applied Physics*, *113*(23), 233913. https://doi.org/10.1063/1.4811539

Avnimelech, Y., Ritvo, G., Meijer, L. E., & Kochba, M. (2001). Water content, organic carbon and dry bulk density in flooded sediments. *Aquacultural Engineering*, *25*(1), 25–33. https://doi.org/10.1016/S0144-8609(01)00068-1

Ballschmiter, K., & Zell, M. (1980). Analysis of polychlorinated biphenyls (PCB) by glass capillary gas chromatography. *Fresenius' Zeitschrift Für Analytische Chemie*, *302*(1), 20–31. https://doi.org/10.1007/BF00469758

Barber, M. C., Suérez, L. A., & Lassiter, R. R. (1988). Modeling bioconcentration of nonpolar organic pollutants by fish. *Environmental Toxicology and Chemistry*, *7*(7), 545–558. https://doi.org/10.1002/etc.5620070703

Barone, V., & Cossi, M. (1998). Quantum Calculation of Molecular Energies and Energy Gradients in Solution by a Conductor Solvent Model. *The Journal of Physical Chemistry A*, *102*(11), 1995–2001. https://doi.org/10.1021/jp9716997

Bates, M. L., Bengtson Nash, S. M., Hawker, D. W., Norbury, J., Stark, J. S., & Cropp, R. A. (2015). Construction of a trophically complex near-shore Antarctic food web model using the Conservative Normal framework with structural coexistence. *Journal of Marine Systems*, *145*(Supplement C), 1–14. https://doi.org/10.1016/j.jmarsys.2014.12.002

Bates, M. L., Bengtson Nash, S. M., Hawker, D. W., Shaw, E. C., & Cropp, R. A. (2017). The distribution of persistent organic pollutants in a trophically complex Antarctic ecosystem model. *Journal of Marine Systems*, *170*(Supplement C), 103–114. https://doi.org/10.1016/j.jmarsys.2017.02.005

Bedard, D. L. (2014). PCB dechlorinases revealed at last. *Proceedings of the National Academy* *of Sciences*, *111*(33), 11919–11920. https://doi.org/10.1073/pnas.1412286111

Bedard, D. L., Bunnell, S. C., & Smullen, L. A. (1996). Stimulation of Microbial para-Dechlorination of Polychlorinated Biphenyls That Have Persisted in Housatonic River Sediment for Decades. *Environmental Science & Technology*, *30*(2), 687–694. https://doi.org/10.1021/es950463i

Bedard, D. L., & May, R. J. (1996). Characterization of the Polychlorinated Biphenyls in the Sediments of Woods Pond: Evidence for Microbial Dechlorination of Aroclor 1260 in Situ. *Environmental Science & Technology*, *30*(1), 237–245. https://doi.org/10.1021/es950262e

Bedard, D. L., Van Dort, H. M., May, R. J., & Smullen, L. A. (1997). Enrichment of Microorganisms That Sequentially meta, para-Dechlorin- ate the Residue of Aroclor 1260 in Housatonic River Sediment. *Environmental Science & Technology*, *31*(11), 3308–3313. https://doi.org/10.1021/es9703483

Borgmann, U., & Whittle, D. M. (1991). Contaminant Concentration Trends in Lake Ontario Lake Trout (Salvelinus Namaycush): 1977 to 1988. *Journal of Great Lakes Research*, *17*(3), 368–381. https://doi.org/10.1016/S0380-1330(91)71373-7

Borja, J., Taleon, D. M., Auresenia, J., & Gallardo, S. (2005). Polychlorinated biphenyls and their biodegradation. *Process Biochemistry*, *40*(6), 1999–2013. https://doi.org/10.1016/j.procbio.2004.08.006

Boyd, C. E. (1995). *Bottom Soils, Sediment, and Pond Aquaculture*. Springer Science & Business Media.

Breivik, K., Sweetman, A., Pacyna, J. M., & Jones, K. C. (2002a). Towards a global historical emission inventory for selected PCB congeners — a mass balance approach: 1. Global production and consumption. *Science of The Total Environment*, *290*(1), 181–198. https://doi.org/10.1016/S0048-9697(01)01075-0

Breivik, K., Sweetman, A., Pacyna, J. M., & Jones, K. C. (2002b). Towards a global historical emission inventory for selected PCB congeners — a mass balance approach: 2. Emissions.

Science of The Total Environment, *290*(1), 199–224. https://doi.org/10.1016/S0048-9697(01)01076-2

Breivik, K., Sweetman, A., Pacyna, J. M., & Jones, K. C. (2007). Towards a global historical emission inventory for selected PCB congeners — A mass balance approach: 3. An update. *Science of The Total Environment*, *377*(2), 296–307. https://doi.org/10.1016/j.scitotenv.2007.02.026

Cai, M., & Reavie, E. D. (2018). Pelagic zonation of water quality and phytoplankton in the Great Lakes. *Limnology*, *19*(1), 127–140. https://doi.org/10.1007/s10201-017-0526-y

Campfens, J., & Mackay, D. (1997). Fugacity-Based Model of PCB Bioaccumulation in Complex Aquatic Food Webs. *Environmental Science & Technology*, *31*(2), 577–583. https://doi.org/10.1021/es960478w

Car, R., & Parrinello, M. (1985). Unified Approach for Molecular Dynamics and Density-Functional Theory. *Physical Review Letters*, *55*(22), 2471–2474. https://doi.org/10.1103/PhysRevLett.55.2471

Christie, W. J. (1974). Changes in the Fish Species Composition of the Great Lakes. *Journal of the Fisheries Research Board of Canada*, *31*(5), 827–854. https://doi.org/10.1139/f74-104

De Laender, F., Van Oevelen, D., Middelburg, J. J., & Soetaert, K. (2010). Uncertainties in ecological, chemical and physiological parameters of a bioaccumulation model: Implications for internal concentrations and tissue based risk quotients. *Ecotoxicology and Environmental Safety*, *73*(3), 240–246. https://doi.org/10.1016/j.ecoenv.2009.11.011

De voogt, P., & Brinkman, U. A. T. (1989). CHAPTER 1 - Production, properties and usage of polychlorinated biphenyls. In R. D. Kimbrough & A. A. Jensen (Eds.), *Halogenated Biphenyls, Terphenyls, Naphthalenes, Dibenzodioxins and Related Products (Second Edition)* (pp. 3–45). Amsterdam: Elsevier. https://doi.org/10.1016/B978-0-444-81029-8.50005-9

Demirtepe, H., Kjellerup, B., Sowers, K. R., & Imamoglu, I. (2015). Evaluation of PCB dechlorination pathways in anaerobic sediment microcosms using an anaerobic dechlorination model. *Journal of Hazardous Materials*, *296*, 120–127. https://doi.org/10.1016/j.jhazmat.2015.04.033

Dolfing, J., & Harrison, B. K. (1992). Gibbs free energy of formation of halogenated aromatic compounds and their potential role as electron acceptors in anaerobic environments. *Environmental Science & Technology*, *26*(11), 2213–2218. https://doi.org/10.1021/es00035a021

Dolfing, J., & Keith Harrison, B. (1993). Redox and reduction potentials as parameters to predict the degradation pathway of chlorinated benzenes in anaerobic environments. *FEMS Microbiology Ecology*, *13*(1), 23–29.

El-Shahawi, M. S., Hamza, A., Bashammakh, A. S., & Al-Saggaf, W. T. (2010). An overview on the accumulation, distribution, transformations, toxicity and analytical methods for the monitoring of persistent organic pollutants. *Talanta*, *80*(5), 1587–1597. https://doi.org/10.1016/j.talanta.2009.09.055

Estepp, L. R., & Reavie, E. D. (2015). The ecological history of Lake Ontario according to phytoplankton. *Journal of Great Lakes Research*, *41*(3), 669–687. https://doi.org/10.1016/j.jglr.2015.06.005

Fagervold, S. K., May, H. D., & Sowers, K. R. (2007). Microbial Reductive Dechlorination of Aroclor 1260 in Baltimore Harbor Sediment Microcosms Is Catalyzed by Three Phylotypes within the Phylum Chloroflexi. *Applied and Environmental Microbiology*, *73*(9), 3009–3018. https://doi.org/10.1128/AEM.02958-06

Fine, P. E., & Carneiro, I. A. (1999). Transmissibility and persistence of oral polio vaccine viruses: implications for the global poliomyelitis eradication initiative. *American Journal of Epidemiology*, *150*(10), 1001–1021.

Frank, R., Thomas, R. L., Holdrinet, M., Kemp, A. L. W., & Braun, H. E. (1979). Organochlorine Insecticides and PCB in Surficial Sediments (1968) and Sediment Cores (1976) from Lake Ontario. *Journal of Great Lakes Research*, *5*(1), 18–27.

https://doi.org/10.1016/S0380-1330(79)72123-X

Gewurtz, S. B., Laposa, R., Gandhi, N., Christensen, G. N., Evenset, A., Gregor, D., & Diamond, M. L. (2006). A comparison of contaminant dynamics in arctic and temperate fish: A modeling approach. *Chemosphere*, *63*(8), 1328–1341. https://doi.org/10.1016/j.chemosphere.2005.09.031

Gibson, D. T., & Parales, R. E. (2000). Aromatic hydrocarbon dioxygenases in environmental biotechnology. *Current Opinion in Biotechnology*, *11*(3), 236–243. https://doi.org/10.1016/S0958-1669(00)00090-2

Gobas, F. A. P. C., Muir, D. C. G., & Mackay, D. (1988). Dynamics of dietary bioaccumulation and faecal elimination of hydrophobic organic chemicals in fish. *Chemosphere*, *17*(5), 943–962. https://doi.org/10.1016/0045-6535(88)90066-5

Gobas, F., & Morrison, H. (2000). Bioconcentration and Biomagnification in the Aquatic Environment. In *Handbook of Property Estimation Methods for Chemicals* (Vols. 1–0). CRC Press. https://doi.org/10.1201/9781420026283.ch9

Goldberg, R. N. (1975). Thermodynamics of hexokinase-catalyzed reactions. *Biophysical Chemistry*, *3*(3), 192–205.

Goldberg, Robert N., Kishore, N., & Lennen, R. M. (2002). Thermodynamic Quantities for the Ionization Reactions of Buffers. *Journal of Physical and Chemical Reference Data*, *31*(No. 2). https://www.nist.gov/publications/thermodynamic-quantities-ionization-reactions-buffers

Grimm, F., Hu, D., Kania-Korwel, I., Lehmler, H., Ludewig, G., Hornbuckle, K., … Robertson, L. (2015). Metabolism and metabolites of polychlorinated biphenyls (PCBs). *Critical Reviews in Toxicology*, *45*(3), 245–272. https://doi.org/10.3109/10408444.2014.999365

Häggblom, M. M., & Bossert, I. D. (Eds.). (2003). *Dehalogenation: Microbial Processes and Environmental Applications* (2003 edition). Boston: Springer.

Harner, T., & Bidleman, T. F. (1996). Measurements of Octanol−Air Partition Coefficients for Polychlorinated Biphenyls. *Journal of Chemical & Engineering Data*, *41*(4), 895–899.

https://doi.org/10.1021/je960097y

Harner, T., & Mackay, D. (1995). Measurement of Octanol-Air Partition Coefficients for Chlorobenzenes, PCBs, and DDT. *Environmental Science & Technology*, *29*(6), 1599–1606. https://doi.org/10.1021/es00006a025

Harrad, S. (2009). *Persistent Organic Pollutants*. John Wiley & Sons.

Held, C., & Sadowski, G. (2016). Thermodynamics of Bioreactions. *Annual Review of Chemical and Biomolecular Engineering*, *7*(1), 395–414. https://doi.org/10.1146/annurev-chembioeng-080615-034704

Hillery, B. R., Basu, I., Sweet, C. W., & Hites, R. A. (1997). Temporal and Spatial Trends in a Long-Term Study of Gas-Phase PCB Concentrations near the Great Lakes. *Environmental Science & Technology*, *31*(6), 1811–1816. https://doi.org/10.1021/es960990h

Hiraishi, A. (2008). Biodiversity of Dehalorespiring Bacteria with Special Emphasis on Polychlorinated Biphenyl/Dioxin Dechlorinators. *Microbes and Environments*, *23*(1), 1–12. https://doi.org/10.1264/jsme2.23.1

Ho, J., Coote, M., Cramer, C., & Truhlar, D. (2015). *Theoretical Calculation of Reduction Potentials*. https://doi.org/10.1201/b19122-8

Hollander, A., Sauter, F., den Hollander, H., Huijbregts, M., Ragas, A., & van de Meent, D. (2007). Spatial variance in multimedia mass balance models: comparison of LOTOS-EUROS and SimpleBox for PCB-153. *Chemosphere*, *68*(7), 1318–1326. https://doi.org/10.1016/j.chemosphere.2007.01.035

Holliger, C., & Schumacher, W. (1994). Reductive dehalogenation as a respiratory process. *Antonie van Leeuwenhoek*, *66*(1–3), 239–246. https://doi.org/10.1007/BF00871642

Hu, D., Martinez, A., & Hornbuckle, K. C. (2011). Sedimentary Records of Non-Aroclor and Aroclor PCB mixtures in the Great Lakes. *Journal of Great Lakes Research*, *37*(2), 359–364. https://doi.org/10.1016/j.jglr.2011.03.001

Hughes, A. S., VanBriesen, J. M., & Small, M. J. (2010). Identification of Structural Properties

Associated with Polychlorinated Biphenyl Dechlorination Processes. *Environmental Science & Technology*, *44*(8), 2842–2848. https://doi.org/10.1021/es902109w

Imamoglu, I., Li, K., & Christensen, E. R. (2002). Modeling polychlorinated biphenyl congener patterns and dechlorination in dated sediments from the Ashtabula River, Ohio, USA. *Environmental Toxicology and Chemistry*, *21*(11), 2283–2291. https://doi.org/10.1002/etc.5620211105

Jones, K. C., & de Voogt, P. (1999). Persistent organic pollutants (POPs): state of the science. *Environmental Pollution*, *100*(1), 209–221. https://doi.org/10.1016/S0269-7491(99)00098-6

Jönsson, A., Gustafsson, Ö., Axelman, J., & Sundberg, H. (2003). Global Accounting of PCBs in the Continental Shelf Sediments. *Environmental Science & Technology*, *37*(2), 245–255. https://doi.org/10.1021/es0201404

Kamaya, H., Kaneshina, S., & Ueda, I. (1981). Partition equilibrium of inhalation anesthetics and alcohols between water and membranes of phospholipids with varying acyl chain-lengths. *Biochimica et Biophysica Acta (BBA) - Biomembranes*, *646*(1), 135–142. https://doi.org/10.1016/0005-2736(81)90280-7

Karcher Sandra C., VanBriesen Jeanne M., & Small Mitchell J. (2007). Numerical Method to Elucidate Likely Target Positions of Chlorine Removal in Anaerobic Sediments Undergoing Polychlorinated Biphenyl Dechlorination. *Journal of Environmental Engineering*, *133*(3), 278–286. https://doi.org/10.1061/(ASCE)0733-9372(2007)133:3(278)

Karickhoff, S. W. (1981). Semi-empirical estimation of sorption of hydrophobic pollutants on natural sediments and soils. *Chemosphere*, *10*(8), 833–846. https://doi.org/10.1016/0045-6535(81)90083-7

Kaur, J., DePinto, J. V., Atkinson, J. F., Verhamme, E., & Young, T. C. (2012). Development of a spatially resolved linked hydrodynamic and exposure model (LOTOX2) for PCBs in Lake Ontario. *Journal of Great Lakes Research*, *38*(3), 490–503. https://doi.org/10.1016/j.jglr.2012.06.011

Kelly, B. C., Gobas, F. A. P. C., & McLachlan, M. S. (2004). Intestinal absorption and biomagnification of organic contaminants in fish, wildlife, and humans. *Environmental Toxicology and Chemistry*, *23*(10), 2324–2336. https://doi.org/10.1897/03-545

Kelly, C. P., Cramer, C. J., & Truhlar, D. G. (2006). Aqueous Solvation Free Energies of Ions and Ion−Water Clusters Based on an Accurate Value for the Absolute Aqueous Solvation Free Energy of the Proton. *The Journal of Physical Chemistry B*, *110*(32), 16066–16081. https://doi.org/10.1021/jp063552y

Klute, E. A. (1986). *Methods of Soil Analysis. Part 1. Physical and Mineralogical Methods* (2 edition). Madison, Wis: American Society of Agronomy-Soil Science Society of America.

Kohn, W., & Sham, L. J. (1965). Self-Consistent Equations Including Exchange and Correlation Effects. *Physical Review*, *140*(4A), A1133–A1138. https://doi.org/10.1103/PhysRev.140.A1133

Krueger, J., & Selin, H. (2002). Governance for Sound Chemicals Management: The Need for a More Comprehensive Global Strategy. *Global Governance*, *8*(3), 323–342.

Krümmel, E. M., Macdonald, R. W., Kimpe, L. E., Gregory-Eaves, I., Demers, M. J., Smol, J. P., … Blais, J. M. (2003). Aquatic ecology: Delivery of pollutants by spawning salmon. *Nature*, *425*(6955), 255–256. https://doi.org/10.1038/425255a

Kuipers, B., Cullen, W. R., & Mohn, W. W. (1999). Reductive Dechlorination of Nonachlorobiphenyls and Selected Octachlorobiphenyls by Microbial Enrichment Cultures. *Environmental Science & Technology*, *33*(20), 3579–3585. https://doi.org/10.1021/es9900712

LimnoTech. (2011, July). DRAFT TMDL Support Document for PCBs in Lake Ontario. http://www.dec.ny.gov/docs/water_pdf/lakeontariopcbtmdl.pdf

Lipmann, F. (1941). Metabolic Generation and Utilization of Phosphate Bond Energy. In F. F. Nord & C. H. Werkman (Eds.), *Advances in Enzymology and Related Areas of Molecular Biology* (pp. 99–162). John Wiley & Sons, Inc. https://doi.org/10.1002/9780470122464.ch4

Mackay, D. (1979). Finding fugacity feasible. *Environmental Science & Technology*, *13*(10), 1218–1223. https://doi.org/10.1021/es60158a003

Mackay, D. (1989). Modeling the Long-Term Behavior of an Organic Contaminant in a Large Lake: Application to PCBs in Lake Ontario. *Journal of Great Lakes Research*, *15*(2), 283–297. https://doi.org/10.1016/S0380-1330(89)71482-9

Mackay, D. (2001). *Multimedia Environmental Models: The Fugacity Approach, Second Edition* (2 edition). Boca Raton: CRC Press.

Mackay, D., Celsie, A. K. D., Arnot, J. A., & Powell, D. E. (2016). Processes influencing chemical biomagnification and trophic magnification factors in aquatic ecosystems: Implications for chemical hazard and risk assessment. *Chemosphere*, *154*(Supplement C), 99–108. https://doi.org/10.1016/j.chemosphere.2016.03.048

Mackay, D., Joy, M., & Paterson, S. (1983). A quantitative water, air, sediment interaction (QWASI) fugacity model for describing the fate of chemicals in lakes. *Chemosphere*, *12*(7), 981–997. https://doi.org/10.1016/0045-6535(83)90251-5

Mackay, D., Shiu, W.-Y., Ma, K.-C., & Lee, S. C. (2006). *Handbook of Physical-Chemical Properties and Environmental Fate for Organic Chemicals, Second Edition* (2 edition). Boca Raton, FL: CRC Press.

MacLeod, M., Fraser, A. J., & Mackay, D. (2002). Evaluating and expressing the propagation of uncertainty in chemical fate and bioaccumulation models. *Environmental Toxicology and Chemistry*, *21*(4), 700–709. https://doi.org/10.1002/etc.5620210403

Marenich, A. V., Cramer, C. J., & Truhlar, D. G. (2009a). Performance of SM6, SM8, and SMD on the SAMPL1 Test Set for the Prediction of Small-Molecule Solvation Free Energies. *The Journal of Physical Chemistry B*, *113*(14), 4538–4543. https://doi.org/10.1021/jp809094y

Marenich, A. V., Cramer, C. J., & Truhlar, D. G. (2009b). Universal Solvation Model Based on Solute Electron Density and on a Continuum Model of the Solvent Defined by the Bulk Dielectric Constant and Atomic Surface Tensions. *The Journal of Physical Chemistry B*, *113*(18), 6378–6396. https://doi.org/10.1021/jp810292n

May, H. D., Miller, G. S., Kjellerup, B. V., & Sowers, K. R. (2008). Dehalorespiration with Polychlorinated Biphenyls by an Anaerobic Ultramicrobacterium. *Applied and Environmental Microbiology*, *74*(7), 2089–2094. https://doi.org/10.1128/AEM.01450-07

McFarland, V. A., & Clarke, J. U. (1989). Environmental occurrence, abundance, and potential toxicity of polychlorinated biphenyl congeners: considerations for a congener-specific analysis. *Environmental Health Perspectives*, *81*, 225–239.

McGill, L. M., Gerig, B. S., Chaloner, D. T., & Lamberti, G. A. (2017). An ecosystem model for evaluating the effects of introduced Pacific salmon on contaminant burdens of stream-resident fish. *Ecological Modelling*, *355*, 39–48. https://doi.org/10.1016/j.ecolmodel.2017.03.027

McLeod, A. M., Arnot, J. A., Borgå, K., Selck, H., Kashian, D. R., Krause, A., … Drouillard, K. G. (2015). Quantifying uncertainty in the trophic magnification factor related to spatial movements of organisms in a food web. *Integrated Environmental Assessment and Management*, *11*(2), 306–318. https://doi.org/10.1002/ieam.1599

McNaught, A. D., & Wilkinson, A. (1997). *Compendium of Chemical Terminology - IUPAC Recommendations* (2 edition). Oxford England ; Malden, MA, USA: Wiley.

Mennucci, B., Cancès, E., & Tomasi, J. (1997). Evaluation of Solvent Effects in Isotropic and Anisotropic Dielectrics and in Ionic Solutions with a Unified Integral Equation Method: Theoretical Bases, Computational Implementation, and Numerical Applications. *The Journal of Physical Chemistry B*, *101*(49), 10506–10517. https://doi.org/10.1021/jp971959k

Miertuš, S., & Tomasi, J. (1982). Approximate evaluations of the electrostatic free energy and internal energy changes in solution processes. *Chemical Physics*, *65*(2), 239–245. https://doi.org/10.1016/0301-0104(82)85072-6

Mohn, W. W., & Tiedje, J. M. (1992). Microbial reductive dehalogenation. *Microbiological Reviews*, *56*(3), 482–507.

Munawar, M., & Munawar, I. F. (1986). The seasonality of phytoplankton in the North American Great Lakes, a comparative synthesis. *Hydrobiologia*, *138*(1), 85–115. https://doi.org/10.1007/BF00027234

Neely, W. B. (1983). Reactivity and Environmental Persistence of PCB Isomers. In *Physical Behavior of PCBs in the Great Lakes* (p. 442). Ann Arbor MI.: Ontario Ministry of the Environment. https://search.proquest.com/docview/48536512?accountid=9902

Neely, W. Brock, Branson, D. R., & Blau, G. E. (1974). Partition coefficient to measure bioconcentration potential of organic chemicals in fish. *Environmental Science & Technology*, *8*(13), 1113–1115. https://doi.org/10.1021/es60098a008

Nies, L., & Vogel, T. M. (1991). Identification of the Proton Source for the Microbial Reductive Dechlorination of 2,3,4,5,6-Pentachlorobiphenyl. *Applied and Environmental Microbiology*, *57*(9), 2771–2774.

Oliver, B. G., Charlton, M. N., & Durham, R. W. (1989). Distribution, redistribution, and geochronology of polychlorinated biphenyl congeners and other chlorinated hydrocarbons in Lake Ontario sediments. *Environmental Science & Technology*, *23*(2), 200–208. https://doi.org/10.1021/es00179a011

Oliver, B. G., & Niimi, A. J. (1988). Trophodynamic analysis of polychlorinated biphenyl congeners and other chlorinated hydrocarbons in the Lake Ontario ecosystem. *Environmental Science & Technology*, *22*(4), 388–397. https://doi.org/10.1021/es00169a005

Orio, M., Pantazis, D. A., & Neese, F. (2009). Density functional theory. *Photosynthesis Research*, *102*(2–3), 443–453. https://doi.org/10.1007/s11120-009-9404-8

Parr, R. G., Gadre, S. R., & Bartolotti, L. J. (1979). Local density functional theory of atoms and molecules. *Proceedings of the National Academy of Sciences*, *76*(6), 2522–2526.

Pauly, D., & Palomares, M.-L. (2005). Fishing Down Marine Food Web: It is Far More Pervasive Than We Thought. *Bulletin of Marine Science*, *76*(2), 197–212.

Pearson, R. G. (1988). Absolute electronegativity and hardness: application to inorganic chemistry. *Inorganic Chemistry*, *27*(4), 734–740. https://doi.org/10.1021/ic00277a030

Pieper, D. H. (2005). Aerobic degradation of polychlorinated biphenyls. *Applied Microbiology and Biotechnology*, *67*(2), 170–191. https://doi.org/10.1007/s00253-004-1810-4

Porta, M., & Zumeta, E. (2002). Implementing the Stockholm Treaty on Persistent Organic Pollutants. *Occup Environ Med*, *59*(10), 651–652. https://doi.org/10.1136/oem.59.10.651

Reavie, E. D., Barbiero, R. P., Allinger, L. E., & Warren, G. J. (2014). Phytoplankton trends in the Great Lakes, 2001–2011. *Journal of Great Lakes Research*, *40*(3), 618–639. https://doi.org/10.1016/j.jglr.2014.04.013

Reid, B. J., Jones, K. C., & Semple, K. T. (2000). Bioavailability of persistent organic pollutants in soils and sediments—a perspective on mechanisms, consequences and assessment. *Environmental Pollution*, *108*(1), 103–112. https://doi.org/10.1016/S0269-7491(99)00206-7

Robertson, L. W., & Hansen, L. G. (Eds.). (2001). *PCBs: Recent Advances in Environmental Toxicology and Health Effects*. University Press of Kentucky. http://www.jstor.org/stable/j.ctt130j2pw

Rossberg, M., Lendle, W., Pfleiderer, G., Tögel, A., Dreher, E.-L., Langer, E., … Mann, T. (2000). Chlorinated Hydrocarbons. In *Ullmann's Encyclopedia of Industrial Chemistry*. Wiley-VCH Verlag GmbH & Co. KGaA. https://doi.org/10.1002/14356007.a06_233.pub2

Rukavina, N. A. (1976). Nearshore Sediments of Lakes Ontario and Erie. *Geoscience Canada*, *3*(3). Retrieved from https://journals.lib.unb.ca/index.php/GC/article/view/1195

Safe, S. (1990). Polychlorinated Biphenyls (PCBs), Dibenzo-p-Dioxins (PCDDs), Dibenzofurans (PCDFs), and Related Compounds: Environmental and Mechanistic Considerations Which Support the Development of Toxic Equivalency Factors (TEFs). *Critical Reviews in Toxicology*, *21*(1), 51–88. https://doi.org/10.3109/10408449009089873

Safe, S. H. (1994). Polychlorinated Biphenyls (PCBs): Environmental Impact, Biochemical and Toxic Responses, and Implications for Risk Assessment. *Critical Reviews in Toxicology*, *24*(2), 87–149. https://doi.org/10.3109/10408449409049308

Schneider, A. R., Stapleton, H. M., Cornwell, J., & Baker, J. E. (2001). Recent Declines in PAH, PCB, and Toxaphene Levels in the Northern Great Lakes As Determined from High Resolution Sediment Cores. *Environmental Science & Technology*, *35*(19), 3809–3815. https://doi.org/10.1021/es002044d

Schwarzenbach, R. P., Gschwend, P. M., & Imboden, D. M. (2002). *Environmental Organic Chemistry* (2 edition). New York: Wiley-Interscience.

Scott, A. P., & Radom, L. (1996). Harmonic Vibrational Frequencies: An Evaluation of Hartree−Fock, Møller−Plesset, Quadratic Configuration Interaction, Density Functional Theory, and Semiempirical Scale Factors. *Figshare*. https://doi.org/10.1021/jp960976r

Selck, H., Drouillard, K., Eisenreich, K., Koelmans, A. A., Palmqvist, A., Ruus, A., … van den Heuvel-Greve, M. (2012). Explaining differences between bioaccumulation measurements in laboratory and field data through use of a probabilistic modeling approach. *Integrated Environmental Assessment and Management*, *8*(1), 42–63. https://doi.org/10.1002/ieam.217

Soonthornnonda, P., Zou, Y., Christensen, E. R., & Li, A. (2011). PCBs in Great Lakes sediments, determined by positive matrix factorization. *Journal of Great Lakes Research*, *37*(1), 54–63. https://doi.org/10.1016/j.jglr.2010.11.003

Sowers, K. R., & May, H. D. (2013). In situ treatment of PCBs by anaerobic microbial dechlorination in aquatic sediment: are we there yet? *Current Opinion in Biotechnology*, *24*(3), 482–488. https://doi.org/10.1016/j.copbio.2012.10.004

Ssebiyonga, N., Erga, S. R., Hamre, B., Stamnes, J. J., & Frette, Ø. (2013). Light conditions and photosynthetic efficiency of phytoplankton in Murchison Bay, Lake Victoria, Uganda. *Limnologica - Ecology and Management of Inland Waters*, *43*(3), 185–193. https://doi.org/10.1016/j.limno.2012.09.005

Szabo, A., & Ostlund, N. S. (2012). *Modern Quantum Chemistry: Introduction to Advanced Electronic Structure Theory*. Courier Corporation.

Tewari, Y. B., & Goldberg, R. N. (1991). Thermodynamics of hydrolysis of disaccharides:

Lactulose, α-d-melibiose, palatinose, d-trehalose, d-turanose and 3-o-β-d-galactopyranosyl-d-arabinose. *Biophysical Chemistry*, *40*(1), 59–67. https://doi.org/10.1016/0301-4622(91)85029-P

Then, A. Y., Hoenig, J. M., Hall, N. G., & Hewitt, D. A. (2015). Evaluating the predictive performance of empirical estimators of natural mortality rate using information on over 200 fish species. *ICES Journal of Marine Science*, *72*(1), 82–92. https://doi.org/10.1093/icesjms/fsu136

Tiedje, J. M., Quensen, J. F., Chee-Sanford, J., Schimel, J. P., & Boyd, S. A. (1993). Microbial reductive dechlorination of PCBs. *Biodegradation*, *4*(4), 231–240.

Van den Berg, M, Birnbaum, L., Bosveld, A. T., Brunström, B., Cook, P., Feeley, M., … Zacharewski, T. (1998). Toxic equivalency factors (TEFs) for PCBs, PCDDs, PCDFs for humans and wildlife. *Environmental Health Perspectives*, *106*(12), 775–792.

Van den Berg, Martin, Birnbaum, L. S., Denison, M., De Vito, M., Farland, W., Feeley, M., … Peterson, R. E. (2006). The 2005 World Health Organization Reevaluation of Human and Mammalian Toxic Equivalency Factors for Dioxins and Dioxin-Like Compounds. *Toxicological Sciences*, *93*(2), 223–241. https://doi.org/10.1093/toxsci/kfl055

Van Dort, H. M., Smullen, L. A., May, R. J., & Bedard, D. L. (1997). Priming Microbial meta-Dechlorination of Polychlorinated Biphenyls That Have Persisted in Housatonic River Sediments for Decades. *Environmental Science & Technology*, *31*(11), 3300–3307. https://doi.org/10.1021/es970347a

Walters, W. J., & Christensen, V. (2018). Ecotracer: analyzing concentration of contaminants and radioisotopes in an aquatic spatial-dynamic food web model. *Journal of Environmental Radioactivity*, *181*, 118–127. https://doi.org/10.1016/j.jenvrad.2017.11.008

Wania, F., Breivik, K., Persson, N. J., & McLachlan, M. S. (2006). CoZMo-POP 2 – A fugacity-based dynamic multi-compartmental mass balance model of the fate of persistent organic pollutants. *Environmental Modelling & Software*, *21*(6), 868–884.

https://doi.org/10.1016/j.envsoft.2005.04.003

Whittle, D. M., & Fitzsimons, J. D. (1983). The Influence of the Niagara River on Contaminant Burdens of Lake Ontario Biota. *Journal of Great Lakes Research*, *9*(2), 295–302. https://doi.org/10.1016/S0380-1330(83)71898-8

Wiegel, J., & Wu, Q. (2000). Microbial reductive dehalogenation of polychlorinated biphenyls. *FEMS Microbiology Ecology*, *32*(1), 1–15. https://doi.org/10.1111/j.1574-6941.2000.tb00693.x

Williams, W. A. (1994). Microbial reductive dechlorination of trichlorobiphenyls in anaerobic sediment slurries. *Environmental Science & Technology*, *28*(4), 630–635. https://doi.org/10.1021/es00053a015

Wu, Q., Bedard, D. L., & Wiegel, J. (1997). Effect of Incubation Temperature on the Route of Microbial Reductive Dechlorination of 2,3,4,6-Tetrachlorobiphenyl in Polychlorinated Biphenyl (PCB)-Contaminated and PCB-Free Freshwater Sediments. *Applied and Environmental Microbiology*, *63*(7), 2836–2843.

Zehnder, A. J. B. (1988). *Biology of anaerobic microorganisms*. John Wiley & Sons, Incorporated.

Appendix A: Original Results and Datasets

Table A.1. The mass flows of selected PCB congeners under steady state (high biomass)

PCB-18 (mg/day)	Air	Water	Sediment	Low Trophic Level	High Trophic Level	Beyond System	Net Loss
Air	6.63E+04	1.36E+06	-	-	-	9.08E+02	1.42E+06
Water	8.75E+05	2.56E+06	3.57E+05	4.49E+06	5.38E+02	1.05E+05	8.39E+06
Sediment	-	4.51E+05	2.97E+02	1.51E+06	-	1.39E+03	1.96E+06
Low Trophic Level	-	4.40E+06	1.60E+06	1.43E+03	7.71E+02	-	6.00E+06
High Trophic Level	-	9.39E+02	2.50E+02	-	1.20E+02	-	1.31E+03
Beyond System	5.48E+05	2.19E+06	-	-	-	-	2.74E+06
Net Gain	1.42E+06	8.39E+06	1.96E+06	6.00E+06	1.31E+03	2.74E+06	-
PCB-153 (mg/day)	**Air**	**Water**	**Sediment**	**Low Trophic Level**	**High Trophic Level**	**Beyond System**	**Net Loss**
Air	1.83E+03	3.42E+06	-	-	-	1.80E+03	3.43E+06
Water	2.88E+06	1.16E+05	3.30E+06	2.05E+07	2.00E+03	3.92E+05	2.72E+07
Sediment	-	8.22E+06	5.57E+04	2.85E+07	-	1.66E+06	3.84E+07
Low Trophic Level	-	1.33E+07	3.51E+07	4.86E+05	1.13E+05	-	4.89E+07
High Trophic Level	-	4.34E+04	4.12E+04	-	3.01E+04	-	1.15E+05
Outside	5.48E+05	2.19E+06	-	-	-	-	2.74E+06
Net Gain	3.43E+06	2.72E+07	3.84E+07	4.89E+07	1.15E+05	2.74E+06	-
PCB-194 (mg/day)	**Air**	**Water**	**Sediment**	**Low Trophic Level**	**High Trophic Level**	**Beyond System**	**Net Loss**
Air	2.31E+02	1.32E+06	-	-	-	4.57E+02	1.32E+06
Water	7.75E+05	4.73E+04	3.27E+06	1.63E+07	1.59E+03	3.12E+05	2.07E+07
Sediment	-	7.07E+06	3.15E+04	2.38E+07	-	1.88E+06	3.28E+07
Low Trophic Level	-	1.01E+07	2.95E+07	4.48E+05	8.54E+04	-	4.01E+07
High Trophic Level	-	3.17E+04	3.04E+04	-	2.48E+04	-	8.70E+04
Beyond System	5.48E+05	2.19E+06	-	-	-	-	2.74E+06
Net Gain	1.32E+06	2.07E+07	3.28E+07	4.01E+07	8.70E+04	2.74E+06	-

The flow direction is from the left side to the top. The green color represents an exchange value between the two compartments, while the red color means self-elimination. The eight biotic compartments are compressed into two general groups: the low trophic levels (Plankton, Mysid, Pontoporeia, and Oligochaete) and high trophic levels (Sculpin, Alewife, Smelt, and Samonid).

Table A.2. The mass flows of selected PCB congeners under steady state (low biomass)

PCB-18	Air	Water	Sediment	Low Trophic Levels	High Trophic Levels	Outside	Net Loss
Air	6.63E+04	1.36E+06	-	-	-	9.08E+02	1.42E+06
Water	8.76E+05	2.57E+06	3.57E+05	4.50E+03	5.40E-01	1.05E+05	3.91E+06
Sediment	-	3.56E+05	2.35E+02	1.19E+03	-	1.10E+03	3.59E+05
Low Trophic Levels	-	4.40E+03	1.29E+03	9.18E-02	7.06E-01	-	5.69E+03
High Trophic Levels	-	9.83E-01	2.51E-01	-	1.28E-02	-	1.25E+00
Outside	5.48E+05	2.19E+06	-	-	-	-	2.74E+06
Net Gain	1.42E+06	3.91E+06	3.59E+05	5.69E+03	1.25E+00	2.74E+06	-
PCB-153	Air	Water	Sediment	Low Trophic Levels	High Trophic Levels	Beyond System	Net Loss
Air	4.19E+03	7.83E+06	-	-	-	4.13E+03	7.84E+06
Water	7.30E+06	2.94E+05	8.35E+06	5.19E+04	5.09E+00	9.94E+05	1.70E+07
Sediment	-	6.93E+06	4.69E+04	2.40E+04	-	1.40E+06	8.40E+06
Low Trophic Levels	-	3.28E+04	4.29E+04	4.06E+01	1.22E+02	-	7.59E+04
High Trophic Levels	-	6.29E+01	5.95E+01	-	4.59E+00	-	1.27E+02
Outside	5.48E+05	2.19E+06	-	-	-	-	2.74E+06
Net Gain	7.84E+06	1.70E+07	8.40E+06	7.59E+04	1.27E+02	2.74E+06	-
PCB-194	Air	Water	Sediment	Low Trophic Levels	High Trophic Levels	Beyond System	Net Loss
Air	4.48E+02	2.56E+06	-	-	-	8.83E+02	2.56E+06
Water	2.01E+06	1.23E+05	8.49E+06	4.22E+04	4.14E+00	8.09E+05	1.15E+07
Sediment	-	6.70E+06	2.99E+04	2.25E+04	-	1.78E+06	8.53E+06
Low Trophic Levels	-	2.55E+04	3.91E+04	4.20E+01	9.93E+01	-	6.48E+04
High Trophic Levels	-	5.08E+01	4.86E+01	-	4.11E+00	-	1.03E+02
Beyond System	5.48E+05	2.19E+06	-	-	-	-	2.74E+06
Net Gain	2.56E+06	1.15E+07	8.53E+06	6.48E+04	1.03E+02	2.74E+06	-

The flow direction is from the left side to the top. The green color represents an exchange value between the two compartments, while the red color means self-elimination. The eight biotic compartments are compressed into two general groups: the low trophic levels (Plankton, Mysid, Pontoporeia, and Oligochaete) and high trophic levels (Sculpin, Alewife, Smelt, and Samonid).

Table A.3. PCB-18 Mass flow details under steady state with high biomass density

PCB 18 Flow Chart (mg/day)													
Sign	Name	Unit	Environment Compartments			Biotic Compartments							
			Air	Water	Sediment	Plankton	Mysid	Pontoporeia	Oligochaete	Sculpin	Alewife	Smelt	Salmonid
1	Advection Input	Amount	5.48E+05	2.19E+06	-	-	-	-	-	-	-	-	-
		Percentage	38.49%	26.09%	-	-	-	-	-	-	-	-	-
2	Food Ingestion	Amount	-	-	-8.53E+03	0.00E+00	1.13E+04	5.68E+03	2.85E+03	9.50E+00	7.34E+02	5.62E+01	3.49E+00
		Percentage	-	-	-0.43%	0.00%	18.31%	0.45%	1.13%	51.92%	59.52%	63.93%	88.60%
3	Gill uptake	Amount	-	-4.50E+06	-1.50E+06	4.44E+06	5.04E+04	1.25E+06	2.50E+05	8.80E+00	4.99E+02	3.17E+01	4.49E-01
		Percentage	-	-53.53%	-76.48%	100.00%	81.69%	99.55%	98.87%	48.08%	40.48%	36.07%	11.40%
4	Reaction/ Metabolism	Amount	-6.63E+04	-2.57E+06	-2.98E+02	-3.30E+00	-7.00E+00	-7.74E+01	-2.61E+01	-1.27E-01	-1.27E+01	-4.69E-01	-1.99E-01
		Percentage	-4.66%	-30.54%	-0.02%	0.00%	-0.01%	-0.01%	-0.01%	-0.69%	-1.03%	-0.53%	-5.06%
5	Death Loss (All)	Amount	-	9.42E+04	1.28E+05	-1.83E+05	-5.76E+03	-2.75E+04	-6.40E+03	-2.39E+00	-1.96E+02	-7.21E+00	-1.37E+00
		Percentage	-	1.12%	6.52%	-4.11%	-9.34%	-2.19%	-2.53%	-13.03%	-15.87%	-8.20%	-34.88%
6	Gill release	Amount	-	4.30E+06	1.46E+06	-4.25E+06	-5.09E+04	-1.22E+06	-2.45E+05	-9.92E+00	-7.02E+02	-5.77E+01	-1.06E+00
		Percentage	-	51.17%	74.48%	-95.54%	-82.49%	-96.78%	-97.08%	-54.22%	-56.99%	-65.66%	-26.96%
7	Egestion	Amount	-	2.10E+03	4.95E+03	0.00E+00	-3.92E+03	-1.89E+03	-9.50E+02	-5.03E+00	-2.58E+02	-1.98E+01	-1.30E+00
		Percentage	-	0.03%	0.25%	0.00%	-6.36%	-0.15%	-0.38%	-27.49%	-20.93%	-22.54%	-33.10%
8	Undigested Food	Amount	-	4.85E+03	1.11E+04	-	-	-	-	-	-	-	-
		Percentage	-	0.06%	0.57%	-	-	-	-	-	-	-	-
9	Predation Loss	Amount	-	-	-	-1.59E+04	-1.11E+03	-1.11E+04	0.00E+00	-8.36E-01	-6.37E+01	-2.70E+00	0.00E+00
		Percentage	-	-	-	-0.36%	-1.80%	-0.88%	0.00%	-4.57%	-5.17%	-3.07%	0.00%
10	Advection Output	Amount	-9.08E+02	-1.05E+05	-1.39E+03	-	-	-	-	-	-	-	-
		Percentage	-0.06%	-1.26%	-0.07%	-	-	-	-	-	-	-	-
11	Resuspension	Amount	-	1.22E+03	-1.22E+03	-	-	-	-	-	-	-	-
		Percentage	-	0.01%	-0.06%	-	-	-	-	-	-	-	-
12	Deposition	Amount	-	-6.74E+03	6.74E+03	-	-	-	-	-	-	-	-
		Percentage	-	-0.08%	0.34%	-	-	-	-	-	-	-	-
13	Rain Dissolution	Amount	-1.35E+06	1.35E+06	-	-	-	-	-	-	-	-	-
		Percentage	-95.14%	16.12%	-	-	-	-	-	-	-	-	-
14	Dry Deposition	Amount	-6.36E+00	6.36E+00	-	-	-	-	-	-	-	-	-
		Percentage	0.00%	0.00%	-	-	-	-	-	-	-	-	-
15	Wet Deposition	Amount	-1.14E+01	1.14E+01	-	-	-	-	-	-	-	-	-
		Percentage	0.00%	0.00%	-	-	-	-	-	-	-	-	-
16	Diffusion (In)	Amount	8.76E+05	4.53E+05	3.50E+05	-	-	-	-	-	-	-	-
		Percentage	61.51%	5.39%	17.84%	-	-	-	-	-	-	-	-
17	Diffusion (Out)	Amount	-1.93E+03	-1.23E+06	-4.51E+05	-	-	-	-	-	-	-	-
		Percentage	-0.14%	-14.60%	-22.93%	-	-	-	-	-	-	-	-

Table A.4. PCB-153 Mass flow details under steady state with high biomass density

PCB 153 Flow Chart (mg/day)													
Sign	Name	Unit	Environment Compartments			Biotic Compartments							
			Air	Water	Sediment	Plankton	Mysid	Pontoporeia	Oligochaete	Sculpin	Alewife	Smelt	Salmonid
1	Advection Input	Amount	5.48E+05	2.19E+06	-	-	-	-	-	-	-	-	-
		Percentage	14.01%	6.91%	-	-	-	-	-	-	-	-	-
2	Food Ingestion	Amount	-	-	-7.19E+06	0.00E+00	1.63E+06	4.79E+06	2.40E+06	2.40E+03	1.30E+05	1.03E+04	9.96E+02
		Percentage	-	-	-15.41%	0.00%	88.18%	17.33%	34.49%	98.43%	98.36%	98.68%	99.80%
3	Gill uptake	Amount	-	-2.39E+07	-2.74E+07	2.37E+07	2.19E+05	2.28E+07	4.56E+06	3.83E+01	2.17E+03	1.38E+02	1.95E+00
		Percentage	-	-75.39%	-58.73%	100.00%	11.82%	82.67%	65.51%	1.57%	1.64%	1.32%	0.20%
4	Reaction/ Metabolism	Amount	-2.09E+03	-1.36E+05	-6.76E+04	-2.96E+02	-1.33E+03	-3.79E+04	-1.74E+04	-6.31E+01	-4.71E+03	-3.22E+02	-8.63E+01
		Percentage	-0.05%	-0.43%	-0.14%	0.00%	-0.07%	-0.14%	-0.25%	-2.59%	-3.55%	-3.08%	-8.65%
5	Death Loss (All)	Amount	-	8.78E+06	2.65E+07	-1.64E+07	-1.09E+06	-1.35E+07	-4.27E+06	-1.19E+03	-7.23E+04	-4.95E+03	-5.95E+02
		Percentage	-	27.67%	56.87%	-69.15%	-59.04%	-48.78%	-61.44%	-48.81%	-54.58%	-47.30%	-59.61%
6	Gill release	Amount	-	6.01E+06	9.57E+06	-5.89E+06	-1.22E+05	-7.51E+06	-2.07E+06	-6.23E+01	-3.27E+03	-4.99E+02	-5.79E+00
		Percentage	-	18.95%	20.52%	-24.84%	-6.56%	-27.16%	-29.69%	-2.56%	-2.47%	-4.77%	-0.58%
7	Egestion	Amount	-	2.29E+05	2.03E+06	0.00E+00	-4.26E+05	-1.20E+06	-6.00E+05	-7.05E+02	-2.86E+04	-2.84E+03	-3.11E+02
		Percentage	-	0.72%	4.34%	0.00%	-22.96%	-4.33%	-8.62%	-28.94%	-21.61%	-27.14%	-31.16%
8	Undigested Food	Amount	-	6.21E+05	4.67E+06	-	-	-	-	-	-	-	-
		Percentage	-	1.96%	10.01%	-	-	-	-	-	-	-	-
9	Predation Loss	Amount	-	-	-	-1.42E+06	-2.10E+05	-5.41E+06	0.00E+00	-4.17E+02	-2.36E+04	-1.85E+03	0.00E+00
		Percentage	-	-	-	-6.00%	-11.36%	-19.58%	0.00%	-17.11%	-17.79%	-17.71%	0.00%
10	Advection Output	Amount	-2.06E+03	-4.58E+05	-2.01E+06	-	-	-	-	-	-	-	-
		Percentage	-0.05%	-1.44%	-4.31%	-	-	-	-	-	-	-	-
11	Resuspension	Amount	-	1.77E+06	-1.77E+06	-	-	-	-	-	-	-	-
		Percentage	-	5.58%	-3.79%	-	-	-	-	-	-	-	-
12	Deposition	Amount	-	-2.33E+06	2.33E+06	-	-	-	-	-	-	-	-
		Percentage	-	-7.34%	4.99%	-	-	-	-	-	-	-	-
13	Rain Dissolution	Amount	-3.90E+06	3.90E+06	-	-	-	-	-	-	-	-	-
		Percentage	-99.77%	12.30%	-	-	-	-	-	-	-	-	-
14	Dry Deposition	Amount	-1.54E-01	1.54E-01	-	-	-	-	-	-	-	-	-
		Percentage	0.00%	0.00%	-	-	-	-	-	-	-	-	-
15	Wet Deposition	Amount	-2.76E-01	2.76E-01	-	-	-	-	-	-	-	-	-
		Percentage	0.00%	0.00%	-	-	-	-	-	-	-	-	-
16	Diffusion (In)	Amount	3.36E+06	8.22E+06	1.52E+06	-	-	-	-	-	-	-	-
		Percentage	85.99%	25.91%	3.26%	-	-	-	-	-	-	-	-
17	Diffusion (Out)	Amount	-4.92E+03	-4.89E+06	-8.22E+06	-	-	-	-	-	-	-	-
		Percentage	-0.13%	-15.40%	-17.61%	-	-	-	-	-	-	-	-

Table A.5. PCB-194 Mass flow details under steady state with high biomass density

PCB 194 Flow Chart (mg/day)														
Sign	Name	Unit	Environment Compartments			Biotic Compartments								
			Air	Water	Sediment	Plankton	Mysid	Pontoporeia	Oligochaete	Sculpin	Alewife	Smelt	Salmonid
1	Advection Input	Amount	5.48E+05	2.19E+06	-	-	-	-	-	-	-	-	-
		Percentage	38.19%	9.26%	-	-	-	-	-	-	-	-	-
2	Food Ingestion	Amount	-	-	-6.80E+06	0.00E+00	1.23E+06	4.53E+06	2.27E+06	1.82E+03	9.68E+04	7.35E+03	6.88E+02
		Percentage	-	-	-17.42%	0.00%	87.81%	20.14%	38.78%	98.39%	98.29%	98.56%	99.78%
3	Gill uptake	Amount	-	-1.86E+07	-2.15E+07	1.85E+07	1.70E+05	1.80E+07	3.58E+06	2.98E+01	1.69E+03	1.07E+02	1.52E+00
		Percentage	-	-78.70%	-55.18%	100.00%	12.19%	79.86%	61.22%	1.61%	1.71%	1.44%	0.22%
4	Reaction/ Metabolism	Amount	-2.51E+02	-5.41E+04	-3.75E+04	-2.49E+02	-1.11E+03	-3.39E+04	-1.65E+04	-5.39E+01	-3.81E+03	-2.59E+02	-6.73E+01
		Percentage	-0.02%	-0.23%	-0.10%	0.00%	-0.08%	-0.15%	-0.28%	-2.92%	-3.86%	-3.47%	-9.76%
5	Death Loss (All)	Amount	-	7.37E+06	2.35E+07	-1.38E+07	-9.16E+05	-1.20E+07	-4.04E+06	-1.02E+03	-5.85E+04	-3.98E+03	-4.64E+02
		Percentage	-	31.13%	60.08%	-74.55%	-65.53%	-53.57%	-69.05%	-55.04%	-59.38%	-53.36%	-67.23%
6	Gill release	Amount	-	3.58E+06	6.13E+06	-3.50E+06	-7.21E+04	-4.75E+06	-1.38E+06	-3.77E+01	-1.87E+03	-2.84E+02	-3.20E+00
		Percentage	-	15.11%	15.71%	-18.98%	-5.16%	-21.12%	-23.62%	-2.04%	-1.90%	-3.81%	-0.46%
7	Egestion	Amount	-	1.25E+05	1.36E+06	0.00E+00	-2.33E+05	-8.24E+05	-4.13E+05	-3.82E+02	-1.53E+04	-1.45E+03	-1.56E+02
		Percentage	-	0.53%	3.49%	0.00%	-16.63%	-3.66%	-7.05%	-20.70%	-15.50%	-19.38%	-22.55%
8	Undigested Food	Amount	-	5.47E+05	4.35E+06	-	-	-	-	-	-	-	-
		Percentage	-	2.31%	11.13%	-	-	-	-	-	-	-	-
9	Predation Loss	Amount	-	-	-	-1.19E+06	-1.76E+05	-4.84E+06	0.00E+00	-3.56E+02	-1.91E+04	-1.49E+03	0.00E+00
		Percentage	-	-	-	-6.47%	-12.60%	-21.50%	0.00%	-19.30%	-19.35%	-19.98%	0.00%
10	Advection Output	Amount	-4.95E+02	-3.57E+05	-2.23E+06	-	-	-	-	-	-	-	-
		Percentage	-0.03%	-1.51%	-5.72%	-	-	-	-	-	-	-	-
11	Resuspension	Amount	-	1.97E+06	-1.97E+06	-	-	-	-	-	-	-	-
		Percentage	-	8.31%	-5.04%	-	-	-	-	-	-	-	-
12	Deposition	Amount	-	-2.56E+06	2.56E+06	-	-	-	-	-	-	-	-
		Percentage	-	-10.81%	6.55%	-	-	-	-	-	-	-	-
13	Rain Dissolution	Amount	-1.42E+06	1.42E+06	-	-	-	-	-	-	-	-	-
		Percentage	-98.89%	5.99%	-	-	-	-	-	-	-	-	-
14	Dry Deposition	Amount	-5.23E+03	5.23E+03	-	-	-	-	-	-	-	-	-
		Percentage	-0.36%	0.02%	-	-	-	-	-	-	-	-	-
15	Wet Deposition	Amount	-9.39E+03	9.39E+03	-	-	-	-	-	-	-	-	-
		Percentage	-0.65%	0.04%	-	-	-	-	-	-	-	-	-
16	Diffusion (In)	Amount	8.87E+05	6.46E+06	1.19E+06	-	-	-	-	-	-	-	-
		Percentage	61.81%	27.29%	3.16%	-	-	-	-	-	-	-	-
17	Diffusion (Out)	Amount	-6.06E+02	-2.07E+06	-6.46E+06	-	-	-	-	-	-	-	-
		Percentage	-0.04%	-8.75%	-16.55%	-	-	-	-	-	-	-	-

Table A.6. PCB-18 Mass flow details under steady state with low biomass density

PCB 18 Flow Chart (mg/day)														
Sign	Name	Unit	Environment Compartments			Biotic Compartments								
			Air	Water	Sediment	Plankton	Mysid	Pontoporeia	Oligochaete	Sculpin	Alewife	Smelt	Salmonid
1	Advection Input	Amount	5.48E+05	2.19E+06	-	-	-	-	-	-	-	-	-
		Percentage	38.49%	56.07%	-	-	-	-	-	-	-	-	-
2	Food Ingestion	Amount	-	-	-6.72E+00	0.00E+00	1.04E+01	4.48E+00	2.24E+00	7.85E-03	6.69E-01	5.29E-02	3.32E-03
		Percentage	-	-	0.00%	0.00%	17.04%	0.45%	1.13%	47.15%	57.29%	62.53%	88.07%
3	Gill uptake	Amount	-	-4.50E+03	-1.18E+03	4.45E+03	5.04E+01	9.87E+02	1.97E+02	8.80E-03	4.99E-01	3.17E-02	4.50E-04
		Percentage	-	-0.12%	-0.33%	100.00%	82.96%	99.55%	98.87%	52.85%	42.71%	37.47%	11.93%
4	Reaction/ Metabolism	Amount	-6.63E+04	-2.57E+06	-2.35E+02	-3.30E-03	-6.93E-03	-6.10E-02	-2.05E-02	-1.16E-04	-1.21E-02	-4.53E-04	-1.91E-04
		Percentage	-4.66%	-65.64%	-0.07%	0.00%	-0.01%	-0.01%	-0.01%	-0.69%	-1.03%	-0.54%	-5.06%
5	Death Loss (All)	Amount	-	9.42E+01	1.21E+02	-1.83E+02	-5.70E+00	-2.17E+01	-5.04E+00	-2.18E-03	-1.86E-01	-6.97E-03	-1.31E-03
		Percentage	-	0.00%	0.03%	-4.11%	-9.39%	-2.19%	-2.53%	-13.08%	-15.88%	-8.23%	-34.88%
6	Gill release	Amount	-	4.30E+03	1.15E+03	-4.25E+03	-5.03E+01	-9.60E+02	-1.93E+02	-9.06E-03	-6.66E-01	-5.58E-02	-1.02E-03
		Percentage	-	0.11%	0.32%	-95.54%	-82.88%	-96.78%	-97.08%	-54.40%	-57.01%	-65.91%	-26.96%
7	Egestion	Amount	-	1.93E+00	4.17E+00	0.00E+00	-3.59E+00	-1.49E+00	-7.48E-01	-4.54E-03	-2.44E-01	-1.88E-02	-1.25E-03
		Percentage	-	0.00%	0.00%	0.00%	-5.92%	-0.15%	-0.38%	-27.24%	-20.90%	-22.25%	-33.09%
8	Undigested Food	Amount	-	4.84E+00	9.80E+00	-	-	-	-	-	-	-	-
		Percentage	-	0.00%	0.00%	-	-	-	-	-	-	-	-
9	Predation Loss	Amount	-	-	-	-1.59E+01	-1.10E+00	-8.71E+00	0.00E+00	-7.64E-04	-6.05E-02	-2.61E-03	0.00E+00
		Percentage	-	-	-	-0.36%	-1.81%	-0.88%	0.00%	-4.58%	-5.17%	-3.08%	0.00%
10	Advection Output	Amount	-9.08E+02	-1.05E+05	-1.10E+03	-	-	-	-	-	-	-	-
		Percentage	-0.06%	-2.70%	-0.31%	-	-	-	-	-	-	-	-
11	Resuspension	Amount	-	9.63E+02	-9.63E+02	-	-	-	-	-	-	-	-
		Percentage	-	0.02%	-0.27%	-	-	-	-	-	-	-	-
12	Deposition	Amount	-	-6.75E+03	6.75E+03	-	-	-	-	-	-	-	-
		Percentage	-	-0.17%	1.88%	-	-	-	-	-	-	-	-
13	Rain Dissolution	Amount	-1.35E+06	1.35E+06	-	-	-	-	-	-	-	-	-
		Percentage	-95.14%	34.65%	-	-	-	-	-	-	-	-	-
14	Dry Deposition	Amount	-6.36E+00	6.36E+00	-	-	-	-	-	-	-	-	-
		Percentage	0.00%	0.00%	-	-	-	-	-	-	-	-	-
15	Wet Deposition	Amount	-1.14E+01	1.14E+01	-	-	-	-	-	-	-	-	-
		Percentage	0.00%	0.00%	-	-	-	-	-	-	-	-	-
16	Diffusion (In)	Amount	8.76E+05	3.57E+05	3.51E+05	-	-	-	-	-	-	-	-
		Percentage	61.51%	9.13%	97.76%	-	-	-	-	-	-	-	-
17	Diffusion (Out)	Amount	-1.93E+03	-1.23E+06	-3.55E+05	-	-	-	-	-	-	-	-
		Percentage	-0.14%	-31.37%	-99.03%	-	-	-	-	-	-	-	-

Table A.7. PCB-153 Mass flow details under steady state with low biomass density

PCB 153 Flow Chart (mg/day)													
Sign	Name	Unit	Environment Compartments			Biotic Compartments							
			Air	Water	Sediment	Plankton	Mysid	Pontoporeia	Oligochaete	Sculpin	Alewife	Smelt	Salmonid
1	Advection Input	Amount	5.48E+05	2.19E+06	-	-	-	-	-	-	-	-	-
		Per total flow	6.99%	12.90%	-	-	-	-	-	-	-	-	-
2	Food Ingestion	Amount	-	-	-4.99E+03	0.00E+00	1.66E+03	3.32E+03	1.67E+03	1.76E+00	1.16E+02	9.48E+00	8.89E-01
		Per total flow	-	-	-0.06%	0.00%	77.77%	17.33%	34.49%	95.51%	96.09%	96.94%	99.53%
3	Gill uptake	Amount	-	-5.19E+04	-1.90E+04	5.14E+04	4.75E+02	1.59E+04	3.16E+03	8.30E-02	4.70E+00	2.99E-01	4.24E-03
		Per total flow	-	-0.31%	-0.23%	100.00%	22.23%	82.67%	65.51%	4.49%	3.91%	3.06%	0.47%
4	Reaction/ Metabolism	Amount	-4.19E+03	-2.94E+05	-4.69E+04	-6.43E-01	-1.59E+00	-2.63E+01	-1.21E+01	-4.52E-02	-4.17E+00	-3.03E-01	-7.66E-02
		Per total flow	-0.05%	-1.73%	-0.56%	0.00%	-0.07%	-0.14%	-0.25%	-2.45%	-3.46%	-3.10%	-8.57%
5	Death Loss (All)	Amount	-	1.85E+04	3.08E+04	-3.55E+04	-1.31E+03	-9.36E+03	-2.97E+03	-8.52E-01	-6.40E+01	-4.65E+00	-5.28E-01
		Per total flow	-	0.11%	0.37%	-69.15%	-61.12%	-48.78%	-61.44%	-46.10%	-53.24%	-47.60%	-59.07%
6	Gill release	Amount	-	1.29E+04	6.64E+03	-1.28E+04	-1.45E+02	-5.21E+03	-1.43E+03	-4.46E-02	-2.89E+00	-4.69E-01	-5.14E-03
		Per total flow	-	0.08%	0.08%	-24.84%	-6.80%	-27.16%	-29.69%	-2.41%	-2.41%	-4.80%	-0.57%
7	Egestion	Amount	-	2.32E+02	1.48E+03	0.00E+00	-4.33E+02	-8.31E+02	-4.16E+02	-6.07E-01	-2.83E+01	-2.61E+00	-2.84E-01
		Per total flow	-	0.00%	0.02%	0.00%	-20.25%	-4.33%	-8.62%	-32.88%	-23.54%	-26.68%	-31.78%
8	Undigested Food	Amount	-	1.26E+03	4.07E+03	-	-	-	-	-	-	-	-
		Per total flow	-	0.01%	0.05%	-	-	-	-	-	-	-	-
9	Predation Loss	Amount	-	-	-	-3.09E+03	-2.51E+02	-3.76E+03	0.00E+00	-2.99E-01	-2.09E+01	-1.74E+00	0.00E+00
		Per total flow	-	-	-	-6.00%	-11.76%	-19.58%	0.00%	-16.16%	-17.35%	-17.82%	0.00%
10	Advection Output	Amount	-4.13E+03	-9.94E+05	-1.40E+06	-	-	-	-	-	-	-	-
		Per total flow	-0.05%	-5.85%	-16.63%	-	-	-	-	-	-	-	-
11	Resuspension	Amount	-	1.23E+06	-1.23E+06	-	-	-	-	-	-	-	-
		Per total flow	-	7.23%	-14.63%	-	-	-	-	-	-	-	-
12	Deposition	Amount	-	-5.05E+06	5.05E+06	-	-	-	-	-	-	-	-
		Per total flow	-	-29.73%	60.14%	-	-	-	-	-	-	-	-
13	Rain Dissolution	Amount	-7.83E+06	7.83E+06	-	-	-	-	-	-	-	-	-
		Per total flow	-99.77%	46.06%	-	-	-	-	-	-	-	-	-
14	Dry Deposition	Amount	-3.08E-01	3.08E-01	-	-	-	-	-	-	-	-	-
		Per total flow	0.00%	0.00%	-	-	-	-	-	-	-	-	-
15	Wet Deposition	Amount	-5.54E-01	5.54E-01	-	-	-	-	-	-	-	-	-
		Per total flow	0.00%	0.00%	-	-	-	-	-	-	-	-	-
16	Diffusion (In)	Amount	7.30E+06	5.71E+06	3.30E+06	-	-	-	-	-	-	-	-
		Per total flow	93.01%	33.62%	39.35%	-	-	-	-	-	-	-	-
17	Diffusion (Out)	Amount	-9.87E+03	-1.06E+07	-5.70E+06	-	-	-	-	-	-	-	-
		Per total flow	-0.13%	-62.39%	-67.89%	-	-	-	-	-	-	-	-

Table A.8. PCB-194 Mass flow details under steady state with low biomass density

PCB 194 Flow Chart (mg/day)													
Sign	Name	Unit	Environment Compartments			Biotic Compartments							
			Air	Water	Sediment	Plankton	Mysid	Pontoporeia	Oligochaete	Sculpin	Alewife	Smelt	Salmonid
1	Advection Input	Amount	5.48E+05	2.19E+06	-	-	-	-	-	-	-	-	-
		Per total flow	21.42%	19.10%	-	-	-	-	-	-	-	-	-
2	Food Ingestion	Amount	-	-	-5.41E+03	0.00E+00	1.35E+03	3.60E+03	1.81E+03	1.51E+00	9.41E+01	7.40E+00	6.79E-01
		Per total flow	-	-	-0.06%	0.00%	77.79%	20.14%	38.78%	95.73%	96.09%	96.82%	99.49%
3	Gill uptake	Amount	-	-4.22E+04	-1.71E+04	4.19E+04	3.86E+02	1.43E+04	2.85E+03	6.75E-02	3.83E+00	2.43E-01	3.45E-03
		Per total flow	-	-0.37%	-0.20%	100.00%	22.21%	79.86%	61.22%	4.27%	3.91%	3.18%	0.51%
4	Reaction/ Metabolism	Amount	-4.48E+02	-1.23E+05	-2.99E+04	-5.64E-01	-1.42E+00	-2.69E+01	-1.31E+01	-4.48E-02	-3.73E+00	-2.66E-01	-6.63E-02
		Per total flow	-0.02%	-1.07%	-0.35%	0.00%	-0.08%	-0.15%	-0.28%	-2.84%	-3.81%	-3.48%	-9.71%
5	Death Loss (All)	Amount	-	1.62E+04	2.90E+04	-3.12E+04	-1.17E+03	-9.58E+03	-3.21E+03	-8.45E-01	-5.74E+01	-4.09E+00	-4.57E-01
		Per total flow	-	0.14%	0.34%	-74.55%	-67.02%	-53.57%	-69.05%	-53.49%	-58.56%	-53.54%	-66.92%
6	Gill release	Amount	-	8.04E+03	4.88E+03	-7.94E+03	-9.18E+01	-3.78E+03	-1.10E+03	-3.13E-02	-1.84E+00	-2.92E-01	-3.15E-03
		Per total flow	-	0.07%	0.06%	-18.98%	-5.28%	-21.12%	-23.62%	-1.98%	-1.87%	-3.82%	-0.46%
7	Egestion	Amount	-	1.37E+02	1.12E+03	0.00E+00	-2.56E+02	-6.55E+02	-3.28E+02	-3.62E-01	-1.63E+01	-1.46E+00	-1.56E-01
		Per total flow	-	0.00%	0.01%	0.00%	-14.73%	-3.66%	-7.05%	-22.94%	-16.67%	-19.10%	-22.91%
8	Undigested Food	Amount	-	1.16E+03	4.18E+03	-	-	-	-	-	-	-	-
		Per total flow	-	0.01%	0.05%	-	-	-	-	-	-	-	-
9	Predation Loss	Amount	-	-	-	-2.71E+03	-2.24E+02	-3.85E+03	0.00E+00	-2.96E-01	-1.87E+01	-1.53E+00	0.00E+00
		Per total flow	-	-	-	-6.47%	-12.89%	-21.50%	0.00%	-18.75%	-19.08%	-20.05%	0.00%
10	Advection Output	Amount	-8.83E+02	-8.09E+05	-1.78E+06	-	-	-	-	-	-	-	-
		Per total flow	-0.03%	-7.05%	-20.83%	-	-	-	-	-	-	-	-
11	Resuspension	Amount	-	1.56E+06	-1.56E+06	-	-	-	-	-	-	-	-
		Per total flow	-	13.63%	-18.33%	-	-	-	-	-	-	-	-
12	Deposition	Amount	-	-5.80E+06	5.80E+06	-	-	-	-	-	-	-	-
		Per total flow	-	-50.57%	68.03%	-	-	-	-	-	-	-	-
13	Rain Dissolution	Amount	-2.53E+06	2.53E+06	-	-	-	-	-	-	-	-	-
		Per total flow	-98.89%	22.05%	-	-	-	-	-	-	-	-	-
14	Dry Deposition	Amount	-9.32E+03	9.32E+03	-	-	-	-	-	-	-	-	-
		Per total flow	-0.36%	0.08%	-	-	-	-	-	-	-	-	-
15	Wet Deposition	Amount	-1.67E+04	1.67E+04	-	-	-	-	-	-	-	-	-
		Per total flow	-0.65%	0.15%	-	-	-	-	-	-	-	-	-
16	Diffusion (In)	Amount	2.01E+06	5.14E+06	2.69E+06	-	-	-	-	-	-	-	-
		Per total flow	78.58%	44.78%	3.16%	-	-	-	-	-	-	-	-
17	Diffusion (Out)	Amount	-1.08E+03	-4.70E+06	-5.14E+06	-	-	-	-	-	-	-	-
		Per total flow	-0.04%	-40.94%	-16.55%	-	-	-	-	-	-	-	-

Table A.9 Calculated standard redox potential for PCB dechlorination

Substrate	Product	Dechlorination Type	E (mV)
PCB 4	PCB 1	Unflanked Ortho	363
PCB 5	PCB 1	Ortho Flanked Meta	425
PCB 5	PCB 2	Single Flanked Ortho	491
PCB 6	PCB 1	Unflanked Meta	341
PCB 6	PCB 2	Unflanked Ortho	407
PCB 7	PCB 1	Unflanked Para	365
PCB 7	PCB 3	Unflanked Ortho	421
PCB 8	PCB 1	Unflanked Para	341
PCB 8	PCB 3	Unflanked Ortho	397
PCB 9	PCB 1	Unflanked Meta	360
PCB 9	PCB 2	Unflanked Ortho	425
PCB 10	PCB 1	Unflanked Ortho	422
PCB 11	PCB 2	Unflanked Meta	353
PCB 12	PCB 2	Single Flanked Para	420
PCB 12	PCB 3	Para Flanked Meta	411
PCB 13	PCB 2	Unflanked Para	343
PCB 13	PCB 3	Unflanked Meta	333
PCB 14	PCB 2	Unflanked Meta	370
PCB 15	PCB 3	Unflanked Para	335
PCB 16	PCB 4	Ortho Flanked Meta	432
PCB 16	PCB 5	Unflanked Ortho	370
PCB 16	PCB 6	Single Flanked Ortho	454
PCB 17	PCB 4	Unflanked Para	346
PCB 17	PCB 7	Unflanked Ortho	344
PCB 17	PCB 8	Unflanked Ortho	368
PCB 18	PCB 4	Unflanked Meta	372
PCB 18	PCB 6	Unflanked Ortho	394
PCB 18	PCB 9	Unflanked Ortho	375
PCB 19	PCB 4	Unflanked Ortho	399
PCB 19	PCB 10	Unflanked Ortho	340
PCB 20	PCB 5	Unflanked Meta	341
PCB 20	PCB 6	Ortho Flanked Meta	425
PCB 20	PCB 11	Single Flanked Ortho	479
PCB 21	PCB 5	Single Flanked Para	437
PCB 21	PCB 7	Doubly Flanked Meta	497
PCB 21	PCB 12	Single Flanked Ortho	507
PCB 22	PCB 5	Unflanked Para	341
PCB 22	PCB 8	Ortho Flanked Meta	425
PCB 22	PCB 13	Single Flanked Ortho	489
PCB 23	PCB 5	Unflanked Meta	381
PCB 23	PCB 9	Ortho Flanked Meta	447
PCB 23	PCB 14	Single Flanked Ortho	502
PCB 24	PCB 5	Unflanked Ortho	405
PCB 24	PCB 9	Single Flanked Ortho	470
PCB 24	PCB 10	Ortho Flanked Meta	408
PCB 25	PCB 6	Unflanked Para	365
PCB 25	PCB 7	Unflanked Meta	342
PCB 25	PCB 13	Unflanked Ortho	429
PCB 26	PCB 6	Unflanked Meta	362
PCB 26	PCB 9	Unflanked Meta	343
PCB 26	PCB 11	Unflanked Ortho	416
PCB 27	PCB 6	Unflanked Ortho	401
PCB 27	PCB 10	Unflanked Meta	320
PCB 28	PCB 7	Unflanked Para	343
PCB 28	PCB 8	Unflanked Para	366
PCB 28	PCB 15	Unflanked Ortho	429
PCB 29	PCB 7	Para Flanked Meta	442
PCB 29	PCB 9	Single Flanked Para	447
PCB 29	PCB 12	Unflanked Ortho	452
PCB 30	PCB 7	Unflanked Ortho	448
PCB 30	PCB 10	Unflanked Para	391
PCB 31	PCB 8	Unflanked Meta	360
PCB 31	PCB 9	Unflanked Para	341
PCB 31	PCB 13	Unflanked Ortho	424
PCB 32	PCB 8	Unflanked Ortho	396
PCB 32	PCB 10	Unflanked Para	315

PCB	33	PCB	6	Single Flanked Para	417	PCB	45	PCB	19	Ortho Flanked Meta	451
PCB	33	PCB	8	Para Flanked Meta	417	PCB	45	PCB	24	Unflanked Ortho	383
PCB	33	PCB	12	Unflanked Ortho	403	PCB	46	PCB	16	Unflanked Ortho	403
PCB	34	PCB	6	Unflanked Meta	366	PCB	46	PCB	19	Ortho Flanked Meta	436
PCB	34	PCB	14	Unflanked Ortho	403	PCB	46	PCB	27	Single Flanked Ortho	456
PCB	35	PCB	11	Single Flanked Para	412	PCB	47	PCB	17	Unflanked Para	378
PCB	35	PCB	12	Unflanked Meta	344	PCB	47	PCB	28	Unflanked Ortho	380
PCB	35	PCB	13	Para Flanked Meta	421	PCB	48	PCB	17	Para Flanked Meta	467
PCB	36	PCB	11	Unflanked Meta	362	PCB	48	PCB	18	Single Flanked Para	441
PCB	36	PCB	14	Unflanked Meta	345	PCB	48	PCB	29	Unflanked Ortho	369
PCB	37	PCB	12	Unflanked Para	339	PCB	48	PCB	33	Unflanked Ortho	418
PCB	37	PCB	13	Single Flanked Para	417	PCB	49	PCB	17	Unflanked Meta	392
PCB	37	PCB	15	Para Flanked Meta	415	PCB	49	PCB	18	Unflanked Para	367
PCB	38	PCB	12	Para Flanked Meta	442	PCB	49	PCB	25	Unflanked Ortho	395
PCB	38	PCB	14	Doubly Flanked Para	492	PCB	49	PCB	31	Unflanked Ortho	400
PCB	39	PCB	13	Unflanked Meta	366	PCB	50	PCB	17	Unflanked Ortho	447
PCB	39	PCB	14	Unflanked Para	339	PCB	50	PCB	19	Unflanked Para	394
PCB	40	PCB	16	Ortho Flanked Meta	422	PCB	50	PCB	30	Unflanked Ortho	343
PCB	40	PCB	20	Single Flanked Ortho	450	PCB	51	PCB	17	Unflanked Ortho	436
PCB	41	PCB	16	Single Flanked Para	447	PCB	51	PCB	19	Unflanked Para	383
PCB	41	PCB	17	Doubly Flanked Meta	532	PCB	51	PCB	32	Unflanked Ortho	408
PCB	41	PCB	21	Unflanked Ortho	379	PCB	52	PCB	18	Unflanked Meta	364
PCB	41	PCB	33	Single Flanked Ortho	483	PCB	52	PCB	26	Unflanked Ortho	397
PCB	42	PCB	16	Unflanked Para	362	PCB	53	PCB	18	Unflanked Ortho	403
PCB	42	PCB	17	Ortho Flanked Meta	448	PCB	53	PCB	19	Unflanked Meta	376
PCB	42	PCB	22	Unflanked Ortho	391	PCB	53	PCB	27	Unflanked Ortho	396
PCB	42	PCB	25	Single Flanked Ortho	451	PCB	54	PCB	19	Unflanked Ortho	407
PCB	43	PCB	16	Unflanked Meta	388	PCB	55	PCB	20	Single Flanked Para	443
PCB	43	PCB	18	Ortho Flanked Meta	448	PCB	55	PCB	21	Unflanked Meta	348
PCB	43	PCB	23	Unflanked Ortho	376	PCB	55	PCB	25	Doubly Flanked Meta	503
PCB	43	PCB	34	Single Flanked Ortho	475	PCB	55	PCB	35	Single Flanked Ortho	511
PCB	44	PCB	16	Unflanked Meta	371	PCB	56	PCB	20	Single Flanked Para	423
PCB	44	PCB	18	Ortho Flanked Meta	431	PCB	56	PCB	22	Para Flanked Meta	423
PCB	44	PCB	20	Unflanked Ortho	399	PCB	56	PCB	33	Ortho Flanked Meta	431
PCB	44	PCB	26	Single Flanked Ortho	463	PCB	56	PCB	35	Single Flanked Ortho	491
PCB	45	PCB	16	Unflanked Ortho	418	PCB	57	PCB	20	Unflanked Meta	386
PCB	45	PCB	18	Single Flanked Ortho	478	PCB	57	PCB	23	Unflanked Meta	346

PCB	57	PCB	26	Ortho Flanked Meta	450	PCB	67	PCB	29	Unflanked Meta	331
PCB	57	PCB	36	Single Flanked Ortho	504	PCB	67	PCB	35	Unflanked Ortho	439
PCB	58	PCB	20	Unflanked Meta	374	PCB	68	PCB	25	Unflanked Meta	377
PCB	58	PCB	34	Ortho Flanked Meta	433	PCB	68	PCB	34	Unflanked Para	376
PCB	58	PCB	36	Single Flanked Ortho	491	PCB	68	PCB	39	Unflanked Ortho	440
PCB	59	PCB	20	Unflanked Ortho	421	PCB	69	PCB	25	Unflanked Ortho	426
PCB	59	PCB	24	Unflanked Meta	357	PCB	69	PCB	27	Unflanked Para	390
PCB	59	PCB	26	Single Flanked Ortho	484	PCB	69	PCB	30	Unflanked Meta	320
PCB	59	PCB	27	Ortho Flanked Meta	445	PCB	70	PCB	26	Single Flanked Para	418
PCB	60	PCB	21	Unflanked Para	339	PCB	70	PCB	31	Para Flanked Meta	420
PCB	60	PCB	22	Single Flanked Para	435	PCB	70	PCB	33	Unflanked Meta	363
PCB	60	PCB	28	Doubly Flanked Meta	493	PCB	70	PCB	35	Unflanked Ortho	422
PCB	60	PCB	37	Single Flanked Ortho	507	PCB	71	PCB	27	Single Flanked Para	418
PCB	61	PCB	21	Para Flanked Meta	460	PCB	71	PCB	32	Para Flanked Meta	424
PCB	61	PCB	23	Doubly Flanked Para	515	PCB	71	PCB	33	Unflanked Ortho	402
PCB	61	PCB	29	Doubly Flanked Meta	515	PCB	72	PCB	26	Unflanked Meta	379
PCB	61	PCB	38	Single Flanked Ortho	526	PCB	72	PCB	34	Unflanked Meta	374
PCB	62	PCB	21	Unflanked Ortho	441	PCB	72	PCB	36	Unflanked Ortho	433
PCB	62	PCB	24	Single Flanked Para	473	PCB	73	PCB	27	Unflanked Meta	378
PCB	62	PCB	29	Single Flanked Ortho	497	PCB	73	PCB	34	Unflanked Ortho	412
PCB	62	PCB	30	Doubly Flanked Meta	490	PCB	74	PCB	28	Para Flanked Meta	433
PCB	63	PCB	22	Unflanked Meta	381	PCB	74	PCB	29	Unflanked Para	334
PCB	63	PCB	23	Unflanked Para	341	PCB	74	PCB	31	Single Flanked Para	440
PCB	63	PCB	31	Ortho Flanked Meta	446	PCB	74	PCB	37	Unflanked Ortho	447
PCB	63	PCB	39	Single Flanked Ortho	504	PCB	75	PCB	28	Unflanked Ortho	414
PCB	64	PCB	22	Unflanked Ortho	420	PCB	75	PCB	30	Unflanked Para	309
PCB	64	PCB	24	Unflanked Para	357	PCB	75	PCB	32	Unflanked Para	385
PCB	64	PCB	31	Single Flanked Ortho	486	PCB	76	PCB	33	Para Flanked Meta	444
PCB	64	PCB	32	Ortho Flanked Meta	450	PCB	76	PCB	34	Doubly Flanked Para	495
PCB	65	PCB	23	Single Flanked Ortho	513	PCB	76	PCB	38	Unflanked Ortho	406
PCB	65	PCB	24	Ortho Flanked Meta	490	PCB	77	PCB	35	Single Flanked Para	424
PCB	66	PCB	25	Single Flanked Para	426	PCB	77	PCB	37	Para Flanked Meta	429
PCB	66	PCB	28	Para Flanked Meta	425	PCB	78	PCB	35	Para Flanked Meta	444
PCB	66	PCB	33	Unflanked Para	374	PCB	78	PCB	36	Doubly Flanked Para	493
PCB	66	PCB	37	Unflanked Ortho	438	PCB	78	PCB	38	Unflanked Meta	346
PCB	67	PCB	25	Para Flanked Meta	431	PCB	79	PCB	35	Unflanked Meta	371
PCB	67	PCB	26	Single Flanked Para	435	PCB	79	PCB	36	Single Flanked Para	421

PCB	79	PCB	39	Para Flanked Meta	426	PCB	88	PCB	48	Single Flanked Ortho	506
PCB	80	PCB	36	Unflanked Meta	392	PCB	88	PCB	50	Doubly Flanked Meta	526
PCB	81	PCB	37	Para Flanked Meta	442	PCB	88	PCB	62	Unflanked Ortho	379
PCB	81	PCB	38	Unflanked Para	340	PCB	89	PCB	41	Unflanked Ortho	397
PCB	81	PCB	39	Doubly Flanked Para	492	PCB	89	PCB	46	Single Flanked Para	440
PCB	82	PCB	40	Single Flanked Para	453	PCB	89	PCB	51	Doubly Flanked Meta	493
PCB	82	PCB	41	Ortho Flanked Meta	429	PCB	89	PCB	71	Single Flanked Ortho	478
PCB	82	PCB	42	Doubly Flanked Meta	513	PCB	90	PCB	42	Unflanked Meta	397
PCB	82	PCB	55	Single Flanked Ortho	460	PCB	90	PCB	43	Unflanked Para	372
PCB	82	PCB	56	Single Flanked Ortho	481	PCB	90	PCB	49	Ortho Flanked Meta	453
PCB	83	PCB	40	Unflanked Meta	397	PCB	90	PCB	63	Unflanked Ortho	407
PCB	83	PCB	43	Ortho Flanked Meta	432	PCB	90	PCB	68	Single Flanked Ortho	471
PCB	83	PCB	44	Ortho Flanked Meta	448	PCB	91	PCB	42	Unflanked Ortho	430
PCB	83	PCB	57	Single Flanked Ortho	461	PCB	91	PCB	45	Unflanked Para	374
PCB	83	PCB	58	Single Flanked Ortho	474	PCB	91	PCB	49	Single Flanked Ortho	485
PCB	84	PCB	40	Unflanked Ortho	428	PCB	91	PCB	51	Ortho Flanked Meta	442
PCB	84	PCB	44	Single Flanked Ortho	479	PCB	91	PCB	64	Unflanked Ortho	400
PCB	84	PCB	45	Ortho Flanked Meta	432	PCB	92	PCB	43	Unflanked Meta	370
PCB	84	PCB	46	Ortho Flanked Meta	447	PCB	92	PCB	44	Unflanked Meta	387
PCB	84	PCB	59	Single Flanked Ortho	458	PCB	92	PCB	52	Ortho Flanked Meta	453
PCB	85	PCB	41	Unflanked Para	367	PCB	92	PCB	57	Unflanked Ortho	400
PCB	85	PCB	42	Single Flanked Para	451	PCB	92	PCB	72	Single Flanked Ortho	471
PCB	85	PCB	47	Doubly Flanked Meta	521	PCB	93	PCB	43	Single Flanked Ortho	488
PCB	85	PCB	60	Unflanked Ortho	408	PCB	93	PCB	45	Ortho Flanked Meta	458
PCB	85	PCB	66	Single Flanked Ortho	476	PCB	93	PCB	65	Unflanked Ortho	351
PCB	86	PCB	41	Para Flanked Meta	459	PCB	94	PCB	43	Unflanked Ortho	398
PCB	86	PCB	43	Doubly Flanked Para	518	PCB	94	PCB	46	Unflanked Meta	382
PCB	86	PCB	48	Doubly Flanked Meta	524	PCB	94	PCB	53	Ortho Flanked Meta	442
PCB	86	PCB	61	Unflanked Ortho	378	PCB	94	PCB	73	Single Flanked Ortho	461
PCB	86	PCB	76	Single Flanked Ortho	498	PCB	95	PCB	44	Unflanked Ortho	418
PCB	87	PCB	41	Unflanked Meta	365	PCB	95	PCB	45	Unflanked Meta	370
PCB	87	PCB	44	Single Flanked Para	441	PCB	95	PCB	52	Single Flanked Ortho	484
PCB	87	PCB	49	Doubly Flanked Meta	505	PCB	95	PCB	53	Ortho Flanked Meta	445
PCB	87	PCB	55	Unflanked Ortho	397	PCB	95	PCB	59	Unflanked Ortho	396
PCB	87	PCB	70	Single Flanked Ortho	486	PCB	96	PCB	45	Unflanked Ortho	408
PCB	88	PCB	41	Unflanked Ortho	441	PCB	96	PCB	46	Unflanked Ortho	422
PCB	88	PCB	45	Single Flanked Para	469	PCB	96	PCB	53	Single Flanked Ortho	482

PCB	96	PCB	54	Ortho Flanked Meta	452	PCB	105	PCB	60	Para Flanked Meta	431
PCB	97	PCB	42	Para Flanked Meta	441	PCB	105	PCB	66	Doubly Flanked Meta	500
PCB	97	PCB	44	Single Flanked Para	432	PCB	105	PCB	77	Single Flanked Ortho	509
PCB	97	PCB	48	Ortho Flanked Meta	422	PCB	106	PCB	55	Para Flanked Meta	460
PCB	97	PCB	56	Unflanked Ortho	409	PCB	106	PCB	57	Doubly Flanked Para	517
PCB	97	PCB	67	Single Flanked Ortho	460	PCB	106	PCB	61	Unflanked Meta	348
PCB	98	PCB	42	Unflanked Ortho	444	PCB	106	PCB	67	Doubly Flanked Meta	532
PCB	98	PCB	46	Unflanked Para	403	PCB	106	PCB	78	Single Flanked Ortho	528
PCB	98	PCB	50	Ortho Flanked Meta	445	PCB	107	PCB	56	Unflanked Meta	386
PCB	98	PCB	69	Single Flanked Ortho	469	PCB	107	PCB	57	Single Flanked Para	422
PCB	99	PCB	47	Para Flanked Meta	453	PCB	107	PCB	63	Para Flanked Meta	427
PCB	99	PCB	48	Unflanked Para	365	PCB	107	PCB	70	Ortho Flanked Meta	454
PCB	99	PCB	49	Single Flanked Para	439	PCB	107	PCB	79	Single Flanked Ortho	505
PCB	99	PCB	66	Unflanked Ortho	409	PCB	108	PCB	55	Unflanked Meta	379
PCB	99	PCB	74	Unflanked Ortho	400	PCB	108	PCB	58	Single Flanked Para	448
PCB	100	PCB	47	Unflanked Ortho	475	PCB	108	PCB	68	Doubly Flanked Meta	505
PCB	100	PCB	50	Unflanked Para	407	PCB	108	PCB	79	Single Flanked Ortho	519
PCB	100	PCB	51	Unflanked Para	417	PCB	109	PCB	55	Unflanked Ortho	441
PCB	100	PCB	75	Unflanked Ortho	440	PCB	109	PCB	59	Single Flanked Para	463
PCB	101	PCB	48	Unflanked Meta	374	PCB	109	PCB	62	Unflanked Meta	347
PCB	101	PCB	49	Para Flanked Meta	448	PCB	109	PCB	67	Single Flanked Ortho	512
PCB	101	PCB	52	Single Flanked Para	450	PCB	109	PCB	69	Doubly Flanked Meta	518
PCB	101	PCB	67	Unflanked Ortho	412	PCB	110	PCB	56	Unflanked Ortho	416
PCB	101	PCB	70	Unflanked Ortho	429	PCB	110	PCB	59	Single Flanked Para	418
PCB	102	PCB	48	Unflanked Ortho	407	PCB	110	PCB	64	Para Flanked Meta	419
PCB	102	PCB	51	Para Flanked Meta	437	PCB	110	PCB	70	Single Flanked Ortho	484
PCB	102	PCB	53	Single Flanked Para	444	PCB	110	PCB	71	Ortho Flanked Meta	445
PCB	102	PCB	71	Unflanked Ortho	422	PCB	111	PCB	57	Unflanked Meta	378
PCB	103	PCB	49	Unflanked Ortho	431	PCB	111	PCB	58	Unflanked Meta	390
PCB	103	PCB	50	Unflanked Meta	377	PCB	111	PCB	72	Ortho Flanked Meta	449
PCB	103	PCB	53	Unflanked Para	395	PCB	111	PCB	80	Single Flanked Ortho	489
PCB	103	PCB	69	Unflanked Ortho	400	PCB	112	PCB	57	Single Flanked Ortho	486
PCB	104	PCB	50	Unflanked Ortho	415	PCB	112	PCB	59	Ortho Flanked Meta	451
PCB	104	PCB	51	Unflanked Ortho	426	PCB	112	PCB	65	Unflanked Meta	318
PCB	104	PCB	54	Unflanked Para	402	PCB	113	PCB	58	Unflanked Ortho	410
PCB	105	PCB	55	Single Flanked Para	422	PCB	113	PCB	59	Unflanked Meta	363
PCB	105	PCB	56	Single Flanked Para	443	PCB	113	PCB	72	Single Flanked Ortho	469

PCB	113	PCB	73	Ortho Flanked Meta	431	PCB	123	PCB	66	Para Flanked Meta	445
PCB	114	PCB	60	Para Flanked Meta	461	PCB	123	PCB	68	Doubly Flanked Para	494
PCB	114	PCB	61	Unflanked Para	340	PCB	123	PCB	76	Unflanked Para	375
PCB	114	PCB	63	Doubly Flanked Para	514	PCB	123	PCB	81	Unflanked Ortho	441
PCB	114	PCB	74	Doubly Flanked Meta	521	PCB	124	PCB	70	Para Flanked Meta	455
PCB	114	PCB	81	Single Flanked Ortho	526	PCB	124	PCB	72	Doubly Flanked Para	494
PCB	115	PCB	60	Unflanked Ortho	440	PCB	124	PCB	76	Unflanked Meta	374
PCB	115	PCB	62	Unflanked Para	337	PCB	124	PCB	78	Unflanked Ortho	434
PCB	115	PCB	64	Single Flanked Para	454	PCB	125	PCB	71	Para Flanked Meta	442
PCB	115	PCB	74	Single Flanked Ortho	500	PCB	125	PCB	73	Doubly Flanked Para	483
PCB	115	PCB	75	Doubly Flanked Meta	519	PCB	125	PCB	76	Unflanked Ortho	400
PCB	116	PCB	61	Single Flanked Ortho	535	PCB	126	PCB	77	Para Flanked Meta	438
PCB	116	PCB	62	Doubly Flanked Meta	554	PCB	126	PCB	78	Single Flanked Para	419
PCB	116	PCB	65	Doubly Flanked Para	537	PCB	126	PCB	79	Doubly Flanked Para	492
PCB	117	PCB	63	Single Flanked Ortho	488	PCB	126	PCB	81	Para Flanked Meta	425
PCB	117	PCB	64	Ortho Flanked Meta	448	PCB	127	PCB	78	Unflanked Meta	384
PCB	117	PCB	65	Unflanked Para	315	PCB	127	PCB	79	Para Flanked Meta	457
PCB	118	PCB	66	Para Flanked Meta	433	PCB	127	PCB	80	Doubly Flanked Para	485
PCB	118	PCB	67	Single Flanked Para	428	PCB	128	PCB	82	Single Flanked Para	442
PCB	118	PCB	70	Single Flanked Para	444	PCB	128	PCB	85	Doubly Flanked Meta	503
PCB	118	PCB	74	Para Flanked Meta	425	PCB	128	PCB	105	Single Flanked Ortho	480
PCB	118	PCB	77	Unflanked Ortho	443	PCB	129	PCB	82	Para Flanked Meta	460
PCB	119	PCB	66	Unflanked Ortho	423	PCB	129	PCB	83	Doubly Flanked Para	516
PCB	119	PCB	69	Single Flanked Para	423	PCB	129	PCB	86	Ortho Flanked Meta	429
PCB	119	PCB	71	Unflanked Para	395	PCB	129	PCB	97	Doubly Flanked Meta	532
PCB	119	PCB	75	Para Flanked Meta	433	PCB	129	PCB	106	Single Flanked Ortho	460
PCB	120	PCB	67	Unflanked Meta	386	PCB	129	PCB	122	Single Flanked Ortho	493
PCB	120	PCB	68	Para Flanked Meta	441	PCB	130	PCB	82	Unflanked Meta	393
PCB	120	PCB	72	Single Flanked Para	443	PCB	130	PCB	83	Single Flanked Para	449
PCB	120	PCB	79	Unflanked Ortho	455	PCB	130	PCB	87	Ortho Flanked Meta	456
PCB	121	PCB	68	Unflanked Ortho	412	PCB	130	PCB	90	Doubly Flanked Meta	509
PCB	121	PCB	69	Unflanked Meta	363	PCB	130	PCB	107	Single Flanked Ortho	488
PCB	121	PCB	73	Unflanked Para	376	PCB	130	PCB	108	Single Flanked Ortho	475
PCB	122	PCB	56	Para Flanked Meta	447	PCB	131	PCB	82	Unflanked Ortho	442
PCB	122	PCB	58	Doubly Flanked Para	497	PCB	131	PCB	84	Single Flanked Para	467
PCB	122	PCB	76	Ortho Flanked Meta	435	PCB	131	PCB	88	Ortho Flanked Meta	430
PCB	122	PCB	78	Single Flanked Ortho	494	PCB	131	PCB	97	Single Flanked Ortho	515

PCB	131	PCB	98	Doubly Flanked Meta	511	PCB	139	PCB	88	Unflanked Para	372
PCB	131	PCB	109	Single Flanked Ortho	462	PCB	139	PCB	91	Single Flanked Para	468
PCB	132	PCB	82	Unflanked Ortho	422	PCB	139	PCB	99	Single Flanked Ortho	514
PCB	132	PCB	84	Single Flanked Para	447	PCB	139	PCB	100	Doubly Flanked Meta	492
PCB	132	PCB	87	Single Flanked Ortho	485	PCB	139	PCB	115	Unflanked Ortho	414
PCB	132	PCB	89	Ortho Flanked Meta	454	PCB	140	PCB	85	Unflanked Ortho	424
PCB	132	PCB	91	Doubly Flanked Meta	505	PCB	140	PCB	89	Unflanked Para	394
PCB	132	PCB	110	Single Flanked Ortho	486	PCB	140	PCB	98	Single Flanked Para	431
PCB	133	PCB	83	Unflanked Meta	398	PCB	140	PCB	100	Doubly Flanked Meta	470
PCB	133	PCB	92	Ortho Flanked Meta	459	PCB	140	PCB	119	Single Flanked Ortho	477
PCB	133	PCB	111	Single Flanked Ortho	481	PCB	141	PCB	86	Unflanked Meta	368
PCB	134	PCB	83	Single Flanked Ortho	500	PCB	141	PCB	87	Para Flanked Meta	462
PCB	134	PCB	84	Ortho Flanked Meta	469	PCB	141	PCB	92	Doubly Flanked Para	516
PCB	134	PCB	93	Ortho Flanked Meta	444	PCB	141	PCB	101	Doubly Flanked Meta	519
PCB	134	PCB	112	Single Flanked Ortho	476	PCB	141	PCB	106	Unflanked Ortho	398
PCB	135	PCB	83	Unflanked Ortho	428	PCB	141	PCB	124	Single Flanked Ortho	493
PCB	135	PCB	84	Unflanked Meta	397	PCB	142	PCB	86	Single Flanked Ortho	509
PCB	135	PCB	92	Single Flanked Ortho	489	PCB	142	PCB	88	Doubly Flanked Meta	527
PCB	135	PCB	94	Ortho Flanked Meta	462	PCB	142	PCB	93	Doubly Flanked Para	539
PCB	135	PCB	95	Ortho Flanked Meta	459	PCB	142	PCB	116	Unflanked Ortho	353
PCB	135	PCB	113	Single Flanked Ortho	492	PCB	143	PCB	86	Unflanked Ortho	398
PCB	136	PCB	84	Unflanked Ortho	424	PCB	143	PCB	89	Para Flanked Meta	461
PCB	136	PCB	95	Single Flanked Ortho	486	PCB	143	PCB	94	Doubly Flanked Para	518
PCB	136	PCB	96	Ortho Flanked Meta	449	PCB	143	PCB	102	Doubly Flanked Meta	516
PCB	137	PCB	85	Para Flanked Meta	462	PCB	143	PCB	125	Single Flanked Ortho	496
PCB	137	PCB	86	Unflanked Para	371	PCB	144	PCB	87	Unflanked Ortho	448
PCB	137	PCB	90	Doubly Flanked Para	517	PCB	144	PCB	88	Unflanked Meta	373
PCB	137	PCB	99	Doubly Flanked Meta	530	PCB	144	PCB	95	Single Flanked Para	472
PCB	137	PCB	114	Unflanked Ortho	409	PCB	144	PCB	101	Single Flanked Ortho	505
PCB	137	PCB	123	Single Flanked Ortho	494	PCB	144	PCB	103	Doubly Flanked Meta	522
PCB	138	PCB	85	Para Flanked Meta	446	PCB	144	PCB	109	Unflanked Ortho	405
PCB	138	PCB	87	Single Flanked Para	447	PCB	145	PCB	88	Unflanked Ortho	410
PCB	138	PCB	97	Single Flanked Para	457	PCB	145	PCB	89	Unflanked Ortho	454
PCB	138	PCB	99	Doubly Flanked Meta	514	PCB	145	PCB	96	Single Flanked Para	472
PCB	138	PCB	105	Unflanked Ortho	422	PCB	145	PCB	102	Single Flanked Ortho	509
PCB	138	PCB	118	Single Flanked Ortho	489	PCB	145	PCB	104	Doubly Flanked Meta	521
PCB	139	PCB	85	Unflanked Ortho	446	PCB	146	PCB	90	Para Flanked Meta	448

PCB	146	PCB	92	Single Flanked Para	449	PCB	154	PCB	102	Unflanked Para	396
PCB	146	PCB	97	Unflanked Meta	404	PCB	154	PCB	103	Single Flanked Para	446
PCB	146	PCB	101	Ortho Flanked Meta	452	PCB	154	PCB	119	Unflanked Ortho	423
PCB	146	PCB	107	Unflanked Ortho	427	PCB	155	PCB	100	Unflanked Ortho	406
PCB	146	PCB	120	Single Flanked Ortho	478	PCB	155	PCB	104	Unflanked Para	398
PCB	147	PCB	90	Single Flanked Ortho	521	PCB	156	PCB	105	Para Flanked Meta	461
PCB	147	PCB	91	Ortho Flanked Meta	488	PCB	156	PCB	106	Single Flanked Para	423
PCB	147	PCB	93	Unflanked Para	404	PCB	156	PCB	107	Doubly Flanked Para	518
PCB	147	PCB	117	Unflanked Ortho	440	PCB	156	PCB	114	Para Flanked Meta	431
PCB	148	PCB	90	Unflanked Ortho	432	PCB	156	PCB	118	Doubly Flanked Meta	528
PCB	148	PCB	94	Unflanked Para	406	PCB	156	PCB	126	Single Flanked Ortho	532
PCB	148	PCB	98	Unflanked Meta	385	PCB	157	PCB	105	Para Flanked Meta	449
PCB	148	PCB	103	Ortho Flanked Meta	454	PCB	157	PCB	108	Doubly Flanked Para	493
PCB	148	PCB	121	Single Flanked Ortho	491	PCB	157	PCB	122	Single Flanked Para	444
PCB	149	PCB	91	Para Flanked Meta	440	PCB	157	PCB	123	Doubly Flanked Meta	504
PCB	149	PCB	95	Single Flanked Para	443	PCB	157	PCB	126	Single Flanked Ortho	520
PCB	149	PCB	97	Unflanked Ortho	429	PCB	158	PCB	105	Unflanked Ortho	437
PCB	149	PCB	101	Single Flanked Ortho	477	PCB	158	PCB	109	Single Flanked Para	419
PCB	149	PCB	102	Ortho Flanked Meta	444	PCB	158	PCB	110	Single Flanked Para	464
PCB	149	PCB	110	Unflanked Ortho	421	PCB	158	PCB	115	Para Flanked Meta	429
PCB	150	PCB	91	Unflanked Ortho	438	PCB	158	PCB	118	Single Flanked Ortho	504
PCB	150	PCB	96	Unflanked Para	404	PCB	158	PCB	119	Doubly Flanked Meta	514
PCB	150	PCB	98	Unflanked Ortho	423	PCB	159	PCB	106	Unflanked Meta	379
PCB	150	PCB	103	Single Flanked Ortho	492	PCB	159	PCB	108	Para Flanked Meta	461
PCB	150	PCB	104	Ortho Flanked Meta	454	PCB	159	PCB	111	Doubly Flanked Para	519
PCB	151	PCB	92	Single Flanked Ortho	496	PCB	159	PCB	120	Doubly Flanked Meta	525
PCB	151	PCB	93	Unflanked Meta	378	PCB	159	PCB	127	Single Flanked Ortho	523
PCB	151	PCB	95	Ortho Flanked Meta	466	PCB	160	PCB	106	Single Flanked Ortho	512
PCB	151	PCB	112	Unflanked Ortho	411	PCB	160	PCB	109	Doubly Flanked Meta	532
PCB	152	PCB	93	Unflanked Ortho	418	PCB	160	PCB	112	Doubly Flanked Para	544
PCB	152	PCB	94	Single Flanked Ortho	508	PCB	160	PCB	116	Unflanked Meta	325
PCB	152	PCB	96	Ortho Flanked Meta	468	PCB	161	PCB	108	Unflanked Ortho	473
PCB	153	PCB	99	Para Flanked Meta	459	PCB	161	PCB	109	Unflanked Meta	411
PCB	153	PCB	101	Single Flanked Para	450	PCB	161	PCB	113	Single Flanked Para	511
PCB	153	PCB	118	Unflanked Ortho	434	PCB	161	PCB	120	Single Flanked Ortho	537
PCB	154	PCB	99	Unflanked Ortho	438	PCB	161	PCB	121	Doubly Flanked Meta	566
PCB	154	PCB	100	Para Flanked Meta	416	PCB	162	PCB	107	Para Flanked Meta	452

PCB	162	PCB	111	Doubly Flanked Para	496	PCB	170	PCB	157	Single Flanked Ortho	498
PCB	162	PCB	122	Unflanked Meta	390	PCB	171	PCB	128	Unflanked Ortho	449
PCB	162	PCB	124	Ortho Flanked Meta	451	PCB	171	PCB	131	Single Flanked Para	448
PCB	162	PCB	127	Single Flanked Ortho	500	PCB	171	PCB	132	Single Flanked Para	469
PCB	163	PCB	107	Single Flanked Ortho	496	PCB	171	PCB	138	Single Flanked Ortho	506
PCB	163	PCB	110	Ortho Flanked Meta	465	PCB	171	PCB	139	Doubly Flanked Meta	506
PCB	163	PCB	112	Single Flanked Para	433	PCB	171	PCB	140	Doubly Flanked Meta	528
PCB	163	PCB	117	Para Flanked Meta	436	PCB	171	PCB	158	Single Flanked Ortho	491
PCB	164	PCB	110	Para Flanked Meta	453	PCB	172	PCB	129	Unflanked Meta	387
PCB	164	PCB	113	Doubly Flanked Para	508	PCB	172	PCB	130	Para Flanked Meta	454
PCB	164	PCB	122	Unflanked Ortho	421	PCB	172	PCB	133	Doubly Flanked Para	505
PCB	164	PCB	124	Single Flanked Ortho	482	PCB	172	PCB	141	Ortho Flanked Meta	448
PCB	164	PCB	125	Ortho Flanked Meta	456	PCB	172	PCB	146	Doubly Flanked Meta	515
PCB	165	PCB	111	Single Flanked Ortho	495	PCB	172	PCB	159	Single Flanked Ortho	467
PCB	165	PCB	112	Unflanked Meta	387	PCB	172	PCB	162	Single Flanked Ortho	490
PCB	165	PCB	113	Ortho Flanked Meta	475	PCB	173	PCB	129	Single Flanked Ortho	525
PCB	166	PCB	114	Single Flanked Ortho	507	PCB	173	PCB	131	Doubly Flanked Meta	542
PCB	166	PCB	115	Doubly Flanked Meta	529	PCB	173	PCB	134	Doubly Flanked Para	541
PCB	166	PCB	116	Unflanked Para	313	PCB	173	PCB	142	Ortho Flanked Meta	445
PCB	166	PCB	117	Doubly Flanked Para	534	PCB	173	PCB	160	Single Flanked Ortho	473
PCB	167	PCB	118	Para Flanked Meta	454	PCB	174	PCB	129	Unflanked Ortho	430
PCB	167	PCB	120	Doubly Flanked Para	495	PCB	174	PCB	132	Para Flanked Meta	468
PCB	167	PCB	123	Para Flanked Meta	442	PCB	174	PCB	135	Doubly Flanked Para	518
PCB	167	PCB	124	Single Flanked Para	443	PCB	174	PCB	141	Single Flanked Ortho	492
PCB	167	PCB	126	Unflanked Ortho	458	PCB	174	PCB	143	Ortho Flanked Meta	461
PCB	168	PCB	119	Para Flanked Meta	447	PCB	174	PCB	149	Doubly Flanked Meta	534
PCB	168	PCB	121	Doubly Flanked Para	507	PCB	174	PCB	164	Single Flanked Ortho	502
PCB	168	PCB	123	Unflanked Ortho	426	PCB	175	PCB	130	Unflanked Ortho	447
PCB	168	PCB	125	Unflanked Para	400	PCB	175	PCB	131	Unflanked Meta	398
PCB	169	PCB	126	Para Flanked Meta	460	PCB	175	PCB	135	Single Flanked Para	468
PCB	169	PCB	127	Doubly Flanked Para	494	PCB	175	PCB	144	Ortho Flanked Meta	456
PCB	170	PCB	128	Para Flanked Meta	467	PCB	175	PCB	146	Single Flanked Ortho	508
PCB	170	PCB	129	Single Flanked Para	449	PCB	175	PCB	148	Doubly Flanked Meta	524
PCB	170	PCB	130	Doubly Flanked Para	516	PCB	175	PCB	161	Single Flanked Ortho	449
PCB	170	PCB	137	Doubly Flanked Meta	508	PCB	176	PCB	131	Unflanked Ortho	428
PCB	170	PCB	138	Doubly Flanked Meta	525	PCB	176	PCB	132	Unflanked Ortho	448
PCB	170	PCB	156	Single Flanked Ortho	486	PCB	176	PCB	136	Single Flanked Para	471

PCB	176	PCB	144	Single Flanked Ortho	485	PCB	183	PCB	138	Unflanked Ortho	446
PCB	176	PCB	145	Ortho Flanked Meta	448	PCB	183	PCB	139	Para Flanked Meta	446
PCB	176	PCB	149	Single Flanked Ortho	514	PCB	183	PCB	144	Single Flanked Para	445
PCB	176	PCB	150	Doubly Flanked Meta	516	PCB	183	PCB	149	Single Flanked Para	474
PCB	177	PCB	130	Single Flanked Ortho	495	PCB	183	PCB	153	Single Flanked Ortho	500
PCB	177	PCB	132	Ortho Flanked Meta	466	PCB	183	PCB	154	Doubly Flanked Meta	521
PCB	177	PCB	134	Single Flanked Para	443	PCB	183	PCB	158	Unflanked Ortho	431
PCB	177	PCB	147	Doubly Flanked Meta	482	PCB	184	PCB	139	Unflanked Ortho	435
PCB	177	PCB	163	Single Flanked Ortho	487	PCB	184	PCB	140	Unflanked Ortho	457
PCB	178	PCB	133	Single Flanked Ortho	525	PCB	184	PCB	145	Unflanked Para	397
PCB	178	PCB	134	Unflanked Meta	423	PCB	184	PCB	150	Single Flanked Para	465
PCB	178	PCB	135	Ortho Flanked Meta	495	PCB	184	PCB	154	Single Flanked Ortho	511
PCB	178	PCB	151	Ortho Flanked Meta	488	PCB	184	PCB	155	Doubly Flanked Meta	521
PCB	178	PCB	165	Single Flanked Ortho	511	PCB	185	PCB	141	Single Flanked Ortho	526
PCB	179	PCB	134	Unflanked Ortho	427	PCB	185	PCB	142	Unflanked Meta	385
PCB	179	PCB	135	Single Flanked Ortho	499	PCB	185	PCB	144	Doubly Flanked Meta	540
PCB	179	PCB	136	Ortho Flanked Meta	472	PCB	185	PCB	151	Doubly Flanked Para	545
PCB	179	PCB	151	Single Flanked Ortho	492	PCB	185	PCB	160	Unflanked Ortho	412
PCB	179	PCB	152	Ortho Flanked Meta	452	PCB	186	PCB	142	Unflanked Ortho	420
PCB	180	PCB	137	Para Flanked Meta	448	PCB	186	PCB	143	Single Flanked Ortho	531
PCB	180	PCB	138	Para Flanked Meta	464	PCB	186	PCB	145	Doubly Flanked Meta	538
PCB	180	PCB	141	Single Flanked Para	450	PCB	186	PCB	152	Doubly Flanked Para	541
PCB	180	PCB	146	Doubly Flanked Para	516	PCB	187	PCB	146	Single Flanked Ortho	499
PCB	180	PCB	153	Doubly Flanked Meta	519	PCB	187	PCB	147	Para Flanked Meta	426
PCB	180	PCB	156	Unflanked Ortho	425	PCB	187	PCB	149	Ortho Flanked Meta	474
PCB	180	PCB	167	Single Flanked Ortho	499	PCB	187	PCB	151	Single Flanked Para	452
PCB	181	PCB	137	Single Flanked Ortho	545	PCB	187	PCB	163	Unflanked Ortho	430
PCB	181	PCB	139	Doubly Flanked Meta	562	PCB	188	PCB	147	Unflanked Ortho	411
PCB	181	PCB	142	Unflanked Para	407	PCB	188	PCB	148	Single Flanked Ortho	499
PCB	181	PCB	147	Doubly Flanked Para	541	PCB	188	PCB	150	Ortho Flanked Meta	461
PCB	181	PCB	166	Unflanked Ortho	447	PCB	188	PCB	152	Unflanked Para	397
PCB	182	PCB	137	Unflanked Ortho	440	PCB	189	PCB	156	Para Flanked Meta	451
PCB	182	PCB	140	Para Flanked Meta	479	PCB	189	PCB	157	Para Flanked Meta	463
PCB	182	PCB	143	Unflanked Para	413	PCB	189	PCB	159	Doubly Flanked Para	495
PCB	182	PCB	148	Doubly Flanked Para	525	PCB	189	PCB	162	Doubly Flanked Para	517
PCB	182	PCB	154	Doubly Flanked Meta	533	PCB	189	PCB	167	Doubly Flanked Meta	525
PCB	182	PCB	168	Single Flanked Ortho	509	PCB	189	PCB	169	Single Flanked Ortho	524

PCB	190	PCB	156	Single Flanked Ortho	519	PCB	197	PCB	171	Unflanked Ortho	453
PCB	190	PCB	158	Doubly Flanked Meta	542	PCB	197	PCB	176	Single Flanked Para	473
PCB	190	PCB	160	Single Flanked Para	430	PCB	197	PCB	183	Single Flanked Ortho	513
PCB	190	PCB	163	Doubly Flanked Para	541	PCB	197	PCB	184	Doubly Flanked Meta	524
PCB	190	PCB	166	Para Flanked Meta	442	PCB	198	PCB	172	Single Flanked Ortho	563
PCB	191	PCB	157	Unflanked Ortho	480	PCB	198	PCB	173	Unflanked Meta	425
PCB	191	PCB	158	Para Flanked Meta	491	PCB	198	PCB	175	Doubly Flanked Meta	569
PCB	191	PCB	161	Doubly Flanked Para	500	PCB	198	PCB	178	Doubly Flanked Para	543
PCB	191	PCB	164	Single Flanked Para	503	PCB	198	PCB	185	Ortho Flanked Meta	485
PCB	191	PCB	167	Single Flanked Ortho	541	PCB	198	PCB	192	Single Flanked Ortho	469
PCB	191	PCB	168	Doubly Flanked Meta	558	PCB	199	PCB	172	Single Flanked Ortho	540
PCB	192	PCB	159	Single Flanked Ortho	561	PCB	199	PCB	174	Ortho Flanked Meta	496
PCB	192	PCB	160	Unflanked Meta	428	PCB	199	PCB	177	Para Flanked Meta	499
PCB	192	PCB	161	Doubly Flanked Meta	549	PCB	199	PCB	178	Doubly Flanked Para	520
PCB	192	PCB	165	Doubly Flanked Para	585	PCB	199	PCB	187	Doubly Flanked Meta	556
PCB	193	PCB	162	Single Flanked Ortho	542	PCB	199	PCB	193	Single Flanked Ortho	487
PCB	193	PCB	163	Para Flanked Meta	498	PCB	200	PCB	173	Unflanked Ortho	426
PCB	193	PCB	164	Ortho Flanked Meta	511	PCB	200	PCB	174	Single Flanked Ortho	521
PCB	193	PCB	165	Doubly Flanked Para	543	PCB	200	PCB	176	Doubly Flanked Meta	541
PCB	194	PCB	170	Para Flanked Meta	469	PCB	200	PCB	179	Doubly Flanked Para	540
PCB	194	PCB	172	Doubly Flanked Para	531	PCB	200	PCB	185	Single Flanked Ortho	487
PCB	194	PCB	180	Doubly Flanked Meta	529	PCB	200	PCB	186	Ortho Flanked Meta	451
PCB	194	PCB	189	Single Flanked Ortho	503	PCB	201	PCB	175	Single Flanked Ortho	502
PCB	195	PCB	170	Single Flanked Ortho	520	PCB	201	PCB	176	Ortho Flanked Meta	472
PCB	195	PCB	171	Doubly Flanked Meta	538	PCB	201	PCB	177	Unflanked Ortho	455
PCB	195	PCB	173	Single Flanked Para	444	PCB	201	PCB	179	Single Flanked Para	472
PCB	195	PCB	177	Doubly Flanked Para	542	PCB	201	PCB	187	Single Flanked Ortho	512
PCB	195	PCB	181	Doubly Flanked Meta	483	PCB	201	PCB	188	Doubly Flanked Meta	527
PCB	195	PCB	190	Single Flanked Ortho	487	PCB	202	PCB	178	Single Flanked Ortho	464
PCB	196	PCB	170	Unflanked Ortho	445	PCB	202	PCB	179	Ortho Flanked Meta	459
PCB	196	PCB	171	Para Flanked Meta	463	PCB	203	PCB	180	Single Flanked Ortho	522
PCB	196	PCB	174	Single Flanked Para	464	PCB	203	PCB	181	Para Flanked Meta	424
PCB	196	PCB	175	Doubly Flanked Para	514	PCB	203	PCB	183	Doubly Flanked Meta	540
PCB	196	PCB	180	Single Flanked Ortho	505	PCB	203	PCB	185	Single Flanked Para	446
PCB	196	PCB	182	Doubly Flanked Meta	513	PCB	203	PCB	187	Doubly Flanked Para	540
PCB	196	PCB	183	Doubly Flanked Meta	524	PCB	203	PCB	190	Unflanked Ortho	429
PCB	196	PCB	191	Single Flanked Ortho	463	PCB	204	PCB	181	Unflanked Ortho	411

PCB	204	PCB	182	Single Flanked Ortho	516	PCB	207	PCB	195	Unflanked Ortho	433
PCB	204	PCB	184	Doubly Flanked Meta	538	PCB	207	PCB	196	Single Flanked Ortho	508
PCB	204	PCB	186	Unflanked Para	398	PCB	207	PCB	197	Doubly Flanked Meta	519
PCB	204	PCB	188	Doubly Flanked Para	542	PCB	207	PCB	200	Single Flanked Para	451
PCB	205	PCB	189	Single Flanked Ortho	534	PCB	207	PCB	201	Doubly Flanked Para	519
PCB	205	PCB	190	Para Flanked Meta	466	PCB	207	PCB	203	Single Flanked Ortho	492
PCB	205	PCB	191	Doubly Flanked Meta	517	PCB	207	PCB	204	Doubly Flanked Meta	505
PCB	205	PCB	192	Doubly Flanked Para	468	PCB	208	PCB	198	Single Flanked Ortho	476
PCB	205	PCB	193	Doubly Flanked Para	509	PCB	208	PCB	199	Single Flanked Ortho	500
PCB	206	PCB	194	Single Flanked Ortho	551	PCB	208	PCB	200	Ortho Flanked Meta	475
PCB	206	PCB	195	Para Flanked Meta	499	PCB	208	PCB	201	Doubly Flanked Meta	544
PCB	206	PCB	196	Doubly Flanked Meta	574	PCB	208	PCB	202	Doubly Flanked Para	556
PCB	206	PCB	198	Doubly Flanked Para	518	PCB	209	PCB	206	Single Flanked Ortho	490
PCB	206	PCB	199	Doubly Flanked Para	542	PCB	209	PCB	207	Doubly Flanked Meta	556
PCB	206	PCB	203	Doubly Flanked Meta	557	PCB	209	PCB	208	Doubly Flanked Para	532
PCB	206	PCB	205	Single Flanked Ortho	520						

1